The role of mitogen-activated protein kinases for developmental and pathogenic processes of *Fusarium graminearum*, the causal agent of the head blight disease of small grain cereals

Dissertation zur Erlangung
des akademischen Grades
Dr. rer. nat.
des Fachbereichs Biologie
der Universität Hamburg

vorgelegt von
Nicole Joan Jenczmionka
aus Kösching

Hamburg 2004

Genehmigt vom
Fachbereich Biologie der
Universität Hamburg
auf Antrag von Herrn Prof. Dr. W. SCHÄFER
Weitere Gutachter der Dissertation:
Herr Prof. Dr. H. LÖRZ

Tag der Disputation: 02. April 2004

Hamburg, den 19. März 2004

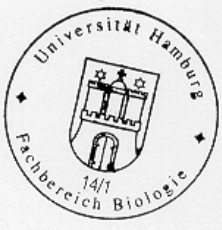

Professor Dr. Arno Frühwald
Dekan

The most exciting phrase to hear in science,
the one that heralds new discoveries,
is not “Eureka” but “That´s funny…”.

Isaac Asimov (1920-1992)

Abbreviations

aa	amino acid (s)
15-ADON	15-acetyldeoxynivalenol
3-ADON	3-acetyldeoxynivalenol
ADP	adenosine diphosphate
ATP	adenosine triphosphate
AZCL	azur cross linked
BCA	disodium 2,2`-bicinchoninate
bp	base pair (s)
cAMP	cyclic adenosine monophosphate
CBH	cellobiohydrolase
cDNA	complementary DNA
CM	complete medium
CMC	carboxymethylcellulose
CSPD	disodium 3-(4-methoxyspiro {I,2-dioxetane-3,2`-(5`-chloro) tricyclo[3.3.1.1^{3,7}]decan}-4-yl) phenylphophate
CWDE	cell wall degrading enzyme (s)
DIG	digoxygenin
DNA	deoxyribonucleic acid
dNTPs	desoxynucleotide triphosphate (s)
DON	deoxynivalenol
dUTP	desoxyuracil triphosphate
EG	endo-1,4-β-glucanase
ERK	extracellular-signal regulated protein kinase
et al.	et alii = and others
FHB	*Fusarium* head blight
Fig.	figure
GC-ECD	gas chromatography-electron capture detection
GC-MS	gas chromatography-mass spectrometry
Gmap1	*Gibberella* MAP kinase 1
Gpmk1	*Gibberella* pathogenicity MAP kinase 1
hph	Hygromycin B phosphotransferase
HPLC-FLD	High Performance Liquid Chromatography-Fluorescence Detector
IPTG	isopropyl-β-D-thiogalactoside
kb	kilo base pairs
LB	Lurea Bertani
MAPK	mitogen-activated protein kinase
MAPKK	mitogen-activated protein kinase kinase
MAPKKK	mitogen-activated protein kinase kinase kinase
MM	minimal medium
MPSS	massively parallel signature sequencing
mRNA	messenger RNA
NIV	nivalenol
OD	optical density
PCR	polymerase chain reaction
PKC	protein kinase C
Pks	polyketide synthase
PMFS	phenylmethylsulfonylflouride
RNA	ribonucleic acid

rpm	rounds per minute
RT-PCR	reverse transcriptase PCR
SAPK	stress-activated protein kinase
SDS	dodecylsulfate sodium salt
SNA	synthetic nutrient poor medium
TAIL-PCR	thermal asymmetric interlaced PCR
Tris	tris-(hydroxymethyl) aminomethane
UV	ultraviolett
v	volume
X-Gal	5-bromo-4-chloro-3-indolyl-β-D-galactopyranoside
YERK	yeast/fungi extracellular-signal regulated protein kinase
YPG	yeast extract/pepton/glucose medium
YSAPK	yeast/fungi stress-activated protein kinase
ZON	zearalenone

Units of measurement according to the international unit system SI (Système Internationale d`Unite) were used. Chemical formulas and molecules are named after IUPAC (International Union of Pure and Applied Chemistry). Other abbreviations for solutions and buffers are explained in the text.

1. Introduction

Fungi represent a highly diverse evolutionary group of eukaryotic, heterotrophic organisms. While many fungi feed saprophytically on dead organic material, most members of fungal groups are able to exploit other organisms as nutrient source during symbiotic or parasitic stages. Plant parasitic fungi have developed a variety of refined mechanisms to invade their hosts and to live at their expense. Necrotrophic fungi rapidly kill their host for example by secretion of toxins and cell wall hydrolysing enzymes. In contrast, biotrophic fungi are able to obtain nutrients from living host cells, thereby, not disturbing the viability of the host for an extended period of time. Fungi using intermediate infection strategies are called hemibiotrophic, because an initial biotrophic phase is followed by tissue destruction and colonisation of dead host tissue (Hahn et al. 1997). Successful infection depends on the correct recognition of the host, attachment to the plant surface, and germination of the spores. Subsequent penetration of the host surface can occur either by invasion through openings such as stomata or wounds, by mechanical force mainly generated by appressoria, and/or by enzymatic degradation of the plant cell wall. Finally, the host tissue is colonised. Secretion of cell wall degrading enzymes can also serve for nutritional purposes. The colonisation can also in some cases be aided by the secretion of toxins (Schäfer 1994). The whole process of infection is a result of differentiation-dependent gene activation utilising complex regulation pathways.
In the following the plant pathogen *Fusarium graminearum* will be introduced. Information will be given on a signaling pathway via mitogen-activated protein kinases. Furthermore, the role of plant cell wall degrading enzymes will be discussed in detail and the function of fungal hydrophobins will be elucidated.

1.1. The plant pathogen *Fusarium graminearum*

The hemibiotrophic, filamentous ascomycete *Fusarium graminearum* Schwabe (teleomorph *Gibberella zeae* [Schwein.] Petch) is the causal agent of the crown rot and the scab diseases, also known as *Fusarium* head blight (FHB), of small grain cereals like wheat, barley and many other grain crops. In small grain cereal crops the symptoms are generally similar. Thereby, the infected spikelets may first show browning or water soaking and later any part or all of the head may appear bleached (Fig. 1 B). The fungus

also may infect the stem immediately below the head, causing a brown/purplish discolouration of the stem tissue. Additional indications of FHB infection are pink to salmon/orange spore masses of the fungus often seen on the infected spikelet and glumes during prolonged humid weather. Infected wheat kernels, called „tombstones“, are shriveled, lightweight, and dull grayish in colour (Fig. 1 D), thus leading to a drastically reduced crop yield (McMullen and Stack 1999; Parry et al. 1995). *F. graminearum* is also associated with stalk and ear rot of corn and can also cause root rot of small grains. Maize ear rot is characterised by growth of pinkish mold on silks, kernels, and husks (Reid and Hamilton 1995). *F. graminearum* also has a wide host range among non crop grasses. The name, in fact, means *Fusarium* „of the grasses“. Being a facultative parasite, *F. graminearum* can, furthermore, effectively colonise compromised or weakened plants of all sorts and in particular senescent maize stalks (Windels and Kommedahl 1984).

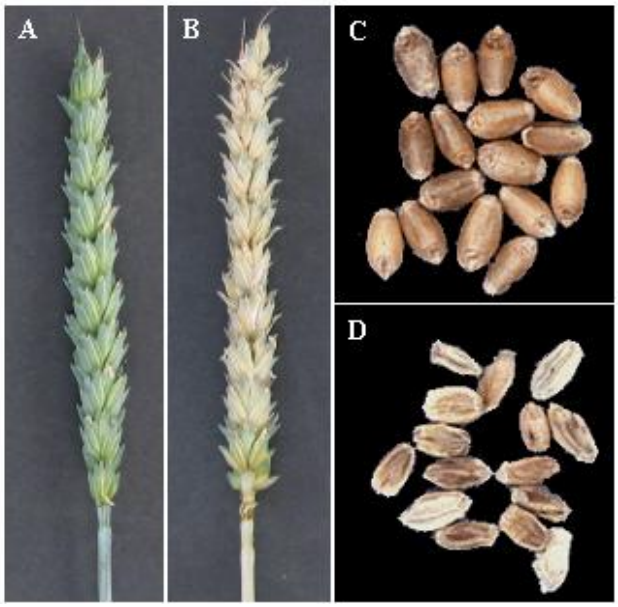

Fig. 1: Symptoms found on wheat spikes after an infection with *Fusarium graminearum*. A) uninfected wheat spike, B) infected, bleached wheat spike, C) uninfected wheat kernels and D) “tombestone” wheat kernels after *F. graminearum* infection.

The most favourable conditions for *F. graminearum* infection are prolonged periods, 48-72 h, of high humidity, e.g. rainfalls and/or heavy dews, as well as warm temperatures of optimally 20-30°C that coincide with the flowering and early kernel-fill period of the crop (McMullen et al. 1997; Bai and Shaner 1994). However, infection does occur at cooler temperatures when high humidity persists for longer that 72 h. Thus, a relatively wide range of environmental conditions can lead to severe FHB infections. Since scab development depends on favourable environmental conditions, disease occurance and

severity varies from year to year. A combination of factors leads to the severest yield and quality losses, e.g. the abundance of inoculum, prolonged or repeated wet periods during flowering through kernel development, microclimatic influences, crop rotation, and susceptibility of the crop cultivar grown. In a severely affected field, virtually every head can show symptoms (McMullen and Stack 1999; Bai and Shaner 1994).

The plant pathogen *F. graminearum* is found worldwide, wherever cereal crops are grown. Nevertheless, frequent rainfalls and high humidity have made areas like USA, Canada, South America, China, Japan, and Central Europe to particularly afflicted regions in the world (Schroeder and Christensen 1963; Bai and Shaner 1994; McMullen et al. 1997; Nicholson et al. 1998). In China, the worlds largest producer of wheat, the scab infection is endemic and has led to losses in excess of 1 million metric tons (Wang et al. 1982). In South Korea severe losses caused by scab of barley in 1963 threatened some of the population with starvation (Vestal 1964). Argentinean epidemics affecting wheat occured from the 1960s up to the 1980s. In the USA and Canada scab outbreaks of varying intensity have been common since 1991, effecting yield and quality of the wheat produced. In 1993 alone, the economic losses surpassed $ 1 billion, making it one of the greatest single-year losses due to any plant disease in North America (McMullen et al. 1997). Although worldwide the principle pathogen for scab diseases is *F. graminearum*, in the United Kingdom and Northern Europe the predominant species is *Fusarium culmorum*, causing comparable symptoms to those of *F. graminearum* (Parry et al. 1995).

F. graminearum is generally classified in the major groups 1 and 2. Group 1 is primarily soilborne and causes crown rot or dryland foot rot of wheat, barley, and other grasses. It is found in arid regions. Group 1 strains do not produce perithecia in culture and rarely in nature. Members of group 1 are presumed to be heterothallic and/or infertile. Group 2 strains are mostly airborne and are associated with scab of small grains, and stalk and ear rot of corn in humid climates. Members of this group are homothallic and are able to undergo sexual reproduction in nature and in culture. Within this group two types were distinguished. Type 2A, being the most prevalent of the strains, grows rapidly, forms red-pigmented colonies with abundant aerial mycelia, and is pathogenic to maize. Furthermore, the mycotoxin zearalenone (ZON) is only produced in low amounts. Type 2B grows slowly, forms appressed brownish-yellow colonies, is nonpathogenic to maize and mostly

produces high levels of ZON (Bai and Shaner 1994; Bowden and Leslie 1999). The wild type strain used in the course of this work belongs to the 2A group.

F. graminearum can exist as mycelia, ascospores, macroconidia, and chlamydospores. The existence of microconidia has not been observed so far. Mycelia, macroconidia, and chlamydospores are produced by the asexual *F. graminearum* stage, whereas the ascospores are the propagules of the sexual stage. In this stage the fungus is called *Gibberella zeae*. In soil macroconidia or mycelium can be transformed into chlamydospores (Bai and Shaner 1994).
In the winter months *F. graminearum* survives saprophytically on dead host tissues. Thus, debris of wheat, corn or rice on the soil surface are the most important source of inoculum (Sutton 1982). In spring perithecia formed in crop debris discharge their ascospores after a drop in relative humidity, such as the drying of previously wetted ascocarps (Trail et al. 2002). Furthermore, aerial mycelia from saprophytic living strains can also serve as efficient initial inoculum. The ascospores and/or aerial hyphae become airborne and serve as primary inoculum during the short period from anthesis through the soft dough stage of kernel development, approximately 10 to 20 days (Parry et al. 1995; Schroeder and Christensen 1963). Spores land on the exposed anthers at flowering time and penetrate the anthers, followed by penetration of the ovary and the floral bracts including the glume, the palea, and the lemma, finally leading to the colonisation of the kernels (Adams 1921). Visible lesions in form of brown, water-soaked spots on the glumes are observed within three to four days under conditions favourable for disease development. Later, the entire spikelet becomes blighted containing either no kernels or poorly filled kernels. From the infected floret the fungus can spread, either externally or internally, up and down the spike from one spikelet to another. If the weather is warm and humid, abundant aerial mycelia is formed, which spreads externally from the spike originally infected to the adjacent spikelets. If the fungus spreads internally, brownish chlorotic symptoms extend down into the culm and up to the top of the spike, thereby invading the parenchymatous tissue as well as the vascular tissue. Clogging of the vascular tissue results in the premature ripening of the heads so that even not directly infected grains will be shriveled because of water shortage. If heads are extensively invaded at an early stage, kernels will fail to develop completely. Finally, the entire spike turns the colour of straw. Visible pink mold, containing abundant sporodochia carrying conidia (Fig. 2 A), appear on the spikes

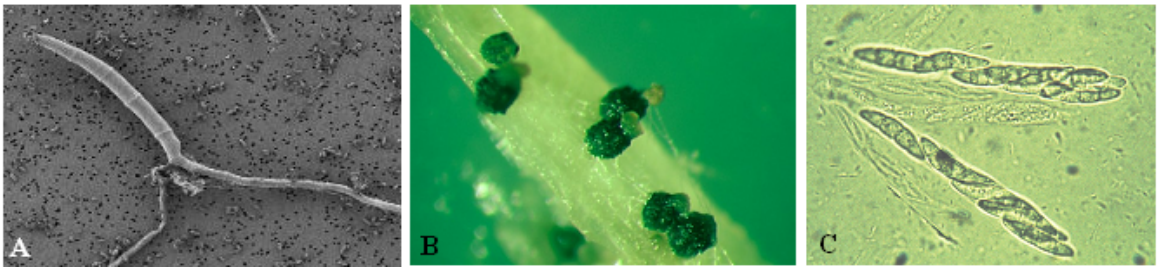

Fig. 2: Reproduction organs from *F. graminearum*. A) scanning electron microscopic picture of a germinated conidia; B) perithecia and C) asci containing ascospores.

after 35 days when the weather continues to be humid (Pritsch et al. 2001; Bai and Shaner 1994; Sutton 1982; Schroeder and Christensen 1963). Dispersal of conidia and aerial mycelia by wind or rain-splashing leads to secondary infections on either the same spike or on other plants. Nevertheless, the fungus is generally limited to one infection cycle per season, as the main period of vulnerability is during anthesis (Parry et al. 1995; Bai and Shaner 1994). Later in the season, perithecia of the sexual stage of *F. graminearum* are formed and can be seen as raised purplish black spots (Fig. 2 B) containing numerous asci (Fig. 2 C). Thus, *F. graminearum* is capable of finishing its total life cycle on one single spike (Fig. 3).

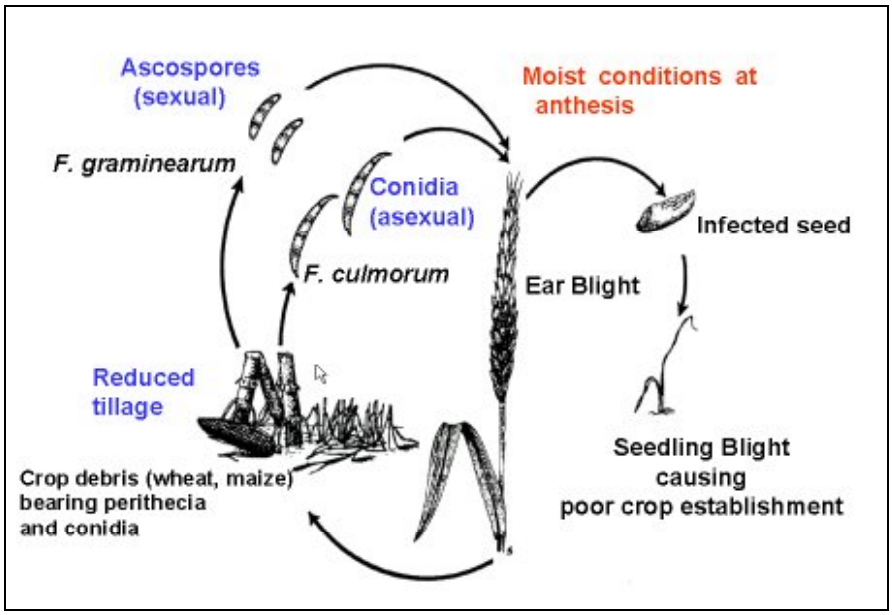

Fig. 3: Disease cycle of *F. graminearum*. (adapted from Bergstrom 1993)

Sowing cereals into *Fusarium*-infested soil may additionally result in the development of seedlings blight and foot rot (Parry et al. 1995). Susceptibility of maize ears to infection by *F. graminearum* is greatest shortly after the silks emerge and declines rapidly thereafter. Entry into the maize ear can occur through wounds or by growth of the mycelium down the

silks to the kernels and cob from spores germinating on the silks. Pollen was observed to stimulate the conidia germination, germ tube growth, and colonisation of silks (Reid and Hamilton 1995; Sutton 1982). Colonisation of maize ears progresses during eight weeks or more in the field. The pathogen invades the kernels, various tissues of the cob, and sometimes the husk leaves.

Eventhough direct penetration of the glume, palea or rachilla of wheat spikelets have been suggested, this mode of initial wheat infection is most probably not the predominant way (Parry et al. 1995; Bai and Shaner 1994, Pritsch et al. 2000). Various infection assays showed that the strongest FHB symptoms were found, when wheat was infected as the anthers were extruding the spikelets (Parry et al.1995). It has been suggested that anthesis may be the period of greatest susceptibility, because of the high levels of choline and betaine produced by the anthers. Both substances have been shown to stimulate growth of *F. graminearum* and also promote the infection of wheat spikes (Bai and Shaner 1994; Strange et al. 1978; Strange et al. 1974; Strange et al. 1972). Histological studies showed that the anthers were colonised before the fungus spread into other parts of the spikelet, including the ovary. In later infection stages the fungal hyphae were found both intra- and intercellularly throughout the entire kernel (Wanjiru et al. 2002; Parry et al. 1995; Schroeder and Christensen 1963). Nevertheless, the actual mode of penetration and invasion is still not understood to a major extent and is discussed very controversially. Generally, a formation of appressoria has been excluded, as no such structures were found *in vivo* and could not be induced *in vitro*. Thus, a mechanical penetration of the host surface like it has been shown for several other fungal plant pathogens is not the strategy of *F. graminearum* (Dean 1997; Emmet and Parbery 1975). Pritsch and coworkers (Pritsch et al. 2000) showed that during glume infection no direct penetration of the epidermis took place. They only observed that the fungus penetrated through the stomata, followed by an abundant intracellular colonisation of the parenchyma tissues. Subsequently, they postulated a similar mode of penetration of the paleas and lemmas. Furthermore, they reported on subcuticular growth, indicating a possible enzymatic degradation of the cuticle. Recently, some evidence for the role of cell wall degrading enzymes during the infection process of *F. graminearum* and *F. culmorum* were gained (Wanjiru et al. 2002; Kang and Buchenauer 2000). The infection of wheat spikes by *F. culmorum* and *F. graminearum* led to a reduction in cell wall components including cellulose, xylan, and pectin. This suggests

that both *F. culmorum* and *F. graminearum* produce cell wall degrading enzymes to assist the infection.

Besides the losses in grain yield through diseased kernels that have a reduced test weight because they are light and shriveled, the FHB infection also leads to a reduction in grain quality through destruction of starch and proteins (Sutton 1982) and most important by accumulation of non-selective mycotoxins. The most commonly known are the trichothecenes deoxynivalenol (DON, Fig. 4 A), nivalenol (NIV), the precursers 3-acetyldeoxynivalenol (3-ADON), and 15-acetyldeoxynivalenol (15-ADON), as well as the estrogenic zearalenone (ZON, Fig. 4 B) (Kang and Buchenauer 1999; McMullen et al. 1997; Bai and Shaner 1994; Sutton 1982). Thereby, biosynthesis of the mycotoxins depends on many factors, especially the pathogen strain, the substrate, the period of colonisation, temperature, moisture, and competing organisms (McMullen and Stack 1999; Sutton 1982).

Trichothecenes are toxic secondary metabolites of various *Fusarium*, *Myrothecium*, *Stachybotrys*, *Trichoderma*, and *Trichothecium* species. The biosynthesis of trichothecenes proceeds from the hydrocarbon trichodiene through a complex series of steps. Most of the chemical intermediates in the pathway are known and most of the genes known to be required for toxin synthesis are organized in a coordinately regulated gene cluster. To date, ten genes involved in trichothecene biosynthesis have been localized. (Sweeney and Dobson 1999; Desjardins and Hohn 1997; Hohn et al. 1997). Trichothecenes are the causal agent of moldy-grain toxicoses such as feed refusal, dermatitis, anemia, immunosuppression, and hemorrhagic septicemia, when animals or humans consume contaminated food or feed (Kimura et al. 2001; Desjardins and Hohn 1997). Safety threshhold values have been recommended for DON mycotoxin contamination in grain used for human food and animal feed. The United State Food and Drug Administration has a guideline of 1 µg/g for finished flour products (Harris et al. 1999). These sesquiterpene epoxides are potent inhibitors of protein biosynthesis primarily in the liver and the gut of eukaryotes. Protein inhibition occurs by blocking of the peptidyl transferease step (Kang and Buchenauer 1999; Proctor et al. 1995). In plants the trichothecenes DON, 3-ADON, and 15-ADON have been shown to be phytotoxic by strongly inhibiting the growth of wheat seedlings, coleoptile segments, and wheat embryos. A significant correlation was found between the reduction of grain weight and the mycotoxin concentration in *F. graminearum* and *F. culmorum* infected wheat grain (Wang and Miller 1988).

Immunocytochemical localization of these trichothecenes indicated a very close relationship of toxin accumulation with pathogenic changes in host cells, symptom appearance, and colonisation of the host tissue by hyphae. These results suggest that the toxins play an important role in disease development (Kang and Buchenauer 1999). In fact, transformation-mediated disruption of the *tri5* gene of *F. graminearum* led to mutants that were unable to produce DON and that were reduced in virulence towards wheat and maize (Bai et al. 2001; Harris et al. 1999; Desjardins et al. 1996; Proctor et al. 1995). The *tri5* gene encodes a trichodiene synthase that catalyzes the first reaction in the trichothecene pathway. Thus, the trichothecene biosynthesis is the first and up to date only pathogenicity trait identified for *F. graminearum*.

Kang and Buchenauer (Kang and Buchenauer 1999) suggested that the trichothecenes may diffuse into the host tissue prior to fungal invasion, bind to the ribosomes and the endoplasmatic reticulum and subsequently inhibit the plant biosynthesis. Additionally, they postulate that the toxins are also associated with the host cell wall plasmalemma in early infection stages, leading to electrolytic losses through alterations of the cell membrane permeability. Thereby, the trichothecenes may effectively retard post infectional defence reactions, thus, aiding the growth of the pathogen in the plant tissue.

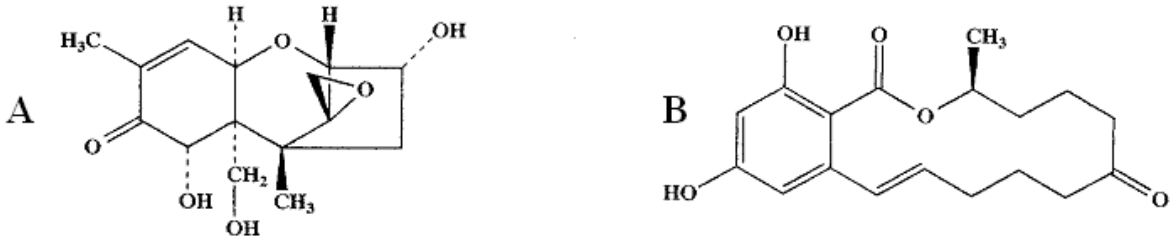

Fig. 4: Structure of two *Fusarium* mycotoxins A) deoxynivalenol (DON), B) zearalenone (ZON). Adapted from Moss (Moss 2002).

Zearalenone (ZON), the second important mycotoxin produced by *F. graminearum*, is produced by the sexual stage of the fungus. It was shown to have influence on perithecia developement and was, therefore, suggested as sex hormone of *F. graminearum* (Wolf and Mirocha 1973). ZON application to plants was shown to influence seed germination, callus induction, differentiation, and plant regeneration (Biesaga-Kościelniak et al. 2003). In animals ZON has an uterotrophic and estrogenic effect, leading to reproductive disorders in farm animals, especially in swine (Moss 2002; Bottalico 1998). Chemically, ZON is a polyketide derived metabolite. The biosynthesis pathway is up to date still unknown. The

role of ZON, if any, in plant infection is also not yet understood, as the actual toxicity of ZON is very low (Moss 2002; Desjardins and Hohn 1997).

None of the currently available commercial cereal cultivars are resistant to *Fusarium* infection, but differences in susceptibility to FHB do occur among different wheats (Gilbert et al. 2002; Miedaner et al. 2001). In order to limit the risk of epidemic FHB infections an extensive disease managment is neccessary. This includes the use of cultural control techniques, the growing of more resistant cultivars, and the use of fungicides. Crop rotation, land preparation, the appropriate use of fertilizers, irrigation and weed control are understood as cultural control techniques and may all contribute to a reduction in the quantity of *Fusarium* inoculum available for dispersal to ears (McMullen and Stack 1999; Parry et al. 1995). Breeding and/or genetical engineering of new resistant grain cultivars focusses on a resistance towards (i) the initial infection, (ii) the pathogen spread within the host, (iii) the ability to degrade DON, and (iv) in gaining a tolerance to high DON concentrations (Buerstmayr et al. 2002; Parry et al. 1995). Seed-treatment fungicides reduce the spread of soil-borne inoculum, but have little effect on head blight because of the large amount of inoculum that can infect the wheat head directly later in the growing season. Although a foliar application of fungicides at anthesis might provide some protection, there are few fungicides available for application. Cost of treatment and the difficulty of determining the optimal time of application also make this method of control less attractive. Even if it reduces direct yield loss, it might not reduce mycotoxin contamination to a tolerable level and the application is neccessary up until shortly before the harvest. Additionally, there have been reports of widespread resistances to several fungicides (Parry et al. 1995; Bai and Shaner 1994). Recently, biological control mechanisms have emerged as a more promissing strategy of disease management (Lutz et al. 2003).

Hence, more detailed information about the molecular mechanisms of *F. graminearum* infection must be gained, in order to find more efficient methods of disease control.

1.2. The role of MAP kinases in fungal pathogenesis

The initial and fundamental step in any successful infection process is the perception of the host. This is mediated by fungal receptors that recognize physical and/or chemical signals from the plant e.g. the hydrophobicity of the cuticle, the elevation of the stomata cells,

various chemical compounds of the plant cuticle, ethylene or gaseous emmision from the stomata. Only if a pathogen recognizes its host correctly, can it initiate specific infection mechanisms that then lead to a successful invasion, e.g. the development of penetration structures like appressoria and/or the secretion of cell wall degrading enzymes (Kolattukudy et al. 1995). The initial perception of the host and the expression of proteins necessary for infection are linked by complex signal transduction pathways, which thus are likely to be crucial factors in disease establishment. The study of signal transduction pathways in fungi is actually the key for getting a complete view of the complex system of interaction between host and pathogen. Therefore, there has been extensive research done on various fungal signal transduction processes. Several genes encoding components of signal transduction pathways have been cloned and disrupted in different fungi and have enabled to gain important information about their infection strategies. Thereby, α-subunits of heterotrimeric G proteins, cAMP dependent protein kinases and mitogen-activated protein (MAP) kinases were shown to play essential roles (Gao and Nuss 1996; Xu and Hamer 1996). It was also demonstrated, that these different pathways interact in many ways to accomplish the multitude of developmental stages (Kinane and Oliver 2003; Lengeler et al. 2000; Xu 2000; Kahmann et al. 1999; Kronstad et al. 1998; Dean 1997; Xu and Hamer 1996). In this work the focus will be on transduction processes via MAP kinase pathways.

Generally, signal transduction processes can be functionally divided into the following steps (Krauss 1997):

1) Perception of a signal by a receptor of a target cell
2) Transduction of the signal in the target cell
3) Translation of the signal into a biochemical reaction
4) Termination of the signal

Ubiquitous MAP kinase pathways regulate growth and differentiation processes from yeast to humans, taking over the transduction of the signal in the target cell. An extracellular signal is registered by a transmembrane receptor, mostly a receptor tyrosine kinase or a G protein-coupled receptor (1). The receptor is activated and passes the signal on by stimulating the tyrosine phosphorylation of the subsequent effector molecules that are arranged in a cascade (2). The first activation step generally occurs by protein kinases associated to the cell membrane, e.g. a heterotrimeric G protein. Finally, the signal is transmitted into the nucleus, resulting in the activation of transcription factors or other

protein kinases that catalyse key reactions of the metabolism (3). The signal termination is mediated by protein phosphatases (4). Signal transduction via cascades of protein kinases is a very flexible and efficient strategy to amplify, diversify and regulate various exogenious signals (Hafen 1998; Krauss 1997; Cobb and Goldsmith 1995).

The key components of the MAP kinase transduction cascade are three cytoplasmatic protein kinases. These three kinases belong to one module that conveys specific exogenious information to target effectors, but also coordinates incoming information from parallel signal pathways. Most organisms possess several such regulation modules. The first kinase of this module is the MAP kinase kinase kinase (MAPKK kinase), a serine/threonine protein kinase. The activated MAPKK kinase phosphorylates the MAP kinase kinase (MAPK kinase) at two serine residues. The dual specifity MAPK kinase with an extraordinary high substrate specifity towards particular MAP kinase isoforms activates the specific MAP kinase by threonine (T) and tyrosine (Y) phosphorylation at the conserved TXY-site (Fig. 5). The MAP kinase, also known as extracellular-signal regulated kinase (ERK), is a serine/threonine protein kinase that has an important function in diversifying MAP kinase signal pathways. Various MAP kinase isoforms with different substrate specifities exist, so that a branching of the signal pathways can occur at this point (Krauss 1997; Cobb and Goldsmith 1995).

The MAP kinase family belongs to one of the largest superfamilies of proteins, the eukaryotic protein kinase superfamily. MAP kinases are proline-directed serine/threonine protein kinases that only phosphorylate substrates with a proline residue (P) at the P-1 site of the substrate recognition consensus motif PX[ST]P. The phosphorylation occurs by linking a phosphate residue of ATP to the hydroxy group of serine and threonine by an ester bond. The activity of most MAP kinases is transiently stimulated within minutes to hours by a large variety of signals, such as mitogens, growth factors, cytokines, T cell antigens, pheromones, phorbol esters, UV light and ionizing radition, osmotic stress, heat shock, oxidative stress, cell adherence and many other factors. Different MAP kinases are characterised by varying degrees of sensitivity to subsets of these stimuli. The specifity of these kinases depends predominantly on the amino acid sequence of the substrate surrounding the serine and threonine, on the accessability of the phosphorylation sites and on the binding of activators, inhibitors and scaffold proteins involved in facilitating the assembly of enzyme-substrate complexes. (Park et al. 2003; Schaeffer and Weber 1999; Kültz 1998). As already mentioned, MAP kinases are activated by dual phosphorylation at the TXY-sequence within the activation loop. Thereby, tyrosine (Y) phosphorylation

regulates the substrate binding, whereas phosphorylation of threonine (T) is needed to position the catalytic residues in the correct manner. Substrate binding may then provoke another conformational change after which ATP can bind (Widmann et al. 1999; Kültz 1998; Marshall 1994). Most MAP kinases have small amino and carboxy terminal regions and consist almost entirely of the eukaryotic protein kinase domain spanning about 300 amino acids and containing 11 conserved subdomains. Structural analysis indicated that MAP kinases might dimerize upon activation by dual phosphorylation. Like the protein kinase domains of other members of the eukaryotic protein kinase superfamily, the MAP kinases fold into a common core structure consisting of two lobes separated by a catalytic cleft (Kültz 1998; Cobb and Goldsmith 1995).

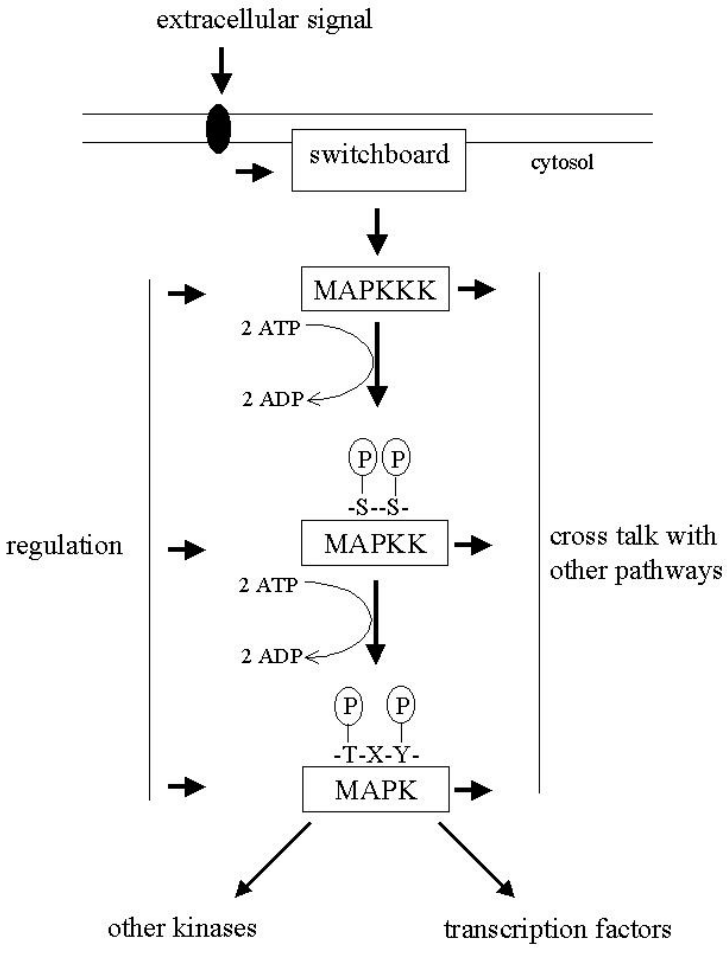

Fig. 5: Schematic illustration of the basic signal transduction processes within a MAP kinase cascade (modified after Krauss 1997). A transmembrane receptor senses a extracellular signal which activates a protein kinase bound to the cell membrane. This kinase, acting like a switchboard, triggers the phosphorylation cascade. A MAPKK kinase (MAPKKK) phosphorylates the dual specifity MAPK kinases (MAPKK) at two serine residues (S), thereby activating the enzyme. The activated MAPK kinase phosphorylates and activates the MAP kinase (MAPK) at a threonine (T) and tyrosine (Y) residue. Finally, the effector molecules, other protein kinases or transcription factors, are phosphorylated and thus activated, leading to a specific cellular answer to the extracellular signal. Regulation can occur at the level of all kinases involved. Furthermore, a cross talk between the MAP kinase cascade and other signal transduction pathways is possible.

The MAP kinase superfamily is divided into at least nine subfamilies. Members of a given subfamily are exclusively found in animals, plants, or yeast/fungi. Based on functional similarities all nine subfamilies can be grouped into three classes, the stress-activated protein kinases (SAPKs), the extracellular signal-activated protein kinases (ERKs), and the MAPK3 subgroup. Each ERK and SAPK subfamily is characterised by a conserved

intermittent amino acid separating the dual phosphorylation sites within a TXY motif. Next to a single signature sequence that is characteristic for all MAP kinases and is sufficient to distinguish MAP kinases from other members of the protein kinase superfamily, further signature sequences were identified that are characterisitic for each of the nine subfamilies. It was found that the amino acids conserved in all MAP kinases are located primarily in the centre of the protein containing the phosphorylation site and the adjacent sequences of the catalytic cleft. On the other hand, amino acids conserved in a given subfamily are located mainly in the periphery, indicating their possible importance for interacting with substrates, activators, and inhibitors, thus enabling a specific regulation of the kinases. Unique amino-terminal regions have been associated with MAPK kinase recognition, whereas the carboxy-terminal part constituting the larger, lower lobe of the molecule has been implicated in substrate recognition (Kültz 1998). Upon activation, the MAP kinases can translocate into the nucleus and activate transcription factors. However, MAP kinase substrates also include cytoplasmic proteins, e.g. phospholipases, transmembrane proteins, and cytoskeleton-associated proteins. In addition, MAP kinases can also phosphorylate MAPK kinases, MAPKK kinases and other protein kinases and, therefore, may be able to reinforce or dampen an induction of its one or other MAP kinase cascades (Widmann et al. 1999; Kültz 1998).

Yeast represents the experimental model where the organisation and regulation of MAP kinase pathways are best understood. Five MAP kinase pathways have been characterised in *Saccharomyces cerevisiae* up to date. Pheromone sensing triggers a MAP kinase cascade which leads to mating processes. One cascade has been shown to regulate filamentous growth after starvation and another is necessary for the response to hypertonic stress, activating the synthesis of osmolytes. Finally, the fifth MAP kinase cascade induces sporulation upon carbon and nitrogen deprivation (Lengeler et al. 2000; Widmann et al. 1999; Banuett 1998). Extensive studies have shown that MAP kinase pathways are a widespread regulatory mechanism for developmental processes, mating and stress response among a multitude of fungi ranging from yeast like to filamentous fungi (Lengeler et al. 2000; Xu 2000). And as initially mentioned, they have in fact also been shown to play an immense role in regulation of pathogenicity in many fungi, such as *Botrytis cinerea* (Zheng et al. 2000), *Candida albicans* (Alonso-Monge et al. 1999; Csank et al. 1998; Navarro-Garcia et al. 1998; Navarro-Garcia et al. 1995), *Claviceps purpurea* (Mey et al. 2002a, Mey et al. 2002b), *Cochliobolus heterostrophus* (Lev and Horwitz 2003; Lev et al. 1999),

Colletotrichum lagenarium (Kojima et al. 2002; Takano et al. 2000), *Fusarium oxysporum* (Di Pietro et al. 2001), *Magnaporthe grisea* (Xu et al. 1998; Xu and Hamer 1996), *Pyrenophora teres* (Ruiz-Roldán et al. 2001) and *Ustilago maydis* (Mayorga and Gold 1999; Müller et al. 1999). Thereby, specific MAP kinases have been found to be important for appressorium formation, invasive hyphal growth and secretion of cell wall degrading enzymes. They were further shown to regulate conidiation, conidia germination and female fertility, thus developmental processes also being important for disease establishment. Another group of MAP kinases participates in the regulation of hyphal growth and virulence. Osmolarity MAP kinases were also found in other fungi. Whereas the osmolarity MAP kinases from yeast is activated mainly by high osmolarity (Brewster et al. 1993), other fungal SAPKs are responsive to various forms of stress, such as hyperosmolarity, temperature shock, fungicide resistance, ultraviolet light irradiation, and oxidative stress (Kawasaki et al. 2002; Soto et al. 2002; Zhang et al. 2002). This indicates that transduction pathways tend to become more versatile in higher fungi. Comparison of all fungal MAP kinases found up to date has led to the speculation that higher, filamentous pathogenic fungi may only have three conserved MAP kinase pathways. One regulating mating and filamentation, hyphal growth, pathogenesis, conidation and conidia germination. A second having in influence on the cell integrity, and nutrient sensing, but also pathogenesis, conidiation and aerial hyphal growth. And a third pathway that regulates response to high osmolarity, stress response and pathogenesis. Because most fungal pathogens have more complicated life cycles and differentiation processes, it was postulated that these three pathways play more diverse roles in pathogenic fungi than in their homologues in *S. cerevisiae* (Xu 2000).

Fungal MAP kinases generally were shown to have pleiotropic regulatory effects which are involved in several developmental pathways, each partially responsible for different extracellular signals. Comparison of the various MAP kinase from different fungal plant pathogens revealed that all seem to use conserved pathways to regulate diverse infection processes. Different signals are sensed and different effector proteins are activated. Therefore, the analysis of regulatory pathways enables to get new insights of specific plant infection processes.

1.3. Cell wall degrading enzymes in the plant infection process

MAP kinases of fungi that are known to penetrate the plant surface directly without the use of appressoria, such as *C. purpurea*, *F. oxysporum* and *B. cinerea*, have been postulated to have a regulatory effect on the production of cell wall degrading enzymes. (Mey at al. 2002b; Di Pietro et al. 2001; Zheng et al. 2000). Additionally, a direct regulatory link between a MAP kinase and cellulolytic enzymes was shown for the phytopathogenic fungus *C. heterostrophus* (Lev and Horwitz 2003). As the cuticle and the cell wall are the main barrier which the plant pathogens have to overcome, one possible mode for MAP kinases to participate in pathogenic processes is by regulating the secretion of cell wall degrading enzymes (CWDE). Hence, a detailed knowledge of the structure and composition of the cell wall is important for understanding infection processes via CWDE. The cuticle covers all above organs of the plant and is chemically made of cutin, a polyester embedded into wax. This polyester is composed of hydroxylated fatty acids, which are crosslinked by ester bonds. The wax consists of hydrocarbons, primary long-chain alcohols, alcanoic acids, and monoesters. Generally, the thickness and composition of the culticle varies among species and can also change during plant development (Hahn et al. 1997; Schäfer 1994). The plant cell wall is the organ that allows the generation of the turgor pressure and provides the cell with its functional form. It is made up of a primary and secondary cell wall. The primary cell wall is adjacent to the middle lamella in young growing cells. After the cell expansion is completed the secondary cell wall is added. The primary cell wall is made up of structural carbohydrates and protein components embedded in a matrix of pectin, a polymer of α-1,4-linked D-galacturonic acid substituted with acetate or various sugar monomers. Pectin is also found as predominant compound of the middle lamella. The major structural compound, with 50 % of the wall mass, is a cellulose-xyloglucan framework. It consists of cellulose microfibrils linked by xyloglucans. Cellulose microfibrils are formed of aggregates of linear β-1,4-linked glucose monomers that give the wall much of its mechanical strength. Xyloglucans are hydrogen-bonded to the cellulose and consist of a backbone of β-1,4-linked D-glucosyl residues with D-xylosyl side chains. Xylans are constituents of the secondary walls of dicotyledons, but in contrast form the main component of some monocotyledon primary walls. They comprise a β-1,4-backbone with linked acetyl residues or arabinose and glucuronic acid side groups. Approximately 10 % of the cell wall mass is made up of a characteristic structural protein component rich in hydroxyproline residues (extensin). As response to microbial attacks,

the synthesis of extensins is often increased and the protein monomers are cross-linked at the penetration sites (Strasburger et al. 2002; Hahn et al. 1997; Keon et al. 1987). Regarding the variety of cell wall components and their complex, interwoven structure, it seems evident that several fungal CWDE need to act synergistically to efficiently degrade the wall polymers. Thus, cutinases, lipases, cellulases, xylanases, pectinases, and proteases might be crucial instruments for the penetration process. Furthermore, amylases could be useful for the degradation of plant tissues high in starch content. Starch is a water insoluble polysaccharide used by many plants as carbohydrate storage and can be found in abundance in seeds and grains. Starch is made up of amylose and amylopectin. Amylose is a long chain of helically wound, unbranched α-1,4-linked D-glucosyl residues, whereas amylopectin is branched having additional α-1,6-linkages (Strasburger et al. 2002).

Cutinases and lipases

Cutinases (EC 3.1.1.74) catalyse the hydrolysis of primary alcohol esters, preferentially those of short chain fatty acids. They represent an enzyme class related to true esterases and true lipases. Synthesis of the enzyme is induced by its substrate and catabolite-repressed by easily utilizable sugars (Hahn et al. 1997). Much research has been done to elucidate the role of cutinases for the virulence of plant pathogens. However, the initial evidence for its importance in pathogenicity could not be confirmed (van Kan et al. 1997; Stahl et al. 1994; Stahl und Schäfer 1992; Sweigard et al. 1992).

Nevertheless, in the recent years secreted lipases have emerged as candidates for virulence factors of human pathogenic fungi (Hube et al. 2000). Lipases (EC 3.1.1.3) are hydrolases acting on the carboxyl ester bonds present in tri-, di-, and monoacylglycerols to liberate fatty acids and glycerol. Generally, lipases are active almost exclusively at oil-water interfaces. Other than the cutinases, also belonging to the family of lipases, not so much is known about the role of secreted lipases for the pathogenicity of plant pathogenic fungi. So far, a participation of lipases in phytopathogenic processes could only be shown for *B. cinerea* and *Alternaria brassicicola*. By supplementing antilipase antibodies to inoculated conidia, the infection of these two pathogens could be reduced dramatically, indicating a requirement of a lipase activity for their infection (Berto et al. 1999; Comménil et al. 1999; Comménil et al. 1998).

Cellulases

There are three main types of enzymes involved in cellulose degradation: the cellobiohydrolases (CBH; EC 3.2.1.91), the endo-1,4-β-glucanases (EG; EC 3.2.1.4), and the β-glucosidases (EC 3.2.1.21). All enzymes appear to exist in multiple forms which

differ in their relative activities on a variety of substrates. The EGs hydrolyse cellulose chains randomly in an endo manner and produce rapid changes in the degree of polymerisation. The CBHs act by removing cellobiose from the nonreducing end of the chain. β-Glucosidases are not strictly speaking cellulases. They cleave glucose from the short-chain cellooligosaccharides and cellobiose (Béguin 1990; Wood and Mahalingeshwara Bhat 1988). The production of cellulases is generally regulated by substrate induction and catabolite repression (Hahn et al. 1997; Béguin 1990). Cellulolytic filamentous fungi mostly produce free cellulases, meaning that the enzymes are secreted and can diffuse directly to the substrate (Lynd et al. 2002; Béguin 1990). The role of cellulases during plant pathogenesis is, so far, not clearly defined. Disruption of major EG genes in phytopathogenic bacteria drastically reduced their virulence (Gough et al. 1988; Roberts et al. 1988). However, in the fungal maize pathogen *Cochliobulus carbonum* deletion of the cellulase *cel1* gene had no effect on the pathogenicity (Sposato et al. 1995).

Xylanases

Because of the heterogenity of xylan, its hydrolysis requires a set of xylanolytic enzymes including β-1,4-endoxylanases (EC 3.2.1.8), β-xylosidases (EC 3.2.1.37), α-L-arabinofuranosidases (EC 3.2.1.55), α-glucuronidases (EC 3.2.1.136), and acetyl xylan esterases (EC 3.1.1.6). The concerted action of these enzymes converts xylan to its constituent sugars. Thereby, the β-1,4-endoxylanase randomly cleaves the internal β-1,4-glycosidic bond of the xylan backbone, decreasing the degree of polymerisation. β-Xylosidases are exo-glycosidases that hydrolyse short xylooligo-saccharides from the non-reducing end, forming xylose as end product. The α-L-arabinofuranosidases, the α-glucuronidases and the acetyl xylan esterases are debranching enzymes that cleave the arabinose, glucuronic acid and acetyl side groups from arabinoxylan, glucuronoxylan and acetylxylan, respectively (Shallom and Shoham 2003; Bertoldo and Antranikian 2002). Secretion of xylanases by fungi has mainly been observed in grass pathogens due to the high amount of glucuronoarabinoxylan in the cell wall of grasses. In these fungi, the xylan secretion is usually induced by xylan and plant cell walls (Komiya et al. 2003; Hahn et al. 1997). Unfortunately, a disruption of a xylanase genes in *Cochliobolus carbonum* (Apel et al. 1993) and in *F. oxysporum* (Gómez-Gómez et al. 2001) was not able to give evidence for the role of these enzymes in pathogenesis. Hence, xylanases are generally not discussed as pathogenicity factors.

Pectinases

Microorganisms, especially plant pathogenic microorganisms, produce a wide spectrum of pectinolytic enzymes. Many of these extracellular enzymes occur in multiple forms, which enhance the adaption of the plant pathogen to different hosts (Bertoldo and Antranikian 2002). Pectin-like substances are degraded by several enzymes classified by their substrates, type of lysis, and mode of action. Both methyl-esterified (pectin) and non-esterified polygalacturonic acid can be degraded by two types of enzymes, hydrolases (EC 3.2.1.15) and lyases (EC 4.2.2.2). Lyases break the α-1,4-bonds of the polymers by inserting a double bond between carbons 4 and 5 of the (methyl) galacturonic acid without adding H^+ and OH^- at the cleavage site. Pectin methylesterases (EC 3.1.1.11) remove the methyl group from esterified galacturonic acid residues in pectin chains, and the polygalacturonate formed is then accessible for cleavage by polygalacturonases and polygalaturonate lyases. Both, lyases and hydrolases, occur as exo- or endo-cleaving enzymes, creating galacturonate dimers or oligomers of various sizes. Pectic enzymes are often induced by pectin degradation products formed by low levels of constitutively expressed enzymes and are catabolite-repressed by simple sugars (Annis and Goodwin 1997; Hahn et al. 1997).

Of all cell wall degrading enzymes produced by plant pathogenic fungi, most research has concentrated on the pectin degrading enzymes. This is because the pectinases are typically produced first, in the largest amount, and are the only cell wall degrading enzyme capable of macerating plant tissue and killing plant cells without the need of other synergistically acting enzymes (Valette-Collet et al. 2003; Annis and Goodwin 1997). In fact, the disruption of pectinolytic enzymes from *B. cinerea*, *C. purpurea*, *Nectria haematococca* and *Aspergillus flavus*, repectively, were sufficient to drastically reduce the fungal virulence, indicating the importance of these enzymes for phytopathogenicity (Valette-Collet et al. 2003; Oeser et al. 2002; Rogers et al. 2000; te Have et al. 1998; Shieh et al. 1997). However, the function of pectinases in plant infection is not always so unequivocal, as various other deletion experiments did not lead to the formation of mutants with reduced virulence (Garcia-Maceira et al. 2000; Scott-Craig et al. 1990).

Proteases

In fungi pathogenic to animals and humans the role of proteases in pathogenicity has been studied extensively (Hube 2000; Schaller et al. 1999). Certain evidence exists, indicating proteases to also be involved in fungal infection of plants (Redman and Rodriguez 2002; Carlile et al. 2000). Generally, proteases are classified according to the nature of their

active centre in serine proteases and cysteine proteases. Furthermore, metal proteases that depend on the presence of bivalent metal ions and aspartic protease, which have a low pH optimum are differentiated. An important feature of proteolytic enzymes of plant pathogenic fungi is their substrate specifity, degrading either fibrious proteins such as extensins or globular proteins like antifungal enzymes, e.g. chitinases (Hahn et al. 1997).

Amylases

Several types of enzymes participate in the degradation of starch. α–Amylases (EC 3.2.1.1) hydrolyse the α-1,4-linkages randomly in an endo manner to produce rapid changes in the degree of polymerisation. Isoamylases (EC 3.2.1.68) cleave the α-1,6-linkages producing dextrins (oligomers of α-1,4-linked D-glucosyl residues), which then are degraded by the α-glucosidases (EC 3.2.1.20) in an exo manner to glucose. Additionally, the glucoamylases (EC 3.2.1.3) can release glucose from the non-reducing ends of amylose and dextrins as well as from amylopectin (Strasburger et al. 2002). Up to date, no information exists as to the importance of amylases in plant pathogenic processes.

Thus, it seems likely that CWDE are utilized by phytopathogenic fungi not only to obtain an important nutrient source but also for penetration of the host cell wall and for spreading through the plant. Nevertheless, it has been very difficult to gain information about the actual importance of these CWDE for the pathogenicity of plant pathogens, as studies on this topic are generally complicated by the multitude of isoenzymes that most fungi are able to produce. Loss of any particular hydrolytic enzyme mostly has little or no effect on pathogenicity, as other enzymes are secreted that can complement for the deleted activity. Lately, research on regulatory genes has been more successful in finding evidence for the importance of CWDE during plant infection (Lev and Horwitz 2003; Tonukari et al. 2000). This is due to the fact that regulatory proteins affect a broad set of targets, and their disruption results in a more severe loss of functions.

1.4. The function and role of hydrophobins

Fungal MAP kinase deletion mutants (Di Pietro et al. 2001; Lev et al. 1999) partially reveal certain phenotypes that have similarity to hydrophobin deletion mutants (Wösten 2001; Talbot et al. 1996; Talbot et al. 1993). Furthermore, it was recently shown that a MAP kinase from *M. grisea* does in fact participate in the induction of a hydrophobin

(Soanes et al. 2002). Hence, a general regulation of hydrophobin secretion via MAP kinase pathways is imaginable.

Hydrophobins are small (~100 aa), moderately hydrophobic proteins that are secreted uniquely by filamentous fungi. These proteins are characterised by similar hydropathy patterns and are composed of two similar domains, each containing four conserved cysteine residues flanked by poorly conserved amino acid areas (Fig. 6). Disulfide bonds are generally formed between the cysteine residues 1 and 2, 3 and 4, 5 and 6 as well as 7 and 8. A typical signal sequence can be found at the amino-terminal end of the protein (Wösten 2001; de Vocht et al. 2000; Ebbole 1997). Most fungi have multiple hydrophobin encoding genes, each tailored for a specific function (Segers et al. 1999; Wessels 1996). The transcriptional regulation of hydrophobins is very complex and seems to be influenced by various factors including different developmental stages, nutritional status, light and circadian clocks. Generally, hydrophobins belong to the highest expressed genes in fungi, e.g. 27 % of the complete cDNAs from an exponentially growing culture of *Cryphonectria parasitica*, the chestnut blight fungus, account for hydrophobin cDNAs (Ebbole 1997).

Motif I:	X_{2-38}-**C**-X_{5-9}-**C**-**C**-X_{11-39}-**C**-X_{8-23}-**C**-X_{5-9}-**C**-**C**-X_{6-18}-**C**-X_{2-13}
Motif II	**C**-X_{5-9}-**C**-**C**-X_{5-18}-G-X_{5-20}-**C**-X_{8-23}-**C**-X_{5-9}-**C**-**C**-X_{2-12}-G-X_{3-10}-**C**-X_{2-13}

Fig. 6: Two possible amino acid motifs found for hydrophobins. C: conserved cysteine residues; X: any other amino acid with a high proportion of non polar amino acids (modified after Wessels 1996 and Ebbole 1997)

Hydrophobins can spontaneously assemble at a hydrophobic/hydrophilic interface, such as air/water or waxy surface/water, into a highly amphiphatic film. One side of the hydrophobin film is moderately to highly hydrophilic, while the other side exposes a surface as hydrophobic as teflon or paraffin. The formation of these hydrophobin aggregates is catalysed by the hydrophobic/hydrophilic interface and results from a conformational change in the protein structure. The intramolecular disulfide bridges were shown to only be essential for the stability of the hydrophobin monomer and not to be involved in the selfassembly process. The disulfide bridges were, thus, proposed to prevent premature selfassembly within the cell or its aqueous environment. (Wösten 2001; de Vocht et al. 2000; de Vocht et al. 1998).

Hydrophobins are grouped into two classes. Class I hydrophobins, e.g. SC3 from *Schizophyllum commune*, form aggregates stable towards detergents and ethanol and are

known to be responsible for the rodlet layers on spores. They are found in fungi belonging to the ascomycetes and basidiomycetes. Class II hydrophobins, e.g. cerato-ulmin from *Ophiostoma ulmi*, however, solubilise into monomers after treatment with 60 % ethanol. Hydrophobins of this class are predominantely found in ascomycetes and have a relatively well conserved amino acid sequence (Wösten 2001; Ebbole 1997; Wessels 1996).

Secretion of hydrophobins fulfills a broad spectrum of functions in fungal development. Fungi normally grow in wet habitats, having generally a hydrophilic surface. Nevertheless, some stages in the fungal life make it neccessary to escape the aqueous environment and grow into the air, e.g. to form aerial reproductive structures. Secreted hydrophobins, thus, lower the surface tension aiding the hyphal tip to break the water surface. As this happens the hydrophobins aggregate at the hydrophobic/hydrophilic interface between the air and the fungal cell wall, thereby covering the hyphae as they grow into the air. This hydrophobic layer effectively protects the hyphae from desiccation and other adverse environmental conditions (Wösten 2001; Ebbole 1997; Wessels et al. 1991). In many fungi, hydrophobins were also shown to be under mating type gene control, thus, indicating hydrophobins to be necessary for sexual reproduction (Ando et al. 2001; Peñas et al. 1998; Schuren and Wessels 1990). Conidia with a rodlet layer formed by selfassembly of secreted hydrophobin monomers become difficult to wet with water, which facilitates their dispersal by wind and mediates the attachment of the conidia and its germ tube to hydrophobic surfaces like plant cuticles. This tight attachment often results in a morphogenetic signal that is important for initial steps of fungal pathogenesis (Wösten 2001). In the case of *M. grisea* the tight binding of the germination tube to the plant surface due to the secretion of the hydrophobin Mpg1 enforces the formation and adhesion of the appressoria. Only by a tight attachment to the host can the appressoria utilise the high pressure of the appressoria to puncture the plant epidermis (Deising et al. 2000; Talbot et al. 1996; Talbot et al. 1993). Hydrophobins have also been discussed as defence of the pathogen against an attack of the host by masking β-glucans and chitin. Derivates of these two main components of the fungal cell wall have been shown to exhibit a high elicitor activity (Wösten 2001). Furthermore, the class II hydrophobin cerato-ulmin from *O. ulmi* is also discussed as toxin causing wilting, reduction in transpiration, increase in leaf respiration, and electrolyte loss after application of purified cerato-ulmin to elms (Wösten 2001).

However, deletion mutants lacking hydrophobins are mostly not reduced in pathogenicity. As for example water soaked conidia or hyphae still can lead to disease development

(Spanu 1998). *M. grisea* Δ*mpg1* were only shown to be reduced in virulence due to a reduced production of appressoria, but the mutants could still infect fully via wounds. Mutants from *O. ulmi* producing no cerato-ulmin had virulence characteristics indistinguishable from those of the wild type. Eventhough all the postulated functions for hydrophobins indicate a major role of this surface active protein in fungal pathogenicity, the conclusion must rather be that hydrophobins seem to be important for general strategies in the life cycle but are dispensable for full pathogenicity.

1.5. Aims of this study

In this work, the role of mitogen-activated protein kinases for the pathogenicity and for various developmental stages of the causal agent of the head blight disease, *Fusarium graminearum*, were investigated. By choosing a strategy of disrupting signal transduction pathways in *F. graminearum* more information was to be gained about the complex interaction between this pathogen and its hosts.

The first aim of this work was to identify MAP kinases from *F. graminearum*. Consequently, the genes that were found to encode MAP kinases were to be isolated in full length and to be characterised concerning intron spacing, resulting amino acid sequence, and transcriptional regulation. From the putative MAP kinase genes found, fungal transformation vectors were to be cloned. Followed by the transformation of *F. graminearum* with these vectors. Through homologous recombination and single crossover the vectors were, thereby, expected to integrate into the fungus leading to the disruption of the endogenous MAP kinase genes. Mutants resulting from these transformations were to be analysed for morphological changes compared to the wild type, including colony morphology, growth speed, biomass production, conidia production, and perithecia formation. The effect of the gene disruption on the virulence of *F. graminearum* was to be assayed in pathogenicity tests on wheat spikes and maize ears. The effect of the identified MAP kinases on potential infection mechanims, such as the production of the mycotoxic deoxynivalenol and the estrogenic zearalenone as well as the secretion of cell wall degrading enzymes was to be elucidated. Finally, a putative hydrophobin of *F. graminearum* was to be identified, cloned in full length, and characterised. A possible regulation of hydrophobin induction by a MAP kinase from *F. graminearum* was to be investigated.

2. Material and Methods

2.1. Material

2.1.1. Chemicals, enzymes and equipment

In this work chemicals, enzymes and equipment were obtained from the companies found in the following list:

Amersham (Braunschweig, Germany), Amresco (USA), Applichem (Darmstadt, Germany), Appligene (Heidelberg, Germany), Biometra (Göttingen, Germany), BioRad (München, Germany), Biozym (Hessisch Oldendorf, Germany), Boehringer/Roche (Mannheim, Germany), Calbiochem (Schwalbach, Germany), Ciba Geigy (Switzerland), Difco (USA), Duchefa (Netherlands), DYNAL (Hamburg, Germany), Eppendorf (Hamburg, Germany), Fluka (Switzerland), Heraeus, (Hanau, Germany), Hybaid (Heidelberg, Germany), Infors (Switzerland), Invitrogen (Netherlands), Kodak (Stuttgart, Germany), Macherey-Nagel (France), MBI Fermentas (St. Leon-Rot, Germany), Megazyme (Ireland), Merck (Darmstadt, Germany), Millipore (Eschenborn, Germany), MWG (Ebersberg, Germany), New England Biolabs (Schwalbach, Germany), Osram (München, Germany), peqLab Biotechnology (Erlangen, Germany), Perkin Elmer (Weiterstadt, Germany), Pharmacia (Sweden), Phase (Lübeck, Germany), Promega (Mannheim, Germany), Puregene (USA), Pütz-Folien (Taunusstein, Germany), Retsch (Haan, Germany), Riedel-de Häen (Seelze, Germany), Roth (Karlsruhe, Germany), Rose GmbH (Trier, Germany), Schleicher und Schüll (Dassel, Germany), Serva (Heidelberg, Germany), Sigma (Deisenhofen, Germany), Sony (USA), Stratagene (Heidelberg, Germany), Universitätsklinikum Eppendorf (Hamburg, Germany), Whatman (Great Britain).

All chemicals were used with the purity degree „pure“ or „per analysis“. If not otherwise mentioned, solutions were made with demineralized water and were sterilized by filtration or by autoclaving.

2.1.2. Organisms

2.1.2.1. *Escherichia coli*

For transformation of recombinant plasmids the *Escherichia coli* strains DH5α, DH10B, Top10 (Invitrogen) and XL1-Blue (Stratagene) were used.

2.1.2.2. *F. graminearum*

The *F. graminearum* wild type strain 8/1 was used throughout the complete work. The strain was kindly provided by Thomas Miedaner of the Landessaatzuchtanstalt Hohenheim, Germany.

As additional control strain for the quantitative enzyme assays the *F. graminearum* strain 31.10A was used. This strain is mutated in one polyketid synthetase (Δ*pks*) and shows, other than an albino colony morphology, no differences in virulence compared to the wild type strain. It was kindly supplied by Sascha Malz, Universität Hamburg.

2.1.2.3. Plants

Virulence assays were conducted with the summer wheat (*Triticum aestivum* L.) cultivars Nandu (Lochow-Petkus, Bergen-Wohlde, Germany) or Munk (Lochow-Petkus, Bergen-Wohlde, Germany). Both wheat cultivars are rated with an assessment of six concerning infections with *Fusarium*, meaning that the cultivars are very susceptible. Furthermore, the maize (*Zea mays*) inbred line A188 (A. Pryor, CSIRO, Canberra, Australia) was used for virulence assays.

2.1.3. Culture media

If not mentioned otherwise, all media were sterilized for 20 min at 121°C and 1.4 bar in the autoclave.

2.1.3.1. Media for *E. coli*

Bacteria were cultivated in Luria Bertani (LB) medium (Sambrook et al. 1989), either as liquid culture or on agar plates. 25 g of the LB Broth or 40 g of the LB Agar mixture (Difco) were dissolved in 1 l deionized water. For seletion of transformed bacterial cultures the antibiotics Ampicilin or Kanamycin (both 100 µg/ml) were added after sterilization. For blue/white selection of transformed bacteria 50 µg/ml X-Gal (solubilized in dimethylformamid) and 200 µM IPTG were supplemented after sterilization of the media.

2.1.3.2. Media for *F. graminearum*

Complete (CM) medium (Leach et al. 1982):

Solution A (100x):	100 g/l $Ca(NO_3)_2$ x 4 H_2O

Solution B (100x):	20 g/l KH_2PO_4; 25 g/l $MgSO_4$ x 7 H_2O; 10 g/l NaCl; (sterilized by filtration)
Solution C:	20 % Glucose (sterilized by filtration)
Suspension D (1000x):	60 mg/l H_3BO_3; 390 mg/l $CuSO_4$ x 5 H_2O; 13 mg/l KI; 60 mg/l $MnSO_4$ x H_2O; 51 mg/l $(NH_4)_6Mo_7O_{24}$ x 4 H_2O; 5.48 g/l $ZnSO_4$ x 7 H_2O; 932 mg/l $FeCl_3$ x 6 H_2O; 2 ml Chloroform (added for sterilization of the suspension)
Solution E:	1 g Yeast extract; 0.5 g casein, hydrolysed by enzymatic cleavage; 0.5 g Casein, hydrolysed by acid degradation; ad 50 ml H_2O
Suspension F (100x):	2.5 g/l Chloramphenicol; 2.5 g/l Kanamycin ; 1 g/l Tetracyclin (sterilized by filtration)

10 ml of solution A was added to 869 ml H_2O and was sterilized in the autoclave. For solid media 16 g/l granulated agar was supplemented prior to sterilization. Then 10 ml of solution B, 50 ml of solution C, 1 ml of suspension D, the complete solution E, and 10 ml of suspension F were added to the medium. Selection of fungal transformants was aided by supplementing the media with 10-50 µg/ml (liquid cultures) or 100-150 µg/ml (agar plates) Hygromycin B.

Media for the osmolarity assay:

For the osmolarity assay different amounts of NaCl were added to CM medium prior to sterilization to reach final concentration of 0.5 M, 0.75 M, 1 M, 1.5 M and 2 M NaCl.

SNA synthetic nutrient poor medium (Nirenberg 1981):

1 g	KH_2PO_4
1 g	KNO_3
0.5 g	$MgSO_4$ x 7 H_2O
0.5 g	KCl
0.2 g	Glucose
0.2 g	Saccharose
1 l	H_2O
16 g	Granulated agar (optional)

Czapek minimal medium (Raper and Thorn 1949):

10 ml salt solution	300 g/l $NaNO_3$; 50 g/l KCl; 50 g/l $MgSO_4$ x 7 H_2O; 1 g/l $FeSO_4$ x 7 H_2O
30 g	Saccharose

0.2-1 g	K_2HPO_4
1 l	H_2O
30 g	Nobel agar, washed with 5 l double deionized H_2O

Regeneration medium:

Solution A:

1 g	Yeast extract
1 g	Casein hydrolysed by enzymatic cleavage
50 ml	H_2O

Solution B:

342 g	Saccharose
500 ml	H_2O

Solution C:

16 g	Granulated agar
450 ml	H_2O

All three components were sterilized separately by autoclaving, and were mixed after cooling down to 50-60°C.

Hygromycin selection agar

16 g	Granulated agar
1 l	H_2O
300 µg/ml	Hygromycin B, added after medium was autoclaved

Carrot agar (Klittich and Leslie 1988)

400 g	Fresh carrots, cooked for 10 min in 400 ml H_2O and puréed
20 g	Granulated agar
500 ml	H_2O

The medium was sterilized for 30 min at 121°C in the autoclave.

Media for enzymatic plate assays:

Basic minimal medium:

1 g	KH_2PO_4
1 g	KNO_3
0,5 g	$MgSO_4$ x 7 H2O
0,5 g	KCl
18 g	Granulated agar
1 l	H_2O

If not mentioned otherwise, the following carbon source supplements were added prior to sterilization:

Amylolytic activity:	0.05 %	AZCL-Amylase (Megazyme)
Xylanolytic activity:	0.05 %	AZCL-Xylan (Megazyme)
Proteolytic activity:	0.05 %	AZCL-Casein (Megazyme)
Cellulolytic activity:	0.5 %	carboxymethylcellulose, sodium salt (Serva)
Lipolytic activity:	2 %	olive oil (Sigma, sterilized by filtration, added after sterilization of the medium)
	0,001 %	Rhodamine B (Sigma; sterilized by filtration, added after sterilization of the medium)

Media used for precultivation and induction of extracellular enzyme secretion

The fungal strains were precultivated in liquid glucose rich medium. 75 µg/ml Hygromycin B was added to all transformant cultures.

1 %	Glucose
0.05 %	Yeast extract
1 x	Yeast Nitrogen Base, with amino acids and vitamines (Difco); 10 x Yeast Nitrogen Base = 67 g/l Yeast Nitrogen Base mixture

Production of polymeric carbohydrate degrading enzymes and proteases were induced in a salt minimal medium modified from the Czapek minimal medium (Raper and Thorn 1949) and supplemented prior to sterilization in the autoclave with one sole carbon source.

Salt minimal medium:

10 ml salt solution	300 g/l $NaNO_3$; 50 g/l KCl; 50 g/l $MgSO_4$ x 7 H_2O; 1 g/l $FeSO_4$ x 7 H_2O
0.5 g	K_2HPO_4
1 l	H_2O

Carbon source supplements:

Amylolytic activity:	0.5 %	soluble starch (Merck)
Endoglucanase activity:	0.5 %	carboxymethylcellulose, sodium salt (Serva)
Cellulolytic activity:	0,5 %	crystalline cellulose (Avicel PH 105; Serva)
Pectinolytic activity:	0.25 %	pectin from citrus fruit (Sigma)
Xylanolytic activity:	0.25 %	xylan from oat spelts (Roth)
Proteolytic activity:	3 %	casein from bovine milk (Sigma)

For induction of extracellular lipolytic enzymes the fungal strains were precultivated in liquid YPG-medium. 75 µg/ml Hygromycin B was added to all transformant cultures. The cultures were then induced in 0.7 % NaCl containing 2 % wheat germ oil (Roth, sterilized by filtration).

YPG-medium (Sambrook et al. 1989):

1 %	Yeast extract
2 %	Pepton
2 %	Glucose

Media for growth assays on one carbon source:

The same basic minimal medium as found under „Media for enzymatic plate assays“ was used. If not mentioned otherwise, this medium was supplemented prior to sterilization with the following carbon sources:

Amylolytic activity:	1 %	soluble starch (Merck)
Endoglucanase activity:	1 %	carboxymethylcellulose, sodium salt (Serva)
Cellulolytic activity:	1 %	crystalline cellulose (Avicel PH 105; Serva)
Cellulolytic activity:	1	cellophane foil, Ø 45 mm (Pütz)
Pectinolytic activity:	1 %	pectin from citrus fruit (Sigma)
Pectinolytic activity:	1 %	polygalacturonic acid, sodium salt (Sigma)
Xylanolytic activity:	1 %	xylan from oat spelts (Roth)
Proteolytic activity:	1 %	casein from bovine milk (Sigma)
Lipolytic activity:	1 %	wheatgerm oil (Roth, sterilized by filtration)

The cellophane foil was whelled in demineralized water for at least 15 min and sterilized in the autoclave between filter paper and then laid on the agar surface.

2.1.4. Plasmids

2.1.4.1. Plasmids for subcloning in *E. coli* and for transformation of *F. graminearum*

- pGEM®-T (Promega), pCR®-XL-TOPO® (Invitrogen) and pCR®2.1-TOPO® (Invitrogen)
  These three plasmids were used for subcloning PCR-products in *E. coli*.
- pAN7-1M (Punt et al. 1987)
  The pAN7-1M plasmid (6782 bp) was used for constructing transformation vectors for the *F. graminearum* transformation. The plasmid contains the gene encoding the

Hygromycin phosphotransferase (*hph*) from *E. coli*, which is under the control of the *gpd1*-promotor from *Aspergillus nidulans*. Therefore, this gene allows the selection of transformed *F. graminearum* strains with Hygromycin B. The pAN7-1M plasmid differs from the original pAN7-1 plasmid by one deleted *Nco*I restriction site at the base pair position 2648. The deletion of this site led to the generation of a new *Bsr*DI restriction site.

2.1.4.2. Plasmids used or generated in the course of this work

• pGEM-T*::*gmap1

This plasmid was constructed prior to this work by Dr. F. J. Maier. With degenerate primers (DP2 and DP4, DP1 and DP3; Hanks and Quinn 1991) designed from conserved gene regions of various fungal MAP kinases a products of 556 bp was amplified and ligated into the pGEM-T plasmid resulting in the vector pGEM-T*::*gmap1.

• pGEM-T*::*gpmk1

This plasmid was also constructed prior to this work by Dr. F. J. Maier. With degenerate primers (DP2 and DP4, DP1 and DP3; Hanks and Quinn 1991) designed from conserved gene regions of various fungal MAP kinases a products of 490 bp was amplified and ligated into the pGEM-T plasmid resulting in the vector pGEM-T*::*gpmk1.

• pGEM-T*::*TAILgmap1F

A PCR-product (1679 bp) was amplified with a TAIL-PCR strategy (see 2.2.7.8.) from the *gmap1* gene using the primers NJ22/AD5 and was inserted into the pGEM-T plasmid. The inserted DNA fragment was situated downstream of the original 556 bp fragment found by PCR with degenerate primers.

• pGEM-T*::*TAILgmap1R

A PCR-product (1106 bp) was amplified with a TAIL-PCR strategy (see 2.2.7.8.) from the *gmap1* gene using the primers NJ19/AD3 and was then inserted into the pGEM-T plasmid. The inserted DNA fragment was situated upstream of the original 556 bp fragment found by PCR with degenerate primers.

• pGEM-T*::*gmap1NJ34/6

A 1278 bp fragment of the *gmap1* gene was amplified from genomic DNA with the primers NJ36 and NJ6 and ligated into the pGEM-T-plasmid.

• pCR2.1TOPO*::*gmap1NJ5/35

A 1956 bp fragment of the *gmap1* gene was amplified from genomic DNA with the primers NJ5 and NJ35 and ligated into the pCR 2.1 TOPO-plasmid.

• pCR2.1TOPO*::*gmap1NJ50/6

A 512 bp fragment of the *gmap1* gene was amplified from cDNA with the primers NJ50 and NJ6 and ligated into the pCR 2.1 TOPO-plasmid.

• pCR2.1TOPO*::*gmap1NJ5/51

A 1074 bp fragment of the *gmap1* gene was amplified from cDNA with the primers NJ5 and NJ51 and ligated into the pCR 2.1 TOPO-plasmid.

• pGEM-T*::*gmap1Pfl23

Using the primers Pfl23-Forw and Pfl23-Rev an inverse-PCR (see 2.2.7.8.) was carried out with the pGEM-T*::*gmap1 plasmid as template resulting in a newly generated *Pfl*23II restriction site in the *gmap1* insert.

• pKOgmap1

The insert from the pGEM-T::gmap1Pfl23 plasmid was excised with the restriction enzyme *Pvu*II and ligated into the *Ehe*I linearized pAN7-1M plasmid.

• pCR2.1TOPO*::*gmap1WT1-3

The 1624 bp wild type PCR *gmap1* fragment that still could be amplified with the primer pair NJ50/52 from genomic DNA of three *F. graminearum* mutants with homologously integrated pKOgmap1-vector was ligated into the pCR 2.1 TOPO-plasmid.

• pCR-XL-TOPO*::*TAILgpmk1F

A PCR-product (1349 bp) was amplified with a TAIL-PCR strategy (see 2.2.7.8.) from the *gpmk1* gene with the primers NJ25/AD7 and was then inserted into the pCR-XL-TOPO-vector. The inserted DNA fragment was situated downstream of the original 490 bp fragment found by PCR with degenerate primers.

• pGEM-T*::*TAILgpmk1R

A PCR-product (469 bp) was amplified with a TAIL-PCR strategy (see 2.2.7.8.) from the *gpmk1* gene with the primers NJ28/AD3 and was then inserted into the pGEM-T plasmid. The inserted DNA fragment was situated upstream of the original 490 bp fragment found by PCR with degenerate primers.

• pCR2.1TOPO*::*gpmk1NJ49/8_gDNA

A 712 bp fragment of the *gpmk1* gene was amplified from genomic DNA with the primers NJ49 and NJ8 and ligated into the pCR 2.1 TOPO-plasmid.

• pCR2.1TOPO*::*gpmk1NJ7/38

A 1530 bp fragment of the *gpmk1* gene was amplified from genomic DNA with the primers NJ7 and NJ38 and ligated into the pCR 2.1 TOPO-plasmid.

• pCR2.1TOPO*::*gpmk1NJ49/8_cDNA

A 598 bp fragment of the *gpmk1* gene was amplified from cDNA with the primers NJ49 and NJ8 and ligated into the pCR 2.1 TOPO-plasmid.

• pCR2.1TOPO*::*gpmk1NJ7/53

A 879 bp fragment of the *gpmk1* gene was amplified from cDNA with the primers NJ7 and NJ53 and ligated into the pCR 2.1 TOPO-plasmid.

• pGEM-T*::*gpmk1PauI

Using the primers PauIMfor and PauIMrev an Inverse-PCR (see 2.2.78.) was carried out with the pGEM-T*::*gpmk1 plasmid as template resulting in a newly generated *Pau*I restriction site in the *gpmk1* insert.

• pKOgpmk1

The insert from the pGEM-T*::*gpmk1PauI plasmid was excised with the restriction enzyme *Pvu*II and ligated into the *Ehe*I linearized pAN7-1M plasmid.

• pKOgpmk1-Del

A fusion-PCR-product, in which two PCR-products amplified with the primer pairs NJ11/pGEM-T349 and NJ12/ pGEM-T2870, respectively, were fused, was ligated into the *Ehe*I linearized pAN7-1M plasmid.

• pGEM-T*::*osmapNJ65/66A_gDNA

A 1800 bp fragment of the gene encoding the osmolarity MAP kinase was amplified from genomic DNA with the primers NJ65 and NJ66A and ligated into the pGEM-T-plasmid.

• pGEM-T*::*osmapNJ65/66A_cDNA

A 1232 bp fragment of the gene encoding the osmolarity MAP kinase was amplified from cDNA with the primers NJ65 and NJ66A and ligated into the pGEM-T-plasmid.

• pGEM-T*::*hydroNJ94B/95

A 1063 bp fragment of the putative hydrophobin gene was amplified from genomic DNA with the primers NJ94B and NJ95 and ligated into the pGEM-T-plasmid.

• pGEM-T*::*hydroNJ59/95

A 589 bp fragment of the putative hydrophobin gene was amplified from cDNA with the primers NJ59 and NJ95 and ligated into the pGEM-T-plasmid.

2.1.5. Primers

The following primers were used in the course of this work for PCR-reactions or sequencing reactions. All primers are listed in 5´-3´-direction. The degenerate primers (DP) were modified after Hanks and Quinn (Hanks and Quinn 1991). All arbitrary primers (AD) used for the TAIL-PCR were modified after Lui and Whittier (Lui and Whittier 1995). The positioning of the gene specific primers can be found in the sequence data found in the appendix.

Vector primers:

M13F	GTA AAA CGA CGG CCA GT
M13R	CAG GAA ACA GCT ATG AC
pGEM-2870	GGG CCT CTT CGC TAT TAC GC
pGEM-349	CGT TGG CCG ATT CAT TAA TG
panehe5´SM	ACT CGA CCT GCA GGC ATG CAA GC
panehe3´SM	TGT CGG GGC TGG CTT AAC TAT G

Degenerated and arbitrary primers:

DP1	CCA ICK IGT NGC IAC RTA YTC
DP2	GCI TAY GGI RTN GTN TG
DP3	GTI GCN ATR AAR AAR AT
DP4	AYY TCI GGI GCI CKR TAV YA
AD1	NGT CGA (G/C)(A/T)G ANA (A/T)GA ANG TCG ASW GAN AWG AA
AD2	GTN CGA (G/C)(A/T)C ANA (A/T)GT TGT NCG ASW CAN AWG TT
AD3	(A/T)GT GNA G(A/T)A NCA NAG AWG TGN AGW ANC ANA GA
AD4	NTC GA(G/C) T(A/T)T (G/C)G(A/T) GTT NTC GAS TWT SGW GTT
AD5	NGT A(G/C)A (G/C)(A/T)G TNA (A/T)CA ANG TAS ASW GTN AWC AA
AD6	TG(A/T) GNA G(A/T)A NCA (G/C)AG ATG WGN AGW ANC ASA GA
AD7	AG(A/T) GNA G(A/T)A NCA (A/T)AG GAG WGN AGW ANC AWA GG
AD9	TCS TIC GNA CIT WGG A

Primers for the Gmap1 MAP kinase gene:

Pfl23-Forw	CGT ACG GAC CTA TTT GTA C

Pfl23-Rev	AAG TTA TCG GGT CG
NJ5 (F)	GCG AGA TCA AGC TGC TCC AGC
NJ6 (R)	GCA GAA CGT TTG CGG AGT GGA
NJ17 (R)	ATT CTC TTC GGG GTC GAC TGA
NJ18 (R)	GTT GAC AAG CAG GTT ACC GGG
NJ19 (R)	CAT CGT CAC TGA CCC TCG TAC A
NJ20 (F)	CCC ATC AGA TCA CAT GTT TGT ACG
NJ21 (F)	TTC AAC GAG ACC TAT TTG TAC GAG
NJ22 (F)	AAG TAC ATC CAC TCC GCA AAC G
NJ29 (F)	ATA TCG CAA GAG AGA CGC GC
NJ30 (R)	TGG GAT GAA GCT ATC AGC ATA CG
NJ31 (R)	CGA TAG TCA TAT TCA TCA TCG TCG C
NJ32 (F)	CCA AAG CTA GTA CGT GTG ATC GAA A
NJ34 (F)	AGT AGC ATA GGT CGT TGT CGC G
NJ35 (R)	AGA ACC AGC AGG AGT CTA GCA AC
NJ44 (F)	ACT GTC ACC AAG GAG CTC GGC C
NJ45 (R)	GAA AGG TCG TCC GCC CAA AAG C
NJ50 (F)	TTC CCC TCG CAA ACC TTG TCG C
NJ51 (R)	TCA ACC CTT GTA CTT TGC GTA GC

Primers for the Gpmk1 MAP kinase gene:

PauIMfor	CAG CGC GCT AAC AAA CAC TGC
PauIMrev	ATC TTA CTA CAG CAA AAC AG
NJ7 (F)	GCG ATA CTT CAA CCA CGA GAA C
NJ8 (R)	GCA GCG GAT CGC GCA AGA CCG
NJ11 (F)	GTG CAT CCG CGC GCA GGA TTT TCC GAC GAC CAC TGC CAG
NJ12 (R)	GAA AAT CCT GCG CGC GGA TGC ACG GTG CAT ATC CGT CTC
NJ23 (F)	GCC ATC AAG AAG ATC ACT CCT TTC GA
NJ24 (F)	CAG AAG CCC CGA AGT TAC GAG
NJ25 (F)	CAC ACA GGA TCT TTC CGA CGA
NJ26 (R)	GAG TGC ATC GCC TTG AGG GC
NJ27 (R)	CTC CTG CAG TGT TTG TTA GCT CG
NJ28 (R)	GCA AAA CAG TGG CGT TTC GTA

NJ38 (R) GCA TAG GGG CCT TGG TTA GGT C

NJ46 (F) GAT ATC CAG GAT GTG GTC GGC G

NJ47 (R) AAT CCT CCA TGG TGG GTG TGC C

NJ49 (F) TTT TCG GTC GCA CGC TCT CCG

NJ53 (R) CAG GTC GTC TTT TTA CAG AGG C

Primers for the β-tubulin gene:

FgBetaTubF TGC TGT TCT GGT CGA TCT TG

FgBetaTubR GAC GGA AGT TTG GAC GTT G

(Compare the accesion number AACM01000261 for the sequences)

Primers for the osmolarity MAP kinase:

NJ65 (F) ACT TCT CGC TCA ACA ACC AC

NJ66A (R) GTG GTG GGA TAG ATC ATG GG

NJ66B (R) ACA CCG GCT TCA ACA TTA TG

NJ70 (F) CCC CAG ATG ACT GGC TAT G

Primers for the hydrophobin gene:

NJ59 (F) ATG CGA TTC ACT GCC TTT CTG

NJ62 (R) CAC CCG GGA CAA GCT TCA GCG TTA GG

NJ94B (F) CTG AAT TCC CTC CTG GTT G

NJ95 (R) CAT GCA GCC AAC CAG TTC AG

2.1.6. DNA-standards

For the qualitative and quantitative analysis of DNA-fragments the DNA-standards „GeneRuler DNA Ladder Mix #SM0331“, „Lambda-*Hin*dIII“ and „pUC *Msp*I“ (MBI-Fermentas) were used.

2.1.7. cDNA library

A cDNA library from *F. graminearum* was kindly supplied by the BASF AG (Ludwigshafen, Germany).

2.2. Methods

2.2.1. Cultivation and storage of organisms

2.2.1.1. Cultivation and storage of *E. coli*

E. coli strains were cultivated for 12-18 h at 37°C in either liquid LB medium (180 rpm) or on LB agar plates. For long term storage an aliquot of a liquid bacterial culture was supplemented with 43 % glycerol (1:1 v/v) and stored at -70°C.

2.2.1.2. Cultivation and storage of *F. graminearum*

If not mentioned otherwise, the cultivation of *F. graminearum* strains occurred at 28°C in the dark either on solid complete medium (CM) or in liquid CM-medium at 135-175 rpm. Fungal strains were stored at –70°C as water-conidia suspensions or as mycelial plugs, both without glycerol.

2.2.1.3. Cultivation of plants

Wheat was grown in 11 cm pots at 20°C with a 16 h photoperiod (8000 Lux) and 70 % relative humidity. Maize plants were grown in 25 cm pots in a green house until the silks started to emerge. Further cultivation of the maize occurred in a growth chamber at 25°C, 16 h, 15000 lux, and 19°C, 8 h, dark.

2.2.2. Transformation of *F. graminearum*

2.2.2.1. Formation of protoplasts

A flask containing 50 ml liquid CM-medium was inoculated with 10^5 conidia and cultivated for three days at 28°C, 140 rpm in the dark. The resulting mycelium was homogenized in a blendor. 8 ml of the homogenized mycelium was used as inoculum for a new 200 ml CM-culture, which was incubated for approximatly 24 h at 24°C and 140 rpm in the dark. The fresh mycelia was separated by filtration and washed twice with sterile demineralized water. 2 g mycelium were resuspended in 20 ml Driselase/Glucanase-solution (5 % Driselase, 3 % Glucanase in 700 mM NaCl, pH 5.6) and digested for 2.5-3 h at 28°C and 75 rpm. Protoplast formation was monitored with the microscope. Protoplasts were separated from the mycelial rests by filtration, first using gauze and then a nylon

membrane with 50 µm pore diameter. According to the method of Royer and coworkers (Royer et al. 1995) the protoplast were pelleted in a swingout rotor at 1300 *g* and 4°C and washed in ice cold 700 mM NaCl, pH 5.45. This procedure was repeated twice, whereas only 830 *g* were used to pellet the protoplasts. Finally, the washed protoplasts were resuspended in ice cold STC (800 mM sorbitol; 50 mM Tris-HCl, pH 8; 50 mM $CaCl_2$). The protoplasts were stored on ice for a maximum of one week. Longer storage led to a drastic loss of transformation efficiency.

2.2.2.2. Transformation

The *F. graminearum* protoplasts (see 2.2.2.1.) were supplemented with STC and SPTC (STC containing 40 % polyethylenglycol 4000) in a volume ratio protoplasts:STC:SPTC = 1:4:1 to accomplish a final protoplast concentration of 0.5-2 x 10^8/ml. To 100 µl of this suspension 5 µl Heparin (5 mg/ml resuspended in STC) and 30 µg linearized transformation vector were added. The suspension was mixed by carefully rotating the reaction tube, and was then incubated for 30 min on ice. Thereby, the probes were mixed every 10 min by rotating the tube. Finally, 1 ml SPTC was added to the probes, which were then incubated for further 20 min at room temperature. The tubes were rotated every 10 min. During this process the linearized transformation vector is translocated into the protoplasts and integrated into the genome via a single crossover in the homologous region of the gene of interest (Fig. 7).

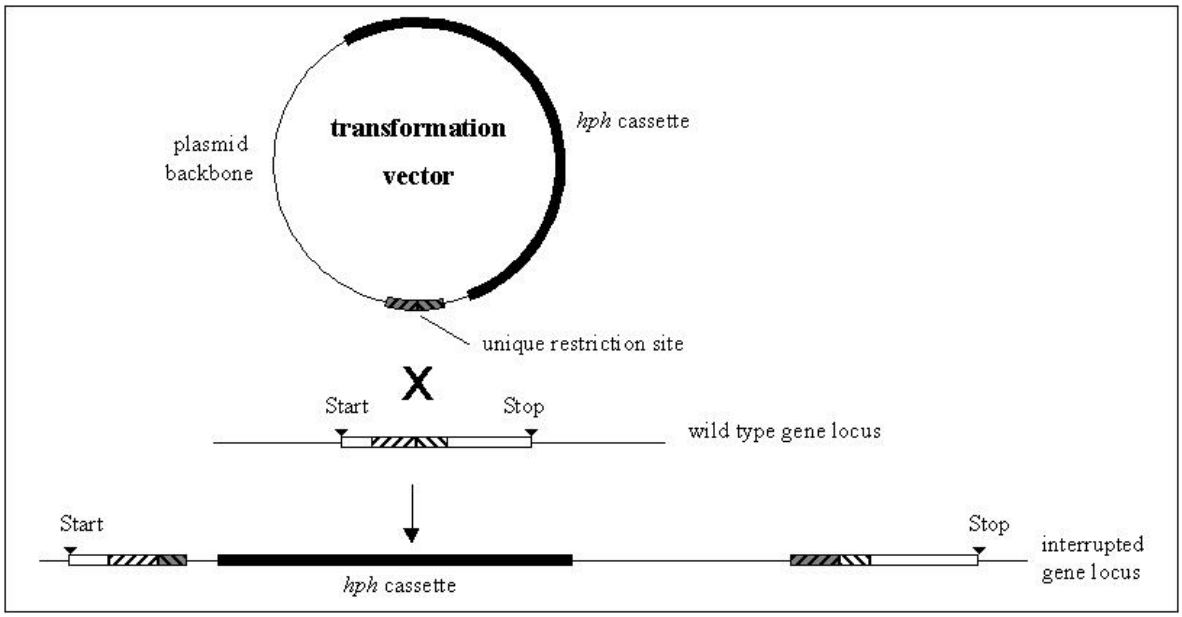

Fig. 7: Gene disruption via homologous integration of a transformation vector into a gene of interest. The transformation vector contained an approximately 500 bp internal fragment of the gene of interest (gray lined bar) next to the Hygromycin B resistance gene *hph* (black bar). The vector was linearized at a unique restriction site, which was introduced into the centre of the internal gene fragment via inverse-PCR or fusion-PCR. The wild type gene locus was interrupted

by homologous recombination of the vector through a single crossover. White lined bars show the homologous regions in the wild type locus. Start and stop codons are indicated by inverted black triangles.

The transformed protoplasts were carefully mixed into 200 ml regeneration medium that had been cooled to 43°C. Petri dishes (Ø 94 mm) were filled with 20 ml of the medium/protoplast-mixture and incubated at 28°C for approximately 12-24 h until the protoplast had visibly started to germinate into hyphae. Then, the petri dishes were covered with 10 ml of Hygromycin selection agar and cultivated for further 5-6 days at 28°C until single colonies had grown through the selection agar. These colonies were placed on CM-medium containing 100 µg/ml Hygromycin B for further selection of transformed strains.

2.2.3. Induction of fungal reproduction

2.2.3.1. Conidiation

To stimulate the production of asexual spores, called conidia, a mycelial plug was placed on agar plates containing SNA minimal medium and incubated for approximatly two weeks at 18°C under near-UV light and white light with a 12 h photoperiod. Condia were also produced on SNA plates covered with cellophane foil. The conidia were then washed from the agar plates with sterile water using a sterile glass rod. The amount of conidia in the suspension was then determined with a Neubauer counting chamber.

Conidia from transformed fungal strains were singled in order to gain homocaryotic mycelia. This step is generally necessary as hyphal cells of *F. graminearum* normally contain several nuclei which can have a different genetical background. Conidia on the other hand are known to derive from one single nucleus (Deacon 1997). Therefore, mycelium which has developed from one conidia should be homocaryotic.

Few conidia were plated on solid CM-medium and incubated for approximately 12-18 h at room temperature. Single, germinated conidia were cut out with a knife and placed on selective medium, CM-agar plates with Hygromycin, to ensure that all false positive transformants are eliminated.

2.2.3.2. Perithecia production

Sexual reproduction of the fungal isolates was induced on carrot agar plates (Klittich and Leslie 1988). Small mycelial plugs from cultures of each parent strain were placed on opposite sides of the agar plate. The plates were incubated at 24°C under a mixture of near-

UV and white light with a 12 h photoperiod. After seven days, the aerial mycelia were knocked down with 1 ml of sterile 2.5 % (v/v) Tween 60 solution using a sterile glass rod, while plates were rotated several times to spread the solution (Bowden and Leslie 1999). After further 7 days of incubation under the conditions mentioned above, perithecia were found covering the plate. In order to examine whether the developed perithecia contained asci with spores, the perithecia were cut out with a knife and placed on a object slide. They were then crushed between object slide and cover slip. Water was added to the probe and then analysed for asci and ascospores under the microscope.

2.2.4. Growth assays

The growth rate of the fungal cultures was determined by placing a mycelial plug (Ø 6 mm) on agar plates containing media with different carbon sources. The culture diameter was measured every day.
To determine the amount of biomass produced, the fungal strains were cultivated in liquid Czapek- and CM-medium for three days on a rotary shaker at 175 rpm and 28°C. The mycelium was then separated from the medium through filtration, lyophilized and weighed.

2.2.5. Pathogenicity tests

The virulence of the fungal strains was elucidated in plant pathogenicity tests. Thereby, the plants were infected with different fungal strains. The symptom development was then observed visually and used as degree of fungal virulence.

2.2.5.1. Pathogenicity test using wheat as host plant

Wheat spikes at anthesis were point-inoculated with the fungal strains by placing a droplet (10 µl) of conidia suspension (5 x 10^4 conidia/ml) or 10 µl of water within the palea and lemma of two basal florets of a spikelet in the middle of the wheat spike tested (modified after Pritsch et al. 2001). Each spike was inoculated twice, as the middle spikelets on both sides of the spike were point-inoculated. To obtain a moist surrounding for infection, the plants were sprayed with water before inoculation with the fungus. The inoculated spikes

were enclosed in small plastic bags during the first three days to ensure a high humidity for infection (Teich and Michelutti 1992) and to prevent a cross contamination of different *F. graminearum* isolates. The inoculated plants were incubated in a growth chamber at 21°C with a 16 h photoperiod (8000 Lux). The plant assays were evaluated three weeks after inoculation with the fungus.

2.2.5.2. Pathogenicity test using maize as host plant

The maize plants were grown until the silks started to emerge. Individual plants were inoculated 2-4 days after silk emergence by injecting 2 ml of macroconidial suspension into the silk channel of primary ears. Thereby, three different spore concentrations were assayed: 10^5, 10^6, 2 x 10^6 (modified after Reid and Hamilton 1995). The inoculated ears were enclosed in small plastic bags during the first four days to ensure a high humidity for infection. Further cultivation occurred in a growth chamber at 25°C, 60 % humidity, 16 h, 15000 Lux and 19°C, 8 h, dark. The plant assays were evaluated 21 days after inoculation with the fungus.

2.2.6.Toxin assays

In order to examine the capability of the fungal strains to produce mycotoxins various plant tissue substrates were used to induce the toxin production. Grinding of the infected probes, mycotoxin extraction (Krska et al. 2001, Rhône Diagnostics LTD 1999) and toxin detection was kindly accomplished at the Institute for Agrobiotechnology (IFA) in Tulln, Austria. Thereby, the probes were analysed for deoxynivalenol (DON) content by GC-ECD and for zearalenone (ZON) content by HPLC-FLD. The amount of toxin found in the probes was related to the ergosterol content. The measurement of ergosterol was also carried out by the IFA in accordance to Lamper and coworkers (Lamper et al. 2000).

2.2.6.1. Toxin induction on wheat kernels

Wheat kernels (30 g) were filled in 100 ml Magenta boxes (Sigma). The boxes were covered with caps and several layers of aluminium foil. After sterilizing the kernels twice in the autoclave for 20 min at 121°C the kernels were whelled with 15 ml sterile water for 24 h.

Agar plates (60 mm Ø) containing CM-medium were inoculated with a fungal conidia suspension. If mutants strains were cultivated, the medium was supplemented with Hygromycin B. The plates were incubated at 28°C until the fungus had covered the complete plate with fresh mycelium. The complete culture, including the agar, was cut into small plugs and mixed into the whelled wheat kernels. These cultures were incubated for 28 days at 28°C in the dark (Dr. T Miedaner, personal information). Then, the cultures were dried for 3-4 days at 45°C and stored in paper bags.

2.2.6.2. Toxin induction on maize kernels

Maize kernels (50 g) were placed in a 500 ml Erlenmeyer flask and supplemented with 25 ml water. The kernels were sterilized in the autoclave for 20 min at 121°C.

The *F. graminearum* strains were precultivated on SNA agar plates (supplemented with Hygromycin B for the mutant strains) until the plate was covered with fresh mycelium. Three mycelial plugs (1 cm^2) were used to inoculate the maize kernels. These cultures were incubated for seven days at 28°C in the dark and for further 14 days at room temperature without direct sun light (Dr. M Lemmens, personal information). Again, the cultures were dried for 3-4 days at 45°C and stored in paper bags.

2.2.6.3. Toxin induction on rice

Baby food jars filled with 25 g rice were supplemented with 8 ml sugar solution (38 g/l saccharose and 2.5 g/l hydrolysed casein), closed with Magenta B caps (Sigma) and whelled for 24 h. This plant tissue substrate was then sterilized in the autoclave for 20 min at 121°C.

Liquid SNA minimal medium (50 ml) was inoculated with mycelial plugs and cultivated for 20 h at 24°C in the dark. The medium inoculated with mutant strains was supplemented with 10 µg/ml Hygromycin B. The resulting fungal suspension (2 ml) was used to inoculate the rice substrate. The cultures were incubated at 28°C in the dark. To ensure a high humidity all jars were kept in plastic bags (Dr. M Lemmens, personal information). After six weeks cultivation the mycelia was dried for 3-4 days at 45°C and stored in paper bags.

2.2.7. Molecular biological methods

2.2.7.1. Standard techniques

Standard molecular biological techniques such as DNA digestion with restriction enzymes, ligation, dephosphorylation of vector backbones and generation of digoxigenin labeled DNA-probes were conducted according to Sambrook and colleagues (Sambrook et al. 1989) or in accordance to the manufacturer´s instructions.

2.2.7.2. DNA purification from agarose gels

DNA was purified from agarose gels using the „Prep-A-Gene Kit“ (BioRad) according to the manufacturer´s instructions.

2.2.7.3. Isolation of DNA from *F. graminearum*

DNA was generally isolated from cultures grown in liquid CM-medium which, in the case of the mutants, was supplemented with Hygromycin. The mycelium of three days old cultures was separated from the culture medium by vacuum filtration. The mycelium was either frozen in liquid nitrogen and ground with mortar and pestle or it was lyophilized and ground in a pebble mill (Retsch). For small amounts, the DNA was extracted from the ground fungal tissue using the „Puregene DNA Isolation Cell and Tissue Kit“ (Biozym) according to the „Plant Tissue Protocols 10-30 mg“. If a greater amount of DNA was needed, DNA extraction was carried out in accordance to Garber and Yoder (Garber and Yoder 1983). The DNA-yield was determined either by comparision of electrophoretically separated DNA with standard markers or photometrically using the formula:

DNA-concentration ng/µl = OD_{260} x 50

2.2.7.4. Transfer of genomic DNA and Southern blot analysis

Enzyme restricted, genomic DNA that had been separated in an agarose gel was transferred to a nylon membrane (Hybond NX, Amersham) either via vacuum blotting with the „VacuGeneXL“ (Pharmacia) according to the manufacturer´s instructions or via capillary transfer (Southern 1975). Prior to blotting the agarose gel had been treated 2 x 5 min with 0.25 M HCl, 2 x 15 min with denaturation solution (1.5 M NaCl, 0.5 M NaOH) and 2 x 15 min with neutralization solution (3 M NaCl, 0.5 M Tris-HCl pH 7.5). The transferred DNA was linked to the nylon membrane using a UV-crosslinker at 1200 µJ/cm^2.

The nylon membrane containing the transferred DNA was first incubated for 2-3 h in prehybridisation buffer (5 x SSC, 0.02 % SDS, 0.1 % Na-Laurylsarcosine, 1 % blocking reagent) at a high stringency hybridization temperature of 68°C. A denaturated digoxygenin (DIG) labeled DNA probe, made via standard-PCR using DIG-11-dUTP (Roche), was added and hybridized for 15-16 h at 68°C. Then, the residual probe was removed under first high and then low stringency conditions: 2 x wash solution I (2 x SSC, 0.1 % SDS) for 5 min at room temperature, 1 x wash solution II (0.2 x SSC, 0.1 % SDS) for 15 min at 68°C, 1 x wash solution III (0.1 x SSC, 0.1 % SDS) for 15 min at 68°C. The nylon membrane was then incubated for 30 min at room temperature in blocking buffer containing 0.1 M maleic acid, 3 M NaCl, and 1 % blocking reagent. The antibody anti-DIG-alkaline phosphatase was added and allowed to bind for 30 min. The residual antibody was removed by washing the membrane 3 x in maleic acid buffer (0.1 M maleic acid, 3 M NaCl, 0.3 % Tween 20) for 15 min. Alkaline reaction conditions needed for the detection were accomplished by incubating the membrane in detection buffer (0.1 M Tris-HCl pH 9.5, 0.1 M NaCl). The detection took place by incubating the filter in a mixture of CSPD and detection buffer (v/v = 1:10) at 37°C and subsequently exposing a film (Hyper-film^{TM}ECL^{TM}) with the filter.

20 x SSC: 3 M NaCl, 0.3 M $Na_3C_6H_5O_7$, pH 7.5
10 % blocking reagent: 100 g/l blocking reagent in 0.1 M maleic acid, 0.15 M NaCl, pH7.5

2.2.7.5. Isolation of total RNA from *F. graminearum*

Total RNA was isolated with the „peqGOLD RNAPure Isolation Kit“ (peqLab Biotechnology) in accordance with the manufacturer`s protocols. Total RNA was isolated from fungal mycelium grown in liquid CM- and SNA-medium, from fungal mycelium grown on solid CM- and SNA-medium covered with cellophane foil, from ungerminated and germinated conidia, from an early stadium of perithecial development and ripe perithecia as well as from uninfected and infected (4 h, 12 h, 24 h, 48 h, and 7 d after inoculation) wheat spikelets. The organic tissues were homogenized prior to RNA extraction by grinding the tissue, frozen in liquid nitrogen, with mortar and pestle. The RNA-yield was determined photometrically using the formula:
RNA-concentration ng/µl = OD_{260} x 40

2.2.7.6. First strand cDNA synthesis and isolation of total mRNA

After isolation of total RNA a DNA digestion step and the first strand cDNA synthesis were accomplished with the DNase I kit (Invitrogen) and the Super Script II kit (Invitrogen). All kits were used according to the manufacturers instructions. First strand cDNA was used for transcription analysis via semiquantitative reverse transcriptase (RT-) PCR.

For a massively parallel signature sequencing (MPSS, Brenner et al. 2000) conducted by the BASF AG (Ludwigshafen) total mRNA was isolated from fungal mycelium grown in liquid CM-medium, from ungerminated and germinated conidia and from an early stadium of perithecial development as well as from ripe perithecia. mRNA was isolated from total RNA with the „Dynabeads mRNA Purification Kit“ (DYNAL) according to the manufacturer´s instructions.

2.2.7.7. Polymerase chain reaction techniques

Polymerase chain reaction

Polymerase chain reactions (PCR) (Mullis 1990) were carried out in thermocyclers from the companies Hybaid (Sprint, Express), Perkin Elmer (Cetus) and MWG-Biotech (Primus and Primus 96plus). Standard amplifications of DNA fragments were done in a reaction volume of 25 µl using the DNA polymerase from *Thermus aquaticus* (*Taq*) from the company Invitrogen. Thereby, the annealing temperature depended on the primers used and the elongation time on the length of the amplified fragment. A standard PCR programme had the following steps: 1 x [94°C, 3 min]; 30 x [94°C, 30 s; 55-60°C, 45 s; 72°C, 1 min]; 1 x [72°C, 5 min]. In order to amplify specific DNA fragments directly from an *E. coli* colony, the first denaturation step was raised to 5 min. Furthermore, various DNA polymerases with proofreading function were used: „DeepVent“ (New England Biolabs) and „Expand“ (Boehringer/Roche). PCRs with these enzymes were carried out according to the manufacturer´s instructions.

Transcription assays via reverse transcriptase (RT-) PCR were carried out as standard PCR with the only difference that first strand cDNA (see 2.2.7.6.) was used as template.

Inverse-PCR

The Inverse-PCR (Ochman et al. 1988) was used to introduce a specific restriction site into DNA-fragments situated in a plasmid. A primer pair (Pfl23-Forw/Pfl23-rev and PauIMfor/

PauIMrev, respectively) was constructed such that the adjacent primers faced the opposite direction (Fig. 8). One primer exhibits the necessary base pair exchanges to generate the restriction site. A PCR was carried out using these primers, the plasmid containing the DNA-fragment of interest as template and the proofreading polymerase „DeepVent“ to gain blunt end PCR-products. During this PCR the complete plasmid was amplified as linear construct. The following cycler programme was used: 1 x [94°C, 4 min]; 30 x [94°C, 1 min; 60°C, 1 min; 75°C, 1.5 min]; 1 x [75°C, 10 min]. The amplified PCR-products were then purified from an agarose gel, ligated via blunt end ligation with the T4-ligase (MBI), and cloned in *E. coli*. Thus, the resulting plasmid contained the insert with modified sequence.

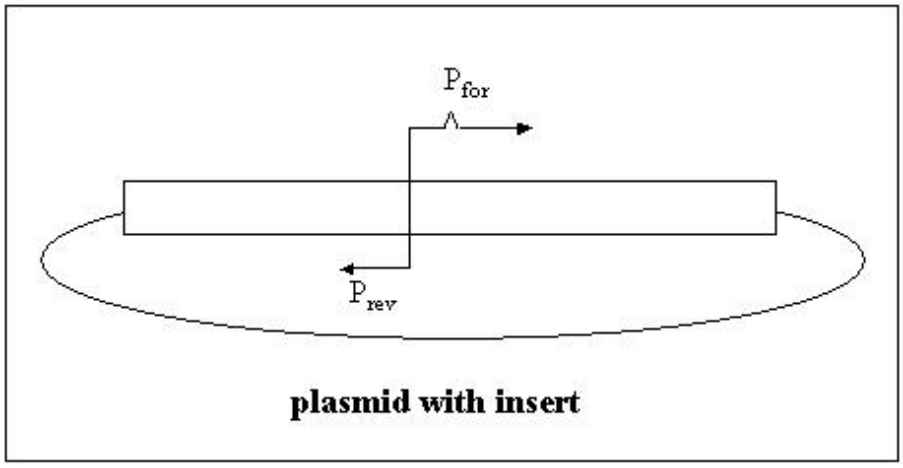

Fig. 8: Schematic illustration of the Inverse-PCR. The box represents the DNA-fragment of interest, which is inserted into a plasmid. Using adjacent forward (P_{for}) and reverse (P_{rev}) primers, symbolized by arrows, the complete plasmid is amplified as linear PCR-product. As P_{for} contains base pair exchanges, symbolised by Λ, the inserted DNA-fragment can be mutated.

Fusion-PCR

The Fusion-PCR (Amberg et al. 1995) was used to insert a new restriction site and two base pair deletions into a specific gene fragment, which had been ligated into a plasmid. Two insert specific primers (NJ11/NJ12) were made with opposite orientation. These 39 bp long primers share overlapping gene regions of approximately 20 bp in length, which contain all necessary base pair exchanges and base pair deletions. In a first PCR using the plasmid mentioned above as template and each one of the insert specific primers with one of the vector primers (pGEM-T2870/pGEM-T349), two PCR-products were amplified. To gain blunt end products the proofreading DNA-polymerase „DeepVent“ was used with the following cycler programme: 1 x [94°C, 3 min]; 35 x [94°C, 1 min; 60°C,

1 min; 75°C, 1 min]; 1 x [75°C, 10 min]. In a second PCR, the two products of the first PCR were used as template. In the primary denaturation step the fragments fuse at the overlapping regions. Using the vector primers M13F and M13R the fusion-product was then amplified by the proofreading DNA-polymerase „DeepVent“ (Fig. 9).

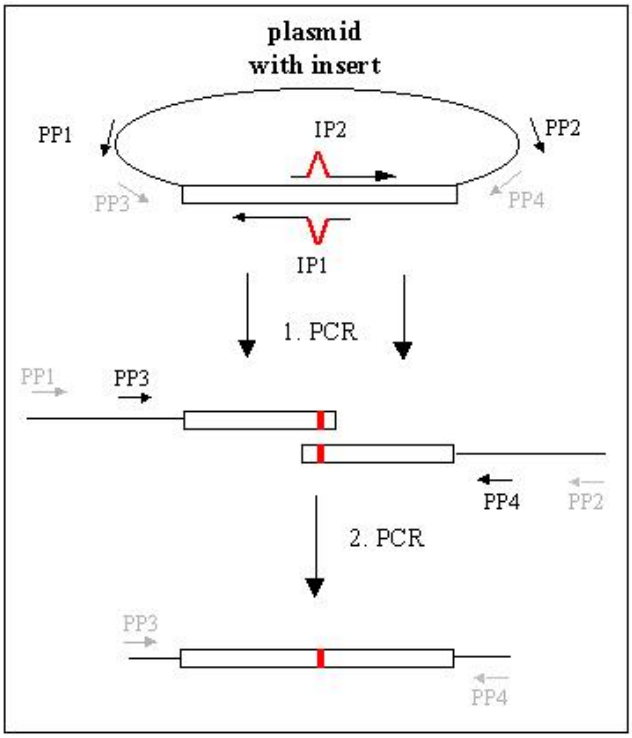

Fig. 9: Schematic illustration of the Fusion-PCR. The white box figures the DNA-fragment of interest, which is inserted in a plasmid symbolized by lines. Arrows mark the position of the primers (PP: plasmid primers; IP: insert primers). A first PCR using the primer pairs PP1/IP1 (pGEM-T2870/NJ12), IP2/PP2 (NJ11/pGEM-T349) and the plasmid as template amplified two products that were fused in a second PCR with the primers PP3/PP4 (M13F/M13R). Red areas indicate the mutated sequence introduced by the primers IP1 and IP2.

The cycler programme 1 x [94°C, 4 min]; 35 x [94°C, 1 min; 60°C, 1 min; 75°C, 2 min]; 1 x [75°C, 10 min] was used. The fusion-product was then purified from an agarose gel, ligated via blunt end ligation with the T4-ligase (MBI) into the *Ehe*I linearized plasmid pAN7-1M, and cloned in *E. coli*.

TAIL PCR

In order to gain upstream and downstream sequence information from a known gene fragment, a thermal asymmetric interlaced (TAIL-) PCR strategy (Lui and Whittier 1995) was carried out (Fig. 10). Three nested gene specific primers were constructed in upstream

and downstream direction, respectively, from the known sequence of the gene of interest. Three nested PCRs were carried out using each one gene specific primer and one of eight different unspecific arbitrary primers (AD primer; modified after Lui and Whittier 1995). In the first PCR-round genomic *F. graminearum* DNA was used as template. The resulting PCR-products were used as template for the second and third PCR, repectively, which increases the product specifity in each PCR-round. All PCRs were carried out with the *Taq* DNA polymerase using the following PCR-conditions:

Reaction mixture: 1 x PCR-buffer; 1.5 mM $MgCl_2$; 0.2 mM dNTPs; 0.4 µM specific primer; 4 µM AD primer; 0.8 U *Taq* DNA polymerase; 20 ng genomic DNA or 1 µl 1/50 dilution of a PCR reaction.

Programme 1.PCR:

Cycles	**Thermal settings**
1 x	94°C, 2 min
5 x	94°C, 1 min; 62°C, 1 min; 72°C, 2.5 min
1 x	94°C, 1 min; 25°C, 3 min
	ramping to 72°C over 3 min; 72°C, 2.5 min
15 x	94°C, 0.5 min; 68°C, 1 min; 72°C, 2.5 min
	94°C, 0.5 min; 68°C, 1 min; 72°C, 2.5 min
	94°C, 0.5 min; 44°C, 1 min; 72°C, 2.5 min
1 x	72°C, 5 min

Programme 2.PCR:

1 x	94°C, 2 min
15 x	94°C, 0.5 min; 68°C, 1 min; 72°C, 2.5 min
	94°C, 0.5 min; 68°C, 1 min; 72°C, 2.5 min
	94°C, 0.5 min; 44°C, 1 min; 72°C, 2.5 min
1 x	72°C, 5 min

Programme 3.PCR:

1 x	94°C, 2 min
15 x	94°C, 1 min; 44°C, 1 min; 72°C, 2.5 min
1 x	72°C, 5 min

The products from the second and third PCR were separated via gel electrophoresis. DNA bands that exhibited a shift from the second to the third PCR, in size of the base pair

difference between the specific primers used for these PCR-rounds, were purified from the gel, ligated into the pGEM-T vector, and cloned in *E. coli*. Sequencing of the inserts revealed whether the amplified fragments consisted of gene regions adjacent to the known gene fragment.

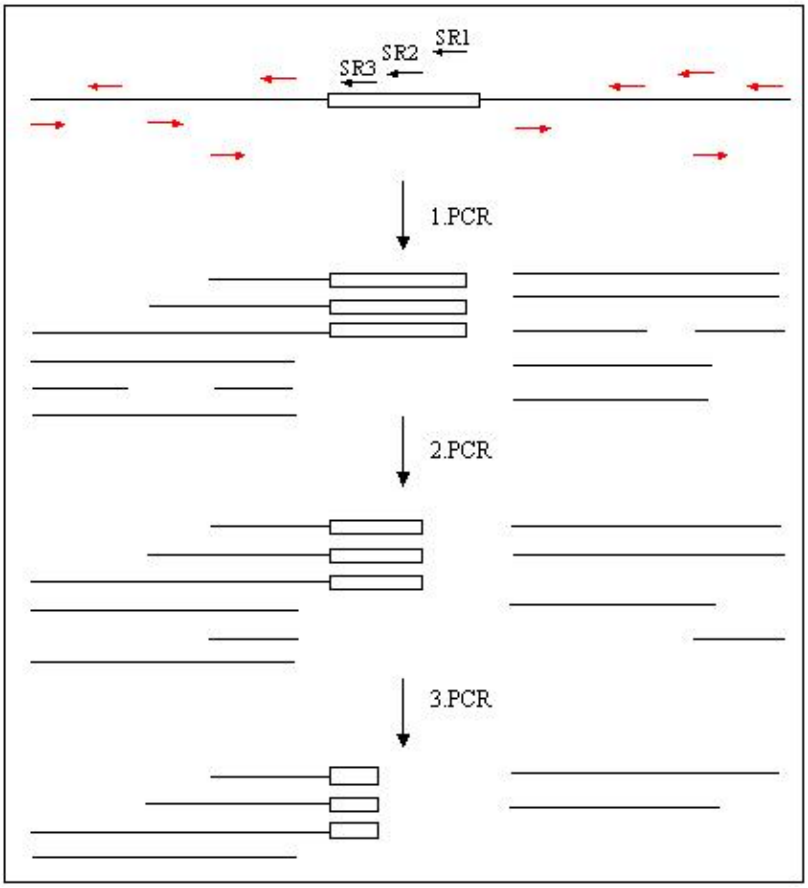

Fig. 10: Schematic illustration of the thermal asymmetric interlaced (TAIL-) PCR. The box symbolizes the known gene fragment, whereas the lines represent unknown DNA-regions upstream and downstream from the known fragment. Three nested gene specific primers bind to the gene of interest in upstream (SR 1-3) direction. Red arrows indicate the eight unspecific AD primers. A first PCR using SR1 and all AD primers amplifies a variety of specific and unspecific products. Unspecific products result from amplifications between two AD primers. In two following PCRs using SR2 (2.PCR), SR3 (3.PCR) and each one of the AD primers the specifity of the PCR-products is raised. This figure only shows a TAIL-PCR amplification in upstream direction with the SR primers.

2.2.7.8. Cloning of PCR-products

Cloning of PCR-fragments amplified with the DNA-polymerase from *T. aquaticus* (Taq), which amplifies the products with 3-´dA sticky ends, was carried out with the „pGEM-T Kit“ from Promega or the „TOPO-TA Kit“ from Invitrogen. Blunt end PCR-products

produced by proof-reading polymerases were cloned into blunt end linearized vectors using the T4-ligase (MBI) according to the manufacturer´s instructions.
Subsequent transformation of *E. coli* with the recombinant plasmids occurred via electroporation (Ausubel et al. 1994) or by heat-shock transformation using the Rubidium-Chloride method to produce competent cells (Sambrook et al. 1989).

2.2.7.9. Plasmid isolation

Recombinant plasmids were isolated from *E. coli* either in accordance to Sambrook and coworkers (Sambrook et al. 1989) or by using the „Plasmid Nucleo Spin Kit“ from Macherey-Nagel in order to gain plasmid with high purity for sequencing reactions.

2.2.7.10. DNA-Sequencing

DNA-sequencing was done by the dideoxynucleotide chain termination method (Sanger et al. 1977) with the ABI PRISM^{TM} BigDye Terminator Cycle Sequencing Ready Reaction (Perkin Elmer). The following cycler programme was used: 1 x [96°C, 5 min]; 25 x [96°C, 30 s; 50°C, 15 s; 60°C, 4 min]. The evaluation of the reaction was carried out at the Universitätsklinikum Eppendorf. DNA-sequencing was also done by the BASF AG.

2.2.8. Biochemical methods

2.2.8.1. Enzymatic plate assays

An initial screening for extracellular enzymes, which are possibly secreted by *F. graminearum*, was carried out on agar plates containing one sole carbon source (see 2.1.3.2.). Mycelial plugs from *F. graminearum* cultures were placed on these media and cultivated for 2-3 days at 28°C in the dark. The enzyme activities were made visible by colour reactions.

Enzyme activity	**Substrate**	**Colour reaction**
Amylolytic activity:	AZCL-Amylase	homogenous blue staining
Xylanolytic activity:	AZCL-Xylan	homogenous blue staining
Proteolytic activity:	AZCL-Casein	homogenous blue staining
Cellulolytic activity:	carboxymethylcellulose	halo formation
Lipolytic activity:	olive oil	orange fluorescent halo

Upon cleavage of the AZCL-substrates the azure blue dye is released, leading to a homogenous blue staining of the agar plates.

Carboxymethylcellulose was stained with 0.1 % Congo Red solution after growth of the fungal strains on the plate. This dye binds to the substrate. After the plate was washed several times with approximately 20 ml of 1 M NaCl the staining disappeared in areas where the substrate had been degraded, thus leading to a halo formation around the colony (Penttilä et al. 1987).

The detection of lipolytic activity (Kouker and Jaeger 1987) was based on the formation of fluorescent complexes, which were formed by free fatty acids and Rhodamine B.

2.2.8.2. Measurement of polymeric carbohydrate degrading enzyme activities

Conidia (10^5) were precultivated in 50 ml glucose rich medium (see 2.1.3.2.) for four days in the dark at 28°C, 150 rpm. Mutant cultures were supplemented with 75 µg/ml Hygromycin B. The mycelium was then separated from the medium by filtration, washed three times with 50 ml deionized water and cultivated for additional two days in 50 ml induction medium containing a polymeric carbohydrate as sole carbon source (see 2.1.3.2.). This was either starch, carboxymethylcellulose, xylan or pectin. Probes (2 ml) of the induced cultures were taken at various time points after induction: 0 h, 6 h, 12 h, 24 h, 36 h, 48 h. The mycelia were separated from the supernatant for 10 min at maximum speed. The culture supernatants were stored at 4°C, the cell pellets at –70°C.

To measure enzyme activites the culture supernatants or the crude cell extracts (see 2.2.8.5.) were incubated in fresh substrate (crude enzyme solution : substrate = 1:10): 50 mM sodium acetate buffer pH 5 containing 1 % substrate (starch, carboxymethyl-cellulose, xylan or pectin). The amount of reducing sugars set free from the subtrate by the enzymes in the culture supernatants or the crude cell extracts was determined with the BCA-assay (Waffenschmidt and Jaenicke 1987). An aliquot of the enzyme reaction mixture (max. 50 µl) was added to 1 ml of a 1:1-mixture of solution A and B (sol. A: 63.5 g/l Na_2CO_3 x H_2O, 24.2 g/l $NaHCO_3$, 1.9 g/l disodium 2.2`-bicinchoninate = BCA; sol. B: 1.25 g/l $CuSO_5$ x 5 H2O, 1.3 g/l LD-serine). These probes were boiled for 15 min in a water bath, cooled to room temperature in the dark followed by the measurement of the absorption at 560 nm. Calibration curves were made from standard glucose solutions ranging from 0.03 mM to 0.5 mM including buffer as reference and 0 mM value. The enzyme activities were calculated as amount of reducing sugars set free from the substrate per minute.

2.2.8.3. Measurement of proteolytic activity

Conidia (10^5) were precultivated in 50 ml glucose rich medium (see 2.1.3.2.) for four days in the dark at 28°C, 150 rpm. Mutant cultures were supplemented with 75 µg/ml Hygromycin B. The mycelium was then separated from the medium by filtration, washed three times with 50 ml deionized water and cultivated for additional two days in 50 ml induction medium containing casein as sole carbon source (see 2.1.3.2.). Probes (2 ml) of the induced cultures were taken at various time points after induction: 0 h, 12 h, 18 h, 24 h, 36 h, 48 h. The mycelia were separated from the supernatant for 10 min at maximum speed. The culture supernatants were stored at 4°C, the cell pellets at –70°C.

The culture supernatants were then incubated for 8 h in fresh substrate (crude enzyme solution:substrate = 1:7): 0.2 M Tris-HCl, pH 7.8, and 0.02 M $CaCl_2$, containing 1 mg/ml Hammarsteen Casein (Merck). The residual protein was then precipitated with 0.25 volumes 20 % trichloric acid for 15 min at room temperature and pelleted for 10 min at maximum speed. The supernatant containing the free amino acids cleaved from the substrate by the secreted proteases was measured photometrically at 280 nm. Thereby, the concentration of the aromatic amino acids, tryptophane and tyrosine within the substrate was determined by comparing the values with a tyrosine calibration curve (0.06 mM - 1 mM tyrosine, including buffer as reference and 0 mM value). Thus, the protease activities were calculated as amount of aromatic amino acids set free from the substrate per minute.

2.2.8.4. Measurement of lipolytic activity

CM-plates (supplemented with Hygromycin B for the mutants) were inoculated with conidia and cultivated for approximately a week at 28°C. The mycelium of two plates was then scratched off the agar surface and used as inoculate for 150 ml YPG-medium (see 2.1.3.2.). The resulting culture were cultivated for further two days in the dark at 28°C, 150 rpm. Mutant cultures were supplemented with 75 µg/ml Hygromycin B. The mycelium was then separated from the medium by filtration, washed three times with 150 ml deionized water and cultivated for several hours in 50 ml induction medium containing wheatgerm oil as sole carbon source (see 2.1.3.2). Probes (2 ml) of the induced cultures were taken at various time points after induction: 0 h, 4 h, 8 h, 12 h. The mycelia were separated from the supernatant for 10 min at maximun speed. The culture supernatants as well as the cell pellets were stored at –70°C.

To measure enzyme activities the culture supernatants or the crude cell extracts (see 2.2.8.5.) were incubated for 30 min in fresh substrate (crude enzyme solution:substrate = 1:10): 50 mM bis-tris-propane, pH 7, containing 1 mg/ml gum arabic, 0.1 % Triton X-100 and 2 mM p-nitrophenol palmitate (Maia et al. 2001). The amount of p-nitrophenol set free from the substrate was measured at 405 nm by comparing the OD-values with a p-nitrophenol calibration curve (15.6 µM - 1000 µM p-nitrophenol, including buffer as reference and 0 mM value). Thus, the lipolytic activities were calculated as amount of p-nitrophenol set free from the substrate per minute.

2.2.8.5. Extraction of a crude cell extract from mycelia

In order to measure intracellular enzyme activities a crude cell extract was gained from deep frozen (-70°C) mycelia from liquid cultures. The liquid cultures had been grown in specific enzyme inducing media. Deep frozen cell pellets from 2 ml liquid culture were homogenized in either 500 µl 50 mM sodium acetate buffer, pH 5, (for polymeric carbohydrate degrading enzyme activity measurements) or in 500 µl 50 mM bis-tris-propane, pH 7.5, (for lipolytic activity measurements) with glass beads by vigorously vortexing the probes for 5 min. Both buffers additionally contained 0.09 mg/ml PMFS to inhibit any proteolytic activities set free from the lysed cells. The resulting supernatant was centrifuged for 10 min at maximum speed to remove the residual cell particles. The supernatant containing the crude cell extract was stored at either 4°C or at -70°C depending on the stability of the enzymes measured.

2.2.8.6. Measurement of total protein concentrations

The total protein concentration in culture supernatants and in crude cell extracts was measured in accordance to Bradford (Bradford 1976), using the Bradford reagent from Amresco. Calibration of the measured values was accomplished with bovine serum albumin (0.6 µg/ml - 40 µg/ml, including water as reference).

2.2.9. In silico methods for the analysis of DNA- and protein sequences

DNA-sequences were analysed with the software programme “Prophet” (National Computing Resource for Life Science Research).

All plamid maps were made with the software programme “Clone Manager” (Scientific & Educational Software).
Protein sequences were analysed with the various software programmes of the “DNA Star” package (DNASTAR Inc.).

3. Results

In the last few years mitogen-activated protein (MAP) kinases have been shown to play an important role in regulating essential processes in the fungal life cycle such as mating, conidiation, cellular integrity, and infection mechanisms (Xu 2000). In this work, genes encoding MAP kinases from the head blight pathogen *Fusarium graminearum* were isolated and their roles in the fungal life cycle were analysed by producing mutants disrupted in these genes and their subsequent characterisation.

Prior to this work, a two round PCR strategy with degenerate primers (DP2 and DP4, DP1 and DP3; Hanks and Quinn 1991), designed from conserved gene regions of various fungal MAP kinases, was carried out. Thereby, two products of 556 bp and 490 bp in length were amplified (Fig. 11 and Fig. 12 in appendix A and B, respectively), ligated into the pGEM-T vector resulting in the vectors pGEM-T::gmap1 and pGEM-T::gpmk1, and were then cloned in *Escherichia coli* DH5α. These two bacterial strains were kindly supplied by Dr. F. J. Maier.

3.1. Isolation and disruption of the gene encoding the Gmap1 MAP kinase of *F. graminearum*

3.1.1. Isolation of the *gmap1* gene

The 556 bp insert of a putative MAP kinase contained in the pGEM-T::gmap1 vector was sequenced using the plasmid specific primers M13 forward and M13 reverse. A similarity search revealed the fragment to show homologies to fungal MAP kinases. Highest similarity was found to the Mps1 MAP kinase (AAC63682) of the phytopathogenic fungus *Magnaporthe grisea*.

Starting from the internal MAP kinase gene fragment of pGEM-T::gmap1, three nested forward and three nested reverse primers (reverse: NJ17, NJ18, NJ19 and forward: NJ20, NJ21, NJ22) were designed. With a thermal asymmetric interlaced (TAIL-) PCR strategy in three rounds, using the nested specific forward and reverse primers as well as eight unspecific arbitrary primers (AD1-AD9; modified after Lui and Whittier 1995), DNA fragments were amplified from genomic DNA of *F. graminearum*. A fragment amplified in forward and in reverse direction, respectively, was ligated into the pGEM-T vector,

resulting in the vectors pGEM-T*::*TAILgmap1F and pGEM-T*::*TAILgmap1R. These vectors were then cloned in the *E. coli* DH10b strain. The TAIL-PCR products were then sequenced by gene walking with the primers M13 forward, M13 reverse, NJ29, NJ30, NJ31, NJ32 and aligned to a sequence of 2937 bp. In order to verify the sequence, the complete gene was amplified in two fragments from genomic DNA using the proofreading polymerase Expand and the primer pairs NJ34/NJ6 for the 5´gene end and NJ5/NJ35 for the 3´gene end. These PCR products were ligated into either the pGEM-T-vector (pGEM-T*::*gmap1NJ34/6) or the pCR 2.1 Topo vector (pCR2.1TOPO*::*gmap1NJ5/35), cloned in *E. coli* and sequenced again. The cDNA of the complete gene was amplified by RT-PCR in two fragments, using the proofreading polymerase Expand and the gene specific primer pairs NJ50/NJ6 for the 5´gene end and NJ5/NJ51 for the 3´gene end. Again the PCR products were ligated into the Topo 2.1. vector (pCR2.1TOPO*::*gmap1NJ50/6 and pCR2.1TOPO*::*gmap1NJ5/51), cloned in *E. coli* and sequenced. Comparisons of the genomic DNA sequence with the cDNA sequence revealed the isolated MAP kinase to have an open reading frame of 1248 bp encoding a 416 aa protein. The gene contained four introns of 114 bp, 62 bp, 59 bp and 55 bp in length (Fig. 13 in appendix A). The amino acid sequence showed high similarities to various other fungal MAP kinases (Fig. 14 in appendix A), such as Maf1 from *Colletotrichum lagenarium*, 88 % identity (AAL50116; Kojima et al. 2002), Mps1 from *M. grisea*, 88 % identity (AAC63682; Xu et al. 1998), Mpk2 from *Blumeria graminis*, 83 % identity (AAG53655; Zhang and Gurr 2001), Cpmk2 from *Claviceps purpurea*, 83 % identity (CAC87145; Mey et al. 2002) and MpkA from *Aspergillus nidulans*, 83 % identity (AAD24428; Bussink and Osmani 1999). The amino acid sequence contained the threonine-glutamate-tyrosine (TEY)-site. The threonine and tyrosine residues of this site were shown to be phosphorylated by the MAP kinase kinase, which is situated upstream in the signal cascade. The dual phosphorylation of this site results in the activation of the MAP kinase (Kültz 1998). Furthermore, it contained all 11 conserved domains of the yeast/fungi extracellular signal regulated kinase subgroup 2 (YERK2; Fig. 14 in appendix A) (Kültz 1998; Hanks and Quinn 1991). Gmap1 also ranged in the YERK2 subgroup, when a multitude of fungal MAP kinases were aligned (Fig. 15 in appendix D). Southern blot analysis, using genomic DNA, digested with several restriction enzymes and a 355 bp gene fragment amplified with the primers NJ5/NJ6 as probe indicated this MAP kinase gene to be present as a single copy in the genome of *F. graminearum*. The gene was named *gmap1* for *Gibberella* MAP kinase 1.

In the course of this work, the described MAP kinase from *F. graminearum* was also isolated by Hou and co-workers (accession number AAM13670; Hou et al. 2002).

3.1.2. Transformation-mediated gene disruption of *gmap1*

3.1.2.1. Cloning of the *gmap1* transformation vector

In order to analyse the function of the Gmap1 MAP kinase from *F. graminearum* a gene disruption strategy was chosen. For the transformation of *F. graminearum* via single crossover vector integration a transformation vector was needed that could be linearized in the centre of the MAP kinase specific sequence (Fig. 16 A). Starting from the initial pGEM-T vector, pGEM-T::gmap1, containing the 556 bp MAP kinase gene fragment, an Inverse-PCR (see 2.2.7.8.; Ochman et al. 1988) was carried out using the primers

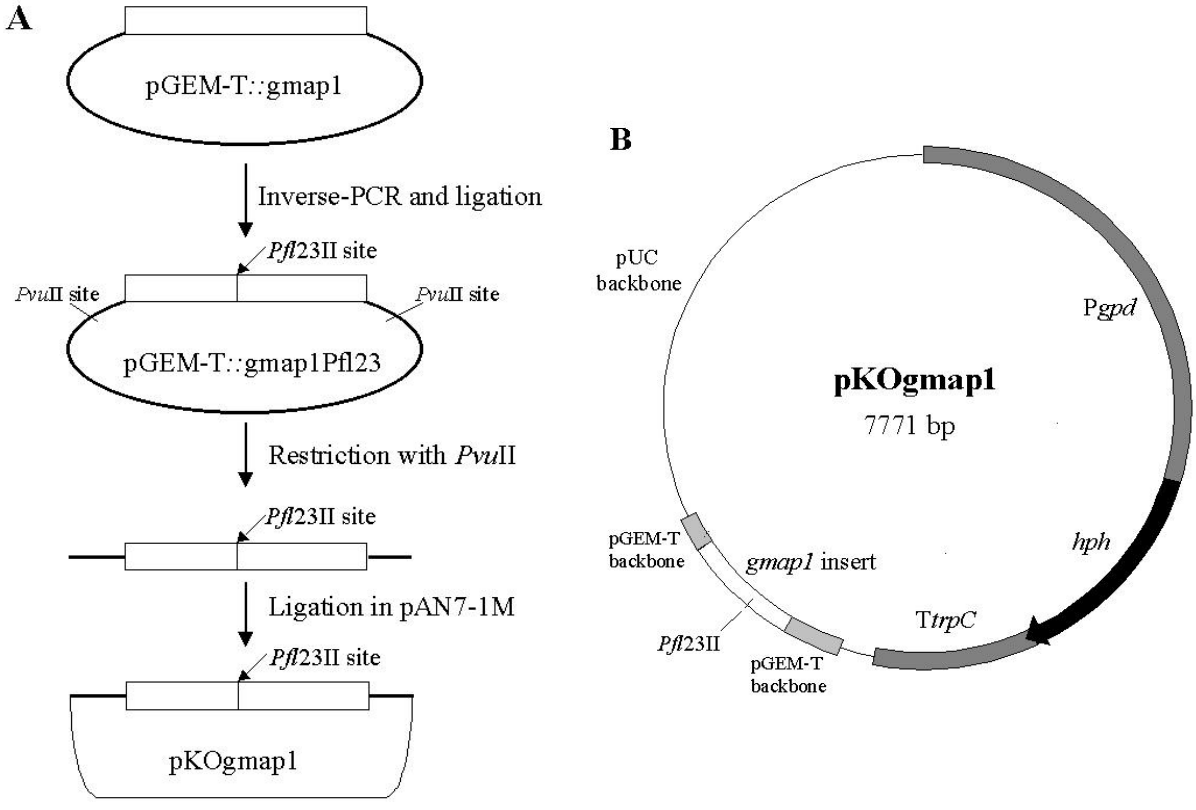

Fig. 16: A) Cloning of the *gmap1* transformation vector. The white boxes show the 556 bp *gmap1* MAP kinase gene fragment that was amplified by PCR with degenerate primers. Black lines indicate the vector backbones. **B)** Detailed map of the pKOgmap1 transformation vector. The vector contains the 556 bp *gmap1* fragment from *F. graminearum* with the *Pfl*23II restriction site and small parts of the pGEM-T cloning vector as well as the *E. coli hph* gene under control of the *Aspergillus nidulans gpd* promotor. Transcription termination is accomplished by the terminator region of the *A. nidulans trp*C gene.

Pfl23-Forw and Pfl23-Rev. The proofreading polymerase DeepVent was used to gain a blunt end PCR product. Thereby, four base pairs were exchanged in the sequence generating an unique *Pfl*23II restriction site in the centre of the *gmap1* specific sequence. The product of the Inverse-PCR (pGEM-T*::*gmap1Pfl23) consists of the complete linear plasmid, which was then ligated and cloned in the *E. coli* DH5α strain. The modified *gmap1* insert was excised from the vector via digestion with *Pvu*II. This restriction enzyme cleaves twice in the vector backbone leaving pGEM-T residues of 158 bp and 275 bp, respectively, next to the *gmap1* specific sequence. The 989 bp fragment was ligated into the *Ehe*I linearized fungal transformation vector pAN7-1M, which contains the Hygromycin B resistance gene, *hph*, as a selective marker. The resulting transformation vector, pKOgmap1 (Fig. 16 B), was cloned in the *E. coli* DH5α strain.

3.1.2.2. Transformation of *F. graminearum* and analysis of transformants

The pKOgmap1 transformation vector was linearized at the unique *Pfl*23II restriction site located in the centre of the *gmap1* specific sequence. 30 µg of the linearized pKOgmap1 transformation vector were used to transform approximately 0.5-2 x 10^8 protoplasts from the *F. graminearum* wild type strain 8/1 (see 2.2.2.; Royer et al. 1995). The transformation vector is thereby introduced into the *F. graminearum* genome by a single crossover at the homologous *gmap1* locus (see Fig. 7, 2.2.2.2.). The emerging transformants were transferred to CM plates containing Hygromycin B for selection, brought to conidiation on SNA plates also containing Hygromycin B, and then single conidiated. Eight transformations yielded 47 transformants in total. Therefrom, 35 transformants were screened for mutants with homologously integrated pKOgmap1 transformation vector. At first this was performed by southern blot, carried out with genomic DNA from the transformants and the wild type strain digested with the restriction enzyme *Eco*47III. The internal MAP kinase fragment, amplified with the primers NJ5/NJ6, was used as a probe (Fig. 17). Thereby, four *gmap1* disruption transformants were found (51.3.1., 203.3.1., 203.13.1., 203.14.1.).

In order to analyse, whether the *gmap1* transcripts were also successfully disrupted in the gained mutants, a RT-PCR was carried out (Fig. 18). RNA from the mutant 51.3.1. and the wild type strain was isolated from cultures grown in liquid CM-medium, followed by DNA digestion and first strand synthesis. A PCR with cDNA as template and two primer

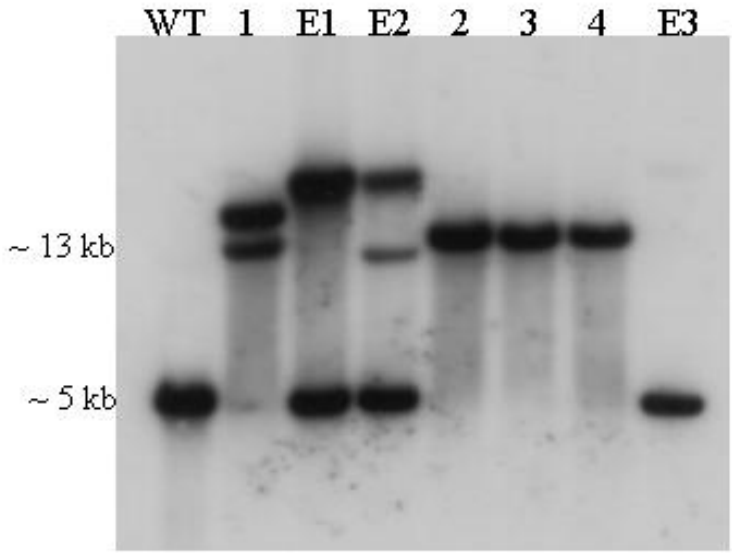

Fig. 17: Southern blot analysis of the genomic DNA from the *F. graminearum* wild type strain (WT), the four *gmap1* disruption mutants (1-4: 51.3.1., 203.13.1., 203.14.1., 203.3.1.) and three ectopic integration transformants (E1-E3). DNA was digested with *Eco*47III. The blot was probed with the 355 bp internal fragment of the *gmap1* gene contained in the transformation vector pKOgmap1. The Δ*gmap1* mutants miss the wild type hybridisation signal of 5 kb. Instead, the signal has shifted in size of the transformation vector, 7771 bp. Next to the shifted wild type band one Δ*gmap1* mutant (1) shows a second higher molecular weight hybridisation signal. Furthermore, it also shows a slight signal at 5 kb. The 5 kb signal did not get more intense after longer exposition times. The ectopic integration transformants show the wild type hybridisation signal as well as 1-2 higher molecular weight hybridisation signals, indicating a random integration of the transformation vector in the genome. The transformant in lane E3 shows only a very faint higher molecular weight signal. But the signal became more intense when longer exposition times were chosen.

combinations was conducted. Primers (NJ44/NJ45) situated upstream and downstream of the homologous locus were used to identify transformants that still showed the wild type gene without homologous vector integration. Under the chosen PCR conditions only an ectopic integration of the transformation vector into the genome of *F. graminearum* would lead to the amplification of a 615 bp DNA fragment. Using the primer pair NJ44/panehe3´SM (the panehe3´SM primer was kindly provided by Sascha Malz), the integration of the vector into the target gene was shown by amplification of a specific 718 bp DNA fragment. The Δ*gmap1* mutant 51.3.1. showed correct integration of the pKOgmap1-vector with the primers NJ44/panehe3´SM, but additionally the wild type PCR product was amplified with the primers NJ44/NJ45. This wild type PCR product could also be amplified from genomic DNA of all four Δ*gmap1* mutants, including the three mutants not tested by RT-PCR. Sequencing of these PCR products confirmed the amplified DNA-fragment to be the *gmap1* wild type gene fragment. This result led to the assumption that the gained Δ*gmap1* mutants either still contained untransformed nuclei or had actively

excised the transformation vector during cultivation. Assuming that the wild type contamination was caused by untransformed nuclei in the Δ*gmap1* mutants, all mutants were single conidiated three more times to find a mutant that would show no wild type background. They were analysed by PCR using genomic DNA as template and the primers NJ44 and NJ45. From each of the mutants, propagates of five picked conidia were tested. After the fourth round of single conidiation the wild type PCR product could still be found, if the PCR was carried out with a high amount of cycles, indicating that the wild type contamination could not be eliminated in this way.

Finally, further 14 transformants gained were examined for homologous integration of the transformation vector by PCR using the primers NJ44/NJ45 and genomic DNA as template. No other mutants with homologously integrated pKOgmap1 vector were found.

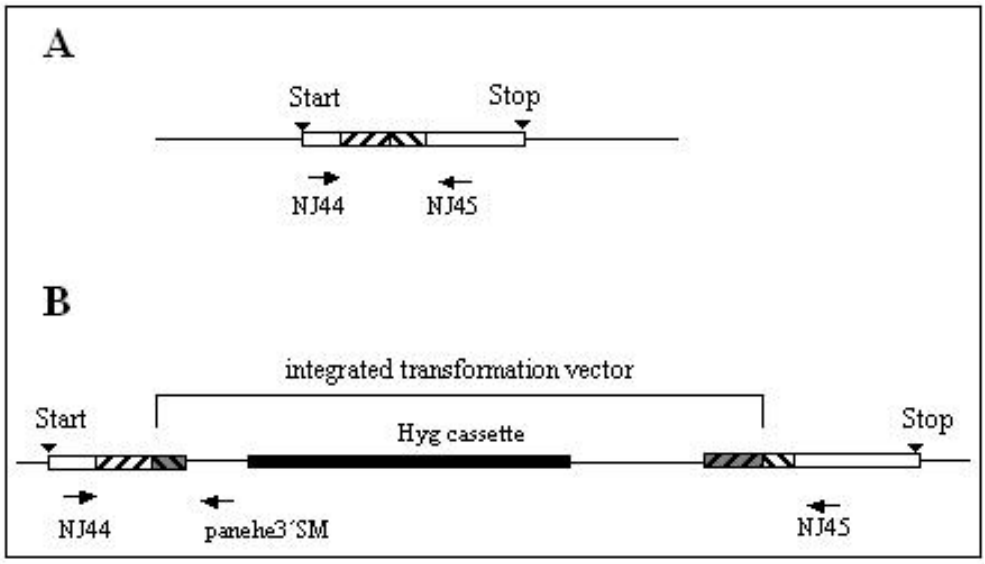

Fig. 18: Positioning of the primers used to analyse the integration of the transformation vector via PCR and RT-PCR. **A**) wild type gene locus, **B**) interrupted gene locus. The gray lined bars figure the vector internal fragment of the gene of interest, whereas the white lined bars show the homologous regions in the wild type gene. In this region the transformation vector integrates via homologous recombination. The Hygromycin B resistance gene *hph*, contained in the transformation vector, is symbolized by a black bar. Start and stop codons are indicated by inverted black triangles. Black arrows indicate the positioning of the gene specific primers NJ44 and NJ45 as well as the primer panehe3´SM that binds to the vector backbone.

3.2. Isolation and disruption of the gene encoding the Gpmk1 MAP kinase of *F. graminearum*

3.2.1. Isolation of the *gpmk1* gene

The 490 bp pGEM-T*::*gpmk1 insert of the second putative MAP kinase was sequenced using the plasmid specific primers M13 forward and M13 reverse. The gained sequence showed a significant homology to the Pmk1 MAP kinases of *M. grisea* (AAC49521) and also to other fungal MAP kinases. Therefore, the 5´and 3´ ends of the corresponding gene were obtained via TAIL-PCR. Three gene specific, nested forward and reverse primers were designed on the basis of the pGEM-T*::*gpmk1 insert sequence (forward: NJ23, NJ24, NJ25 and reverse: NJ26, NJ27, NJ28). In three rounds using the gene specific primers, a set of unspecific arbritary primers (AD1-AD9; modified after Lui and Whittier 1995) and *F. graminearum* genomic DNA as initial template, various DNA fragments were amplified in forward and reverse direction. A reverse and a forward PCR product were ligated into the pGEM-T or the pCR-XL-TOPO vector (pGEM-T*::*TAILgpmk1R and pCR-XL-TOPO*::*TAILgpmk1F) and cloned in *E. coli*. Sequencing of the TAIL-PCR products was kindly done by the BASF AG, Ludwigshafen. In order to verify the sequence the complete gene was amplified in two fragments from genomic DNA with the polymerase Expand, ligated into the pCR 2.1 Topo vector, resulting in the plasmids pCR2.1 TOPO*::*gpmk1NJ7/38 and pCR2.1TOPO*::*gpmk1NJ49/8_gDNA. These plasmids were cloned in *E. coli* and sequenced again. The specific primers used were designed on the basis of the fragments amplified via TAIL-PCR: NJ49 and NJ8 for the 5´gene end and NJ7 and NJ38 for the 3´gene end. Furthermore, the cDNA of the complete gene was amplified by RT-PCR from *F. graminearum* 8/1 RNA isolated from a culture grown in CM-medium. The gene was amplified in two fragments using the polymerase Expand and the gene specific primer pairs NJ49/NJ8 for the 5´gene end and NJ7/NJ53 for the 3´gene end. The PCR products were ligated into the pCR 2.1 Topo vector (pCR2.1TOPO*::*gpmk1 NJ49/8_cDNA and pCR2.1TOPO*::*gpmk1NJ7/53), cloned in *E. coli*, and sequenced. Comparison of the genomic DNA sequence with the cDNA sequence made it possible to find the transcription start and stop as well as the localization of the introns. Three introns of 60 bp, 57 bp and 64 bp were identified. The gene had an open reading frame of 1065 bp and encoded a 355 aa protein (Fig. 19 in appendix B). Comparison of the deduced amino acid sequence with database entries revealed high similarities to other fungal MAP kinases

(Fig. 20 in appendix B), such as Fmk1 from *Fusarium oxysporum*, 98.3 % identity (AF286533; Di Pietro et al. 2001), Pmk1 from *M. grisea*, 97.2 % identity (U70134; Xu and Hamer 1996), Cmk1 from *C. lagenarium*, 96.9 % identity (AJ318517; Takano et al. 2000), Cpmk1 from *C. purpurea*, 95.2 % identity (AF174649; Mey et al. 2002), Ptk1 from *Pyrenophora teres*, 92.4 % identity (AF272831; Ruiz-Roldán et al. 2001) and Chk1 from *Cochliobolus heterostrophus*, 91 % identity (AF178977; Lev et al. 1999). The high similarity of the described *F. graminearum* MAP kinase to Pmk1 from *M. grisea* led to name Gpmk1 (*Gibberella* pathogenicity MAP kinase 1) for the *F. graminearum* kinase. In the Gpmk1 amino acid sequence the threonine-glutamate-tyrosine (TEY)-sequence, a site for threonine-tyrosine phosphorylation, was found (Kültz 1998). Dual phosphorylation of this site by the MAP kinase kinase is needed to activate the MAP kinase. Furthermore, it contains all 11 conserved domains of the yeast/fungi extracellular signal regulated kinase subgroup 1 (YERK1; Fig. 20 in appendix B) (Kültz 1998; Hanks and Quinn 1991). Gpmk1 also ranges in the YERK1 subgroup, when a multitude of fungal MAP kinases are aligned (Fig. 15 in appendix D). Southern blot analysis of genomic DNA, digested with several restriction enzymes, indicated this MAP kinase gene to be present as single copy in the genome of *F. graminearum.* A 355 bp *gpmk1* gene fragment amplified with the primer pair NJ7/NJ8 was used as a probe.

Recently, the *gpmk1* gene has also been isolated by Urban and colleagues (accession number AAL73403; Urban et al. 2003).

3.2.2. Transformation-mediated gene disruption of *gpmk1*

3.2.2.1. Cloning of the *gpmk1* transformation vector

Disruption mutants were produced in order to analyse the function of the Gpmk1 MAP kinase in the fungal life cycle. Two different transformation vectors, pKOgpmk1 and pKOgpmk1-Del, were made to disrupt the *gpmk1* gene. In both cases a point mutation was set to gain a unique *Pau*I restriction site in the centre of the homologous gene region of the transformation vector. The sole difference between the two constructed transformation vectors is, that the pKOgpmk1-Del vector has each one base pair deletion to the right and left of the *Pau*I restriction site.

For the construction of the pKOgpmk1 vector an Inverse-PCR strategy (Fig. 21 A; Ochman et al. 1988) was persued. Therefore, the initial pGEM-T vector, pGEM-T::gpmk1,

containing the 490 bp *gpmk1* gene fragment, was used as template. A PCR with the primers PauIMfor and PauIMrev and the proofreading polymerase DeepVent led to a PCR product that consisted of the complete linear plasmid now containing a *Pau*I restriction site in the *gpmk1* insert due to an exchange of one base pair. This PCR product was ligated (pGEM-T::gpmk1PauI) and cloned in the *E. coli* DH5α strain. Digestion of this vector with the restriction enzyme *Pvu*II allowed the excision of the modified *gpmk1* insert from the vector backbone. This restriction enzyme cleaves twice in the vector backbone leaving pGEM-T residues of 158 bp and 275 bp, respectively, next to the *gpmk1* specific sequence. The resulting 923 bp fragment was ligated into the *Ehe*I linearized fungal transformation vector pAN7-1M, which contains the Hygromycin B resistance gene, *hph*, as a selective marker (Fig. 21 B). The resulting transformation vector, pKOgpmk1, was cloned in the *E. coli* DH5α strain.

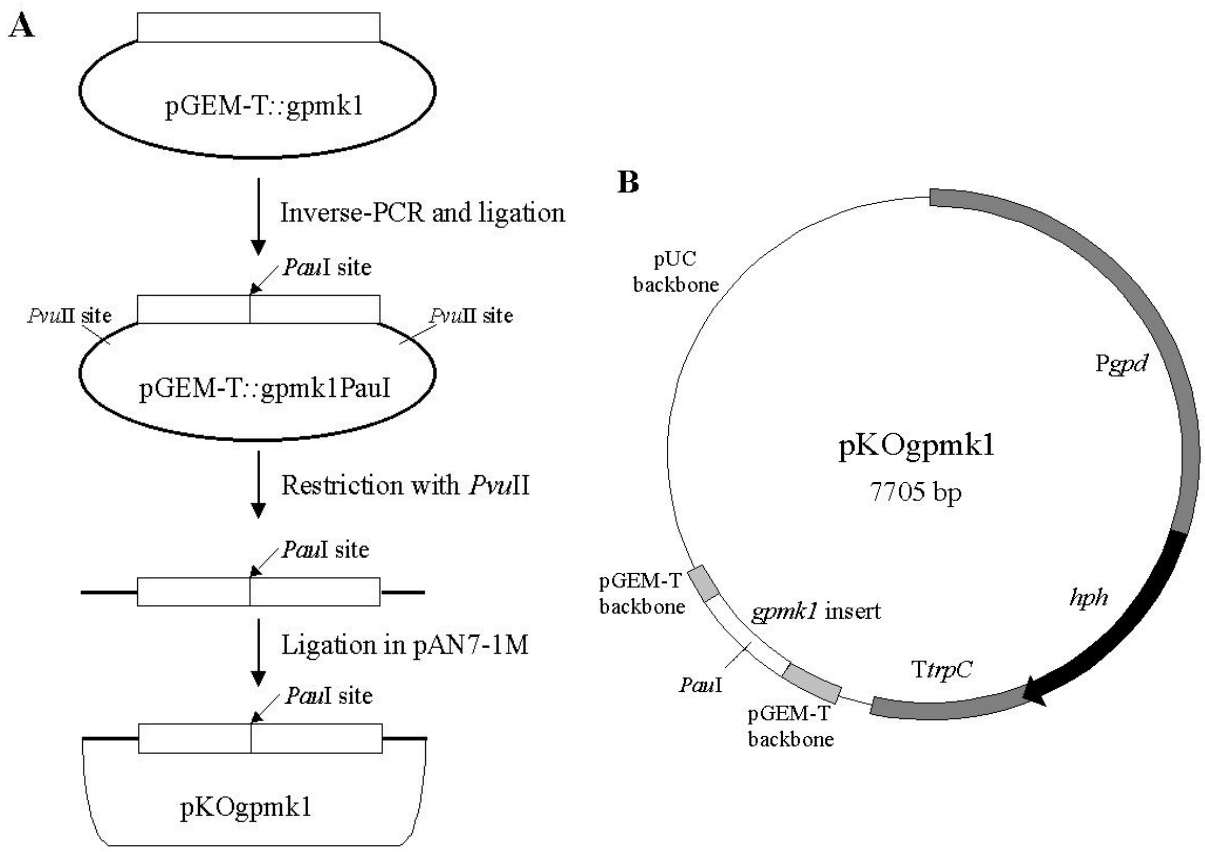

Fig. 21: A) Cloning of the *gpmk1* transformation vector. The white boxes show the 490 bp *gpmk1* MAP kinase gene fragment that was amplified by PCR with degenerate primers. Black lines indicate the vector backbones. **B)** Detailed map of the pKOgpmk1 transformation vector. The vector contains the 490 bp *gpmk1* fragment from *F. graminearum* with the *Pau*I restriction site and small parts of the pGEM-T cloning vector as well as the *E. coli hph* gene under control of the *A. nidulans gpd* promotor. Transcription termination is accomplished by the terminator region of the *A. nidulans trp*C gene.

The point mutation leading to the unique *Pau*I restriction site and the base pair deletions in the *gpmk1* gene specific sequence of the pKOgpmk1-Del transformation vector was accomplished by a Fusion-PCR strategy (Fig. 22 A; Amberg et al. 1995). A PCR using the pGEM-T::gpmk1 vector as template and the primer pairs NJ11/pGEM-T349 and NJ12/pGEM-T2870 led to the amplification of two PCR products, 534 bp and 460 bp in size. In a second PCR round these two products were used as template. The overlaping regions fused in the first cycles and were then amplified with the M13 forward and M13 reverse primers, to form a 708 bp fusion product. This fusion product consisted of the *gpmk1* 490 bp gene fragment with a *Pau*I restriction site and a base pair deletion on both sides of the generated *Pau*I restriction site as well as two pGEM-T residues of 127 bp and 91 bp, respectively. The fusion product was ligated into the fungal transformation vector pAN7-1M, resulting in the vector pKOgpmk1-Del, and transformed in the *E. coli* XL Blue strain (Fig. 22 B).

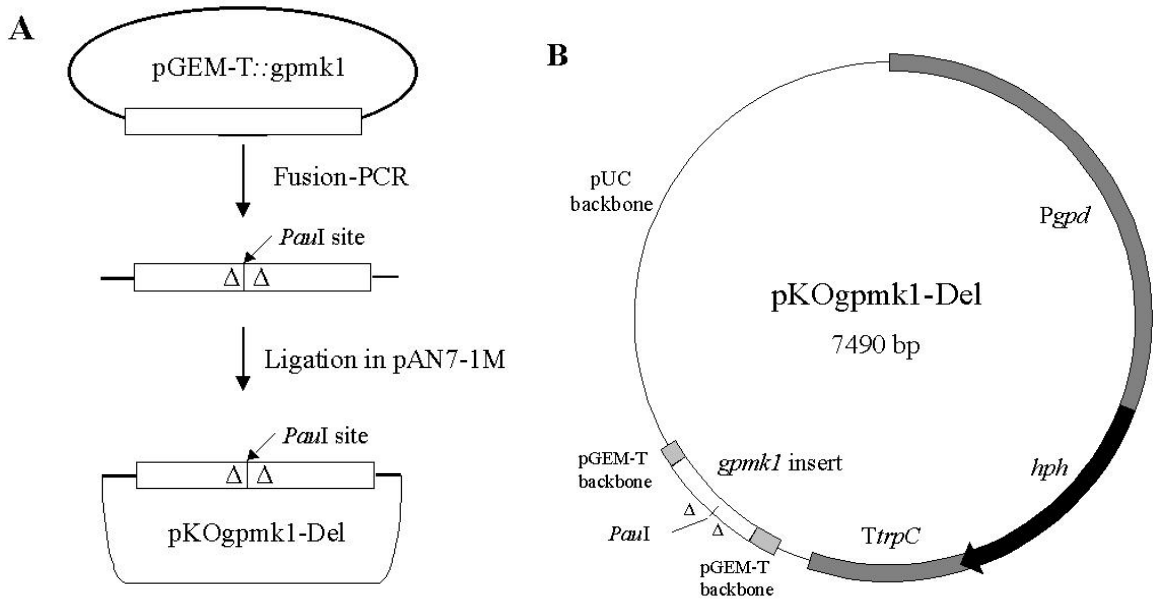

Fig. 22: A) Cloning of the pKOgpmk1-Del transformation vector. The white boxes show the 490 bp *gpmk1* MAP kinase gene fragment that was amplified by PCR with degenerate primers. Black lines indicate the vector backbones. The symbol Δ indicates the base pair deletions added to gain a frame shift in the open reading frame of the *gpmk1* gene. **B)** Detailed map of the pKOgpmk1 transformation vector. The vector contains the 490 bp *gpmk1* fragment from *F. graminearum* with the *Pau*I restriction site and small parts of the pGEM-T cloning vector as well as the *E. coli hph* gene under control of the *A. nidulans gpd* promotor. Transcription termination is accomplished by the terminator region of the *A. nidulans trp*C gene.

3.2.2.2. Transformation of *F. graminearum* and analysis of transformants

Both transformation vectors, pKOgpmk1 and pKOgpmk1-Del, were linearized with the restriction enzyme *Pau*I. Approximately 0.5-2 x 10^8 protoplasts of the *F. graminearum* wild type strain 8/1 were transformed with the linearized pKOgpmk1 and pKOgpmk1-Del vectors, respectively (see 2.2.2.; Royer et al. 1995). The transformation vectors were thereby introduced into the *F. graminearum* genome by a single crossover at the homologous *gpmk1* locus (see Fig. 7, 2.2.2.2.). The resulting transformants were cultivated on CM plates containing Hygromycin B, brought to conidiation on SNA plates with Hygromycin B, and were then single conidiated. Three transformants were gained using the pKOgpmk1 transformation vector. Further 23 transformants resulted from transformation with the pKOgpmk1-Del vector. Southern blot analysis was performed with genomic mutant and wild type DNA digested with the restriction enzyme *Eco*RV to test for mutants that had inserted the transformation vector by homologous recombination (Fig. 23). Therefore, the blots were probed with a digoxygenin labeled PCR product that had been amplified with the primers NJ7 and NJ8. Two *gpmk1* disruption mutants were gained with the pKOgpmk1 vector (57.1.1., 57.2.1.). Only 10 of the 22 generated

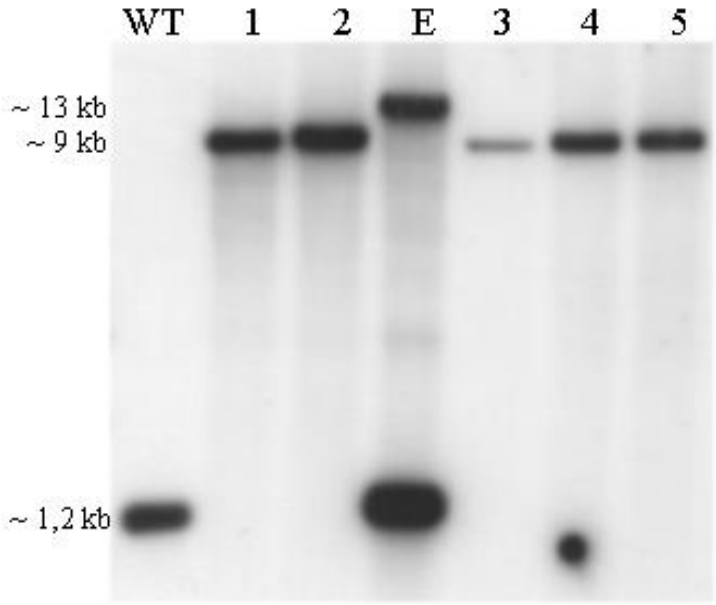

Fig. 23: Southern blot analysis of the genomic DNA from the *F. graminearum* wild type strain (WT), some of the *gpmk1* disruption mutants (1-5: 57.1.1., 57.2.1., 169.6.1., 169.7.1., 169.8.1.), and one ectopic integration transformant (E). DNA was digested with *Eco*RV. The blot was probed with the 355 bp internal fragment of the *gpmk1* gene contained in the transformation vectors. *gpmk1* disruption mutants miss the wild type hybridisation signal of ~1,2 kb. Instead, the signal has shifted in size of the transformation vector, 7705 bp (pKOgpmk1) and 7490 bp (pKOgpmk1-Del), respectively. Next to the wild type hybridisation signal, the ectopic integration transformant shows a second signal, indicating a random integration of the transformation vector in the genome.

transformants resulting from the transformation with the pKOgpmk1-Del vector were tested. All ten transformants showed a homologous integration of the transformation vector (169.6.1., 169.7.1., 169.8.1., 169.9.1., 169.11.1., 169.12.1., 169.13.1., 169.14.1., 169.15.1., 169.17.1.). Fig. 23 only shows the southern blot analysis of five of the twelve *gpmk1* disruption mutants.

The integration of the transformation vector was also tested via RT-PCR to see, whether the *gpmk1* transcript was successfully disrupted (Fig. 24). RNA from mutants and the wild type strain, grown in CM-medium, was isolated. After DNA digestion and first strand synthesis, various PCRs were carried out using two gene specific primers (NJ46 and NJ47), which are situated upstream and downstream of the homologous locus, and two primers binding to the insert flanking regions of the pAN7-1M vector backbone (panehe5´SM and panehe3´SM; kindly provided by Sascha Malz). The 675 bp fragment of the *gpmk1* wild type gene region, using the primers NJ46/NJ47, could not be amplified from mutant cDNA. This indicated that the transcripts were interrupted. A 711 bp fragment from the 5´gene end (NJ46) to the inserted vector (panehe3´SM) was amplified showing

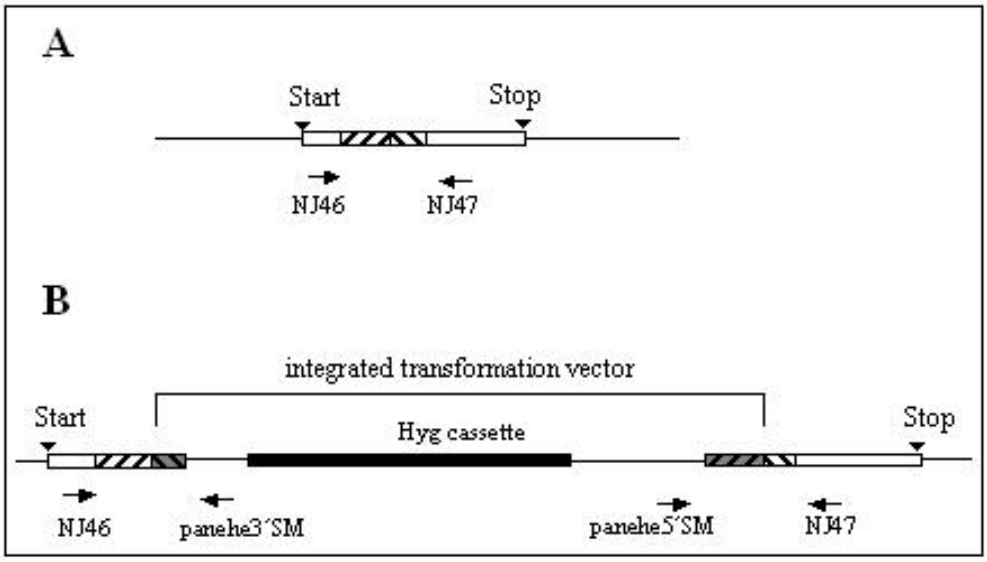

Fig. 24: Positioning of the primers used to analyse the integration of the transformation vector via PCR and RT-PCR. **A**) wild type gene locus **B**) interrupted gene locus. The gray lined bars figure the vector internal fragment of the gene of interest, whereas the white lined bars show the homologous regions in the wild type gene. In this region the transformation vector integrates via homologous recombination. The Hygromycin B resistance gene *hph*, contained in the transformation vector, is symbolized by a black bar. Start and stop codons are indicated by inverted black triangles. Black arrows indicate the positioning of the gene specific primers NJ46 and NJ47 as well as the primers panehe3´SM and panehe5´SM that bind to the vector backbone.

the vector to be integrated correctly. A PCR product starting from the pAN7-1M vector to the 3´gene end could only be amplified from genomic DNA and not from cDNA. This result again exhibits the correct integration of the transformation vector and also shows that the transcription of the *gpmk1* gene is stopped by the integrated vector. Thus, the gained disruption mutants are not expected to express a functional Gpmk1 MAP kinase.

3.3. Transcription analysis of two *F. graminearum* MAP kinase genes

In order to analyse the conditions under which the genes encoding the Gmap1 and the Gpmk1 MAP kinase from *F. graminearum* are transcribed a semi-quantitative RT-PCR analysis was carried out. RNA was isolated from uninfected (24 h incubation with H_2O; kindly provided by Sascha Malz) and from *F. graminearum* infected wheat spikelets (4 h, 12 h, 24 h, 48 h and 7 d after spore inoculation; kindly provided by Sascha Malz) as well as from a *F. graminearum* 8/1 culture grown in CM-medium. After a DNA digestion step and first-strand synthesis a PCR was performed with the *gmap1* specific primers NJ5/NJ6, the *gpmk1* specific primers NJ7/NJ8 and primers for the *F. graminearum* β-tubulin gene (FgBetaTubFor/FgBetaTubRev). The β-tubulin gene was used as control for a constitutively and highly expressed gene. The primers for the β-tubulin gene were designed from a sequence found in the *F. graminearum* cDNA library made by the BASF AG, Ludwigshafen (Germany). This sequence showed high homologies to β-tubulin genes of other fungal organisms. Control PCRs with all three primer pairs were done with genomic DNA as template. Transcripts of the β-tubulin gene could not be found in uninfected wheat spikes. In *F. graminearum* infected wheat spikes the β-tubulin transcripts were first detectable 12 h after inoculation and increased during progress of the infection. An amplification of the β-tubulin fragment was also possible from cDNA isolated from a culture grown in liquid CM-medium. The β-tubulin gene fragment amplified from genomic DNA showed a slightly higher molecular weight, indicating the isolated cDNA to be free from genomic DNA contamination (Fig. 25 C).

Transcripts of the *gmap1* and the *gpmk1* MAP kinase gene could not be detected in uninfected wheat spikelets. Both MAP kinase genes exhibit a constitutive expression pattern comparable to the β-tubulin gene. Transcripts could be found in the culture grown in CM-medium as well as in infected wheat spikelets beginning at 24 h after inoculation, when the fungus had grown enough to be detected by PCR. A shift in molecular weight of

the PCR products from genomic DNA compared to cDNA, due to an intron in the sequence, showed that the isolated cDNA was free from genomic DNA contamination (Fig. 25 A, B).

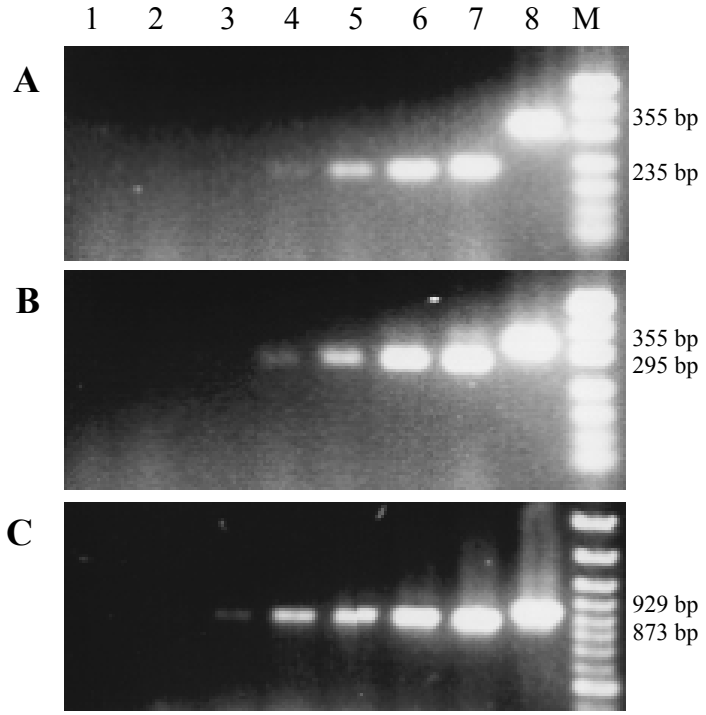

Fig. 25: Expression of the *gmap1* (**A**), the *gpmk1* (**B**) and the β-tubulin (**C**) gene from *F. graminearum* during plant infection and in vitro, as shown via RT-PCR. First-strand cDNA generated from total RNA isolated from uninfected (lane 1) and from *F. graminearum* infected wheat spikelets (4 h, 12 h, 24 h, 48 h and 7 d after spore inoculation; lanes 2-6) as well as from a *F. graminearum* 8/1 culture grown in CM-medium (lane 7) was used as template for PCR with the *gmap1* specific primers NJ5/NJ6, the *gpmk1* specific primers NJ7/NJ8 and primers for the *F. graminearum* β-tubulin gene (FgBetaTubFor/FgBetaTubRev) Lane 8: PCR with genomic DNA as template performed as control. Lane M: GeneRuler DNA Ladder Mix (C) and pUC19 DNA/*Msp*1 marker (A, B).

3.4. Phenotypic characterisation of the MAP kinase disruption mutants

Disruption of MAP kinases in various other fungal plant pathogens resulted in mutants with pleiotropic phenotypes. These results indicated that fungal MAP kinases play a regulatory role during conidiation, mating, vegetative growth but also during parasitic growth on the plant, thereby inducing important infection mechanisms like appressoria formation or secretion of cell wall degrading enzymes (Xu 2000; Lev and Horwitz 2003). Thus, the following experiments were carried out to characterise the gained *F. graminearum* MAP kinase mutants.

3.4.1. Growth assays

Morphology (Fig. 26) and growth rate (Fig. 27) of the gained MAP kinase mutants were assayed on agar plates containing complete medium (CM) and Czapek minimal medium, respectively. Furthermore, the biomass production was determined after growth in liquid CM and Czapek medium and was compared to the *F. graminearum* wild type strain 8/1 (Fig. 28).

On CM plates *F. graminearum* grows as a compact brown colony exhibiting only very little aerial growth. The Δ*gmap1* and Δ*gpmk1* mutants showed a comparable culture morphology. The Δ*gpmk1* mutants grew slightly slower than the wild type. Yet, all Δ*gmap1* mutants were drastically reduced in their growth rate, producing smaller and more compact colonies and having an average growth reduction of 54 % over the entire time course measured. Czapek, a minimal medium lacking amino acid supplements (Raper and Thorn 1949), induces *F. graminearum* to form thick, white aerial mycelia. The colonies produced by the Δ*gmap1* mutants were again more compact in comparison to the wild type strain and the mutants again showed a significant average growth rate reduction of 70 %.

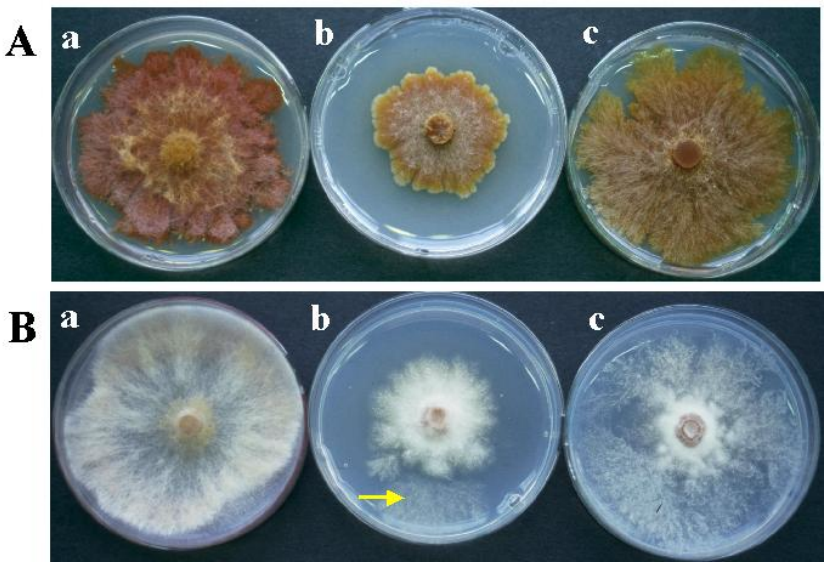

Fig. 26: Colony morphology during growth on CM (A) and Czapek (B) medium, showing the *F. graminearum* wild type strain (a), a Δ*gmap1* mutant (b) and a Δ*gpmk1* mutant (c). Thereby, the mutants only grew with selective Hygromycin B pressure on the CM-plates. The pictures were taken seven days postinoculation. The arrow markes an area where the Δ*gmap1* mutant has lost its growth reduced phenotype and then grows as fast as the wild type strain.

The *gpmk1* mutants exhibited a more drastic difference in colony morphology on Czapek plates. Unlike the wild type strain, no aerial mycelia were formed. The mutants grew within the agar with few long hyphae. These long hyphae were multiply branched with short hyphae that produced conidiophores carrying conidia at their tips. This growth behaviour resulted in an average growth rate reduction ranging from 71 % one day after

inoculation to 28 % at the last time point measured. A *gmap1* and a *gpmk1* ectopic integration transformant, respectively, were also assayed concerning their morphology and growth rate on CM and Czapek plates. In all experiments they exhibited rates comparable to the wild type strain (data not shown).

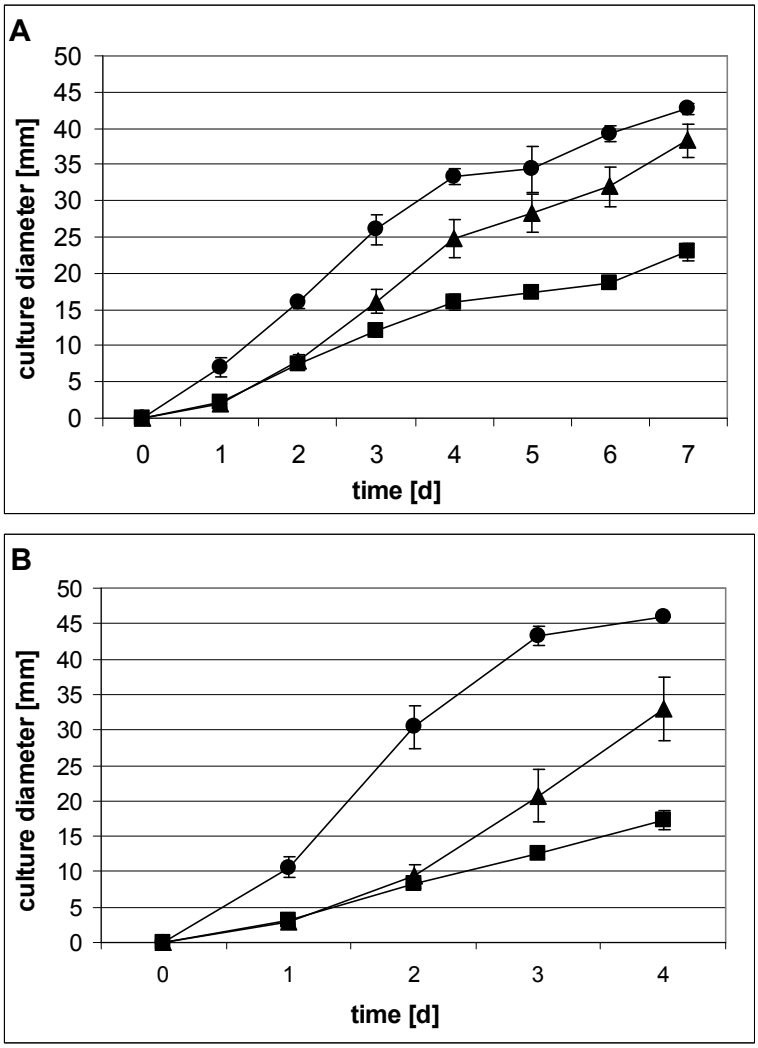

Fig. 27: Growth rate of the *F. graminearum* wild type strain 8/1 (●), the Δ*gmap1* mutants (■) and the Δ*gpmk1* mutants (▲) on CM plates (**A**) and on Czapek plates (**B**). Mycelial plugs of the wild type strain (n=10), three Δ*gmap1* mutants (n=5) and eight Δ*gpmk1* mutants (n=5) were inoculated on CM and Czapek plates, respectively, and incubated at 28°C in the dark.

After several days of growth in medium without selective Hygromycin B pressure, some of the Δ*gmap1* mutant cells started to grow as fast as the wild type cells. Thus, in a few areas of the colony the culture grew out rapidly in a fan shaped manner (compare Fig. 26). The fast growing mycelia had also lost their capability to grow under Hygromycin pressure, when placed on CM-plates containing Hygromycin. This phenomenon indicates the

Δ*gmap1* mutants to have a genetical wild type background, which coincides with the detection of a wild type PCR product during the screening of the transformants (compare 3.1.2.2.).

The biomass production was determined from the *F. graminearum* wild type strain, three Δ*gmap1* mutants, eight Δ*gpmk1* mutants, one *gmap1* and one *gpmk1* ectopic integration transformant (Fig. 28). In all cultures assayed, the biomass production was lower during growth in Czapek medium compared to CM-medium. Both ectopic integration transformants as well as all mutants tested, even the Δ*gmap1* mutants, showed no obvious difference in biomass production in comparison to the wild type strain.

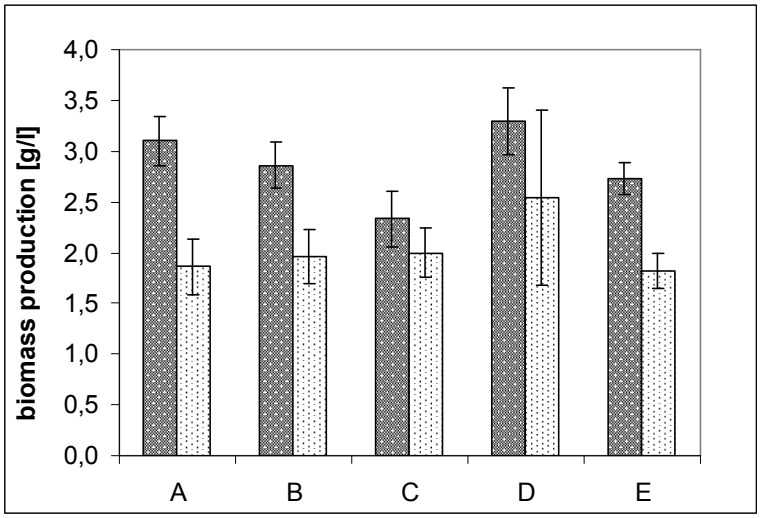

Fig. 28: Biomass production of the *F. graminearum* wild type strain 8/1 (A), three Δ*gmap1* mutants (B), eight Δ*gpmk1* mutants (C) and each one *gmap1* (D) and *gpmk1* (E) ectopic integration transformant in liquid CM (dark bars) and Czapek (light bars) medium. The wild type biomass production was assayed in triplicate and all mutants in duplicate. A mycelial plug (6 mm in diameter) was inoculated in 50 ml liquid CM and Czapek medium, respectively, and grown for three days at 28°C and 175 rpm. All transformants were grown under selective Hygromycin B (75 µg/ml) pressure. Finally, the mycelium was separated by filtration, lyophilized and weighed.

3.4.2. Conidia production

A participation of the described MAP kinases from *F. graminearum* in conidiation processes was examined by determining the conidia production of the wild type strain 8/1, three Δ*gmap1* mutants, eight Δ*gpmk1* mutants, one *gmap1* and one *gpmk1* ectopic

integration transformant (Fig. 29). Initially, the conidia production was plainly measured after growth on SNA plates. However, microscopic analysis of the culture plates revealed that the Δ*gpmk1* mutants produced conidia underneath the surface of the solid medium and only very few conidia on the surface. In addition, the conidia were not formed in typical large round bundles on the conidiophore, so called sporodochia, which were distinctly distributed over the SNA plate. Only three to four conidia were produced per conidiophore and these were found below the surface throughout the whole plate. In order to include the conidia produced under the surface of the solid medium, the fungal strains were grown on SNA covered with cellophane foil as a physical barrier. Under these conditions, conidiation of all strains increased 10- to 20-fold. Under both induction conditions all Δ*gpmk1* mutants tested showed a significant reduction in conidia production as compared to the wild type strain: 91 % on SNA without cellophane foil and 78 % on SNA with cellophane foil. The *gpmk1* ectopic integration transformant exhibited a conidia production similar to the wild type strain. The amount of conidia produced by the Δ*gmap1* mutants was comparable to the Δ*gmap1* ectopic integration mutant. On SNA without cellophane foil no difference was observed. Only on SNA with cellophane foil a 50 % reduction was seen by these mutants in comparison to the 8/1 strain. The viability of the conidia produced by the Δ*gmap1* and Δ*gpmk1* mutants was 90-100 %, which is comparable to the viability of the conidia from the wild type strain.

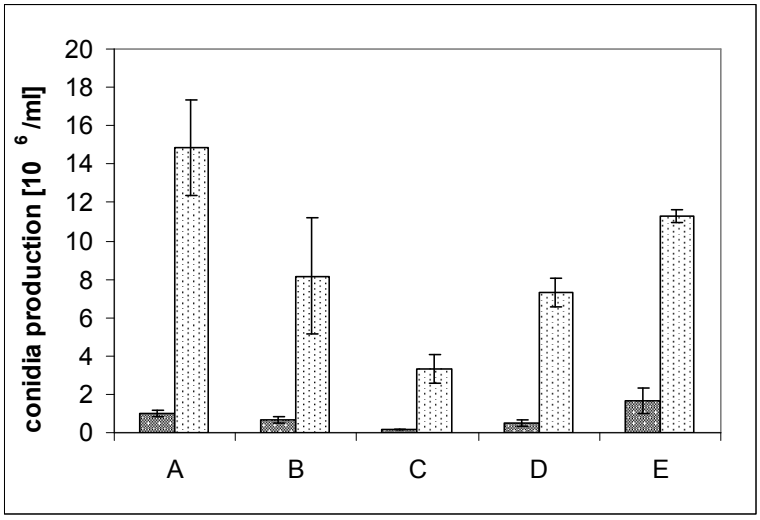

Fig. 29: Conidia production of the *F. graminearum* wild type strain 8/1 (A), three Δ*gmap1* mutants (B), eight Δ*gpmk1* mutants (C) and each one *gmap1* (D) and *gpmk1* (E) ectopic integration transformant on SNA without (dark bars) and with (light bars) cellophane foil. Culture incubation took place at 18°C under near-UV light and white light with a 12 h photoperiod. Conidia were washed off the plates with 1 ml water 16 d after inoculation and counted (n=4).

3.4.3. Sexual reproduction

The fertility of the *F. graminearum* wild type strain, the Δ*gmap1* and Δ*gpmk1* mutants as well as one *gmap1* and one *gpmk1* ectopic integration transformant were determined by counting the number of perithecia produced on carrot agar (compare 2.1.3.2.). All three independent Δ*gmap1* mutants, eight Δ*gpmk1* mutants, the wild type strain and the ectopic integration transformants were selfed several times. The wild type strain produced an average of 15 perithecia/plate. Ascospores could be isolated from the perithecia indicating the wild type strain to be fully fertile. The ectopic integration transformants produced 20-30 perithecia/plate. In all experiments the Δ*gpmk1* mutants were unable to form perithecia. The Δ*gmap1* mutants only showed 1-2 perithecia/plate. On closer view, these few perithecia were formed in the Δ*gmap1* colony zone, which showed the loss of the growth reduced phenotype, as observed for growth in absence of Hygromycin (compare 3.4.1.). This indicates that the perithecia were produced by the wild type contamination in the mutants. Figure 30 shows the perithecial development of the wild type strain, the Δ*gmap1* and Δ*gpmk1* mutants on carrot agar.

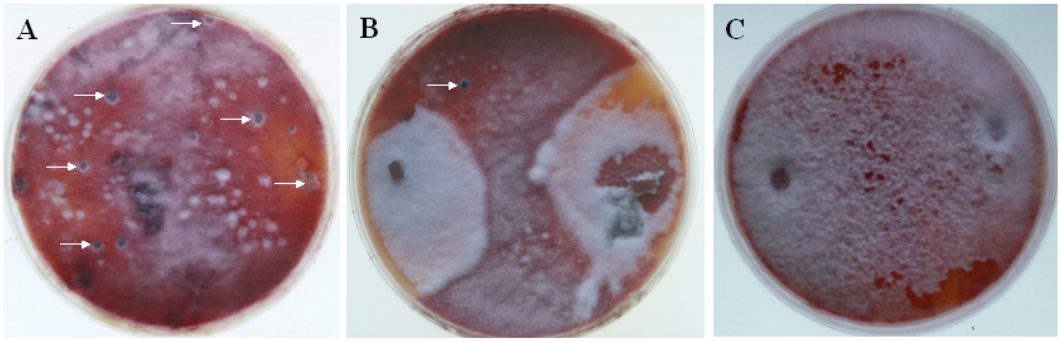

Fig. 30: Perithecial development on carrot agar. Small mycelial plugs from the *F. graminearum* wild type strain (A), a Δ*gmap1* mutant (B) and a Δ*gpmk1* mutant (C) were placed on opposite sides of the carrot agar plates and incubated at 24°C under a mixture of near-UV and white light with a 12 h photoperiod. After seven days the aerial mycelia was knocked down with 1 ml sterile 2.5 % Tween 60 solution. After further seven days perithecia were found covering the plate. Some of the perithecia are marked with white arrows.

The various strains were also outcrossed with each other. Outcrossing of the mutants with the wild type strain led to a clear cut line of mycelial separation, the so-called barrage. Perithecia were only produced on the plate side inoculated with the wild type. The same picture was found when the mutants were outcrossed with the corresponding ectopic integration transformant. Δ*gpmk1* mutants outcrossed with the Δ*gmap1* mutants did not

lead to the production of perithecia. Interestingly, the Δ*gpmk1* mutants also showed a drastic reduction in aerial mycelia formation on carrot agar.

3.4.4. Osmolarity assay

Fungal MAP kinases are also known to regulate stress dependent pathways (Xu 2000). Therefore, an involvment of the Gmap1 and Gpmk1 MAP kinase on the regulation of osmotic stress was tested by placing a mycelial plug on CM plates containing 0 M, 0.5 M, 0.75 M, 1 M, 1.5 M and 2 M NaCl, respectively. After four days the culture diameters were measured and compared to the growth of the wild type strain and the ectopic *gmap1* and *gpmk1* integration. In all cases an addition of 0.5 M NaCl increased the growth of *F. graminearum*. Higher NaCl concentrations led to a rapid decrease in growth. At 2 M NaCl no growth was detected. All MAP kinase mutants tested showed the same reaction towards a high osmotic surrounding as the wild type strain and the ectopic integration transformants (data not shown).

3.4.5. Pathogenicity tests

3.4.5.1. Virulence of Δ*gmap1* and Δ*gpmk1* mutants towards wheat

In order to determine whether the Gmap1 and Gpmk1 MAP kinases participate in signal transduction pathways, which are essential for pathogenicity on wheat spikes, plant inoculation tests were performed. Wheat spikes were point-inoculated with conidia suspensions of the *F. graminearum* wild type strain 8/1, three independent *gmap1* mutants, eight *gpmk1* mutants and the *gmap1* and *gpmk1* ectopic integration transformants, respectively. All strains were assayed several times. The infected spikes were monitored for three weeks. After four days the first symptoms of wild type strain infection could be seen as an obvious growth of aerial mycelia on the point-inoculated spikelet. The wheat spikes browned rapidly after six to seven days on the inoculated and the surrounding spikelets. Bleaching of the infected spikes was clearly visible two to three weeks after inoculation (Fig. 31 A).

The spikelets inoculated with Δ*gmap1* mutant conidia suspensions also showed growth of aerial mycelia. However, inoculation of the wheat spike with the Δ*gmap1* mutants led to browning only directly on the inoculated spikelet (Fig. 31 B).

The spikes inoculated with the Δ*gpmk1* mutant conidia suspensions showed slight growth of aerial mycelia on the surface of the inoculated spikelet 4 days after inoculation. No further signs of infection like browning or bleaching of the wheat spikes occured throughout the 3 weeks monitored, the spikes were totally uninfected (Fig. 31 C).

Fig. 31: Pathogenicity assays on wheat spikes. Wheat spikes at anthesis were point-inoculated twice with 500 conidia/10µl from the *F. graminearum* wild type strain (**A**), a Δ*gmap1* mutant (**B**), a Δ*gpmk1* mutant (**C**) and water as control (**D**). Infected spikes were enclosed in plasic bags for three days and were incubated for 21 days in a growth chamber.

Wheat infection with the ectopic integration mutants led to head blight symptoms comparable to the wild type strain (data not shown). Three weeks after plant inoculation the wheat spikes were removed from the plant and were tested for kernel development (Fig. 32). All spikelets of the spike inoculated with wild type conidia contained small, brown degenerated kernels typical for the head blight disease. Isolation of the kernels from *gmap1* mutant infected wheat spikes showed that kernel degeneration only took place in the visibly infected spikelets. An inoculation with the Δ*gpmk1* mutant had no effect on the kernel development. The inoculated spike exhibited normal, fully developed kernels. Even the kernel of the inoculated spikelet developed normally.

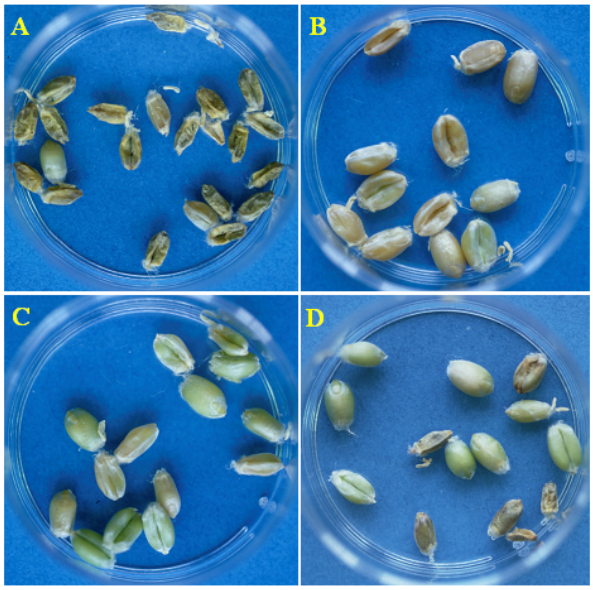

Fig. 32: Wheat kernels isolated from *F. graminearum* infected wheat spikes. Wheat spikes at anthesis were pointinoculated with 2 x 500 conidia/10µl from the *F. graminearum* wild type strain (**A**), a Δ*gpmk1* mutant (**C**), and a Δ*gmap1* mutant (**D**), as well as water as control (**B**). After 21 days cultivation in a growth chamber the kernels were isolated from the spikes and analysed for signs of *Fusarium* infection.

3.4.5.2. Virulence of Δ*gpmk1* mutants towards maize

F. graminearum has a very broad range of virulence and, therefore, this pathogen is also able to infect other host plants including barley and maize. Therefore, it was interesting to analyse, whether the *gpmk1* MAP kinase mutants show the same apathogenic phenotype on a different host, e.g. maize. The wild type strain 8/1 and four independent Δ*gpmk1* mutants were inoculated in three different conidia concentrations ($1x10^5$, $1x10^6$, $2x10^6$/2 ml) in the primary ears of maize plants. Thereby, the wild type was assayed four times and the mutants three times. Ears injected with water served as control. After three weeks cultivation in a growth chamber the infected ears were opened and the grade of infection was assayed (Fig. 33 and 34). Infection of the maize ears is noticeable by obvious browning and softening of the silks and the cob. A strong infection also leads to the browning of the leaves surrounding the cob. In order to determine the virulence of the various strains the total cob length was related to the length of the infected cob area. Corn development only took place occasionally, as the tassels had to be cut off prior to inoculation.

Ears infected with $1x10^5$ conidia from the wild type strain already showed slight signs of infection. Two from three cobs showed browning of the tips. Higher wild type conidia concentrations led to stronger symptoms like browning of the silks, the cob and the surrounding leaves. Thereby, ears infected with $1x10^6$ conidia exhibited an average infection rate of 63 %. A 100 % infection of the cob was found for all three ears inoculated

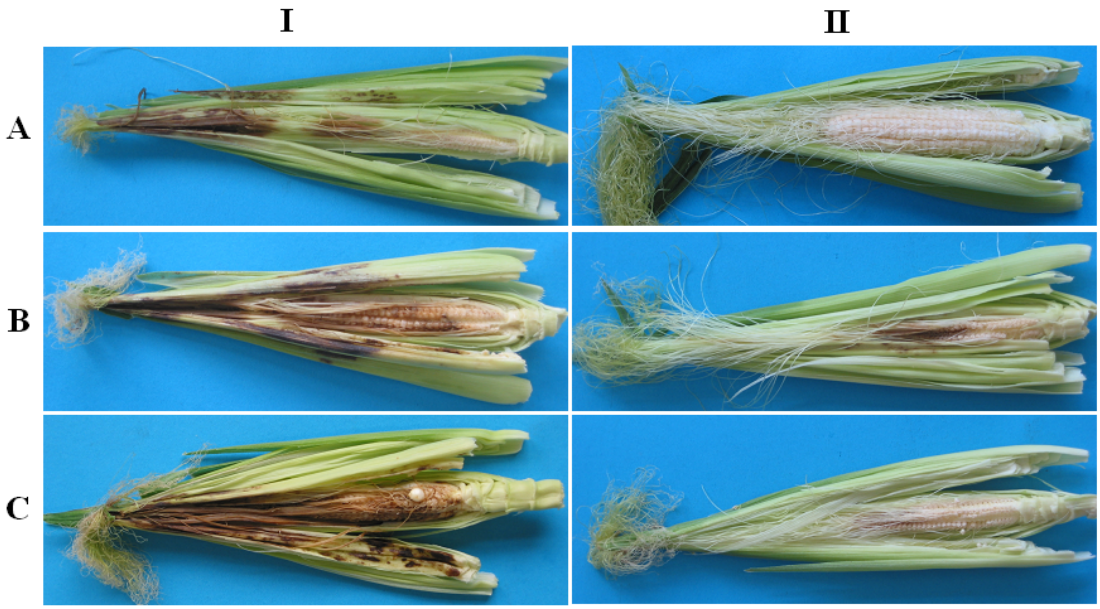

Fig. 33: Pathogenicity assay on maize ears. Maize plants were infected with *F. graminearum* by injecting conidia in three different concentration (A $1x10^5$; B $1x10^6$; C $2x10^6$/ 2 ml) into the silk channel of the primary ears. column I: *F. graminearum* wild type strain 8/1; column II: mutant with disrupted *gpmk1* gene. The inoculated maize plants were cultivated for three weeks in a growth chamber. Then the ears were opened and the infection was monitored.

with $2x10^6$ conidia. Ears infected with conidia from Δ*gpmk1* mutants only led to symptoms on the silks and the tip of the cob. If at all, only little browning of the surrounding leaves occurred. At least $1x10^6$ conidia from the Δ*gpmk1* mutants were needed for an infection. Only two from eight cobs infected with $1x10^6$ conidia showed high infection rates, 61 % and 75 % respectively. In the other six cases tested a maximum infection rate of 10 % was observed. Just the utmost tips of the cobs exhibited slight signs of browning. Higher conidia concentrations ($2x10^6$) only led to a slight increase in symptom development, thus showing an average infection rate of 16 %. Variations in disease establishment result from a generally high fluctuation in the sensitivity of the host. The sensitivity of maize towards *F. graminearum* infections was shown to be very dependent on the exact inoculation time and the general fitness of the inoculated plant (Reid and Hamilton 1995). Figure 33 pictures ears infected with wild type and Δ*gpmk1* mutant conidia in all three concentrations tested. For this figure the ears with the strongest possible infections were used. Analysis of the average grade of cob infection indicated the Δ*gpmk1* mutants to have a drastically reduced virulence toward maize (Fig. 34).

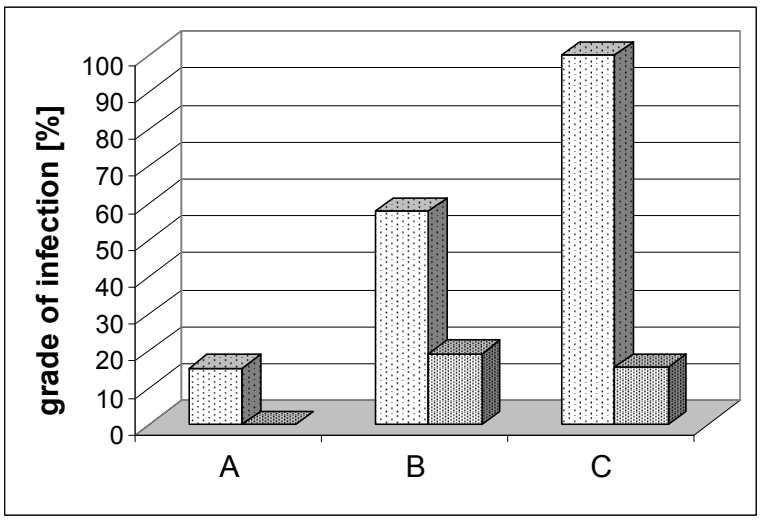

Fig. 34: Average grade of cob infection after inoculation with the *F. graminearum* wild type strain (light bars; n=4) and four Δ*gpmk1* mutants (dark bars; n=3). Maize ears were inoculated with different conidia amounts: 1 x 10^5 (A), 1 x 10^6 (B), and 2 x 10^6 (C). Three weeks post inoculation the ears were opened and the infection rate was determined. The percentage of infection represents the ratio of the length of the infected cob to the total cob length. The results of every single measurement have been summarized to gain a mean value of infection.

3.5. Toxin assays

Secretion of various mycotoxins is one of the most important strategies of *F. graminearum* to colonize the host tissue. Particularly the secretion of deoxynivalenol (DON) has been shown to be essential for the progress of infection over complete wheat spikes (Bai et al. 2001). Other mycotoxins secreted by *F. graminearum*, zeralenone (ZON) and fumonisin, have up to date not been proven to be virulence factors during plant infection. As mycotoxin secretion is such a fundamental mechanism of the *F. graminearum* infection, it was inevitable to examine, whether the Δ*gpmk1* mutants apathogenicity on wheat and drastically reduced virulence on maize is due to a decreased mycotoxin production. This would enable to correlate mycotoxin production directly to the fungal virulence.

After induction of mycotoxin production the probes were sent to the Institute for Agrobiotechnology (IFA) in Tulln, Austria. The isolation and detection of the toxins were accomplished there. To relate the amount of toxins determined in the plant tissue to the fungal biomass, the concentration of ergosterol, an membrane component exclusively found in fungi, was also measured. The ergosterol measurements also took place at the IFA.

Induction of toxin production was carried out on three different substrates: wheat kernels, maize kernels and rice supplemented with sugars. During the cultivation a drastic growth attenuation of the mutants on all substrates was observed. The wild type strain rapidly cultivated the substrate with thick white mycelia, whereas the mutants hardly showed mycelial growth. Obvious growth of the mutants was detected earliest after two to three weeks incubation at 28°C.

3.5.1. Toxin production on wheat kernels

In a first approach to induce mycotoxin production the *F. graminearum* wild type strain 8/1 and four independent Δ*gpmk1* mutants were inoculated as mycelia plugs on sterilized and wheeled wheat kernels followed by a 28 d cultivation at 28°C. All probes were analysed for DON, ZON and ergosterol content.

In all probes, including the wild type strain probe, only an induction of ZON had taken place. No DON was detectable in the probes. The measurement of ZON content in the probes showed that the mutants disrupted in the *gpmk1* gene had a drastic defect in ZON induction. In three from four mutant cultures no ZON was detectable. The fourth mutant had produced a 10 fold lower ZON amount compared to the wild type strain (Fig. 35).

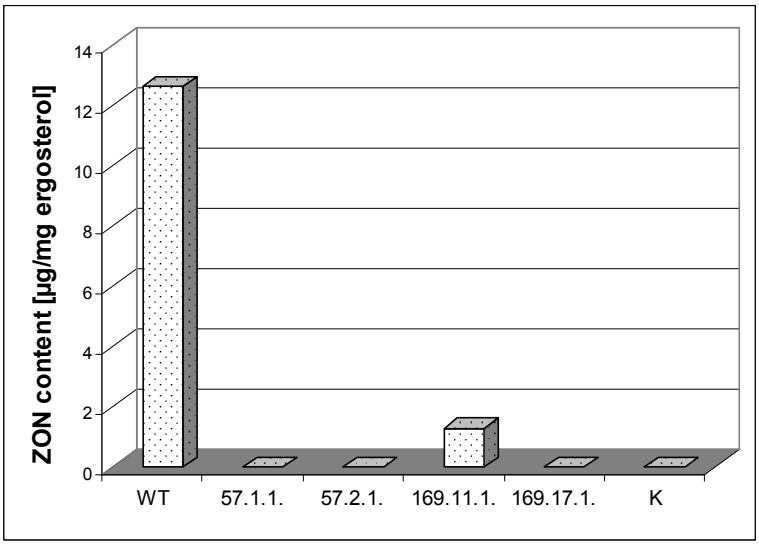

Fig. 35: Wheat induced production of zearalenone (ZON) by the *F. graminearum* wild type strain (WT) and four independent *gpmk1* disruption mutants (57.1.1., 57.2.1., 169.11.1., 169.17.1.). Mycelial plugs from each strain were inoculated on sterile, whelled wheat kernels and cultivated for 28 days in the dark at 28°C. The cultures were then dried for 4 days at 45°C and milled to fine powder. K= uninfected wheat kernels as control. The probes were measured for ZON content by HPLC-FLD. The detection limit of ZON was 3 µg/kg. The ergosterol content was determined by GC-MS, having a detection limit of 0.5 mg/kg.

3.5.2. Toxin production on maize kernels

In order to compare mutants and wild type concerning their DON production, a new mode of cultivation was carried out. Hence, the *F. graminearum* wild type strain 8/1 and four independent Δ*gpmk1* mutants were inoculated as mycelia plugs on sterilized maize kernels followed by one week cultivation at 28°C in the dark and two weeks at room temperature in a semi-light place. All probes were analysed for DON, ZON and ergosterol content.

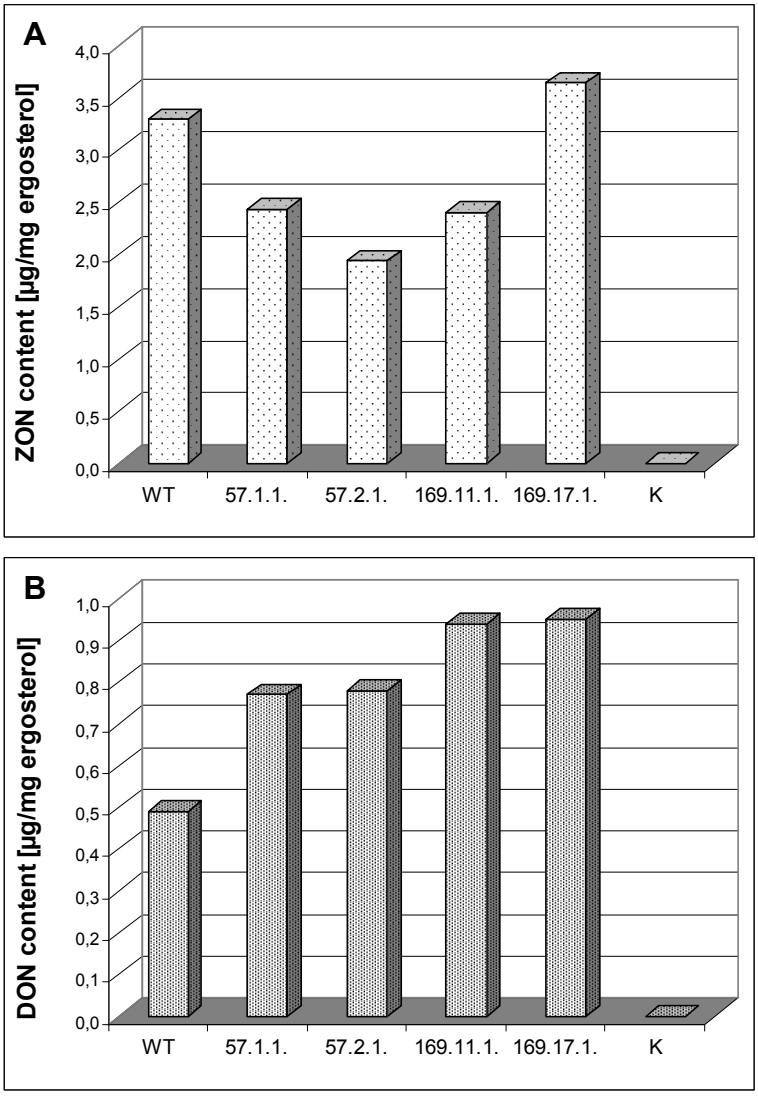

Fig. 36: Maize induced production of **A**) zearalenone (ZON) and **B**) deoxynivalenol (DON) by the *F. graminearum* wild type strain (WT) and four independent *gpmk1* disruption mutants (57.1.1., 57.2.1., 169.11.1., 169.17.1.). Mycelial plugs from each strain were inoculated on sterile maize kernels and cultivated for two weeks at 28°C in the dark and one week at room temperature in a semi-light place. The cultures were then dried for 4 days at 45°C and milled to fine powder. K= uninfected maize kernels as control. The probes were measured for ZON content by HPLC-FLD. The detection limit of ZON was 3 µg/kg. DON was analysed by GC-ECD. The detection limit of DON was 60 µg/kg. The ergosterol content was determined by GC-MS, having a detection limit of 0.5 mg/kg.

This cultivation mode resulted in an induction of ZON as well as DON production (Fig. 36). The wild type strain produced approximately 7 fold higher amounts of ZON than of DON. However, the wild type revealed a 4-fold lower ZON content in the maize culture compared to the induction on wheat kernels. All four mutants tested showed varying amounts of ZON, but the average amount was comparable to the wild type ZON production. The DON contents produced by the analysed MAP kinase mutants were slightly higher than the wild type DON content, indicating the disruption of the *gpmk1* gene to have no influence on the DON induction under the given conditions.

3.5.3. Toxin production on rice

Finally, a third medium for DON and ZON induction was tested. Thereby, the *F. graminearum* wild type strain 8/1 and four independent Δ*gpmk1* mutants were inoculated as mycelial suspension on rice supplemented with saccharose and casein to ensure a high carbon concentration. The probes were cultivated at 28°C for six weeks in special jars that enabled maximum oxygen influx. The DON, ZON and ergosterol content of all probes was analysed. Besides the DON and ZON analysis, all rice cultures were tested for the production of the DON-precursors 3-acetyldeoxynivalenol (3-ADON) and 15-acetyldeoxynivalenol (15-ADON) as well as the trichothecene nivalenol (NIV).
The rice medium had the strongest effect on the toxin induction (Fig. 37). On rice the wild type strain exhibited a 7 fold stronger ZON induction than on maize and a 2 fold stronger induction than on wheat kernels. Its DON production was also 9 fold higher than on the maize substrate. On rice the wild type again produced more ZON than DON. Similar to the wheat induction, the Δ*gpmk1* mutants revealed a drastically reduced ZON content compared to the wild type strain. As average, the mutant cultures produced only 3.5 % of the wild type ZON amount. Hence, on rice the *gpmk1* disruption results in the inability to induce the ZON production. Concerning the DON production, the Δ*gpmk1* mutants exhibited varying amounts of DON, ranging from 42 % to 100 % of the wild type DON content. Therefore, a regulation of DON via the Gpmk1 pathway is questionable. Finally, neither the precursors 3-ADON and 15-ADON, nor NIV could be measured in any of the probes including the wild type strain (data not shown).

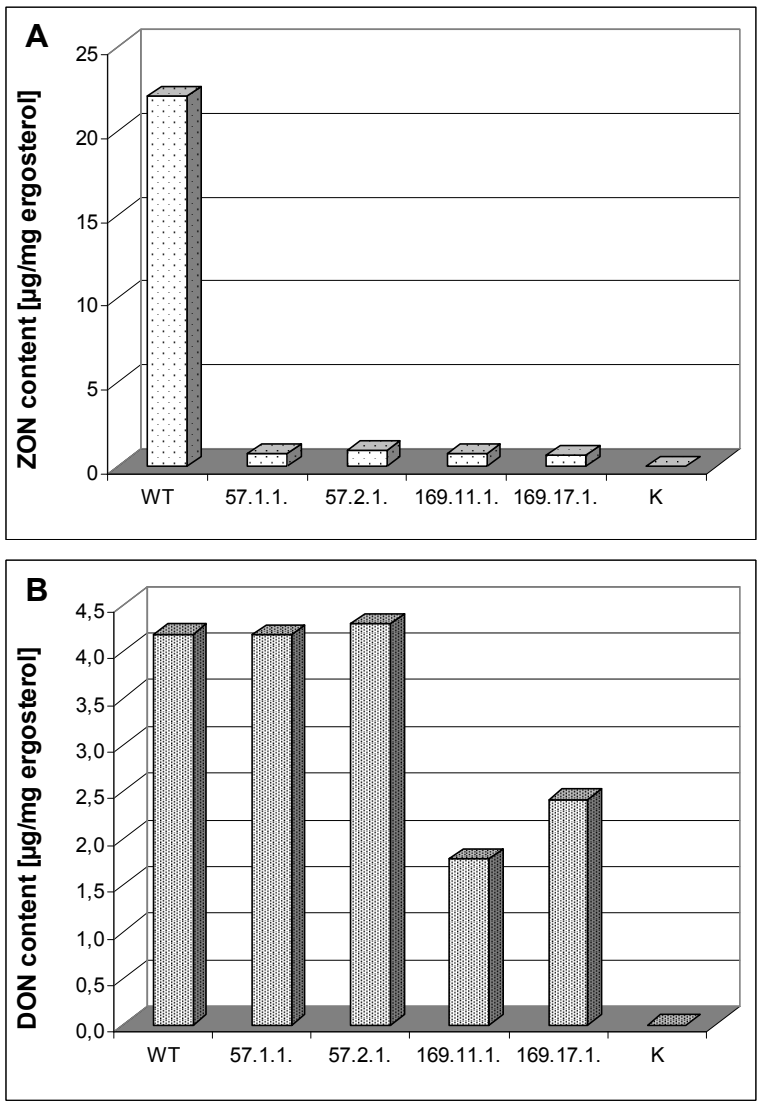

Fig. 37: Rice induced production of **A**) zearalenone (ZON) and **B**) deoxynivalenol (DON) by the *F. graminearum* wild type strain (WT) and four independent *gpmk1* disruption mutants (57.1.1., 57.2.1., 169.11.1., 169.17.1.). A mycelial suspension from each strain was inoculated on sterile rice supplemented with 8 ml sugar solution (38 g/l saccharose and 2.5 g/l hydrolysed casein) and cultivated for six weeks at 28°C in the dark in baby food jars with Magenta B caps (Sigma). The cultures were then dried for 4 days at 45°C and milled to fine powder. K= uninfected maize kernels as control. The probes were measured for ZON content by HPLC-FLD. The detection limit of ZON was 3 µg/kg. DON was analysed by GC-ECD. The detection limit of DON was 60 µg/kg. The ergosterol content was determined by GC-MS, having a detection limit of 0.5 mg/kg.

3.6. The effect of *gpmk1* disruption on the secretion of hydrolytic enzymes

3.6.1. Qualitative plate assays

As *F. graminearum* was shown to be a non-appressoria forming pathogen (Pritsch et al. 2000), an enzymatic digestion of the plant cell wall seems more likely to be its mode of penetration. Therefore, the secretion of cell wall degrading enzymes is necessary. A

possible degradation of the plant cell wall by *F. graminearum* has already been postulated by Wanjiru and co-workers (Wanjiru et al. 2002), who found that the wheat cell wall components were reduced upon invasive growth of *F. graminearum*. Nevertheless, up to date no detailed analysis have been done.

In a first approach, plate assays were conducted to find out which secretory enzymes could be expected. Minimal media containing one sole carbon source were inoculated with the *F. graminearum* wild type strain 8/1. Substrate hydrolysis was generally made visible by a colour reaction within the medium. Either azur cross-linked substrates were used, which upon hydrolysis lead to a blue staining of the medium, or the substrate disappearance or product formation was specifically stained. This screening revealed that *F. graminearum* is able to secrete a range of enzymes needed for degradation of polymers present in the plant cell wall. Amylolytic, xylanolytic, cellulolytic, and proteolytic activities were found (Fig. 38 A, B, C, D).

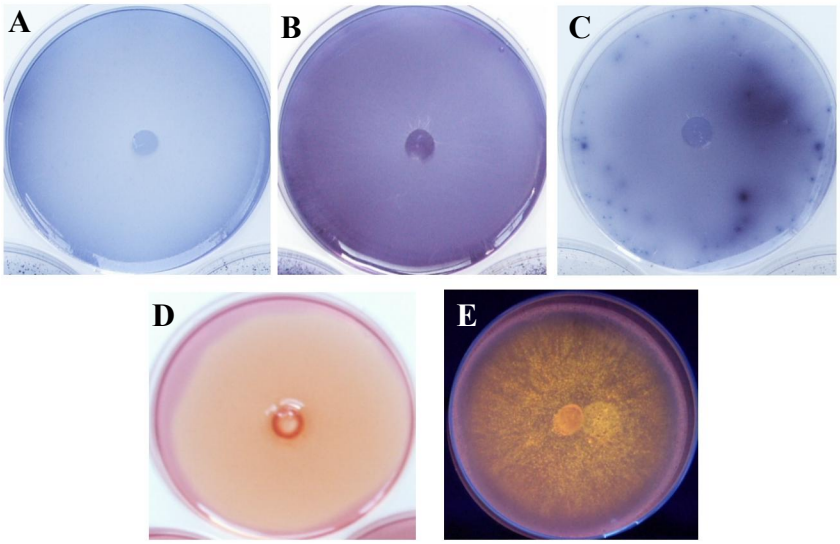

Fig. 38: Secretion of hydrolyzing enzymes by *F. graminearum* wild type strain 8/1 as shown by plate assays. Minimal medium was substituted with one sole carbon source (**A:** amylose; **B:** xylan; **C:** casein; **D:** carboxymethylcellulose; **E:** olive oil). Substrates A, B and C are linked to azur blue. Enzymatic hydrolysis of these substrates leads to a homogenous blue staining of the medium. The plate containing carboxymethylcellulose (D) was dyed with congo red. Degradation of the substrate forms a halo around the colony. Plate E contains Rhodamine B as dye. Cleavage of the olive oil leads to free fatty acids. These form a complex with Rhodamine B, which is visible as a fluorescent halo around the culture if examined under UV light.

The secretion of lipolytic enzymes by *F. graminearum* has already been examined (Christian Haase, unpublished data). Nevertheless, a plate assay (Kouker and Jaeger 1987) using olive oil as substrate and Rhodamine B as dye was also carried out in this set of experiments (Fig. 38 E). All hydrolytic activities could be found in the *gpmk1* disruption

mutants. Yet, a visible reduction of Δ*gpmk1* mutant enzyme secretion was detectable only on the plates containing olive oil as substrate, giving a first indication that these mutants might show an altered lipoylic activity (Fig. 39).

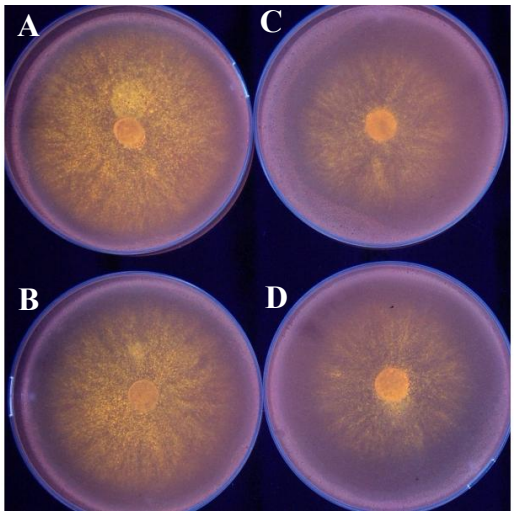

Fig. 39: Plate assay showing the secretion of lipolytic enzymes. **A**: *F. graminearum* wild type strain, **B**: *gpmk1* ectopic integration transformant, **C** and **D**: two of the six tested *gpmk1* disruption mutants. The fungal strains were inoculated on plates containing olive oil as substrate and Rhodamine B as dye. Three days after inoculation the plates were examined under UV light. Fatty acids set free from the substrate by lipolytic enzymes form orange fluorescent complexes with Rhodamine B.

3.6.2. Quantitative, photometric enzyme assays

Qualitative plate assays however do not suffice to analyse enzyme reductions in mutants effectively. Even if enzymes are secreted in lower amounts, they accumulate in the plate and continuously degrade the substrate, so that differences in enzyme secretion can hardly be seen. In order to quantify the secretion of hydrolyzing enzymes that were found to be produced by *F. graminearum* (compare 3.6.1.), the enzyme activities within the culture supernatants were determined with photometric assays. Comparison of enzyme activities from the Δ*gpmk1* mutants and the *F. graminearum* wild type strain could then possibly give a clue to find out which hydrolytic enzymes are particularly important for the infection process and, thus being a potential cause for the apathogenic phenotype of these MAP kinase mutants.

The wild type strain 8/1, in general four independant Δ*gpmk1* mutants, and the Δ*pks* mutant 31.10A as control (kindly provided by Sascha Malz), were precultured in liquid medium and then induced in liquid minimal medium containing soluble starch, pectin, carboxymethylcellulose, xylan, casein or wheat germ oil as sole carbon source, respectively. The cultures were induced over several hours during which probes were taken. The enzyme activities of these samples were assayed. The hydrolysis of the

polymeric carbohydrate cell wall components, such as cellulose, starch, pectin, and xylan, were assayed by determination of the released reducing sugars.

3.6.2.1. Amylolytic activity

Secretion of amylolytic enzymes was induced by cultivating the *F. graminearum* strains in medium with soluble starch as sole carbon source. The culture supernatant from samples taken at different time points were then incubated in buffer with soluble starch as substrate. Figure 40 shows the specific amylolytic activities of the *F. graminearum* wild type strain 8/1, the Δ*pks* mutant, and four independent Δ*gpmk1* mutants. In the wild type culture supernatant an obvious amylolytic activity was detectable six hours after induction. A maximum activity of 540 nmol/min*mg was reached after 24 hours followed by a rapid decrease in amylolytic activity. This decrease in activity suggests a reduction in enzyme secretion or an inactivation of amylase activity by e.g. changes in the pH conditions of the culture. The Δ*pks* mutant exhibited a similar pattern of amylase induction. Among the four Δ*gpmk1* mutants the measured amylolytic activities varied considerably. Nevertheless, the average amylase activity showed only little difference to the wild type values. Thus, under the chosen conditions, the disruption of the *gpmk1* gene has no influence on the amylolytic enzyme activity within the supernatant.

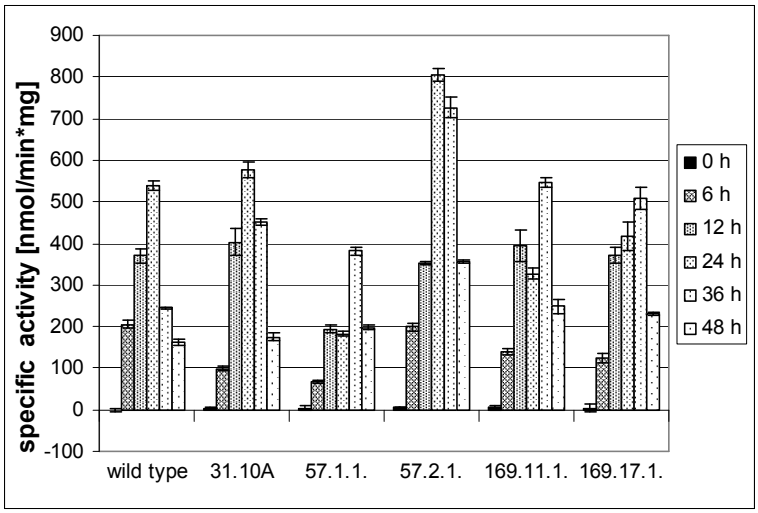

Fig. 40: Specific amylolytic activity within the culture supernatant. The *F. graminearum* wild type strain 8/1, the Δ*pks* mutant 31.10A, and four independent Δ*gpmk1* mutants (57.1.1., 57.2.1., 169.11.1., 169.17.1.) were induced with soluble starch. Culture probes were withdrawn at six time points after induction. The supernatants were then incubated at 37°C in 50 mM sodium acetate, pH 5, containing 1 % soluble starch as substrate. The amylase activity was determined by measuring the amount of reducing sugars set free from the substrate per minute and mg protein (n=4).

3.6.2.2. Polygalacturonase activity

Pectin as sole carbon source was used to induce secreted pectinase activity in *F. graminearum* cultures. As the enzyme assay was conducted under acidic conditions, the assay was only able to detect polygalacturonases activity. Pectate lyases, another pectin cleaving enzyme, generally have their reaction optimum around pH 9 and are, therefore, not expected to be active under the given conditions. Only the wild type strain 8/1 and two Δ*gpmk1* mutants were tested for their polygalacturonases activity (Fig. 41).

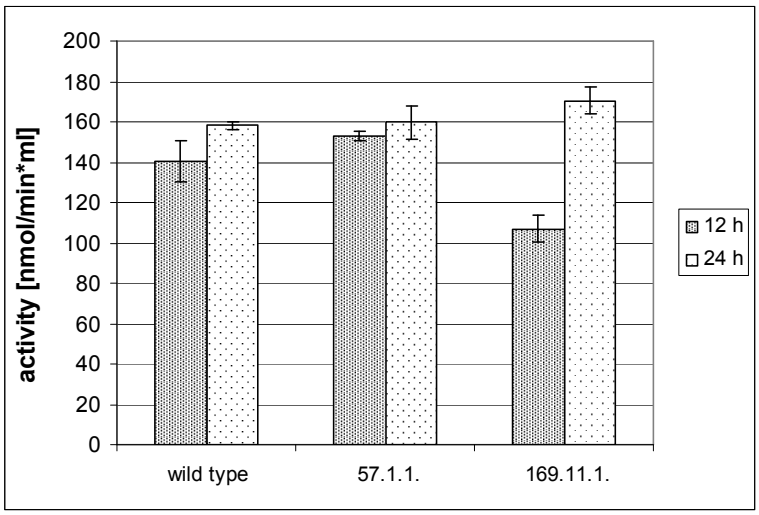

Fig. 41: Polygalacturonases activity within the culture supernatant. The *F. graminearum* wild type strain 8/1 and two independent Δ*gpmk1* mutants (57.1.1., 169.11.1.) were induced with pectin. Culture probes were withdrawn at two time points after induction. The supernatants were then incubated at 37°C in 50 mM sodium acetate, pH 5, containing 1 % pectin as substrate. The polygalacturonase activity was expressed as the amount of reducing sugars set free from the substrate per minute and ml culture supernatant (n=4).

Culture supernatant probes were incubated in buffer with pectin as substrate. These enzyme activities were calculated for a total of 1 ml culture supernatant and not refered to the protein content, as the residual pectin in the culture supernatant interfered with the protein assays used. At both time points, 12 h and 24 h after inoculation, the Δ*gpmk1* mutants exhibited extracellular polygalacturonases activitiy levels comparable to the wild type strain, indicating no effect of the Gpmk1 MAP kinase on pectinase induction. Therefore, no further experiments including more mutants and more time points were done.

3.6.2.3. Proteolytic activity

In a first approach to find the optimal substrate for protease induction, the *F. graminearum* wild type was induced with casein, casein hydrolysate, skim milk, and bovine serum

albomin (data not shown). The test showed skim milk and casein to be the best inducters of secreted protease activity. Therefore, in the following assay the *F. graminearum* wild type strain 8/1, the Δ*pks* mutant, and four Δ*gpmk1* mutants were induced in minimal medium with casein as sole carbon source. The culture supernatant from probes taken at various time points were then incubated in buffer with casein as substrate. Total proteolytic activity was determined by measuring the release of the aromatic amino acids after trichloric acid precipitation of the residual substrate (Fig. 42). Again the obtained activities were calculated per ml culture supernatant as the total amount of protein secreted by the fungal strains can not be distinguished from the protein added to the medium as substrate.

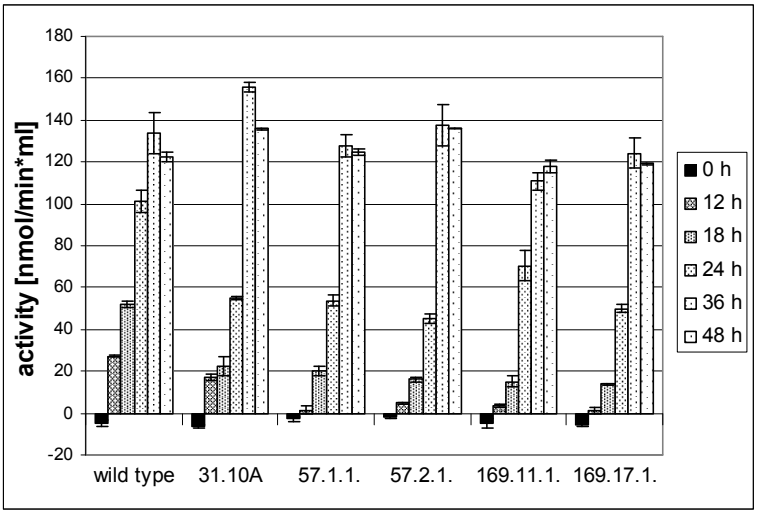

Fig. 42: Proteolytic activity within the culture supernatant. The *F. graminearum* wild type strain 8/1, the Δ*pks* mutant 31.10A, and four independent Δ*gpmk1* mutants (57.1.1., 57.2.1., 169.11.1., 169.17.1.) were induced with casein. Culture probes were withdrawn at six time points after induction. The supernatants were then incubated at 37°C in 0.2 M Tris HCl and 0.02 M $CaCl_2$, pH7.8; containing 1 mg/ml Hammarsteen casein as substrate. After precipitation of the residual casein with 20 % trichloric acid, the release of aromatic amino acids was determined and calculated per minute and ml culture supernatant (n=2).

The wild type extracellular protease activity was detectable 12 h after inoculation and continued to increase until it reached a maximum of 130 nmol/min*ml at 36 h followed by a slight decrease. The Δ*pks* mutant showed a similar protease induction pattern, thereby, reaching maximum activities of 150 nmol/min*ml. All Δ*gpmk1* mutants showed a slight time lag in protease induction. Enzyme activity was first detectable 18 h after inoculation i.e. six hours later than in the wild type and the Δ*pks* mutant supernatants. Nevertheless, the proteolytic activities of the mutants then rapidly reached wild type levels and also had their maximum activity at 36 h.

3.6.2.4. Xylanolytic activity

Xylanase secretion was induced by using xylan as sole carbon source in the growth medium. The xylanolytic activity levels were determined from the *F. graminearum* wild type strain 8/1, the Δ*pks* mutant, and four independent Δ*gpmk1* mutants at six different induction time points. These probes were then incubated in buffer with xylan as substrate. Similar to pectin, the residue xylan in the culture supernatant also interacts with the protein assays tested, so that the total protein concentration of the supernatant could not be measured. Therefore, the activities were again calculated per ml culture supernatant.

Figure 43 displays the xylanolytic activities measured for the mentioned *F. graminearum* strains. Wild type xylanolytic activity was detectable six hours after infection and then drastically increased up to activity values of 185 nmol/min*ml during the complete time range tested. The Δ*pks* mutant, only had a slight induction lag in the first 12 h (~50 % reduction). Otherwise it exhibited a comparable activity pattern. One Δ*gpmk1* mutant (57.1.1.) surprisingly showed similar xylanolytic activity levels to the Δ*pks* mutant. Nevertheless, the other three MAP kinase disruption mutants (57.2.1., 169.11.1., 169.17.1.) clearly displayed a delayed induction of xylanase secretion, as the mutants activity levels in the first 12 h were in average reduced to approximately 95 % of the wild type xylanolytic activity. Xylanase induction started to take place in the mutant cultures after

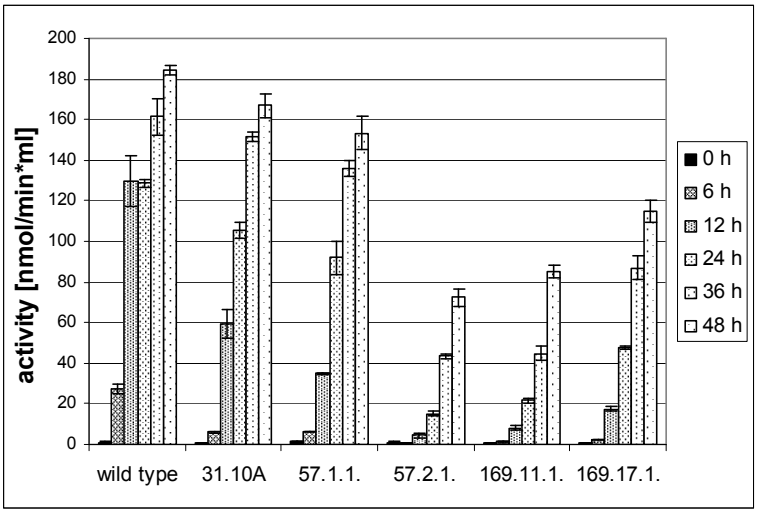

Fig. 43: Xylanolytic activity within the culture supernatant. The *F. graminearum* wild type strain 8/1, the Δ*pks* mutant 31.10A, and four independent Δ*gpmk1* mutants (57.1.1., 57.2.1., 169.11.1., 169.17.1.) were induced with xylan. Culture probes were taken at six time points after induction. The supernatants were then incubated at 37°C in 50 mM sodium acetate, pH 5, containing 1 % xylan as substrate. The xylanase activity was determined by measuring the amount of reducing sugars set free from the substrate per minute and ml culture supernatant (n=4).

24 h. However, during the complete time range tested, all three mutants did not reach the enzyme activity levels of the wild type strain, indicating the gpmk1 disruption to have an effect on the xylanase production.

3.6.2.5. Endoglucanase activity

The cellulase activity was measured using carboxmethylcellulose as sole carbon source during growth of the cultures and as substrate for the enzyme assay. With this specific substrate it is only possible to assay the activity of one enzyme type of the cellulose degrading complex, the endo-1,4-β-glucanases (EG; Béguin 1990). Figure 44 shows the specific EG activities of the *F. graminearum* wild type strain 8/1, the Δ*pks* mutant, and four independent Δ*gpmk1* mutants. Wild type strain EG activities rapidly increased after induction with carboxmethylcellulose and reached maximum values of 60 nmol/min*mg after 48 h in the induction medium. Again, the Δ*pks* mutant showed a slightly slower induction compared to the wild type strain, but it did reach the same activity levels as the wild type after 48 h induction. In all mutants tested, the disruption of the *gpmk1* gene had a drastic effect on the EG induction. Mutant EG activity was first detectable, when the wild type strain had almost reached maximum activity levels. This indicates the MAP kinase to play a role in early enzyme induction. After induction had taken place, the various Δ*gpmk1*

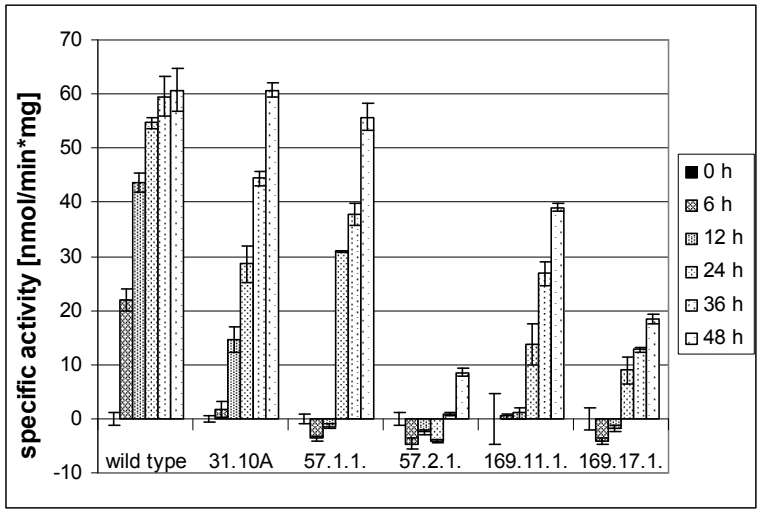

Fig. 44: Specific endo-1,4-β-glucanase activity within the culture supernatant. The *F. graminearum* wild type strain 8/1, the Δ*pks* mutant 31.10A, and four independent Δ*gpmk1* mutants (57.1.1., 57.2.1., 169.11.1., 169.17.1.) were induced with carboxymethylcellulose. Culture probes were withdrawn at six time points after induction. The supernatants were then incubated at 37°C in 50 mM sodium acetate, pH 5, containing 1 % carboxymethylcellulose as substrate. The endoglucanase activity is expressed as the amount of reducing sugars set free from the substrate per minute and mg protein (n=4).

mutants showed different rates of enzyme secretion. Similar to the xylanase assay, the mutant 57.1.1. exhibited fast induction and high enzyme activities, whereas the mutants 57.2.1., 169.11.1., and 169.17.1. additionally displayed a drastic reduction in overall EG activity.

An additional measurement of the complete cellulolytic activity using crystalline cellulose as substrate for the minimal medium and the enzyme assay failed. No enzyme activities were detected in all cultures tested, so that one can conclude that crystalline cellulose does not suffice for the induction of cellulase secretion in a liquid culture.

3.6.2.6. Lipolytic activity

The highest induction of lipolytic activity was detected when the cultures were precultivated in YPG medium and then induced in water with wheatgerm oil as substrate. Thereby, it is excessively important to clear all residual sugars, as the expression of secreted lipases from *F. graminearum* are strongly glucose repressable (Christian Haase, unpublished data). Probes were taken at four different time points and the supernatants were incubated in buffer with p-nitrophenol palmitate as substrate. The secreted lipases from the supernatant cleave fatty acids from the substrate releasing p-nitrophenol, which concentration is determined photometrically. The lipase activity was described as the amount of p-nitrophenol released over a certain time course.

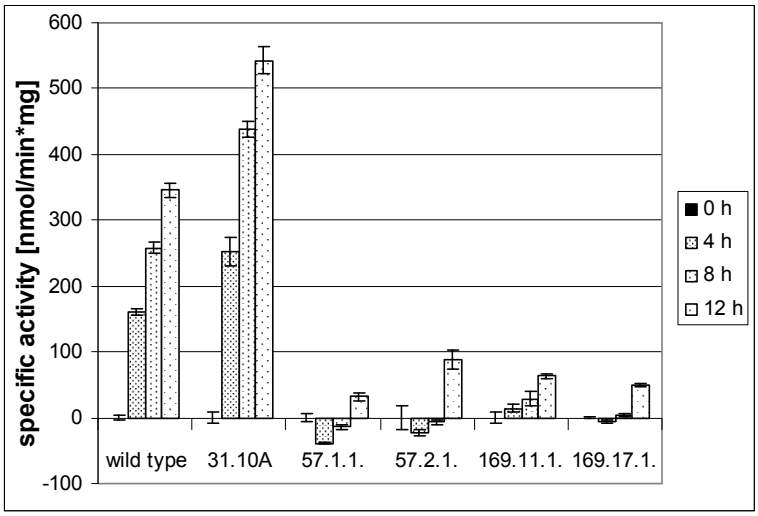

Fig. 45: Specific lipolytic activity within the culture supernatant. The *F. graminearum* wild type strain 8/1, the Δ*pks* mutant 31.10A, and four independent Δ*gpmk1* mutants (57.1.1., 57.2.1., 169.11.1., 169.17.1.) were induced with wheatgerm oil. Culture probes were taken at four time points after induction. The supernatants were then incubated at 37°C in 50 mM bis-tris-propane, pH 7.5, containing 1 mg/ml gum arabic, 0.1 % Triton X-100 and 2 mM p-nitrophenol palmitate as substrate. The lipolytic activity was determined by measuring the amount of p-nitrophenol released from the substrate per minute and mg protein (n=3).

The wild type strain and the Δ*pks* mutant showed lipolytic activity already four hours after induction with wheatgerm oil. The activities increased over the following eight hours to maximum activity levels of 350 nmol/min*mg for the wild type strain and 550 nmol/min*mg for the Δ*pks* mutant (Fig. 45). The Δ*pks* mutant showed over all time points measured an obviously higher lipolytic activity compared to the wild type strain. Disruption of the gene encoding the Gpmk1 MAP kinase led to dramatic effects concerning the induction of lipolytic activity. All mutants showed a 8-12 h delay in enzyme induction. Even after obvious induction had taken place the total lipolytic activities of the mutants only reached an average of 20 % of wild type strain activity.

Additionally, the lipolytic activities in the crude extracts from the cell pellets (8 h induced) of all strains were measured (Fig. 46). No significantly higher enzyme activities were found in the cell pellets of the mutant strains compared to the wild type, indicating the reductions in mutant enzyme activities in the supernatant to not be due to an insufficient secretion. Thus, reductions in enzyme activities can be attributed to delayed enzyme induction either on transcriptional or poststranscriptional level. Nevertheless, the mutants showed a higher lipolytic activity in the crude cell extract than in the supernatant,

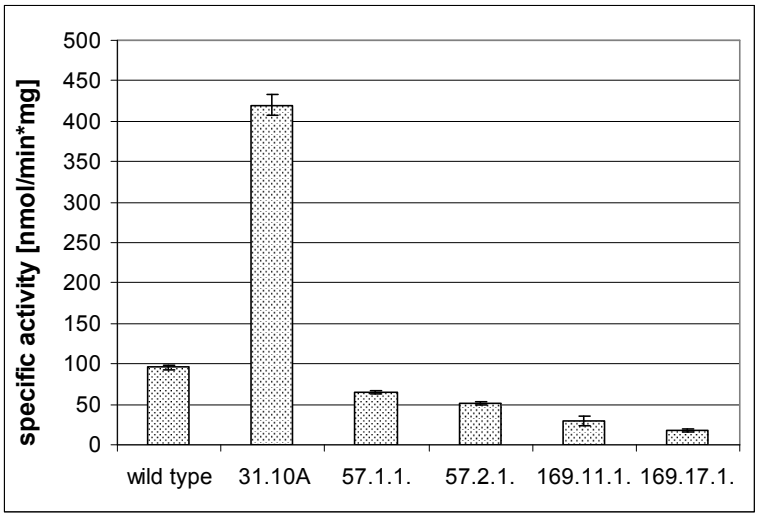

Fig. 46: Specific lipolytic activity within the crude cell extract. The *F. graminearum* wild type strain 8/1, the Δ*pks* mutant 31.10A, and four independent Δ*gpmk1* mutants (57.1.1., 57.2.1., 169.11.1., 169.17.1.) were induced with wheatgerm oil. Culture probes were taken after 8 h induction. An extract was isolated from the cell pellet by homogenizing the pellet in 50 mM bis-tris-propane, pH 7.5. The crude cell extracts were then incubated for 30 min at 37°C in 50 mM bis-tris-propane, pH 7.5, containing 1 mg/ml gum arabic, 0.1 % Triton X-100 and 2 mM p-nitrophenol palmitate as substrate. The lipolytic activity was determined by measuring the amount of p-nitrophenol set free from the substrate per minute and mg protein (n=3).

indicating some additional intracellular lipolytic activity, which does not seem to be influenced by the disruption of the *gpmk1* gene. The Δ*pks* mutant also exhibits the highest lipolytic activity in the crude cell extract, when compared to the other strains.
Furthermore, the mutant cultures exhibited a visible red colouring of the supernatant and the mycelium after 24 h growth in the water-wheatgerm oil suspension (Fig. 47), indicating the mutants to have suffered from stress symptoms. These results suggest the participation of the Gpmk1 MAP kinase in the regulation of secreted lipolytic enzymes.

Fig. 47: *F. graminearum* cultures after 24 h growth in water-wheatgerm oil suspension. **A**) Δ*pks* mutant 31.10A, **B**) wild type strain, **C**) Δ*gpmk1* mutant 57.2.1., and **D**) Δ*gpmk1* mutant 169.17.1.. After two days precultivation in YPG the cultures were washed and grown for an additional day in water with 2 % wheatgerm oil.

3.6.3. Growth assays

In order to examine, whether a reduction in enzyme activity consequently limits the growth of *F. graminearum* on media containing the specific substrates as sole carbon source, further growth assays were carried out. A minimal medium was supplemented with one sole carbon source as substrate. Thereby, the following substrates were tested: crystalline cellulose, carboxymethylcellulose, cellophane foil, xylan, wheatgerm oil, soluble starch, pectin, and casein. Mycelial plugs of the *F. graminearum* wild type strain 8/1, the Δ*pks* mutant, and four Δ*gpmk1* mutants were set on 60 mm plates containing the media mentioned above. The cultures were incubated at 28°C until the wild type strain had cultivated the complete plate. Figure 48 summarizes the results of all growth assays. In general, the Δ*pks* and Δ*gpmk1* mutants showed a slight reduction of growth speed compared to the wild type strain, indicating a certain transformational effect on the growth rate of the mutants. Nevertheless, the *gpmk1* disruption mutants exhibited an obvious

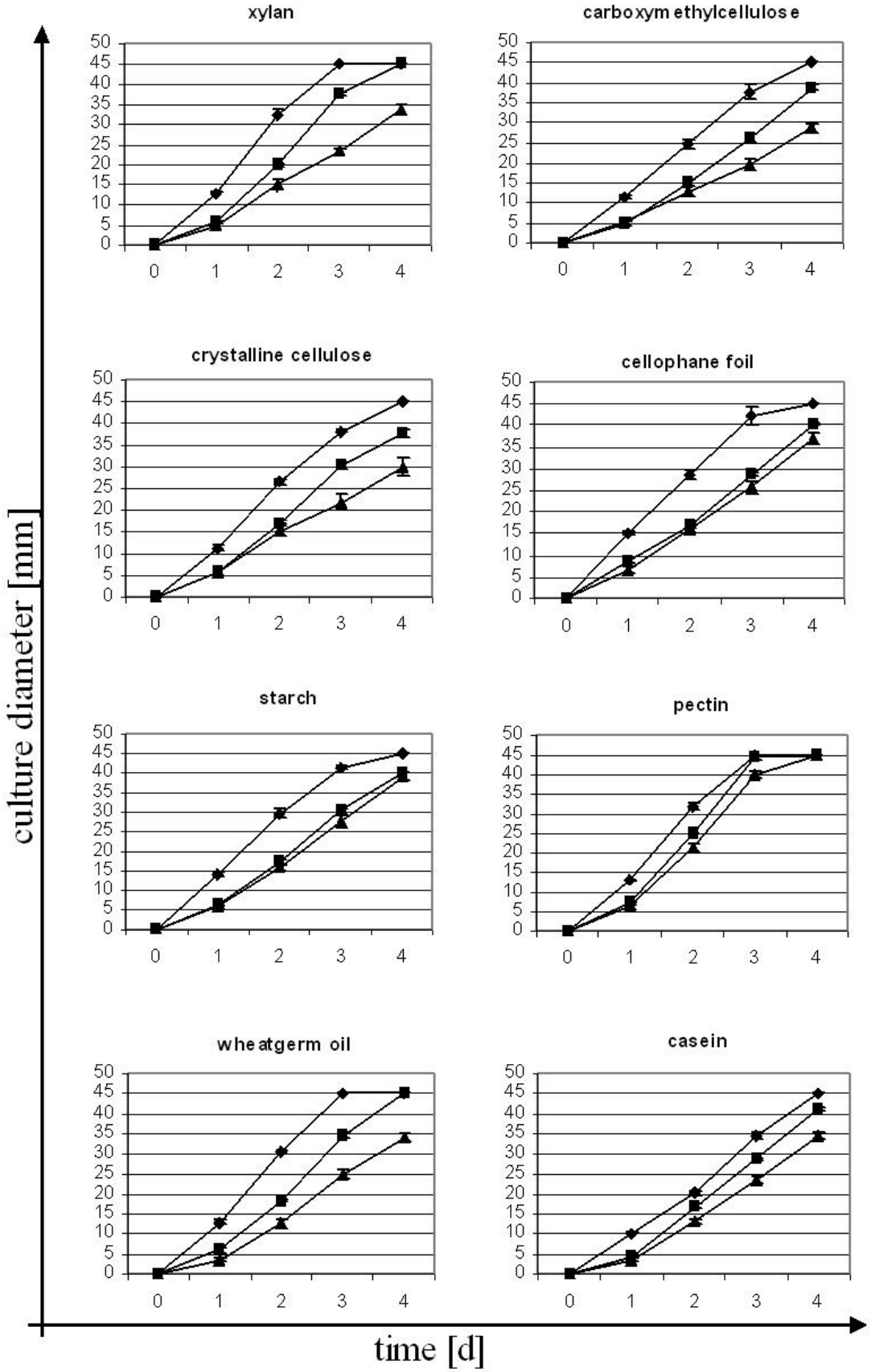

Fig. 48: Growth rate of the *F. graminearum* wild type strain 8/1 (♦), the Δ*pks* mutant (■), and the Δ*gpmk1* mutants (▲) on various substrates. The wild type strain (n=4), the Δpks mutant (n=3) and four Δ*gpmk1* mutants (n=3) were inoculated on minimal medium containing one sole carbon source and were then incubated for four days at 28°C in the dark.

attenuation in growth speed compared to the Δ*pks* mutant when cultivated on carbon sources that were shown to be degraded less efficiently by the MAP kinase mutants, such as xylan, carboxymethylcellulose, and wheatgerm oil (compare 3.6.2.). A growth reduction of the Δ*gpmk1* mutants was also observed on crystalline cellulose. The reduction was first observed one to two days after inoculation, when probably all reserves were utilized from the mycelium/agar plug which served as inoculate. On soluble starch, pectin, and casein the MAP kinase mutants displayed a similar growth speed as the Δ*pks* mutant, indicating that the offered carbon sources can be metabolized at a comparable rate. During the conducted photometric enzyme assays starch and pectin degrading enzymes were shown to be secreted by the Δ*gpmk1* mutants at a rate comparable to the wild type strain and the Δ*pks* mutant. The enzymatic degradation of casein was only reduced in the very early induction times.

After five days growth on cellophane foil the wild type strain and the Δ*pks* mutant had degraded the complete foil and had started to grow into the medium below. The Δ*gpmk1* mutant colonies had not been able to degrade the foil and could, on the contrary, be completely washed off the foil by adding water to the plate. A degradation of the cellophane foil under the mutant strains was first detectable after a longer cultivation periode. This effect coincides with the result that these mutants were shown to have an obviously delayed production of cellulose degrading enzymes.

On media that induced the wild type to vigorous aerial growth the mutants disrupted in the *gpmk1* gene again showed a reduced or delayed formation of aerial mycelia. This morphology was particularly obvious on plates containing casein, starch, pectin, and xylan as sole carbon source.

3.7. Isolation and characterisation of a gene encoding an osmolarity MAP kinase from *F. graminearum*

During the search for MAP kinase genes from *F. graminearum* prior to this work via PCR with degenerate primers, only two genes encoding for MAP kinases (3.1. amd 3.2.) were found, one with homologies to the cell integrity MAP kinases, and one MAP kinase obviously involved in regulation of pathogenicity. Nevertheless, it has been postulated that higher fungi could have three of these regulatory proteins (Xu 2000). The third kinase generally plays a role in regulation of osmolarity. As neither the disruption of the Gmap1

nor the Gpmk1 MAP kinase of *F. graminearum* seemed to have an effect on the growth of the mutants on high osmolarity media (3.4.4.), it was to be expected that *F. graminearum* also has at least one more MAP kinase involved in the response to hyperosmolarity. In an attempt to find this missing MAP kinase, a cDNA database from *F. graminearum* (kindly supplied by the BASF AG, Ludwigshafen, Germany) was analysed by blast search with the amino acid sequence of the Osm1 MAP kinase from *M. grisea*. The clone containing the sequence with the highest homology to Osm1 was sequenced in full length by the BASF AG. The complete gene was then amplified from cDNA and genomic DNA using the primers NJ65 and NJ66A, ligated into the pGEM-T vector, resulting in the plasmids pGEM-T::osmapNJ65/66A_gDNA and pGEM-T::osmapNJ65/66A_cDNA. These plasmids were cloned into *E. coli* and sequenced. Comparison of the genomic DNA sequence with the cDNA sequence enabled to find the start and stop of the gene transcription as well as the positioning of the introns. An open reading frame of 1071 bp was found containing eight introns 71 bp, 62 bp, 120 bp, 77 bp, 76 bp, 56 bp, 56 bp, and 49 bp in length (Fig. 49 in appendix C). The deduced amino acid sequence of 357 aa shows significant homologies to various fungal osmolarity MAP kinases (Fig. 50 in appendix C) such as the osmotic sensitive-2 MAP kinase from *Neurospora crassa*, 94 % identity (AAK83124; Zhang et at. 2002), Osm1 from *M. grisea*, 93 % identity (AF184980; Dixon et at. 1999), Hog1p-like protein from *Hotaea werneckii*, 88 % identity (AAM64214; Turk and Plemenitas, 2002), and Hog1 from *S. cerevisiae*, 80 % identity (AAA34680; Brewster et at. 1993). The deduced amino acid sequence contained the threonine-glycine-tyrosine (TGY)-sequence. At this site the dual specifity MAP kinase kinase phosphorylates the threonine and tyrosine residues, resulting in the activation of the MAP kinase (Kültz 1998). Furthermore, it contained all 11 conserved domains of the yeast/fungi stress-activated protein kinase subgroup (YSAPK) (Kültz 1998; Hanks and Quinn 1991). The putative osmolarity MAP kinase from *F. graminearum* also ranged in the YSAPK subgroup, when a multitude of fungal MAP kinases were aligned (Fig. 15 in appendix D).

A semi-quantitative RT-PCR analysis of the putative osmolarity MAP kinase gene from *F. graminearum* was carried out to investigate the mode of transcriptional regulation of this gene. RNA was isolated from uninfected (24 h incubation with H_20; kindly provided by Sascha Malz) and from *F. graminearum* infected wheat spikelets (4 h, 12 h, 24 h,48 h and 7 d after spore inoculation; kindly provided by Sascha Malz) as well as from a *F. graminearum* 8/1 culture grown in CM-medium. After a DNA digestion step and first-strand synthesis a PCR was performed with the specific osmolarity MAP kinase primers

NJ70/NJ66B and primers for the *F. graminearum* β-tubulin gene (FgBetaTubFor/ FgBetaTubRev). Thereby, the β-tubulin gene was used as control for a constitutively and highly expressed gene. Comparable to the other two MAP kinase genes investigated in this work, the osmolarity MAP kinase from *F. graminearum* showed a constitutive mode of regulation (Fig. 51). Transcripts were found in cultures grown in CM-medium as well as in wheat spikes infected with *F. graminearum*. No transcript could be detected in uninfected wheat spikes and in early wheat infection time points. The latter indicating that the fungus had not grown far enough to be detectable with the chosen PCR conditions. This pattern resembles the constitutively expressed β-tubulin gene with the only difference that the β-tubulin gene can be detected earlier, thus being stronger transcribed. The PCR control with genomic DNA showed the expected shift in size resulting from introns that can be found in the amplified sequence.

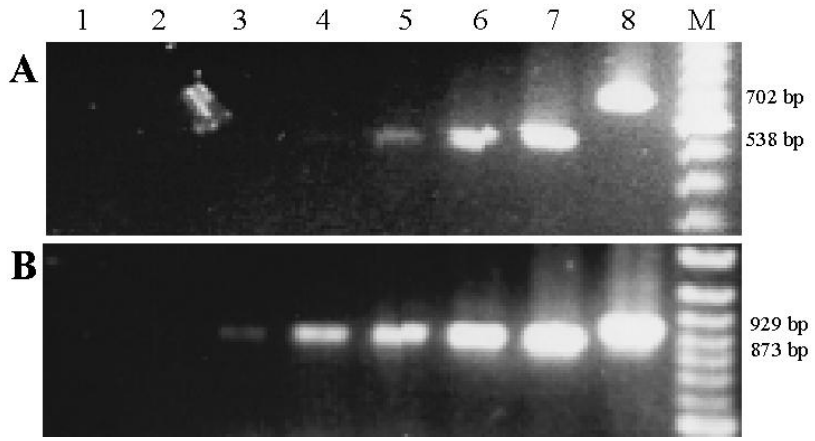

Fig. 51: Expression of the gene encoding the putative osmolarity MAP kinase (**A**) and the β-tubulin gene (**B**) from *F. graminearum* during plant infection and *in vitro*, as shown via RT-PCR. First-strand cDNA generated from total RNA isolated from uninfected (line 1) and from *F. graminearum* infected wheat spikelets (4 h, 12 h, 24 h, 48 h and 7 d after spore inoculation; lines 2-6) as well as from a *F. graminearum* 8/1 culture grown in CM-medium (line 7) was used as template for PCR with the osmolarity MAP kinase specific primers NJ70/NJ66B and primers for the *F. graminearum* β-tubulin gene (FgBetaTubFor/FgBetaTubRev) Lane 8 PCR with genomic DNA as template performed as control. Lane M: GeneRuler Ladder Mix.

3.8. Isolation and characterisation of a putative hydrophobin gene from *F. graminearum*

Earlier on, the *F. graminearum* mutants disrupted in the gene encoding the Gpmk1 MAP kinase were shown to have a reduced production of aerial mycelia (3.4.1.) and to be sexually sterile (3.4.3.). These results led to the idea that the reduced formation of aerial

mycelia could arise from a lack of hydrophobin secretion. Hydrophobins are moderately hydrophobic proteins that are able to assemble into stable aggregates at hydrophobic/hydrophilic interphases. They have been shown to be important during aerial growth and fruiting body formation of various fungi (Wessels et al. 1991). The idea was encouraged by recently published results concerning a regulatory effect of the Pmk1 MAP kinase from *M. grisea* on the induction of its hydrophobin Mpg1 (Soanes et al. 2002). For *F. graminearum* no hydrophobins are so far known. The aim was, therefore, to see whether a gene enconding a hydrophobin from *F. graminearum* could be found. The cDNA database of *F. graminearum* was analysed for proteins that were anotated with similarities to fungal hydrophobins. Three sequences were found, of which only one showed a putative open reading frame that, translated into the amino acid sequence, showed a placing of cysteine residue typical for hydrophobins. This cDNA fragment exhibited low homologies to the hydrophobin from *Flammulina velutipes* (BAB17622; Ando et al. 2001) and the well-known hydrophobin Sc3 from *Schizophyllum commune* (AAA96324; Schuren and Wessels, 1990). Most hydrophobins only show such low overall sequence homologies, as they only share a typical placing of eight conserved cysteine residues. The complete cDNA clone carrying this gene was sequenced by the BASF AG (Ludwigshafen, Germany). In the mean time the complete genomic library of *F. graminearum* had been published, so that primers could be made in sequence areas upstream and downstream of the gene. Using these primers the complete gene was amplified from genomic DNA (primers NJ94B and NJ95) and from cDNA (primers NJ59 and NJ95) and ligated into the pGEM-T vector, resulting in the plasmids pGEM-T::hydroNJ94B/95 and pGEM-T::hydroNJ59/95. These plasmids were cloned into *E. coli* and sequenced again. Comparison of the genomic DNA sequence with the cDNA sequence enabled to find the start and stop of the gene transcription as well as the positioning of the introns. An open reading frame of 510 bp containing two introns of 51 bp and 58 bp encodes a protein of 170 aa in length (Fig. 52 in appendix E). The deduced amino acid sequence exhibited the typical spacing of eight cysteine residues known to be essential for the hydrophobin structure. A structural difference could only be found in an additional, ninth cysteine residue in the N-terminal protein region (Fig. 53 in appendix E). Additionally, sequence homologies were found on amino acid level to other hydrophobins such as the Fvh1 hydrophobin from *F. velutipes*, 36 % identity (BAB17622; Ando et al. 2001), the hydrophobin 1 from *Dictyonema glabratum*, 35 % identity (CAC86002; Trembley et al. 2002), and Sc3 from *S. commune*, 31 % identity (AAA96324; Schuren and Wessels, 1990). Hydrophobin amino acid

sequences generally display a typical hydropathy pattern which enables the correct folding of the protein. The hydropathy blot of the deduced amino acid sequence from the putative *F. graminearum* hydrophobin was compared to hydropathy blots of other fungal hydrophobins (Fig. 54 in appendix E). Thereby, the hydropathy pattern of the described protein showed a great likeliness to the known fungal hydrophobins. Furthermore, a calculation with Signal P neural network programme as well as Signal P Markow model programme revealed a cleavage site with a high probability between positions 17 and 18 of the amino acid sequence. The presence of a signal sequence gives strong evidence for a extracellular localization of the described protein.

To gain information over the transcriptional regulation and induction mode of the putative hydrophobin gene from *F. graminearum*, various semi-quantitative RT-PCR analysis were carried out (Fig. 55). The *F. graminearum* wild type strain 8/1 was cultivated in several different ways: in liquid culture using CM-medium or SNA medium, on solid CM and SNA medium with cellophane foil to prevent the fungus from growing into the medium and on aerial mycelia inducing Czapek plates. Futhermore, conidia and germinated conidia, an early stadium of perithecia development and ripe perithecia, as well as

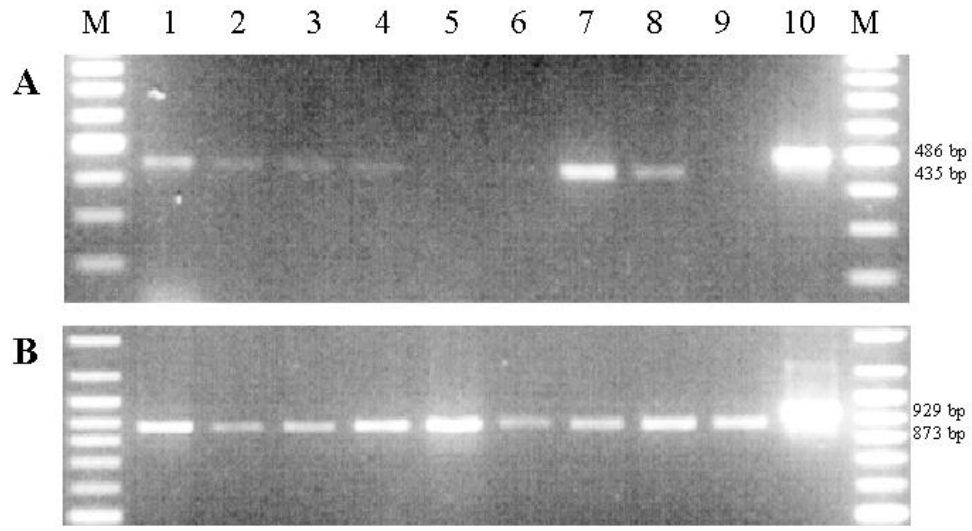

Fig. 55: Expression of the gene encoding the putative hydrophobin (**A**) and the β-tubulin gene (**B**) from the *F. graminearum* wild type strain. First strand cDNA was generated from cultures grown in liquid CM (line 1) and SNA (line 2) medium, from cultures grown on solid CM (line 3) and SNA (line 4) covered with cellophane foil and from Czapek plates (line 5), as well as from conidia (line 6), germinating conidia (line 7), an early stadium of perithecial development (line 8) and ripe perithecia (line 9). The hydrophobin transcripts were amplified with the primer pair NJ59/NJ62, the β-tubulin transcripts with the primer pair FgBetaTubFor/FgBetaTubRev. The products in line 10 were amplified from genomic DNA as control for DNA contamination of the cDNA. Lane M: GeneRuler Ladder Mix.

uninfected and infected wheat spikes were assayed for hydrophobin transcripts. RNA from all mentioned cultures was isolated followed by DNA digestion and first-strand synthesis. A subsequent PCR using cDNA as template and the hydrophobin specific primer pair NJ59/NJ62 was performed. A PCR using primers for the β-tubulin gene (FgBetaTubFor/ FgBetaTubRev) as well as a PCR with genomic DNA were done as control. In all probes tested, the β-tubulin transcript could be amplified. Concerning the various culture media tested, hydrophobin transcripts were found in the cultures grown in liquid CM- and SNA-medium, as well as in the cultures grown on solid CM and SNA covered with cellophane foil. A transcription of the hydrophobin gene could also be detected in germinating conidia and in early stages of perithecia development. The obviously strongest transcription of the putative hydrophobin was found in germinating conidia (Fig. 55). No induction of the putative hydrophobin gene took place during the infection prossess on wheat (data not shown). Conidia as such and ripe perithecia also showed no signs of hydrophobin induction (Fig. 55).

As Soanes and coworkers (Soanes et al. 2002) had shown that hydrophobin expression can be regulated by MAP kinases, it was interesting to find out, whether the *F. graminearum* Δ*gpmk1* MAP kinase mutants possibly showed a reduced transcription of the putative *F. graminearum* hydrophobin. Thus, in the hope of finding an explanation for some of the phenotypes found in the Δ*gpmk1* mutants, RNA was isolated from germinating conidia of the wild type strain and three Δ*gpmk1* mutants. After a DNA digestion step and

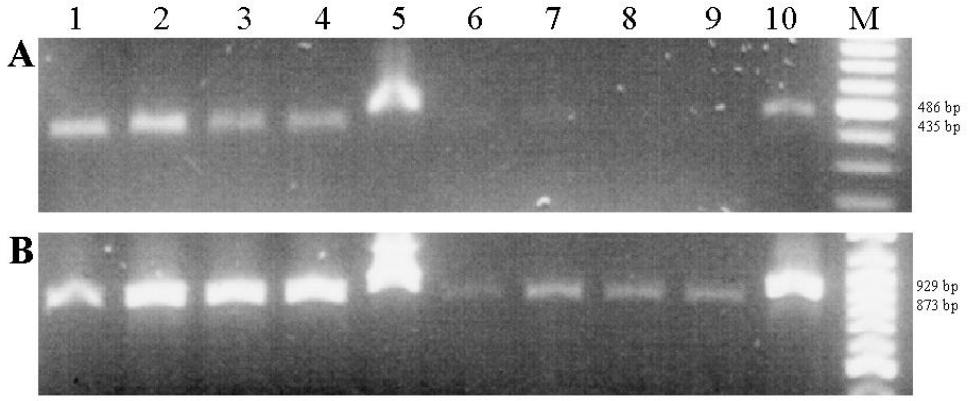

Fig. 56: Expression of the gene encoding the putative hydrophobin (**A**) and the β-tubulin gene (**B**) by the *F. graminearum* wild type strain (lanes 1 and 6), and by three Δ*gpmk1* mutants (lanes 2-4 and 7-9). First strand cDNA was generated from germinating conidia of the wild type strain and three independant Δ*gpmk1* mutants. The hydrophobin transcripts were amplified with the primer pair NJ59/NJ62, the β-tubulin transcripts with the primers FgBetaTubFor and FgBetaTubRev. The products in lanes 5 and 10 were amplified from genomic DNA as control for DNA contamination of the cDNA. The products of lanes 1-5 were amplified with 30 cycles, whereas the products of lanes 6-10 were amplified with 25 cycles. Lane M: GeneRuler Ladder Mix.

first-strand synthesis, PCRs were performed with the hydrophobin primers and the β-tubulin primers (see above). Wild type and mutant cDNA from germinated conidia were used as template. In one set the PCR was run with 25 cycles and in another set with 30 cycles, respectively (Fig. 56). The β-tubulin transcript could be amplified in all strains and under both PCR conditions chosen. From all cDNAs gained from the Δ*gpmk1* mutants transcripts of the putative hydrophobin could be amplified in the same intensity as from the wild type strain. This result indicates that the disruption of the *gpmk1* gene seems to have no effect on the transcription of the putative hydrophobin from *F. graminearum*.

4. Discussion

Fusarium graminearum is the causal agent of the head blight disease of small grain cereals and of the ear rot of maize in humid and semihumid regions of the world. This devastating disease is able to cause severe grain yield losses. Additionally, the grain is contaminated with a variety of mycotoxins, causing moldy-grain toxicoses of humans and animals after consumption. Therefore, an extensive disease management is necessary. Dispite of its great importance, neither cereal cultivars with resistance against *F. graminearum* nor fungicides working efficiently against *F. graminearum* are available so far. In order to find new methods for disease control the precise infection mechanisms of this plant pathogen must be studied in detail. So far, only the mycotoxic trichothecenes were shown to be involved in the disease establishment of *F. graminearum* (Bai et al. 2001; Desjardins et al. 1996; Proctor et al. 1995).

Since a few years, research on signal transduction pathways of fungi have become the key for obtaining an insight in the complex interactions between host and pathogen. In this work, therefore, a strategy using mitogen-activated protein (MAP) kinase deletion mutants was used to investigate which developmental and pathogenic processes of *F. graminearum* are possibly regulated by MAP kinase signal transduction pathways.

4.1. The three MAP kinases of *F. graminearum*

In order to analyse the role of MAP kinase pathways in *F. graminearum* the specific genes encoding putative MAP kinases had to be identified. Via PCR with degenerate primers two gene fragments were amplified, which showed homologies to fungal MAP kinases. The DNA regions flanking these gene fragments were isolated by a thermal asymmetric interlaced PCR-strategy (Lui and Whittier 1995). Comparison of the genomic DNA and cDNA sequences allowed to derive a putative amino acid sequence. Both MAP kinases revealed significant homologies to fungal MAP kinases. One, having the highest sequence identity of 88 % to the cell integrity MAP kinase Mps1 from *Magnaporthe grisea* (Xu et al. 1998), was named Gmap1 for *Gibberella* MAP kinase 1. The second kinase showed an 97.2 % identity to the pathogenicity MAP kinase Pmk1 from *M. grisea* (Xu and Hamer 1996) and was, hence named Gpmk1 for *Gibberella* pathogenicity MAP kinase. Both MAP kinases, Gmap1 and Gpmk1, contained the threonine-glutamate-tyrosine (TEY)-site for

MAP kinase activation. The threonine and tyrosine residues of this site are phosphorylated by the MAP kinase kinase, which is situated upstream in the signal cascade. The dual phosphorylation of this site results specifically in the activation of MAP kinases (Krauss 1997; Cobb and Goldsmith 1995). The glutamate (E) situated between threonine and tyrosine of the phosphorylation site enables to classify the MAP kinases Gmap1 and Gpmk1 into the subgroup of extracellular-signal regulated kinases (ERKs). This already indicates that the regulatory processes in which Gmap1 and Gpmk1 take part probably enable *F. graminearum* to react to certain exogenious signals. A detailed analysis of the deduced amino acid sequences of both MAP kinases from *F. graminearum* allowed to further classify the identified kinases in two different ERK groups. Gpmk1 as well as Gmap1 revealed the 11 conserved MAP kinase domains. Thereby, Gpmk1 showed the specifities of the yeast/fungi extracellular-signal regulated kinase 1 subgroup (YERK1) and Gmap1 those of the yeast/fungi extracellular-signal regulated kinase 2 subgroup (YERK2) (Kültz 1998; Hanks and Quinn 1991). By transformation-mediated disruption of the *F. graminearum* genes encoding Gmap1 and Gpmk1 the participation of these MAP kinases in processes involved in the regulation of various developmental stages, pathogenicity and cell growth could also be elucidated on functional level. Yet, this will be discussed in detail later.

By screening a cDNA library of *F. graminearum* a third MAP kinase was found. Isolation and comparison of the genomic DNA and cDNA of the gene led to a putative amino acid sequence with high homologies to osmotic sensitive MAP kinases, such as Osm1 from *M. grisea* (93 % identity; Dixon et at. 1999). Studies on various osmolarity MAP kinases have shown that these regulatory enzymes are responsive to various stress situations and specifically influence the accumulation of compatible solutes such as glycerol, trehalose or arabitol as response to hyperosmotic stress in *Schizosaccharomyces pombe* (Paredes et al. 2003), *Neurospora crassa* (Zhang et al. 2002), *Candida albicans* (Alonso-Monge et al. 1999), *M. grisea* (Dixon et al. 1999), and *Saccharomyces cerevisiae* (Wojda et al. 2003; Nevoigt and Stahl 1997). An osmosensitive MAP kinase has also been shown to be involved in repression of sexual development as well as spore stress resistance and survival in *Aspergillus nidulans* (Kawasaki et al. 2002). Generally, the osmosenstive MAP kinases are dispendable for pathogenicity in plant pathogens. In *M. grisea* Osm1, for example, does not regulate the hydrostatic turgor in the appressoria, which is generated by an accumulation of glycerol in molar concentrations (Dixon et al. 1999). Nevertheless, certain

evidence exists that support a role for the osmolarity MAP kinase pathway during pseudohyphae formation and thus virulence of *C. albicans* (Alonso-Monge et al. 1999).
According to the specifities of the 11 conserved MAP kinase domains found in this putative osmolarity MAP kinase from *F. graminearum*, it groups into the yeast/fungi stress-activated protein kinase subgroup (YSAPK) of MAP kinases. Additionally, the MAP kinase activation site TXY reveals a glycine at the X position. This characteristic is also specific for the subgroup of yeast and fungal stress-activated protein kinases (Kültz 1998; Hanks and Quinn 1991). As the YSAPK subgroup has less sequence similarities in common with the YERK1 and YERK2 subgroup than these to YERK groups amongs each other, it does not seem astonishing why the osmolarity MAP kinase could not be found using degenerate primers derived from MAP kinases of the YERK groups. Eventhough the high sequence homology of the third MAP kinase from *F. graminearum* to protein kinases of the YSAPK subgroup indicates its function as osmotic sensitive MAP kinase, the actual regulatory function of this kinase must still be verified by the characterisation of disruption mutants. These studies are currently being carried out.

Transcription analysis of the three genes encoding MAP kinases from *F. graminearum* showed all three genes to be constitutively expressed, as transcripts were present during vegetative growth as well as during the infection process on the plant. Hence, regulation of these MAP kinases might only be posttranscriptional, which is a widely described regulational mode for other protein kinases (Hunter 1995). This includes, next to the phosphorylation at the TXY-site, the cellular localisation and the attachment of various scaffold proteins (Schaeffer and Weber 1999). A constitutive expression of MAP kinase was also found for the Ubc3 (= Kpp2) MAP kinase from *Ustilago maydis* (Brachmann et al. 2003) and Ptk1 from *Pyrenophora teres* (Ruiz-Roldán et al. 2001). Nevertheless, some fungal MAP kinases have also been shown to be constitutively expressed at low levels but were then upregulated during certain developmental stages (Brachmann et al. 2003; Xu 2000). The transcripts of all three *F. graminearum* MAP kinases amplified from infected wheat spikes were detected approximately 12 hours later than the β-tubulin transcripts. This indicates that the MAP kinases are transcribed at a much lower rate than the β-tubulin gene. But, a comparatively low level of transcription is to be expected for every kind of regulatory protein (Hunter 1995).

Within the present work, three MAP kinases of the phytopathogenic fungi *F. graminearum* were found, indicating the fungus to have three regulatory pathways utilizing cascades of MAP kinases. This makes *F. graminearum*, next to *M. grisea* (Dixon et al. 1999; Xu et al. 1998; Xu and Hamer 1996) and *Aspergillus nidulans* (Kawasaki et al. 2002; Bussink and Osmani 1999; Park H J, Jahng K-Y, Chae K-S, Han D M unpublished), the third filamentous fungus, in which MAP kinases of all three pathways postulated for higher fungi are known.

4.2. The regulatory role of the Gmap1 MAP kinase of *F. graminearum*

MAP kinases belonging like the Gmap1 kinase from *F. graminearum* to the YERK2 subgroup, have been found in several fungal organisms such as *S. cerevisiae* (Slt2/Mpk1; Lee et al. 1993), *Pneumocystis carinii* (Mpk1; Fox and Smulian 1999), *Cryptococcus neoformans* (Mpk1; Kraus et al. 2003), *C. albicans* (Mck1; Navarro-García et al. 1998; Navarro-García et al. 1995), *Pichia pastoris* (Pim1; Cosano et al. 2001). *Claviceps purpurea* (Cpmk2; Mey et al. 2002a), *Colletotrichum lagenarium* (Maf1; Kijoma et al. 2002), *B. graminis* (Mpk2; Zhang and Gurr 2001), *A. nidulans* (MpkA; Bussink and Osmani 1999), and *M. grisea* (Mps1; Xu et al. 1998). Functional characterisation of these MAP kinases, have shown that they were responsible for regulating processes necessary for cell integrity. MAP kinase deletion mutants formed weak cell walls that had a low resistance towards digestion with cell wall lytic enzymes and often showed growth defects on solid medium. Some, additionally, displayed alterations in their cell surface (Xu 2000; Navarro-Garcia et al. 1998).

In order to analyse the function of the Gmap1 MAP kinase from *F. graminearum*, Δ*gmap1* mutants were produced by transformation mediated gene disruption. Comparable to other fungal cell integrity MAP kinase mutants (Lee et al. 1993; Navarro-Garcia et al. 1998; Bussink and Osmani 1999; L. Zheng and J.-R. Xu unpublished data) the *F. graminearum* strains disrupted in the *gmap1* gene showed a significantly reduced growth speed on solid media and a more compact colony morphology compared to the wild type. This phenotype was observed on complete medium as well as on minimal medium, indicating that the growth reduction was not related to the specific media used. This growth defect was restored, when the mutants were cultivated in liquid media. They produced comparable amounts of biomass as the wild type strain. A similar restoration of growth defects in cell

integrity MAP kinase mutants has been observed for *M. grisea* (Xu et al. 1998), *A. nidulans* (Bussink and Osmani 1999) and *Botrytis cinerea* (L. Zheng and J.-R. Xu unpublished data). The growth reduction on solid medium, the formation of compact colonies and the restoration of the growth reduction in liquid medium therefore might suggest that the *F. graminearum* Δ*gmap1* mutants are defective in the elongation of aerial hyphae and normal polarized growth, possibly due to severe cell wall defects. This speculation was strengthened by Hou and coworkers (Hou et al. 2002), who characterised the same MAP kinase from *F. graminearum* parallel to this work and observed that the cell wall of the MAP kinase deletion mutants was much weaker than the wild type and showed sensitivity towards treatment with cell wall lytic enzymes. It is also possible that the Gmap1 kinase from *F. graminearum* could be involved in actin cytoskeleton organisation, as it is postulated for *S. cerevisiae* (Gustin et al. 1998).

Unlike Mps1 from *M. grisea* (Xu et al. 1998), Maf1 from *C. lagenarium* (Kojima et al. 2002), Cpmk2 from *C. purpurea* (Mey et al. 2002a), and MpkA from *B. cinerea* (L. Zheng and J.-R. Xu unpublished data) the Gmap1 Map kinase did not affect the conidiation of *F. graminearum*. On SNA agar (compare 2.1.3.2.) the mutants produced an amount of conidia comparable to the wild type. If the conidiation was induced on cellophane foil the conidiation of the Δ*gmap1* mutants was reduced in comparison to the wild type, but showed rates similar to an ectopic mutant tested. This indicates the reduction to be due to a transformation effect and not due to the gene disruption. Furthermore, the conidia produced by the Δ*gmap1* mutants were as viable as the wild type conidia. On the contrary, *A. nidulans* strains with deleted MpkA MAP kinase were shown to have a germination defect. This defect could, however, be largely remediated on complex high osmolarity media (Bussink and Osmani 1999). Thus, it can be concluded that the Gmap1 MAP kinase from the plant pathogen *F. graminearum* has no regulatory effect on conidia production and germination.

F. graminearum mutants disrupted in the *gmap1* gene were practically unable to form perithecia. If at all, only one to two perithecia/plate were produced by the colony areas, that lost their growth reduced phenotype. A comparable regulatory effect of a cell integrity MAP kinase was found in *M. grisea*. Mutants deleted in the *mps1* gene were shown to be female-sterile (Xu et al. 1998). The cell integrity MAP kinase Slt2 of *S. cerevisiae* also responds to mating pheromones (Xu 2000). Therefore, it seems likely that cell integrity

MAP kinases could genereally respond to mating signals, which then lead to major rearrangements of the cell walls that are necessary for a successful reproduction process. The same role could also be postulated for Gmap1 from *F. graminearum*.

The deletion of cell integrity MAP kinases from various fungal pathogens always led to the formation of mutants that had a drastically reduced virulence (Kraus et al. 2003; Mey et al. 2002a; Kojima et al. 2002; Xu et al. 1998; Diez-Orejas et al. 1997; L. Zheng and J.-R. Xu unpublished data). Or, transcripts of the genes encoding these MAP kinases were predominately found during the infection process (Zhang and Gurr 2001). Comparable to the other pathogenic fungi, disruption of the gene encoding the Gmap1 MAP kinase from *F. graminearum* also led to a drastic reduction of fungal virulence. After point-inoculation of wheat spikes with Δ*gmap1* mutant conidia, the blight symptoms could solely be observed directly on the inoculated spikelet. No disease spreading occurred over the complete spike. Regarding the reduction in growth speed of the MAP kinase mutants that was observed in this work on solid *in vitro* medium, it is possible that the reduction in virulence may be solely a consequence of this reduced growth rate. Thus, defining the Gmap1 MAP kinase as a fitness factor that has no influence on effects directly linked to pathogenicity. However, Hou and colleagues (Hou et al. 2002) showed that the *F. graminearum* mutants deleted in the same MAP kinase were also dramatically impaired in their ability to produce DON and 15-ADON. This indicates that the Gmap1 kinases has a regulatory function in the trichothecene induction. Therefore, it is more likely that the reduced virulence is caused by the lack of toxins produced during wheat infection. Particularly, as the phenotype found *in planta* was very similar to infections carried out with *F. graminearum* Δ*tri5* mutants. These Δ*tri5* mutants have a deleted trichodiene synthase, the enzyme that catalyses the first reaction in the trichothecene biosynthesis pathway, and are thus unable to produce DON. *In planta* the conidia were shown to germinate and infect the inoculated spikelet, but the disease symptoms were also limited to the inoculated spikelet and did not spread over the complete spike (Bai et al. 2001).

During cultivation of the gained *F. graminearum* Δ*gmap1* mutants it was observed, that the mutants sporadically lost their growth reduced phenotype while growing on medium without Hygromycin pressure. The two following hypothesis might explain this effect.
(i) The mutant cultures contained untransformed wild type nuclei. If protoplasts are successfully transformed they are, due to the resistance marker, able to proliferate on

selective medium. As a protoplast contains several nuclei and it is not necessary for all nuclei to be transformed to gain resistance, it seems evident that the colony formed from these proliferated, transformed protoplasts can be heterokaryotic for the inserted mutation. Thus, all transformants were single conidiated in order to gain homokaryotic mutants. This is possible, as it is genereally assumed that *Fusarium* species have multinucleate, homokaryotic spores, developed from a single nucleus that enters the spore and then divides (Deacon 1997). However, in the case of the *gmap1* mutants it could be, that the mutant conidia might occasionally contain amongst transformed nuclei also nuclei with the wild type genotype, possibly due to their phenotype. If this were the case, it was to be expected that the "contamination" with wild type nuclei would be lost, if several rounds of single conidiation under selective pressure were carried out. But, even after four single conidiation rounds the wild type *gmap1* locus could still be detected. So that it was concluded, that the Δ*gmap1* mutant colonies were initially homocaryotic.

(ii) The integrated vector was actively excised during cultivation. Homologous recombination occurs at much higher rates in fungi than in plants and mammals (Schiestl and Petes 1991). Therefore, it is tempting to assume that the opposite reaction is just as likely possible. The vector ends would again be subject of a homologous recombination event, leading to the formation of a hair pin structure and the excision of this hair pin. Up to date, the basis of this instability is not yet clear. However, it does seem imaginable that an inserted mutation, leading to a drastic impairment of vegetative growth, like observed for the *F. graminearum* Δ*gmap1* mutants, could result in a high selective pressure of reversion. Particularly, when the Hygromycin pressure for the mutation is removed. Besides, the *F. graminearum* mutants disrupted in the gene encoding the second MAP kinase Gpmk1 exhibited no vital growth impairment and showed no phenotypic or genotypic signs of reversion. The presumption that the mitotic stability of a vector insertion is dependent on the importance of the mutated gene for normal vegetative growth is supported by the comparision of the targeting efficiency of the *gmap1* and the *gpmk1* gene. Whereas the *gpmk1* gene was targeted with a efficiency of 92 %, the *gmap1* gene only had a transformation efficiency of 11 % eventhough the transformation procedure was identical for both gene disruptions. This result indicates that protoplasts failing to produce the Gmap1 MAP kinase have a lower viability and/or proliferation rate, possibly due to severe cell wall defects. The level of gene expression has also been discussed as factor influencing the targeting frequency (Thyagarajan et al. 1995; Srikantha et al. 1995). However, as both the *gmap1* and the *gpmk1* gene were shown to be constitutively

expressed at a low level, it seems unlikely that the transcriptional status is the reason for these drastic differences in targeting frequency. Other factors that have been postulated to be influencing the targeting frequency (Bird and Bradshaw 1997) such as the chromosomal position and the level of methylation must remain unsettled. Hence, the mitotic instability of the *gmap1* gene locus is attributed to the importance of the Gmap1 kinase for the normal vegetative life of *F. graminearum.* Despite the mutants being mitotically instable, the phenotypic characterisation of the Δ*gmap1* mutants done in this work can for two reasons definitely be associated with the absence of the regulatory influence from the *F. graminearum* cell integrity MAP kinase Gmap1. First, the experiments were done as far as possible under Hygromycin selection pressure. To ensure that the observed phenotypes did not result from the selection pressure, ectopic transformants were carried along with the experiments under the same conditions. Secondly, Hou and coworkers (Hou et al. 2002) found parallel to this work identical phenotypes when analysing stable Δ*mgv1* (*mgv1* = *gmap1*) mutants gained by gene replacement. This knockout strategy is generally safer, as it guarantees the removal of the complete gene locus, but unfortunately has the great drawback of having an extremely low transformation efficiency. But, as the excision of a vector integrated into the genome by single crossover only occurs very seldom and the transformation efficiency of the single crossover gene disruption is drastically higher than the gene replacement (Malz 2003), the gene disruption via single crossover is nevertheless an effective method for the gene knockout in *F. graminearum.*

4.3. The regulatory role of the Gpmk1 MAP kinase of *F. graminearum*

MAP kinases from fungal pathogens belonging to the YERK1 subgroup, like the Gpmk1 MAP kinase from *F. graminearum* isolated in this work, have been shown to be wide range regulators of infection-related morphogenesis and pathogenicity. Comparing the function of these MAP kinases of various fungal pathogens, it is obvious that highly conserved MAP kinases are able to trigger divergent infection processes and thus finally initiate a multitude of different diseases. This ranges from infections of foliar pathogens via appressoria penetration (Takano et al. 2000; Xu and Hamer 1996) over nectrotrophic broad-host-range infections of soil-bourne or fruit pathogens (Di Pietro et al. 2001; Zheng et al. 2000) to highly organ-specific pathogens (Mey et al. 2002b). MAP kinases of this type have been found in the fungal pathogens *B. graminis* (Mpk1; Zhang and Gurr 2001),

N. heamatococca (FsMAPK; Li et al. 1997), *B. cinerea* (Bmp1; Zheng et al. 2000), *C. lagenarium* (Cmk1; Takano et al. 2000), *F. oxysporum* (Fmk1; Di Pietro et al. 2001), *C. heterostrophus* (Chk1; Lev et al. 1999), *P. teres* (Ptk1, Ruiz-Roldán et al. 2001), *U. maydis* (Ubc3; Mayorga and Gold 1999; Müller et al. 1999), *C. albicans* (Cek1; Csank et al. 1998), *C. purpurea* (Cpmk1; Mey at al. 2002b), and *M. grisea* (Pmk1; Xu and Hamer 1996). In each pathogen these YERK1 subgroup MAP kinases specifically regulate the main infection mechanisms needed for the establishment of the specific diseases. Characterisation of these MAP kinases should therefore give vital information about infection mechanisms. Hence, it was promising to elucidate the function of the Gpmk1 MAP kinase from *F. graminearum* in detail. But besides being involved in infection processes, these pathogenicity MAP kinases from different fungi additionally play diverse roles in fungal growth and differentiation such as hyphal growth, mating, condidation, and conidia germination, indicating that the pathogenicity MAP kinases can respond to various signals and regulate different processes.

In order to analyse the function of the YERK1 subgroup MAP kinase Gpmk1 for development and pathogenicity of *F. graminearum*, disruption mutants were produced by transformation-mediated disruption of the *gpmk1* gene. Subsequent functional characterisation of the gained mutants revealed certain functional redundancies to other fungal YERK1 knockout mutants. Concerning the vegetative hyphal growth, the Δ*gpmk1* mutants displayed an obvious reduction in aerial hyphae formation and had a slight retardation in radial growth speed compared to the wild type strain. The lack of aerial hyphae was observed on several media, indicating the growth defect to be media independent. However, no difference was found in the biomass production. Generally, YERK1 deletion mutants showed no changes in vegetative growth (Mey et al. 2002b; Ruiz-Roldán et al. 2001; Takano et al. 2000; Mayorga and Gold 1999; Müller et al. 1999; Xu and Hamer 1996). Nevertheless, minor growth reductions were found for the *B. cinerea* Δ*bmp1* mutants (Zheng et al. 2000) and the *C. albicans* Δ*cek1* mutants (Csank et al. 1998). Furthermore, a reduced aerial hyphae formation was observed for the Δ*fmk1* mutants from *F. oxysporum* (Di Pietro et al. 2001) and the Δ*chk1* mutants from *C. heterostrophus* (Lev et al. 1999). In contrast to the Δ*chk1* mutants, the *F. graminearum* MAP kinase mutants do not undergo autolysis in the central part of the colony. The Fmk1 MAP kinase deletion mutants from *F. oxysporum* additionally revealed an easily wettable phenotype and were also impaired in breaching the liquid-air interphase. Therefore, Di Pietro and colleagues (Di Pietro et al. 2001) suggested that these MAP kinase mutants could have a lower surface

hydrophobicity. This could indicate a possible regulatory role of Fmk1 on hydrophobin production. Having in mind that the Fmk1 MAP kinase showed the highest sequence homology to the Gpmk1 kinase, it is tempting to assume a similar regulatory effect for Gpmk1.

Disruption of the *gpmk1* gene from *F. graminearum* led to mutants with defects in conidia formation. Sporodochia were not produced by these mutants. Instead, their conidia were spread evenly over the agar plate, resulting in a reduced conidia production. Furthermore, the conidia were mainly found under the agar surface, again indicating that the mycelium exhibited a diminished capability of growing in an aerial phase. The reduced conidia production was not due to the formation of the conidia under the agar surface, as the amount of conidia produced by the Δ*gpmk1* mutants was still lower than the wild type production, if cellophane was used as physical barrier. Interestingly, the cellophane foil increased the conidiation of both the wild type and the mutants by 1000-2000 %. This suggests that the cellophane surface must act as topographic and/or chemical signal for the induction of conidiation. The signal must then be transduced by a pathway independent of the Gpmk1 MAP kinase.

The conidia produced by the Δ*gpmk1* mutants were completely viable. Therefore, it seems likely that no major process of conidia production had been disturbed, as it was described for the Δ*ptk1* mutants from *P. teres* (Ruiz-Roldán et al. 2001) and the Δ*chk1* mutants from *C. heterostrophus* (Lev et al. 1999). Deletion of the gene encoding the Cmk1 MAP kinase in *C. lagenarium* also led to mutants that had an obviously reduced conidia production. The conidia of these mutants additionally were only able to germinate under high nutrient conditions (Takano et al. 2000). As no other fungi with deleted pathogenicity MAP kinase showed effects during conidiation, it seems likely that these pathogenicity MAP kinases only in some cases transduce signals involved in the conidiation process. Concerning *F. graminearum*, it is rather more likely that the conidiation is only indirectly linked to the Gpmk1 pathway. The reduced amount of conidia produced by Δ*gpmk1* mutants seem to be a result of the failure to produce full sporodochia. Sporodochia, however, might only be formed by aerial hyphae. Thus, the conidiation phenotype of the Δ*gpmk1* mutants rather seems to be an effect of the reduced formation of aerial mycelium, maybe due to a reduced hydrophobin secretion. Particularly as the deletion of the Mpg1 hydrophobin from *M. grisea* led to mutants that showed, comparable to the Δ*gpmk1* mutants, reduced conidia production but normal conidia germination rates (Talbot et al. 1993).

YERK1 pathogenicity MAP kinases have in several cases been shown to be involved in the regulation of mating processes. Deletion of the corresponding MAP kinases in the filamentous fungi *C. heterostrophus* and *M. grisea* led to female sterile mutants (Lev et al. 1999; Xu and Hamer 1998). The Ubc3 (= Kpp2) MAP kinase from *U. maydis* was shown to be responsible for the production of and the answer to pheromone signals (Mayorga and Gold 1999; Müller et al. 1999). In the yeasts *C. neoformans* and *S. cerevisiae* the corresponding Gpmk1 homologues are solely responsible for mating processes (Davidson et al. 2003; Gustin et al. 1998; Herskowitz 1995). *F. graminearum* mutants disrupted in the *gpmk1* gene were unable to form perithecia, indicating the Gpmk1 MAP kinase to also play a regulatory role in the mating process of this cereal pathogen. Generally, an inability of filamentous fungi to form aerial hyphae has been shown to have a drastic effect on the formation of sexual fruiting bodies, e.g. the deletion of the Chk1 MAP kinase from *C. heterostrophus* (Lev et al. 1999). Hence, the sexually sterile phenotype of the Δ*gpmk1* mutants from *F. graminearum* could also be explained by the obvious reduction of aerial mycelia as exhibited by these mutants. A participation of the Gpmk1 MAP kinase in the production and secretion of mating pheromones could also be possible. Similar to the Δ*ubc3* mutants from *U. maydis* (Mayorga and Gold 1999; Müller et al. 1999) the disruption of the Gpmk1 pathway might render *F. graminearum* unable to sense the mating partner. As a result, no sexual reproduction processes are initiated. However, the occurrence of pheromones for the mating processes of *F. graminearum* and if so, the regulatory role of Gpmk1, still need to be examined in detail.

Functional characterisation of deletion mutants, however, displayed the major role of the MAP kinases belonging to the YERK1 subgroup to be the highly specific regulation of processes involved in pathogenic, invasive growth. Deletion of these MAP kinases in various fungi led in most cases to apathogenic mutants or mutants that were drastically impaired in virulence (Mey at al. 2002b; Di Pietro et al. 2001; Ruiz-Roldán et al. 2001; Takano et al. 2000; Zheng et al. 2000; Lev et al. 1999; Mayorga and Gold 1999; Müller et al. 1999; Csank et al. 1998; Xu and Hamer 1996). Therefore, these YERK1 kinases have generally been referred to as pathogenicity MAP kinases. As already mentioned, these highly homologous MAP kinases are able to regulate infection processes specific for each fungal organism. In *P. teres* (Ruiz-Roldán et al. 2001), *C. lagenarium* (Takano et al. 2000), *C. heterostrophus* (Lev et al. 1999), and *M. grisea* (Xu and Hamer 1996) appressoria, the penetration structures essential for these fungi, are not formed by the MAP kinase deletion

mutants. Pathogenicity MAP kinases of those fungi that are known to penetrate the plant surface directly without the use of appressoria, *C. purpurea* (Mey at al. 2002b), *F. oxysporum* (Di Pietro et al. 2001) and *B. cinerea* (Zheng et al. 2000), have been postulated to have a regulatory effect on the induction of cell wall degrading enzymes (CWDE). These findings demonstrate that the characterisation of pathogenicity MAP kinase deletion mutants is an effective tool to gain information about infection mechanisms of any fungal organism. Hence, the Δ*gpmk1* mutants from *F. graminearum* were to be analysed in detail concerning their pathogenicity.

The Δ*gpmk1* mutants revealed to be completely apathogenic on wheat spikes. A slight formation of aerial mycelia showed that the conidia must have been able to germinate in the inoculated spikelets, but no signs of infection could be found after 21 days incubation on the spikes and on the kernels. These results suggest that the mutants were unable to penetrate the plant surface after germination of the conidia. In fact, a preliminary histological experiment gave first evidence that the mutants hyphae failed to penetrate the surface of the glumes. Instead, they formed coiled and looped hyphae on the plant surface (data not shown). Eventhough this result must certainly be reproduced, it does seem tempting to compare it with the hyphal growth of the Δ*cmk1* mutants from *C. lagenarium* (Takano et al. 2000) and the Δ*chk1* mutants from *C. heterostrophus* (Lev et al. 1999). Pathogenicity MAP kinase deletion mutants of both fungi produced curled and hooked penetration hyphae in place of functional appressoria, indicating this hyphal deformity to result from a unsuccessful penetration event. As *F. graminearum* is a non-appressoria forming plant pathogen, the failure to penetrate the host surface might also come from a reduced ability to produce CWDE like it was suggested for *C. purpurea*, *F. oxysporum*, and *B. cinerea* (Mey at al. 2002b; Di Pietro et al. 2001; Zheng et al. 2000). A second possible reason for a failed penetration event could be the insufficient attachment of the pathogen to the host surface. The tight attachment of the pathogen to the host is a prerequisite for the induction of penetration mechanisms (Nicholson and Epstein 1991). That the Δ*gpmk1* mutants from *F. graminearum* might be impaired in their surface adhesion was suggested when the mutants were cultivated on minimal medium covered with cellophane foil. Unlike the wild type strain, the Δ*gpmk1* mutant colonies did not attach firmly to the foil, but could be washed off by adding water to the plates. Fungal attachment is generally accomplished by the secretion of mucilage and by the formation of a hydrophobic layer around the hyphae after secretion of hydrophobins (Wösten 2001; Nicholson and Epstein 1991). As the Δ*fmk1* MAP kinase deletion mutants from

F. oxysporum showed next to a reduced aerial growth also an impairment in root attachment, Di Pietro and colleagues (Di Pietro et al. 2001) suggested both phenotypes to results from a lack of hydrophobin secretion. MAP kinases, therefore, might take part in the regulation of fungal attachment. In fact, in humans MAP kinase pathways have already been linked to adhesion-dependent gene regulation (Aplin et al. 2002; Defilippi and Vallés 2002).

Additionally, maize pathogenicity tests were performed with the Δ*gpmk1* mutants from *F. graminearum*. Unlike the wheat infection, the mutants were not totally apathogenic on maize. Instead, they were able to infect the host to a minor degree, suggesting that the regulation of infection processes by Gpmk1 could be partially host dependent. However, the experimental procedure of the maize infection assay conducted in this work had a clear shortcoming. Due to the size of the growth chambers the tasles had to be cut off the maize plants. The cobs therefore were not able to form ripe kernels, so that the infection conditions of the assay differed quite drastically from the natural conditions. The strength of infection might be reduced by developing kernels, as the kernels represent a much tougher barrier to overcome by the pathogen than the relatively soft tissue of the cob. A new assay under more natural conditions must be carried out, in order to get clearer informations about the host specific infections. Nevertheless, the Δ*gpmk1* mutants were able to macerate the cob tissue to a certain degree, suggesting that the Gpmk1 MAP kinase from *F. graminearum* does not regulate all infection processes under every condition.

The apathogenic phenotype on wheat and the reduced virulence on maize led to the question which infection mechanisms of *F. graminearum* are regulated by the pathogenicity MAP kinase Gpmk1. Up to date, only one factor, the trichothecene production, has been clearly determinded to be relevant for the virulence of *F. graminearum*. Deletion of the *tri5* gene led to mutants that were not able to produce any trichothecenes and that showed a reduced virulence (Bai et al. 2001; Proctor et al. 1995). Therefore, it was necessary to analyse whether the Gpmk1 MAP kinase regulates the trichothecene production. A down-regulation of trichothecenes in the Δ*gpmk1* mutants could explain a virulence reduced phenotype. Another possible pathogenicity factor are CWDE. The degradation of wheat cell wall components was observed microscopically after infections with *F. graminearum* and *F. culmorum* (Wanjiru et al. 2002; Kang and Buchenauer 2000). Therefore, the secretion of CWDE was postulated. However, up to date it is not known which hydrolytic enzymes can be secreted by *F. graminearum* at all. A

down-regulation of CWDE in the Δ*gpmk1* mutants could demonstrate the importance of these enzymes for the pathogenic life of *F. graminearum*.

The toxin production of the Gpmk1 MAP kinase disruption mutants had to be assayed *in vitro*, because the mutants were not able to cultivate living wheat spikes. Three different *in vitro* induction substrates were tested: wheat kernels, maize kernels, and rice. The three induction methods used also differed in various conditions (incubation time and temperature, light intensity, oxygen accessability, additional nutrient supply, and amount of inoculum). The wild type and Δ*gpmk1* mutant cultures of all three induction conditions were analysed for the production of the trichothecene deoxynivalenol (DON) and the estrogenic zearalenone (ZON).

Fungal strains growing on whelled wheat kernels only produced ZON. DON was neither detectable in the mutants nor in the wild type strain. The failed DON induction is most likely due to a poor oxygen supply of the cultures, resulting from tightly closed culture jars. According to Dr. M. Lemmens (personal information) a low oxygen pressure can inhibit the induction of DON completely. The mutants produced either no or drastically reduced amounts of ZON compared to the wild type. These results suggested a regulation of ZON induction under the given conditions by the Gpmk1 MAP kinase.

A cultivation of the *F. graminearum* strains on maize kernels, a substrate that is generally used to determine the complete mycotoxin spectrum of an isolate (Dr. M. Lemmens, personal information), resulted in the induction of DON and ZON in the wild type as well as in the mutant strains. The ZON content of the wild type culture was nearly 4-fold lower than the content of the wheat culture. This reduction might be caused by the shorter incubation time, the lower incubation temperature, and a lower air moisture in the maize assay (Jimenez et al. 1996; Montani et al. 1988). The mutants produced a comparable amount of ZON and a slightly higher amount of DON. Hence, the mutants are generally capable of producing the toxins DON and ZON at levels comparable to the wild type, despite the missing MAP kinase Gpmk1.

A third toxin induction took place on rice. The medium was supplemented with saccharose and casein, because high amounts of carbon can promote the toxin production. Additionally, special cultivation jars were used to aid the oxygen influx. These measures lead to an obviously stronger DON and ZON induction of the wild type strain than on wheat or maize. This result coincides with the fact that rice has already been shown to be the best solid, natural substrate for the induction of *F. graminearum* toxins (Lori et al. 1990; Megalla et al. 1986). On rice all Gpmk1 MAP kinase deletion mutants were

drastically reduced by 96.5 % in their ZON production compared to the wild type strain. Thus, the ZON induction seems to be regulated by the Gpmk1 MAP kinases during growth of *F. graminearum* on rice. Concerning the DON production on rice, the Δ*gpmk1* mutant cultures contained varying amounts of toxins. Two mutants produced wild type DON levels, whereas the other two showed an obvious reduction (~50 %) in DON production. These results make a regulation of DON by Gpmk1 during growth on rice questionable. Besides the DON and ZON analysis, all rice cultures were tested for the production of the DON-precursors 3-acetyldeoxynivalenol (3-ADON) and 15-acetyldeoxynivalenol (15-ADON) as well as the trichothecene nivalenol (NIV). NIV was not found in any of the analysed probes, indicating the isolate 8/1, which was used in the course of this work, to belong to the DON chemotype of the type B trichothecenes producers (Bottalico 1998). Furthermore, the main end product of its trichothecene pathway seems to be DON, as none of the precursors 3-ADON and 15-ADON could be measured in the rice probes.

Generally, not much information exists concerning the conditions for the toxin induction in *Fusarium* species and its regulation is expected to be very complex. However, the biosynthesis of mycotoxins is known to be influenced by many factors, such as the strain, the substrate, the period of colonisation, the temperature, moisture, the availability of certain nutrients, oxygen, and pH (Sutton 1982; Ueno et al. 1975). Additionally, certain evidence hints at a regulation of trichothecenes via signal transduction pathways mediated by a G-protein α-subunit (Tag et al. 2000). The results of this work suggest a differential regulation of DON and ZON induction in *F. graminearum* by various signal transduction pathways depending on the substrate the fungus is cultured on. The analysed MAP kinase Gpmk1 seems to regulate the induction of ZON production on wheat and on rice, whereas on maize a different pathway is chosen for its induction. Altered chemical and/or topographical signals on the surface of the substrates could be one clue for the activation of different transduction pathways. Eventhough DON seems to be partially regulated by the Gpmk1 MAP kinase during growth on wheat (Urban et al. 2003), a DON regulation via Gpmk1 on maize and rice is very questionable. Generally, one must keep in mind that most regulational events can not be regarded as mere linear pathways, but instead are very complex. Pathways can be either activated or inhibited by cross talk from other pathways. Furthermore, additional regulatory events can occur at the level of the transcription factors.

According to Wolf and Mirocha (Wolf and Mirocha 1973) ZON could act as sex pheromone in *F. graminearum*, helping the mating partners to find each other. Bringing into mind, that the Δ*gpmk1* mutants are completely unable to form sexual fruiting bodies

and that they also are reduced in ZON production, it does seem tempting to conclude that the sexual sterility of the MAP kinase disruption mutants results from the lack of ZON secretion. However, this conclusion must be verified by measuring the ZON amount produced by the wild type strain and the mutants during growth on sexual reproduction stimulating carrot medium (compare 2.1.3.2.). Particularly, as the regulation of ZON via the Gpmk1 MAP kinase cascade seems to be medium dependent.

Eventhough Wanjiru and colleagues (Wanjiru et al. 2002) have postulated a secretion of certain CWDE by *F. graminarum*, up to date no detailed information exists, as to which CWDE the pathogen actually can secrete. Only the secretion of lipolytic enzymes had been shown so far (Christian Haase, unpublished data). Using qualitative plate assays and quantitative photometric enzyme assays, it was possible to display the actual production and secretion of amylolytic, pectinolytic, cellulolytic, xylanolytic, and proteolytic enzymes by *F. graminearum* in the present work. The fungal wild type strain 8/1 produced high amounts of starch degrading enzymes and lower levels of pectin, carboxymethylcellulose (CMC), xylan, and casein degrading enzymes.
The regulatory effect of the Gpmk1 MAP kinase on the secretion of CDWE was assayed by measuring the ability of the Δ*gpmk1* mutants to degrade components of the plant cell wall *in vitro*. The disruption of the *gpmk1* gene had no effect on the production of amylolytic enzymes and polygalacturonases, indicating these enzymes to firstly not be regulated by the Gpmk1 MAP kinase and secondly to not be responsible for the apathogenic phenotype of the mutants. However, it can not be postulated that all types of pectin degrading enzymes (e.g. pectate lyases and pectin methylesterases) are irrelevant for the pathogenicity of *F. graminearum*. Particularly as pectinolytic enzymes are often the first CWDE produced by pathogens when cultured on purified plant cell walls and during infection. Purified pectinases can cause tissue maceration, a major symptom of some plant diseases (Annis and Goodwin 1997). Furthermore, the disruption of single pectinolytic enzymes in *B. cinerea* (Valette-Collet et al. 2003; te Have et al. 1998), *C. purpurea* (Oeser et al. 2002), and *Aspergillus flavus* (Shieh et al. 1997) was sufficient to reduce the fungal virulence, indicating the importance of these enzymes for fungal pathogenicity. In *Nectria haematococca* the simultanious disruption of two pectate lyase genes also led to mutants with impaired virulence (Rogers et al. 2000). Pectinases of *F. oxysporum* were shown to be differentially regulated, partially even by the pathogenicity MAP kinase Fmk1. This regulatory kinase was demonstrated to induce a pectate lyase but not a polygalacturonase

(Di Pietro et al. 2001). Similar to Fmk1 from *F. oxysporum*, the Gpmk1 MAP kinase might regulate the pectate lyases. Polygalacturonases show an optimal activity at approximately pH 5 and pectate lyases at approximately pH 9. As the assay was performed at pH 5, the pectate lyase activity might not be detected at those conditions. Maybe a difference in enzyme activity could have been found for the mutants at alkaline conditions. Hence, pectate lyases might turn out to be the enzymes that are relevant for pectin degradation during pathogenic processes of *F. graminearum*.

Proteases have been extensively studied as potential virulence factors in pathogens of animals and humans, whose intercellular matrix is mainly proteinaceous. Secreted aspartic proteinases have been shown to contribute to tissue damage during infection (Schaller et al. 1999). Lately, however, proteases have also started to emerge as potential virulence factors of phytopathogenic fungi. A protease of the tomato pathogen *Colletotrichum coccodes* was shown to be essential for pathogenicity and virulence (Redman and Rodriguez 2002) and in the wheat pathogen *Stagonospora nodorum* a trypsin-like protease is suggested to participate in the degradation of host cell walls during infection (Carlile et al. 2000). In *F. graminearum* secretion of proteases could be particularly important for the degradation of protein depositions, which have been shown to be produced in wheat cell walls upon attack of *F. graminearum* (El-Glendy et al. 2001). The *F. graminearum* Gpmk1 MAP kinase mutants only exhibited a retardation of protease induction, indicating Gpmk1 to possibly be responsible for the early enzyme induction. But other regulatory pathways rapidly take over the protease induction. A participation of Gpmk1 regulated proteases during the pathogenic phase of *F. graminearum* can only be assumed for the early infection time points.

The Gpmk1 MAP kinase also seems to regulate the early induction of xylanase and endoglucanse expression, as in the supernatants of the Δ*gpmk1* mutants xylanolytic and endoglucanase activities were later detectable than in the wild type strain. In fact, a similar regulational influence on cellulase production was already postulated for the Chk1 pathogencity MAP kinase from *C. heterostrophus* (Lev and Horwitz 2003). In a study of uncharacterised mutants of *C. lagenarium*, cellulases were also suggested to play a role in initial penetration of this pathogen (Katoh et al. 1988). Furthermore, a xylanase of *F. oxysporum* was exclusively expressed during the initial stages of infection in tomato roots (Gómez-Gómez et al. 2001), indicating the importance of xylan degradation for the disease initiation. Eventhough it has never been possible to demonstrate the importance of xylanases for phytopathogenicity, it is generally assumption that xylanases might be a

pathogenicity factor of pathogens of monocotyledons, because xylan is the most abundant component of the cell walls in this group of plants (Apel et al. 1993). Furthermore, Wanjiru and colleagues (Wanjiru et al. 2002) saw a tremendous decrease in the xylan content of the wheat cell wall after *F. graminearum* infection. Besides the delay in xylanase and endoglucanase induction, the Δ*gpmk1* mutants also displayed an obvious overall reduction in these enzyme activities. However, comparison of the mutants amongst each other, exhibit the mutants to show quite different xylanases and endoglucanses induction levels. It is imaginable, that the Gpmk1 MAP kinase initially regulates the induction of these enzymes. But starvation might result in the activation of a different pathway, that also can induce xylanase and endoglucanse activities. This process might occur in each mutant at a different speed. Nevertheless, the results of this work certainly suggest a participation of xylanases and endoglucanases during early pathogenic life stages of *F. graminearum*. This coincides with results found for the pathogenic fungi *C. heterostrophus* (Lev and Horwitz 2003), *F. oxysporum* (Gómez-Gómez et al. 2001), and *C. lagenarium* (Katoh et al. 1988), as well as the bacterium *Xanthomonas campestris* (Gough et al. 1988). CWDE are, furthermore, proposed to participate in fungal adhesion to surfaces (Nicholson and Epstein 1991). The reduced production of endoglucanases could therefore explain why the mutant colonies were not able to adhere properly to the cellophane foil and were subsequently hardly able to degrade the foil.

The disruption of the *gpmk1* MAP kinase gene finally had the most drastic affect on the lipolytic activity of *F. graminearum*. MAP kinase disruption mutants only had 20 % residual lipolytic activity compared to the wild type strain as found in the quantitative enzyme assays. The lipolytic activity of the Δ*gpmk1* mutants was so far reduced that the difference could even be detected in qualitative plate assays. Thus, the induction of lipolytic activity is obviously regulated by the Gpmk1 MAP kinases. An activation of lipase activity by MAP kinase cascades has in fact already been shown for humans (Krauss 1997). Furthermore, the data of this work also indicates the importance of lipase secretion for the infection process of *F. graminearum*. Up to date, the importance of lipases for phytopathogenicity has only been shown for *Alternaria brassicicola* (Comménil et al. 1998) and *B. cinerea* (Berto et al. 1999). Lipase antibody inhibition experiments showed that fungal lipases play an essential role during the early infection stages, e.g. the spore adhesion, of the plant pathogens *A. brassicicola* and *B. cinerea*. As Pritsch and coworkers (Pritsch et al. 2000) had observed a subcuticular growth of *F. graminearum* after host penetration, the secreted lipases might participate in cuticle degradation, thereby helping

the fungus to establish itself in the host. However, lipases may also be essential for liberating fatty acids from wax lipids, oil droplets or from the plant cell membrane. The free fatty acids are then generally utilized directly from the pathogen (Agrios 1997). Additionally, lipase products, diacylglycerol and fatty acids, have also been shown to function as second messengers in *M. grisea* (Thines et al. 1997) and *Colletotrichum trifolii* (Dickman et al. 2003), activating protein kinase A or protein kinase C dependant signal transduction pathways. Activation of these pathways was required for appressorium formation in both fungi (Dickman et al. 2003; Thines et al. 2000) and was demonstrated to be induced by plant cutin in *C. trifolii* (Dickman et al. 2003). Concerning *F. graminearum*, lipase products might have similar regulatory effects in this pathogen.

Finally, all results gathered from the quantitative enzyme assays suggest the Gpmk1 pathogenicity MAP kinase from *F. graminearum* to regulate several CWDE such as lipases, endoglucanases, and xylanases. A defect in protein secretion could be excluded, as the mutants did not have higher enzyme activity levels in the mycelial cell pellet compared to the wild type strain. Gpmk1 is, furthermore, responsible for the early induction of proteases, but not for the regulation of amylase and polygalacturonase production. The ability of the mutants to degrade certain cell wall components could in all cases be correlated to their radial growth speed on the corresponding substrate. Additionally, the mutants showed a reduced growth speed on crystalline cellulose, indicating the *gpmk1* disruption to not just influence the endoglucanase activity, that was quantitatively determined in this work, but to also have an effect on the production of other enzymes of the cellulase complex. The simultaneous reduction of different CWDE is one clue to understanding the apathogenic phenotype of the Δ*gpmk1* mutants during growth on wheat. In fact, it is generally understood that CWDE act synergistically on the pathogenesis of plant pathogens (Annis and Goodwin 1997). Therefore, the characterisation of regulatory genes, such as the *snf1* gene from *Cochliobolus carbonum* (Tonukari et al. 2000), is more promissing in gaining information about the effect of CWDE on the virulence of plant pathogens than the deletion of single genes encoding CWDE.

Comparison of the toxin results and the results from the quantitative enzyme assays with the results gathered from the pathogenicity tests leads to a possible hypothesis for the host specific infection of the Δ*gpmk1* mutants during growth on wheat and maize (Fig. 57). First of all, the reduced production and secretion of CWDE affects the initial infection process. The penetration of the host is either totally inhibited or occurs much slower. This

gives the host more time to recognize the attack and initate its defence mechanisms. Thereby, leading to a reduced impact of the infection. If secondly, a substrate specific toxin regulation is postulated for *F. graminearum* as mentioned above, the availability of DON could further influence the strength of the infection. A regulation of DON and ZON production through the Gpmk1 MAP kinase on wheat suggests that the Δ*gpmk1* mutants do not produce these toxins during a wheat infection and are therefore, unable to hamper the hosts defence response. Particularly, as DONs main phytotoxic effect seems to be the inhibition of the rapid translation of defence response proteins, thereby aiding the growth

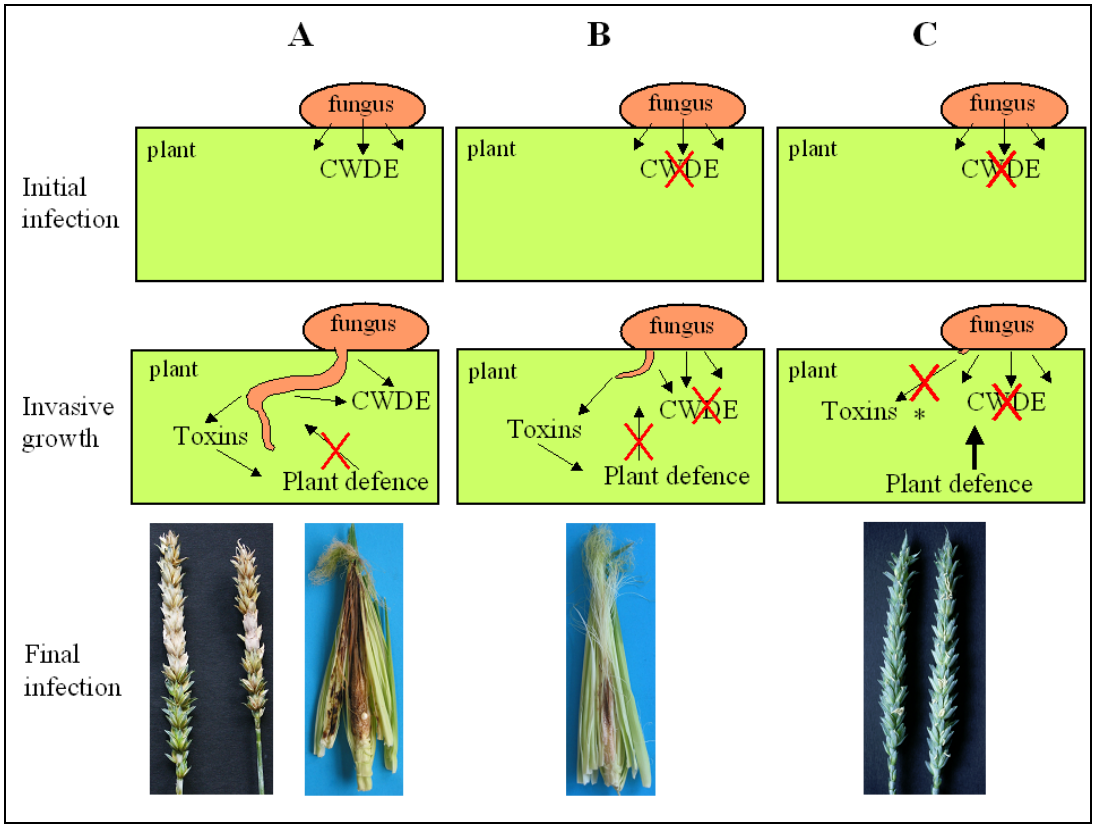

Fig. 57: Scheme illustrating the host specifity of the *F. graminearum* Δ*gpmk1* mutants. **A**) wild type strain on either wheat or maize; **B**) Δ*gpmk1* mutants on maize; **C**) Δ*gpmk1* mutants on wheat. A red X symbolises a reduction or an inhibition. * result partially gathered by Urban and colleagues (Urban et al. 2003).

of the pathogen in the plant tissue (Kang and Buchenauer 1999). The combination of slow or no penetration and missing toxin production on wheat could be the reason for the apathogenicity of the Δ*gpmk1* mutants on wheat. As discussed earlier on, the toxin induction during growth on maize is regulated by other pathways than the Gpmk1 MAP kinase. Thus, the Δ*gpmk1* mutants still produce DON and ZON during maize infection, which in turn interact with the host. Finally resulting in the invasion of the host. But as the mutants continue to be impaired in CWDE production, the symptom development stays

drastically reduced. The secretion of CWDE, therefore seems to be crucial for the initial infection including the penetration and early disease establishment, whereas toxin secretion aids the invasive growth of the pathogen. Up to date, no evidence for the importance of ZON during the infection process exists. However, the results of this work might also suggest a participation of ZON as phytotoxin in *Fusarium* disease establishment, since the apathogenic Δ*gpmk1* mutants show a stronger reduction in ZON than in DON production.

4.4. A putative hydrophobin from *F. graminearum*

In the last decade hydrophobins have been shown to play an important role during attachment of the fungus to the plant cuticle, infection court preparation, and topological signaling (Schäfer 1994). It has been shown that hydrophobins are essential for the development of aerial hyphae, fruiting bodies (Ando et al. 2001; Lugones et al. 1996; Wessel et al. 1991), and full virulence (Talbot et al. 1993). These phenotypes are also found in the *gpmk1* deficient mutants of *F. graminearum*. Similar to *M. grisea* mutants deleted in the hydrophobin gene *mpg1* (Talbot et al. 1996; Talbot et al. 1993), the Gpmk1 MAP kinase deficient mutants of *F. graminearum* exhibit a reduced conidia production in general as well as a failure to form sporodochia. The few conidia made by the Δ*gpmk1* mutants are found under the agar, again indicating that the mycelia exhibit diminished capability of growing in an aerial phase. Comparable to the Δ*gpmk1* mutants, the deletion of the Mpg1 hydrophobin from *M. grisea* led to mutants with reduced conidia production but normal conidia germination rates (Talbot et al. 1993). An inability of filamentous fungi to form aerial hyphae also has been shown to have a drastic effect on the formation of sexual fruiting bodies, e.g. the deletion of the *chk1* MAP kinase from *C. heterostrophus* (Lev et al. 1999). Hence, the sexually sterile phenotype of the Δ*gpmk1* mutants from *F. graminearum* might also be explained by an obvious reduction of aerial mycelia as is exhibited by these mutants. Eventhough a direct participation of hydrophobins in fungal virulence was only shown for *M. grisea* (Talbot et al. 1993), it is still generally assumed, that hydrophobins are involved in disease establishment by aiding the fungal attachment to the host. All Δ*gpmk1* phenotypes mentioned above as well as the observation that the Δ*gpmk1* mutants are impaired in adhesion to cellophane foil could indicate a possible defect of the *F. graminearum* Δ*gpmk1* mutants in the production and/or secretion of hydrophobins. A regulation of hydrophobin production by pathogenicity MAP kinases has

in fact already been displayed for *M. grisea* (Soanes et al. 2002) and has also been postulated for *F. oxysporum* (Di Pietro et al. 2001). In order to analyse a regulatory effect of the Gpmk1 MAP kinase on hydrophobin secretion, it was first necessary to identify genes in *F. graminearum* encoding such putative hydrophobins. Via screening of a cDNA library (kindly provided by the BASF AG) made from *F. graminearum* after growth on minimal medium, an open reading frame was identified that showed after translation a cysteine spacing typical for hydrophobins. The complete gene sequence was gained from genomic DNA and cDNA and a subsequent comparison of both sequences, and the translation of the open reading frame led to a protein sequence with obvious hydrophobin characteristics. The deduced amino acid sequence contained a signal sequence, indicating the protein to be secreted, which is a prerequisite for hydrophobins. The spacing of eight cysteines in the deduced amino acid sequence and the hydropathy blot of the sequence revealed this protein from *F. graminearum* to have high similarities to other fungal hydrophobins. Hence, the isolated gene was suggested to encode a putative hydrophobin from *F. graminearum*. This putative hydrophobin had a rather long N-terminal protein region, indicating it to probably belong to the class I hydrophobins (Wösten 2001). Transcripts of the putative hydrophobin gene were found during growth of *F. graminearum* on liquid and solid complete and minimal medium, during conidia germination, and in early phases of sexual reproduction. Thereby, the strongest gene induction seemed to take place during conidia germination. The *F. graminearum* hydrophobin was not transcribed on Czapek medium, in conidia themselves, in ripe perithecia, and during plant infection. These results suggest the isolated hydrophobin to be involved in the formation of aerial mycelia on solid medium as well as the reduction of the water tension in liquid culture to aid the fungus by breaching the water/air interface. Furthermore, the hydrophobin could be needed for the formation of aerial mycelia for early sexual reproduction events. The hydrophobin from *F. graminearum* obviously has its main function during conidia germination, thereby possibly enabling the germ tube to adhere to the surface it is growing on. Conidia of *F. graminearum*, however, do not rely on the putative hydrophobin. But as conidia from *F. graminearum* are not very hydrophobic, the absence of transcripts in conidia was not so astonishing. As the analysed hydrophobin is not transcribed during growth of *F. graminearum* on Czapek medium, it can not be associated with the drastic aerial hyphae reduced morphology of the Δ*gpmk1* mutants on this medium. Finally, it is evident that the identified hydrophobin has no functional role during plant infection and invasive growth in the host. Besides the transcriptional analysis,

the putative hydrophobin from *F. graminearum* must be purified from a liquid culture and analysed in order to understand its actual function, e.g. the purified hydrophobin could be added externally to the Δ*gpmk1* mutant cultures. A subsequent remediation of some of the mutant phenotypes, e.g. sexual sterility, formation of aerial hyphae and reduced adhesion to cellophane foil, would then give clear evidence for the participation of the hydrophobin during these developmental processes.

The initial question concerning the hydrophobins was to clarify whether the Gpmk1 MAP kinase from *F. graminearum* regulates the hydrophobin induction. Therefore, a transcription analysis was carried out with the wild type strain and the Δ*gpmk1* mutants. A down-regulation of the hydrophobin transcript levels could, however, not be found in the Δ*gpmk1* mutants, indicating the hydrophobin from *F. graminearum* to not be regulated by the Gpmk1 MAP kinase. Hence, the discussed phenotypes of the MAP kinase mutants do not result from a reduced amounts of the identified hydrophobin. But as most fungi have multiple hydrophobins (Trembley et al. 2002; Segers et al. 1999; Wessels 1996), it is very likely that *F. graminearum* also has several hydrophobin genes. The transcription of at least one of the still unknown genes might be regulated by the Gpmk1 MAP kinase and could be responsible for the observed Δ*gpmk1* phenotypes.

4.5. Conclusion and future prospects

As previously postulated for higher filamentous fungi, *F. graminearum* has three MAP kinases each taking over various functions during vegetative growth, asexual and sexual reproduction as well as pathogenicity, and each partially responsible for different extracellular signals. Figure 58 summarizes the results obtained during this work, giving the potential roles of the *F. graminearum* MAP kinases. The MAP kinases Gmap1, Gpmk1 and FgOsm are in the centre of three regulatory pathways. As the signals that induce each specific MAP kinase cascades are still unknown, one can only speculate about the nature of the signals in this context. Gmap1 might sense various differentiation signals or even pheromones that induce cell wall remodeling, sexual reproduction, and aerial growth. Furthermore, it takes part in *Fusarium* disease establishment by inducing the production of the phytotoxic thrichothecene DON (Hou et al. 2002) and by promoting hyphal growth. Characterisation of the Gpmk1 pathway has given first valuable informations concerning

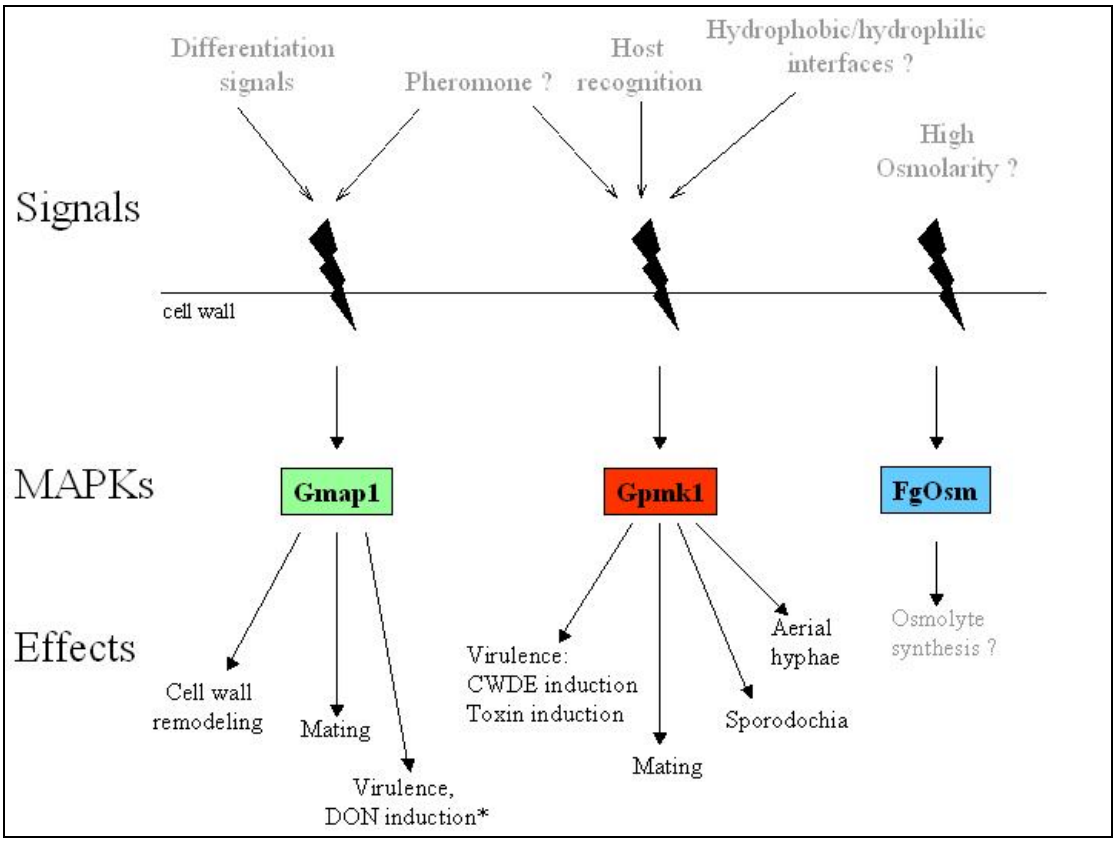

Fig. 58: Overview of the putative functions of the three MAP kinases from *F. graminearum*. Black letters indicate experimental results gathered in the course of this work. Grey letters indicate speculative signals or effects. * result gathered by Hou and coworkers (Hou et al. 2002).

the pathogenic life of *F. graminearum*. Gpmk1 seems to be particularly important during early stages of infection, as it regulates the production of many important CWDE such as pectinases, cellulases, xylanases, and particularly lipases that are maybe needed to penetrate the host surface. At later time points, a host specific triggering of toxin production via the Gpmk1 MAP kinase could result in differential disease establishment. This type of "fine tuned" toxin regulation might be necessary for the switch of *F. graminearum* from a short biotrophic phase to a necrotrophic life style. Hence, it can be postulated that *F. graminearum* has two main virulence determinants, the CWDE and the toxins. A concerted secretion of various CWDE is crucial for initial infection processes. A subsequent secretion of DON and possibly ZON is then necessary for disease establishment and invasive growth by hampering the plant defence response. Further secretion of CWDE would aid the breakdown of the plant tissue. Furthermore, Gpmk1 has an effect on mating processes, sporodochia, and aerial hyphae formation. The FgOsm pathway still remains to be functionally characterised. However, due to its high sequence homologies to many other YSAPK MAP kinases, it can be expected that FgOsm could

respond to high osmotic shocks and thus induce stress responses such as the synthesis of osmolytes.

Hence, each MAP kinase pathway seems to have one main, unique regulatory function, but is also able to share the regulation of various other processes with other existing pathways. Thus, it can happen that the interruption of different pathways leads to similar mutant phenotypes. However, pleiotropic mutant phenotypes can also result from the down-regulation of certain functional units that effect several developmental stages. Hydrophobins e.g., are known to be important for the formation of aerial hyphae, the conidiation, the sexual reproduction, and cell adhesion. A down-regulation of the hydrophobin production, thus, would result in mutants with pleiotropic phenotypes. Therefore, it is important to keep in mind that fungi mutated in regulatory genes can either have phenotypes that are directly linked to the missing regulational pathway or they can show phenotypes that themselves result from a different phenotype and not because the corresponding genes were actually regulated by the MAP kinase. Figure 59 shows, how the occurrence of all different phenotypes found for the various MAP kinase mutants could be explained. The asexual phenotype of the Δ*gmap1* mutants can be an indirect effect of the

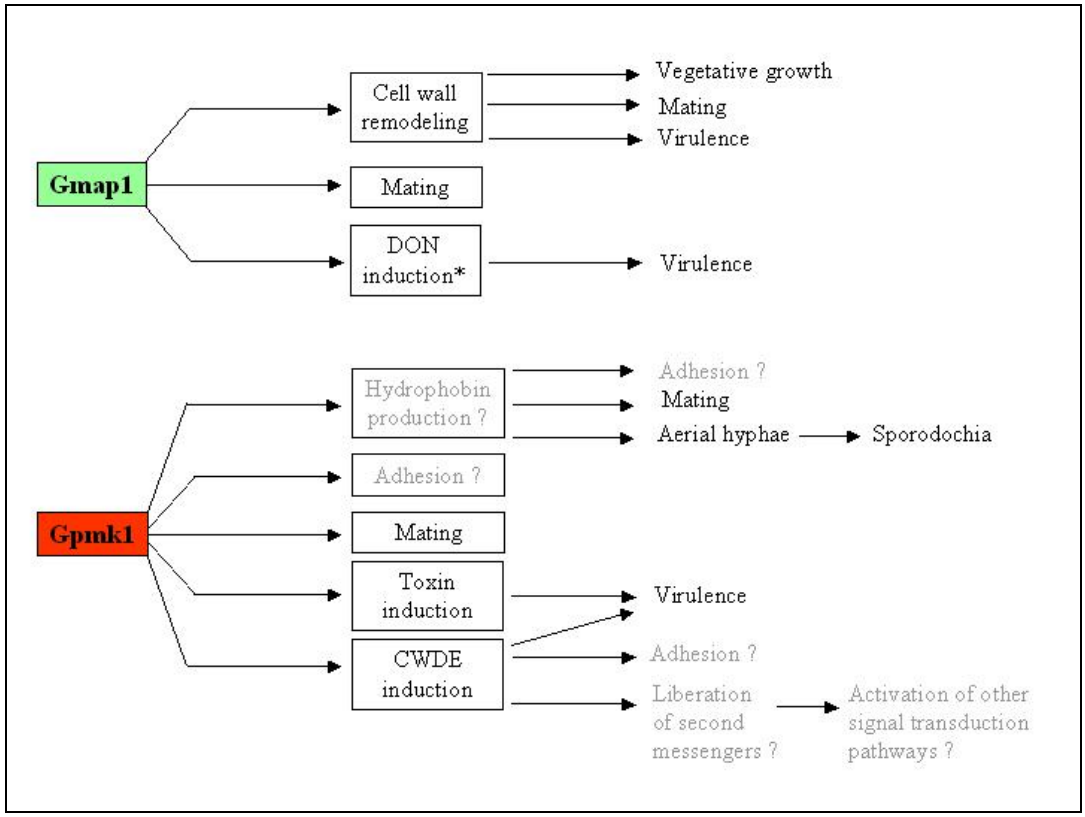

Fig. 59: The Gmap1 and the Gpmk1 MAP kinase from *F. graminearum* and how they cause certain phenotypes. Black letters indicate experimental results gathered in the course of this work. Grey letters indicate speculative effects of the Gpmk1 MAP kinase. * result gathered by Hou and coworkers (Hou et al. 2002).

failed cell wall remodeling. However, Gmap1 could also be involved in recognition of the mating partners by pheromone sensing, leading directly to the expression of mating related genes. Similarly, the reduced virulence of these mutants might be a joint effect of a reduced toxin production and a reduction in polarized growth due to cell wall defects.
Various phenotypes of the Δ*gpmk1* mutants, such as the sterility, as well as the formation of aerial hyphae, could result from a regulatory effect of Gpmk1 on hydrophobin production. A reduced formation of aerial hyphae might subsequently lead to malformation of sporodochia. Nevertheless, the regulation of hydrophobins via Gpmk1 still needs to be verified. This also holds true for any defect of the mutants in surface adhesion. Here again, mating type genes could be under Gpmk1 control, giving another explanation for the sexual sterility. Finally, as already mentioned before, the *in planta* phenotype of the Δ*gpmk1* mutants results from the direct regulation of toxin and CDWE induction via the Gpmk1 pathway. Furthermore, products of secreted lipases might translocate into the fungal cells and act as second messengers, inducing other signal transduction pathways, which also partake in regulation of infection related processes.

The results of this work show that the characterisation of regulatory proteines, such as MAP kinases, is a powerful tool for studying processes essential for pathogenicity. Nevertheless, it must be kept in mind, that most developmental processes can not be fully understood through the characterisation of single transduction pathways. In various other fungal organisms, the intricacies of the connections between signaling pathways are beginning to unfold and interactions appear to frequently exist between different pathways, such as the phosphoinositide, the cAMP, and the MAP kinase signaling pathways. In *S. cerevisiae* the Slt2 cell integrity MAP kinase pathway was shown to be crosslinked with a lipid independent protein kinase C (PKC) pathway and a phosphoinositide signaling pathway. Thereby, the PKC was postulated to control a bifurcated pathway, one arm of which contains the Slt2 MAP kinase module. The cross talk is supposed to take place at the level of the MAPKK kinase and be supported by various scaffold proteins (Herskowitz 1995). The Slt2 MAP kinase pathway and the phosphoinositide signaling pathway were shown to be distinctly separated but act together in regulating the polarised deposition of chitin for septum organisation during the cell division (Tahirovic et al. 2003). In the plant-pathogenic, filamentous fungi *M. grisea* a cross talk between a cAMP dependent pathway and the Pmk1 pathogenicity MAP kinase pathway was shown to regulate the formation of appressoria. The Δ*pmk1* mutants were still responsive to exogeniously added cAMP for

early stages of appressoria formation, which indicates Pmk1 to act downstream of a cAMP signal for infection structure formation (Xu and Hamer 1996). In fact, a single G subunit was suggested to be the link between the two pathways (Choi and Dean 1997; Xu et al. 1997). An interaction of these two pathways during appressoria formation was also proposed for *C. heterostrophus* (Lev et al. 1999) and *B. graminis* (Kinane and Oliver 2003). An interaction between cAMP dependent pathways and MAP kinase pathways was also found in several other fungi, such as *S. cereviseae*, *S. pombe*, *U. maydis*, and *Cryptococcus neoformans* (Kronstad et al. 1998). Hence, it is extremely likely, that some of the developmental processes and infection mechanisms found to be regulated by the MAP kinases Gmap1 and Gpmk1 in *F. graminearum* are also influenced by other pathways. This would certainly include the induction of toxins and CWDE, especially pectinases and amylases, as well as the regulation of conidiation and the secretion of hydrophobins.

This work enabled to gain some evidence towards the regulation of various developmental processes of *F. graminearum*, as well as some new insights into the infection mechanisms and their regulation of this devastating plant pathogen. Future studies must now focus on using these informations to find better methods for disease management, such as efficient targets for fungicides. The MAP kinases themselves can not function as target, as they do not fulfill the condition of being a specific fungal element. They are found from yeast to human (Widmann et al. 1999) and in plants they are an important regulator of the defence reponse mechanisms (Suzuki 2002; Morris 2001; Zhang and Klessig 2001). Fungizides acting against MAP kinases would, thus, not only inhibit the natural plant defence but also have toxic effects on the consumers. Hence, it is necessary to find specific fungal proteins that also are an element of the infection processes. These could be either specific effectors of MAP kinase regulation or their inductors, such as transmembrane receptors. MAP kinase deletion mutants can be helpful in finding genes that encode such proteins. Transcriptional profiling (Madhani et al. 1999) and suppression subtractive hybridisation (Lev and Horwitz 2003; Xue et al. 2002) of MAP kinase mutants have been two of the many methods used to find specific genes that are regulated by certain MAP kinases. These techniques could also be the clue for finding specifically virulence regulated genes in *F. graminearum* and for finding putative targets for disease managment.

5. Summary

The ascomycete *Fusarium graminearum* is the main causal agent of the head blight disease of small grain cereals and the stalk and ear rot of corn. It is found all over the world and is one of the most important cereal pathogens. The head blight disease causes grain yield losses and reductions in grain quality through the accumulation of non-selective mycotoxins. So far no cereal cultivars with resistance against *F. graminearum* and no fungicides working efficiently against *F. graminearum* are available.

In the present work, a strategy using mitogen-activated protein (MAP) kinase deletion mutants was used to investigate, which developmental and pathogenic processes of *F. graminearum* are possibly regulated by MAP kinase signal transduction pathways and which mechanisms might be essential for its pathogenicity. First of all, three genes encoding MAP kinases were isolated from *F. graminearum*. They were named Gmap1, Gpmk1 and FgOsm, respectively. Functional characterisation of Gmap1 and Gpmk1 was carried out by producing Δ*gmap1* and Δ*gpmk1* mutants via transformation mediated gene disruption. The function of FgOsm still remains to be analysed. But, according to its amino acid sequence homologies FgOsm belongs to the yeast/fungi stress-activated MAP kinases, which generally regulate responses to hyperosmotic shocks in other fungi.

Gmap1 belongs to the yeast/fungi extracellular-signal regulated MAP kinase subgroup 2 that are known to be involved in cell integrity processes. Characterisation of the Δ*gmap1* mutants revealed a growth defect on solid media, an asexual phenotype, and a drastic reduction of virulence. These results suggested the Gmap1 kinase to regulate cell developmental processes that are important for mating and full virulence. However, the generated Δ*gmap1* mutants exhibited an obvious genetical instability. Therefore, they were not further characterised.

Disruption of the gene encoding the Gpmk1 MAP kinase from *F. graminearum*, a kinase of the yeast/fungi extracellular-signal regulated MAP kinase subgroup 1, led to mutants that displayed a reduced ability to produce aerial hyphae and were unable to form sporodochia, resulting in a reduced conidia production. Furthermore, they were completely unable to form sexual fruiting bodies. Infection tests revealed the mutants to have a drastically reduced virulence towards maize and be completely apathogenic on wheat. These results indicated the Gpmk1 MAP kinase to be involved in developmental processes, such as aerial growth, sporodochia formation, mating processes, as well as in host penetration and invasive growth.

The reduced ability to form aerial mycelia after *gpmk1* disruption suggested a regulation of hydrophobins via the identifed Gpmk1 MAP kinase. Therefore, a gene encoding a putative hydrophobin was isolated from *F. graminearum*. The deduced amino acid sequence showed all characteristics of hydrophobins. The hydrophobin gene was transcribed predominantely in germinating conidia, but could also be found during growth of the fungus on liquid and solid complete and minimal medium, as well as in early stages of perithecial development. No transcription occurred *in planta*, indicating the identified hydrophobin to have no obvious function during plant infection. A regulation of hydrophobin production by the Gpmk1 MAP kinase could however not be verified, so that the growth defects of the Δ*gpmk1* mutants could not be explained by the failure to secrete the identified hydrophobin. But, as most fungi secrete several hydrophobins, it remains to be examined, if a regulatory role of Gpmk1 on other still unknown hydrophobins could be the clue to some of the mutants phenotypes.

Since the trichothecene mycotoxins are so far the only virulence factors known for *F. graminearum*, the mutants were analysed for their ability to produce the trichothecene deoxynivalenol (DON) and additionally the mycotoxin zearalenone (ZON). The experiments revealed DON and ZON to be differentially regulated depending on the substrate the strains were cultivated on. Gpmk1 regulates the induction of ZON production on wheat and on rice, whereas on maize a different pathway is utilized for its induction. Gpmk1 only showed a slight regulatory effect on DON induction during cultivation on rice and no effect during cultivation on maize.

Recently, cell wall degrading enzymes (CWDE) have also been postulated to partake in the head blight disease establishment. In this work, it could be shown that *F. graminearum* can secrete amylolytic, cellulolytic, xylanolytic, pectinolytic, and proteolytic enzymes. Biochemical analysis of the Δ*gpmk1* mutants revealed a regulatory effect of the Gpmk1 MAP kinase on the early induction of an endoglucanase, a xylanase, and a protease activity as well as the overall induction of a lipolytic activity. These results suggest the infection processes of *F. graminearum* to depend on CWDE secretion particularly during the early infection stages. After host penetration the secretion of toxins aids the invasive growth of the pathogen. Hence, differential toxin secretion might result in a varying disease severity. As Gpmk1 influences the ZON induction by far stronger than the DON induction, these results could possibly give a first hint as to a role of ZON in plant infection.

6. Zusammenfassung

Der Ascomycet *Fusarium graminearum* ist ein weltweit verbreiteter Erreger von Ährenfusariosen kleinkörniger Gräser sowie der Halm- und Kolbenfäule des Maises. Er zählt zu den bedeutendsten Getreidepathogenen. Die Fusariose verursacht Ertrags- und Qualitätseinbußen durch leichtgewichtige, „taube“ Körner sowie durch Anreicherung von unspezifisch wirkenden Mycotoxinen im Getreide. Bis dato gibt es noch keine resistenten Getreidesorten und keine effizient gegen *F. graminearum* wirksamen Fungizide.

In der vorliegenden Arbeit wurde eine Strategie über mitogen-aktivierte Protein- (MAP) kinase Deletionsmutanten gewählt, um zu untersuchen, welche Entwicklungs- und Pathogenitätsprozesse von *F. graminearum* über MAP-Kinase-Signaltransduktionswege reguliert werden und welche Mechanismen für die Pathogenität essentiell sind. Zunächst wurden drei für MAP-Kinasen kodierende Gene aus *F. graminearum* isoliert. Sie wurden als Gmap1, Gpmk1 bzw. FgOsm bezeichnet. Die funktionale Charakterisierung von Gmap1 und Gpmk1 erfolgte durch die Herstellung von Δ*gmap1* and Δ*gpmk1* Mutanten mittels transformationsvermittelter Gendisruption. Die Funktion von FgOsm muß noch untersucht werden. Auf Grund seiner Aminosäuresequenzhomologien kann FgOsm jedoch zu den stressaktivierten MAP-Kinasen gezählt werden, welche in anderen Pilzen an der Regulation der Reaktion auf hyperosmotischen Schock beteiligt sind.

Gmap1 gehört zu der pilzlichen Untergruppe 2 der extrazellulären signalregulierten MAP-Kinasen, die an Prozessen des Zellbestands beteiligt sind. Die Δ*gmap1* Mutanten zeigten einen Wachstumsdefekt auf festen Medien, einen asexuellen Phänotyp und eine drastische Reduktion der Virulenz. Diese Ergebnisse deuten darauf hin, daß Gmap1 Prozesse der Zellentwicklung reguliert, die bei der Kreuzung und der vollen Virulenz eine Rolle spielen. Da die Δ*gmap1* Mutanten jedoch eine starke genetische Unbeständigkeit aufwiesen, wurden sie nicht weiter untersucht.

Die Disruption des Gens für die Gpmk1 MAP-Kinase von *F. graminearum*, eine Kinase der Untergruppe 1 der extrazellulären signalregulierten MAP-Kinasen, führte zu Mutanten, die eine reduzierte Bildung von Luftmyzel zeigten und die nicht mehr in der Lage waren Sporodochien zu bilden, was zu einer allgemeinen Senkung der Konidiationsrate führte. Außerdem bildeten sie keine sexuellen Fruchtkörper mehr. Infektionstests zeigten, dass die Mutanten reduziert virulent auf Mais und völlig apathogen auf Weizen waren. Diese Ergebnisse deuten darauf hin, daß die MAP-Kinase Gpmk1 an Entwicklungsprozessen, wie der Luftmyzelbildung, der Sporodochienbildung und der Kreuzung beteiligt ist, sowie an der Wirtspenetration und dem invasivem Wachstum im Wirt.

Die Beeinträchtigung der Luftmyzelbildung nach *gpmk1* Disruption ließ eine Regulation von Hydrophobinen durch die identifizierte Gpmk1 MAP-Kinase vermuten. Daher wurde ein Gen für ein potentielles Hydrophobin aus *F. graminearum* isoliert. Die abgeleitete Aminosäuresequenz wies alle Charakteristika der Hydrophobine auf. Das entsprechende Gen wurde hauptsächlich in keimenden Konidien transkribiert, konnte aber auch während des Wachstums in flüssigem und festem Komplett- und Minimalmedium sowie in Perithezienvorstufen nachgewiesen werden. *In planta* wurde es nicht transkribiert, so dass eine Rolle des identifizierten Hydrophobins bei der Pflanzeninfektion unwahrscheinlich ist. Eine Regulation des Hydrophobingens durch die Gpmk1 MAP-Kinase konnte nicht bestätigt werden. Folglich können die Wachstumsveränderungen der Δ*gpmk1* Mutanten nicht durch die mangelnde Sekretion des identifizierten Hydrophobins erklärt werden. Da die meisten Pilze aber mehrere Hydrophobine sekretieren, bleibt es allerdings noch offen, ob Gpmk1 auf andere, noch unbekannte Hydrophobine eine regulatorische Funktion ausübt, die wiederum die Δ*gpmk1*-Phänotypen erklären könnte.

Da bis dato die Trichothecen-Mycotoxine die einzig bekannten Virulenzfaktoren von *F. graminearum* sind, wurden die Δ*gpmk1*-Mutanten auf ihre Fähigkeit untersucht, das Trichothecen Deoxynivalenol (DON) und zusätzlich das Mycotoxin Zearalenon (ZON) zu produzieren. Die Experimente zeigten, dass DON und ZON abhängig vom jeweiligen Substrat unterschiedlich reguliert werden. Gpmk1 scheint die ZON-Produktion auf Weizen und Reis zu regulieren, wohingegen auf Mais ein anderer Regulationsweg eingeschlagen wird. Gpmk1 zeigte einen geringen regulatorischen Einfluß auf die DON-Induktion während des Wachstums auf Reis und keinen Einfluß beim Wachstum auf Mais.

Wiederholt wurde die Bedeutung zellwandabbauender Enzyme (CWDE) für die Fusariosenentstehung postuliert. In dieser Arbeit konnte gezeigt werden, dass *F. graminearum* amylolytische, cellulolytische, xylanolytische, pektinolytische und proteolytische Enzyme sekretieren kann. Biochemische Analysen der Δ*gpmk1* Mutanten zeigten, dass die Gpmk1 MAP-Kinase die frühe Induktion einer Endoglucanase-, einer Xylanase- und einer Proteaseaktivität reguliert, sowie die gesamte Induktion einer Lipaseaktivität. Diese Ergebnisse deuten darauf hin, daß der Infektionsmechanismus von *F. graminearum* insbesondere in frühen Infektionstadien von der Sekretion verschiedener CWDE abhängt. Nach der Penetration helfen die Toxine bei der Ausbreitung des Pilzes im Wirtsgewebe. Folglich könnte die differentielle Sekretion von Toxinen zu einer Variation in der Krankheitsausbreitung führen. Da Gpmk1 die ZON-Produktion viel stärker beeinflusst als die des DON, könnten diese Ergebnisse den ersten Hinweis auf eine mögliche Beteiligung von ZON bei der Pflanzeninfektion geben.

7. References

Adams J F (1921) Observations on wheat scab in Pennsylvania and its pathological history. Phytopathology 11: 115-124

Agrios G N (1997) Plant Pathology. Fourth Edition, Academic Press, San Diego

Alonso-Monge R, Navarro G F, Molero G, Diez O R, Gustin M, Pla J, Sanchez M, Nombela C (1999) Role of the mitogen-activated protein kinase Hog1p in morphogenesis and virulence of *Candida albicans*. J Bacteriol 181: 3058-3068

Amberg D C, Botstein D, Beasley E M (1995) Precise gene disruption in *Saccharomyces cerevisiae* by double fusion polymerase chain reaction. Yeast 11:1275-1280.

Ando A, Harada A, Miura K, Tamai Y (2001) A gene encoding a hydrophobin, *fvh1*, is specifically expressed after induction of fruiting in the edible mushroom *Flammulina velutipes*. Curr Genet 39: 190-197

Annis S, Goodwin P H (1997) Recent advances in the molecular genetics of plant cell wall-degrading enzymes produced by plant pathogenic fungi. European Journal of Plant Pathology 103: 1-14

Apel C P, Panaccione D G, Holden F R, Walton J D (1993) Cloning and targeted gene disruption of *XYL1*, a β1,4-xylanase gene from the maize pathogen *Cochliobolus carbonum*. Mol Plant-Microbe Interact 6: 467-473

Aplin A E, Hogan B P, Tomeu J, Juliano R L (2002) Cell adhesion differentially regulates the nucleocytoplasmic distribution of active MAP kinases. J Cell Science 115: 2781-2790

Ausubel F M, Brent R, Kingston R E, Moore D D, Seidman J G, Smith J A, Struhl K, Albright L M, Coen D M, Varki A, Janssen K (1994). Current Protocols in Molecular Biology. New York: John Wiley and Sons. chapter 1.8.4.

Bai G-H, Desjardins A E, Plattner R D (2001) Deoxynivalenol-nonproducing *Fusarium graminearum* causes initial infection, but does not cause disease spread in wheat spikes. Mycopathologia 153: 91-98

Bai G, Shaner G (1994) Scab of wheat: prospects for control. Plant Dis 78: 760-766

Banuett F (1998) Signalling in the yeasts: an informational cascade with links to the filamentous fungi. Microbiol Mol Biol Rev 62: 249-274

Béguin P (1990) Molecular biology of cellulose degradation. Annu Rev Microbiol 44: 219-248

Bergstrom G C (1993) Scab (Fusarium head blight). In Seed-borne Diseases and Seed Health Testing of Wheat (Mathur S B, Cunter B M, Eds.) p. 84, Jordbrugsfortaget, Frederiksberg

Berto P, Comménil P, Belingheri L, Dehorter B (1999) Occurrence of a lipase in spores of *Alternaria brassicicola* with a crucial role in the infection of cauliflower leaves. FEMS Microbiol Lett 180: 183-189

Bertoldo C, Antranikian G (2002) Natural polysaccharide degrading enzymes. In Enzyme catalysis in organic chemistry (Draus K, Waldmann H, Eds.) pp 653-685, Wiley-VCH, Weinheim

Biesaga-Kościelniak J, Marcińska M, Wędzony M, Kościelniak J (2003) Effect of zearalenone treatment on the production of wheat haploids via the maize pollination system. Plant Cell Rep 21: 1035-1039

Bird D, Bradshaw R (1997) Gene targeting is locus dependant in the filamentous fungus *Aspergillus nidulans*. Mol Gen Genet 255: 219-225

Bottalico A (1998) *Fusarium* disease of cereals: species complex and related mycotoxin profiles, in Europe. J Plant Pathol 80: 85-103

Bowden R L, Leslie J F (1999) Sexual recombination in *Gibberella zeae*. Phytopathology 89: 182-188

Brachmann A, Schirawski J, Müller P, Kahmann R (2003) An unusual MAP kinase is required for efficient penetration of the plant surface by *Ustilago maydis*. The EMBO Journal 22: 2199-2210

Bradford M (1976) A rapid and sensitive method for the quantification of microgramm quantities of protein utilizing the principle of protein-dye binding. Anal Biochem 72: 248-254

Brenner S, Johnson M, Bridgham J, Golda G, Lloyd D H, Johnson D, Luo S, McCurdy S, Foy M, Ewan M, George D, Eletr S, Albrecht G, Vermaas E, Williams S R, Moon K, Burcham T, Pallas M, DuBridge R B, Kirchner J, Fearon K, Mao J, Corcoran K (2000) Gene expression analysis by massively parallel signature sequencing (MPSS) on microbead arrays. Nature Biotechnology 18: 630-634

Brewster J L, de Valoir T, Dwyer N D, Winter E, Gustin M C (1993) An osmosensing signal transduction pathways in yeast. Science 259: 1760-1763

Buerstmayr H, Lemmens M, Hartl L, Doldi L, Steiner B, Stierschneider M, Ruckenbauer P (2002) Molecular mapping of QTLs for Fusarium head blight resistance in spring wheat. I. Resistance to fungal spread (Type II resistance). Theor Appl Genet 104: 84-91

Bussink H J, Osmani S A (1999) A mitogen-activated protein kinase (MPKA) is involved in polarized growth in the filamentous fungus *Aspergillus nidulans*. FEMS Microbiol Lett 173 (1): 117-125

Carlile A J, Bindschedler L V, Bailey A M, Bowyer P, Clarkson J M, Cooper R M (2000) Characterization of SNP1, a cell wall-degrading trypsin, produced during infection by *Stagonospora nodorum*. Mol Plant-Microbe Interact 13: 538-550

Choi W, Dean R A (1997) The adenylate cyclase gene *MAC1* of *Magnaporthe grisea* controls appressorium formation and other aspects of growth and development. Plant Cell 9: 1973-1983

Cobb M H, Goldsmith E J (1995) How MAP kinases are regulated. J Biol Chem 270: 14843-14846

Comménil P, Belingheri L, Dehorter B (1998) Antilipase antibodies prevent infection of tomato leaves by *Botrytis cinerea*. Physiol Mol Plant Pathol 52: 1-14

Comménil P, Belingheri L, Bauw G, Dehorter B (1999) Molecular characterization of a lipase induced in *Botrytis cinerea* by components of grape berry cuticle. Physiol Mol Plant Pathol 55: 37-43

Cosano I C, Martín H, Flández M, Nombela C, Molina M (2001) Pim1, a MAP kinase involved in cell wall integrity *in Pichia pastoris*. Mol Genet Genomics 265: 604-614

Csank C, Schroppel K, Leberer E, Harcus D, Mohamed O, Meloche S, Thomas D Y, Whiteway M (1998) Roles of the *Candida albicans* mitogen-activated protein kinase homologue, Cek1p, in hyphal development and sytemic candidosis. Infect Immun 66: 2713-2721

Davidson R C, Nichols C B, Cox G M, Perfect J R, Heitmann J (2003) A MAP kinase cascade composed of cell type specific and non-specific elements controls mating and differentiation of the fungal pathogen *Cryptococcus neoformans*. Mol Microbiol 49: 469-485

Deacon J W (1997) Modern Mycology, 3rd Edition, Chapter 8 Genetics, Blackwell Science, S.143

Dean R A (1997) Signal pathways and appressoria morphogenesis. Annu Rev Phytopathol 35: 211-234

Defilippi P, Vallés A M (2002) The winding road from adhesive receptors to the nucleus. EMBO Reports 3: 312-316

Deising H B, Werner S, Wernitz M (2000) The role of fungal appressoria in plant infection. Microbes and Infection 2: 1631-1641

Desjardins A E, Hohn T M (1997) Mycotoxins in plant Pathogenesis. Mol Plant-Microbe Interact 10: 147-152

Desjardins A E, Proctor R H, Bai G, McCormick S P, Shaner G, Buechley G, Hohn T M (1996) Reduced virulence of trichothecene-nonproducing mutants of *Gibberella zeae* in wheat field tests. Mol Plant-Microbe Interact 9: 775-781

de Vocht M L, Reviakine I, Wösten H A B, Brisson A, Wessels J G H, Robillard G T (2000) Structural and functional role of the disulfide bridges in the hydrophobin SC3. J Biol Chem 275: 28428-28432

de Vocht M L, Scholtmeijer K, van der Vegte E W, de Vries O M H, Sonveaux N, Wösten H A B, Ruysschaert J-M, Hadziioannou G, Wessels J G H, Robillard G T (1998) Structural characterisation of the hydrophobin SC3, as a monomer and after self-assembly at hydrophobic/hydrophilic interfaces. Biophys J 74: 2059-2068

Dickman M B, Ha Y-S, Yang B, Adams B, Huang C (2003) A protein kinase from *Colletotrichum trifolii* is induced by plant cutin and is required for appressorium formation. Mol Plant-Microbe Interact 16: 411-421

Diez-Orejas R, Molero G, Navarro-Garcia F, Pla J, Nombela C, Sanchez-Perez M (1997) Reduced virulence of *Candida albicans MCK1* mutants: a role for mitogen-activated protein kinases in pathogenicity. Infect Immun 65: 833-837

Di Pietro A, García-Maceira F I, Méglecz E, Roncero M I G (2001) A MAP kinase of the vascular wilt fungus *Fusarium oxysporum* is essential for root penetration and pathogenesis. Mol Microbiol 39: 1140-1152

Dixon K P, Xu J-R, Smirnoff N, Talbot N J (1999) Independent signaling pathways regulate cellular turgor during hyperosmotic stress and appressoria-mediated plant infection by *Magnaporthe grisea*. Plant Cell 11: 2045-2058

Ebbole D J (1997) Hydrophobins and fungal infection of plants and animals. Trends Microbiol 5: 405-408

El-Glendy W, Brownleader M D, Ismail H, Clarke P J, Gilbert J, El-Bordiny F, Trevan M, Hopkins J, Naldrett M, Jackson P (2001) Rapid deposition of wheat cell wall structural proteins in response to *Fusarium*-derived elicitors. J Exp Bot 54: 85-90

Emmet R W, Parbery D G (1975) Appressoria. Annu Rev Phytopathol 13: 147-167

Fox D, Smulian A G (1999) Mitogen-activated protein kinase Mpk1 of *Pneumocystis carinii* complements the slt2Δ defect in the cell integrity pathway of *Saccharomyces cerevisiae*. Mol Microbiol 34: 451-462

Garber R C, Yoder O C (1983) Isolation of DNA from filamentous fungi and separation into nuclear, mitochondrial, ribosomal, and plasmid components. Anal Biochem 135:416-422.

Garcia-Maceira F I, Di Pietro A, Roncero M I (2000) Cloning and disruption of *pgx4* encoding an in planta expressed exopolygalacturonase from *Fusarium oxysporum*. Mol Plant-Microbe Interact 13: 359-365

Gao S, Nuss D L (1996) Distinct roles for two G protein alpha subunits in funcal virulence, morphology, and reproduction revealed by targeted gene disruption. Proc Natl Acad Sci 93: 14122-14127

Gilbert J, Abramson D, McCallum B, Clear R (2002) Comparison of canadian *Fusarium graminearum* isolates for aggressiveness, vegetative compatibility, and production of ergosterol and mycotoxins. Mycopathologia 153: 209-215

Gómez-Gómez E, Roncero M I G, Di Pietro A, Hera C (2001) Molecular characterization of a novel endo-*β*-1,4-xylanase gene from the vascular wilt fungus *Fusarium oxysporum*. Curr Genet 40: 268-275

Gough C L, Dow J M, Barber C E, Daniels M J (1988) Cloning of two endoglucanase genes of *Xanthomonas campestris* pv *campestris*: analysis of the role of the major endoglucanase in pathogenicity. Mol Plant-Microbe Interact 1: 275-281

Gustin M C, Albertyn J, Alexander M, Davenport K (1998) MAP kinase pathways in the yeast *Saccharomyces cerevisiae*. Microbiol Mol Biol Rev 62: 1264-1300

Hafen E (1998) Kinases and phosphatases - a marriage is consummated. Science 280: 1212-1213

Hahn M, Deising H, Struck C, Mendgen K (1997) Fungal morphogenesis and enzyme secretion during pathogenesis. In Resistance of crop plants against fungi (Hartleb H, Heitefuss R, Hoppe H-H, Eds.) pp 33-57, Fischer Verlag, Jena

Hanks S K, Quinn A M (1991) Protein kinase catalytic domain sequence database: Identification of conserved features of primery structure and classification of family members. Methods Enzymol 200: 38-62

Harris L J, Desjardins A E, Plattner R D, Nicholson P, Butler G, Young J C, Weston G, Proctor R H, Hohn T M (1999) Possible Role of trichothecene mycotoxins in virulence of *Fusarium graminearum* on maize. Plant Dis 83: 954-960

Herskowitz I (1995) MAP kinase pathways in yeast: for mating and more. Cell 80: 187-197

Hohn T M, McCormick S P, Alexander N J, Desjardins A E, Proctor R H (1997) Function and biosynthesis of trichothecenes produced by *Fusarium* species. In Molecular Genetics of Host-Specific Toxins in Plant Disease (Kohmoto K and Yoder O C, Eds), Kluwer Academic Publishers, Dordrecht/Boston/London

Hou Z, Xue C, Peng Y, Katan T, Kistler H C, Xu J-R (2002) A mitogen-activated protein kinase gene (*mgv1*) in *Fusarium graminearum* is required for female fertility, heterocaryon formation, and plant infection. Mol Plant-Microbe Interact 15: 1119-1127

Hube B (2000) Extracellular proteinases of human pathogenic fungi. In Dimorphism in human pathogenic and apathogenic yeasts. (Ernst J F, Schmidt A, Eds.) pp 126-137, Karger, Sydney

Hube B, Stehr F, Bossenz M, Mazur A, Schäfer W (2000) Secreted lipases of *Candida albicans*: cloning, characterization and expression analysis of a new family of putative virulence genes with at least ten members. Arch Microbiol 174: 362-374

Hunter T (1995) Protein kinases and phosphatases: the ying and yang of protein phosphorylation and signaling. Cell 80: 225-248

Jimenez M, Manez M, Hernandez E (1996) Influence of water activity and temperature on the production of zearalenone in corn by three Fusarium species. Int J Food Microbiol 29: 417-421

Kahmann R, Basse C, Feldbrügge M (1999) Fungal-plant signalling in the *Ustilago maydis*-maize pathosystem. Curr Opin Mircobiol 2: 647-650

Kang Z, Buchenauer H (2000) Ultrastructural and cytochemical studies on cellulose, xylan and pectin degrataion in wheat spikes infected by *Fusarium culmorum*. J Phytopathology 148: 263-275

Kang Z, Buchenauer H (1999) Immunocytochemical localization of *Fusarium* toxins in infected wheat spikes by *Fusarium culmorum*. Physiol Mol Plant Pathol 55: 275-288

Katoh M, Hirose I, Kubo Y, Hikichi Y, Kunoh H, Furusawa I, Shishiyama J (1988) Use of mutants to indicate factors prerequisite for penetration of *Colletotrichum lagenarium* by appressoria. Physiol Mol Plant Pathol 32: 177-184

Kawasaki L, Sanchez O, Shiozaki K, Aguirre J (2002) SakA MAP kinase is involved in stress signaling, sexual development and spore viability in *Aspergillus nidulans*. Mol Microbiol 45: 1153-1163

Keon J P R, Byrde R J W, Cooper R M (1987) Some aspects of fungal enzymes that degrade plant cell walls. In Fungal infection of plants (Pegg G F, Ayres P G, Eds.) pp 133-157, Cambridge University Press, Cambridge

Kimura M, Anzai H, Yamaguchi I (2001) Microbial toxins in plant-pathogen interactions: Biosynthesis, resistance mechanisms, and significance. J Gen Appl Microbiol 47: 149-160

Kinane J, Oliver R P (2003) Evidence that the appressorial development in barley powdery mildew is controlled by MAP kinase activity in conjunction with the cAMP pathway. Fungal Genet Biol 39: 94-102

Klittich C J R, Leslie J F (1988) Nitrate reduction mutants of *Fusarium moniliforme* (*Gibberella fujikuroi*). Genetics 118: 417-423

Kojima K, Kikuchi T, Takano Y, Oshiro E, Okuno T (2002) The mitogen-activated protein kinase gene MAF1 is essential for the early differentiation phase of appressorium formation in *Colletotrichum lagenarium*. Mol Plant-Microbe Interact 15 (12): 1268-1276

Kolattukudy P E, Rogers L M, Li D, Hwang C-S, Flaishman M A (1995) Surface signaling in pathogenesis. Proc Natl Acad Sci 92: 4080-4087

Komiya Y, Suzuki S, Kunoh H (2003) Release of xylanase from conidia and germlings of *Blumeria graminis* f. sp. *tritici* and expression of a xylanase gene. J Gen Plant Pathol 69: 109-114

Kouker G, Jaeger K-E (1987) Specific and sensitive plate assay for bacterial lipases. Appl Environ Microbiol 53: 211-213

Kraus P R, Fox D S, Cox G M, Heitman J (2003) The *Cryptococcus neoformans* MAP kinase Mpk1 regulate cell integrity in response to antifungal drugs and loss of calcineurin function. Mol Microbiol 48: 1377-1387

Krauss G (1997) Biochemie der Regulation und Signaltransduktion. Wiley-VCH, Weinheim

Kronstad J, De Maria A, Funnell D, Laidlaw R D, Lee N, Moniz de Sá M, Ramesh M (1998) Signaling via cAMP in fungi: interconnections with mitogen-activated protein kinase pathways. Arch Microbiol 170: 395-404

Krska R, Baumgartner S, Joseph R (2001) The state-of-art in the analysis of type-A and –B trichothecene mycotoxins in cereals. Fresenius J Anal Chem 371: 285-299

Kültz D (1998) Phylogenetic and functional classification of mitogen- and stress-activated protein kinases. J Mol Evol 46: 571-588

Lamper C, Téren J, Bartók T, Komoróczy R, Mesterházy À, Sági F (2000) Predicting DON contamination in Fusarium-infected wheat grains via determination of the ergosterol content. Cereal Research Communications 28: 337-344

Leach J, Lang B R, Yoder O C (1982) Methods for selection of mutants and *in vitro* culture of *Cochliobolus heterostrophus*. J Gen Microbiol 128: 1719-1729

Lee K S, Irie K, Gotoh Y, Watanabe Y, Araki H, Nishida E, Matsumoto K, Levin D E (1993) A yeast mitogen-activated protein kinase homolog (Mpk1p) mediates signalling by protein kinase C. Mol Cell Biol 13: 3067-3075

Lengeler K B, Davidson R C, D´Souza C, Harashima T, Shen W-C, Wang P, Pan X, Waugh M, Heitman J (2000) Signal transduction cascades regulating fungal development and virulence. Microbiol Mol Biol Rev 64: 746-785

Lev S, Sharon A, Hadar R, Ma H, Horwitz B A (1999) A mitogen-activated protein kinase of the corn leaf pathogen *Cochliobolus heterostrophus* is involved in conidiation, appressorium formation and pathogenicity: diverse roles for mitogen-activated protein kinase homologs in foliar pathogens. Proc Natl Acad Sci USA 96: 13541-13547

Lev S, Horwitz B A (2003) A mitogen-activated protein kinase pathway modulates the expression of two cellulase genes in *Cochliobolus heterostrophus* during plant infection. Plant Cell 15: 835-844

Li D, Rogers L, Kolattukudy P E (1997) Cloning and expression of cDNA encoding a mitogen-activated protein kinase from a phytopathogenic filamentous fungi. Gene 195: 161-166

Lugones L G, Bosscher J S, Scholtmeyer K, de Vries O M, Wessels J G (1996) An abundant hydrophobin (ABH1) forms hydrophobic rodlet layers in *Agaricus bisporus* fruiting bodies. Microbiology 142: 1321-1329

Lori G A, Henning C P, Violante A, Alippi H E, Varsavsky E (1990) Relation between the production of deoxynivalenol and zearalenone and mycelial growth of *Fusarium graminearum* on solid natural substrates. Microbiologia 6: 76-82

Lui Y-G, Whittier R F (1995) Thermal asymmetric interlaced PCR: Automatable amplification and sequencing of insert end fragments from YAC clones for chromosome walking. Genomics 25: 674-681

Lutz M P, Feichtinger G, Défago G, Duffy B (2003) Mycotoxigenic *Fusarium* and deoxynivalenol production repress chitinase gene expression in the biocontrol agent *Trichoderma atroviride* P1. Appl Env Microbiol 69: 3077-3084

Lynd L R, Weimer P J, van Zyl W H, Pretorius I S (2002) Microbial cellulose utilization: fundamentals and biotechnology. Microbiol Mol Biol Rev 66: 506-577

Madhani H D, Galitski T, Lander E S, Fink G R (1999) Effectors of a developmental mitogen-activated protein kinase cascade revealed by expression signatures of signaling mutants. Prot Natl Acad Sci 96: 12530-12535

Megalla S E, Bennett G A, Ellis J J, Shotwell O I (1986) Production of deoxynivalenol and zearalenone by isolates of *Fusarium graminearum* Schw. J Basic Microbiol 26: 415-419

Maia M M D, Heasley A, Camargo de Morais M M, Melo E H M, Morais Jr. M A, Ledingham W M, Lima Filho J L (2001) Effect of culture conditions on lipase production by *Fusarium solani* in batch fermentation. Bioresource Technology 76: 23-27

Malz S (2004) Untersuchungen zur Physiologie des getreidepathogenen Pilzes *Fusarium graminearum* Schabe durch gezielte Gendisruption. Doktorarbeit der Universität Hamburg

Marshall C J (1994) Hot lips and phosphorylation of protein kinases. Nature 367: 199

Mayorga M E, Gold S E (1999). A MAP kinase encoded by the *ubc3* gene of *Ustilago maydis* is required for filamentous growth and full virulence. Mol Microbiol 34: 485-497

McMullen M P, Stack R W (1999) Fusarium Head Blight (Scab) of small grains. North Dakota State Universitity Extension Service, PP-804

McMullen M P, Jones R, Gallenberg D (1997) Scab of wheat and barley: a re-emerging disease of devastating impact. Plant Dis 81: 1340-1348

Mey G, Held K, Scheffer J, Tenberge K B, Tudzynski P (2002a) CPMK2, an SLT2-homologous mitogen-activated protein (MAP) kinase, is essential for pathogenesis of *Claviceps purpurea* on rye: evidence for a second conserved pathogenesis-related MAP kinase cascade in phytopathogenic fungi. Mol Microbiol 46 (2): 305-318

Mey G, Oeser B, Lebrun M H, Tudzynski P (2002b) The biotrophic, non-appressorium-forming grass pathogen *Claviceps purpurea* needs a *Fus3*/*Pmk1* homologous mitogen

activated protein kinase for colonization of rye ovarian tissue. Mol Plant-Microbe Interact 15: 303-312

Miedaner T, Schilling A G, Geiger H H (2001) Molecular genetic diversity and variation for aggressiveness in populations of *Fusarium graminearum* and *Fusarium culmorum* sampled from wheat fields in different countries. J Phytopathology 149: 641-648

Montani M L, Vaamonde G, Resnik S L, Buera P (1988) Influence of water activity and temperature on the accumulation of zearalenone in corn. Int J Food Microbiol 6: 1-8

Morris P C (2001) MAP kinase signal transduction pathways in plants. New Phytologist 151: 67-89

Moss M O (2002) Mycotoxin review – 2. Fusarium. Mycologist 16: 158-161

Müller P, Aichinger C, Feldbrügge M, Kahmann R (1999) The MAP kinase Kpp2 regulates mating and pathogenic development in *Ustilago maydis*. Mol Microbiol 34: 1007-1017

Mullis K B (1990) Eine Nachtfahrt und die Polymerase Ketten Reaktion. Spektrum der Wissenschaft 6: 60-67

Navarro-Garcia F, Alonso-Monge R, Rico H, Pla J, Sentandreu R, Nombela C (1998) A role for the MAP kinase gene *MKC1* in cell wall construction and morphological transitions in *Candida albicans*. Microbiology 144: 411-424

Navarro-Garcia F, Sánchez M, Pla J, Nombela C (1995) Functional characterization of the *MKC1* gene of *Candida albicans*, which encodes a mitogen-activated protein kinase homolog related to cell integrity. Mol Cell Biol 15: 2197-2206

Nevoigt E, Stahl U (1997) Osmoregulation and glycerol metabolism in the yeast *Saccheromyces cerevisiae*. FEMS Microbiol Rev 21: 231-241

Nicholson P, Simpson D R, Eston G W, Rezanoor H N, Lees A K, Parry D W, Joyce D (1998) Detection and quantification of *Fusarium culmorum* and *Fusarium graminearum* in cereals using PCR assays. Physiol Mol Plant Pathol 53: 17-37

Nicholson R L, Epstein L (1991) Adhesion of fungi to the plant surface. Prerequisite for pathogenesis. In The fungal spore and disease initiation in plants and animals (Cole G T, Hoch H C, Eds.) pp 3-23, Plenum Press, New York and London

Nirenberg H (1981) A simpilified method for identifying *Fusarium* spp. occuring on wheat. Can J Bot 59: 1599-1609

Ochman H, Gerber A S, Hartl D L (1988) Genetic applications of an inverse polymerase chain reaction. Genetics 120: 621-623

Oeser B, Heidrich P M, Müller U, Tudzynski P, Tenberge K B (2002) Polygalacturonase is a pathogenicity factor in the *Claviceps purpurea/rye* interaction. Fungal Genet Biol 36: 176-186

Paredes V, Franco A, Soto T, Vicente-Soler J, Gacto M, Cansado J (2003) Different roles for the stress-activated protein kinase pathway in the regulation of trehalose metabolism in *Schizosaccharomyces pombe*. Microbiology 149: 1745-1752

Park S-H, Zarrinpar A, Lim W A (2003) Rewiring MAP kinase pathways using alternative scaffold assembly mechanisms. Science 299: 1061-1065

Parry D W, Jenkinson P, McLeod L (1995) *Fusarium* ear blight (scab) in small grain cereals – a review. Plant Pathology 44: 207-238

Peñas M M, Ásgeirsdóttir S A, Lasa I, Culiañez-Marcià F A, Pisabarro A G, Wessels J G H, Ramírez L (1998) Indentification, characterisation, and in situ detection of a fruit-body-specific hydrophobin of *Pleurotus ostreatus*. Appl Env Microbiol 64: 4028-4034

Penttilä M, Saloheimo A, Lehtovaara P, Knowles J K C (1987) Expression of two *Trichoderma reesei* endoglucanases in the yeast *Saccharomyces cerevisiae*. Yeast 3: 175-185

Pritsch C, Vance C P, Bushnell W R, Somers D A, Hohn T M, Muehlbauer G J (2001) Systemic expression of defence response genes in wheat spikes as a response to *Fusarium graminearum* infection. Physiol Mol Plant Pathol 58: 1-12

Pritsch C, Muehlbauer G J, Bushnell W R, Somers D A, Vance C P (2000) Fungal development and induction of defence response genes during early infection of wheat spikes by *Fusarium graminearum*. Mol Plant-Microbe Interact 13: 159-169

Proctor R H, Hohn T M, McCormick S P (1995) Reduced virulence of *Gibberella zeae* caused by disruption of a trichothecene toxin biosynthetic gene. Mol Plant-Microbe Interact 8: 593-601

Punt P J, Oliver R P, Dingemanse M A, Pouwels P H, Van den Hondel C A M J J (1987) Transformation of *Aspergillus* based on the hygromycin B resistance marker from *Escherichia coli*. Gene 56: 117-124

Raper K B, Thorn C (1949) A Manual of the Penicillia. Waverly Press Inc., The Williams & Wilkins Company, Baltimore, 64-65

Redman R S, Rodriguez R J (2002) Characterization and isolation of an extracellular serine protease from the tomato pathogen *Colletotrichum coccodes*, and its role in pathogenicity. Mycol Res 106: 1427-1434

Reid L M, Hamilton R I (1995) Effect of macroconidial suspension volume and concentration on expression of resistance to *Fusarium graminearum* in maize. Plant Dis 79: 461-466

Rhône Diagnostics LTD (1999) Technical Notes, SA-45 (VO1)

Roberts D P, Denny T P, Schell M A (1988) Cloning of the *egl* gene of *Pseudomonas solanacearum* and analysis of its role in phytopathogenicity. J Bacteriol 173: 6547-6552

Rogers L M, Kim Y K, Gou W, Gonzales-Candelas L, Li D, Kolattukudy P E (2000) Requirement for either host- or pectin-induced pectate lyase for infection of *Pisum sativum* by *Nectria haematococca*. Proc Natl Acad Sci USA 97: 9813-9818

Royer J C, Moyer D L, Reiwitch S G, Madden M S, Bech Jensen E, Brown S H, Yonker C C, Johnstone J A, Golightly E J, Yoder W T, Shuster J R (1995) *Fusarium graminearum* A 3/5 as a novel host for heterologous protein production. Biotechnology 13: 1479-1483

Ruiz-Roldán M C , Maier F J, Schäfer W (2001) PTK1, a mitogen-activated-protein kinase gene, is required for conidiation, appressorium formation, and pathogenicity of *Pyrenophora teres* on barley. Mol Plant-Microbe Interact 14: 116-125

Sambrook J, Fritsch E F, Maniatis T (1989) Molecular Cloning: A Laboratory Manual, 2nd Ed. Cold Spring Harbor Laboratory, Cold Spring Harbor, NY

Sanger F, Nicklen S, Coulsen A R (1977) DNA sequencing with chain terminating inhibitors. Proc Natl Acad Sci USA 74: 5463-5467

Schaeffer H J, Weber M J (1999) Mitogen-activated protein kinases: specific messages from ubiquitous messengers. Mol Cell Biol 19: 2435-2444

Schäfer W (1994) Molecular mechanism of fungal pathogenicity to plants. Annu Rev Phytopathol 32: 461-477

Schaller M, Korting H C, Schäfer W, Bastert J, Chen W, Hube B (1999) Secreted aspartic proteinase (Sap) activity contributes to tissue damage in a model of human oral candidosis. Mol Microbiol 34: 169-180

Schiestl R H, Petes T D (1991) Integration of DNA fragments by illegitimate recombination in *Saccharomyces cerevisiae*. Proc Natl Acad Sci 88: 7585-7589

Schroeder H W, Christensen J J (1963) Factors affecting resistance of wheat scab caused by *Gibberella zeae*. Phytopathology 53: 831-838

Schuren F H, Wessels J G (1990) Two genes expressed in fruiting dikaryons of *Schizophyllum commune*: homologies with a gene not regulated by mating-type genes. Gene 90: 199-205

Scott-Craig J S, Panaccione D G, Cervone F, Walton J D (1990) Endopolygalacturonase is not required for pathogenicity of *Cochliobolus carbonum* on maize. Plant Cell 2: 1191-1200

Segers G C, Hamada W, Oliver R P, Spanu P D (1999) Isolation and characterisation of five different hydrophobin-encoding cDNAs from the fungal tomato pathogen *Cladosporium fulvum*. Mol Gen Genet 261: 644-652

Shallom D, Shoham Y (2003) Microbial hemicellulases. Curr Opin Microbiol 6: 219-228

Shieh M, Brown R L, Whitehead M P, Carey J W, Cotty P L, Cleveland T E, Dean R A (1997) Molecular genetic evidence for the involvement of a specific polygalaturonase,

P2c, in the invasion and spread of *Aspergillus flavus* in cotton bolls. Appl Environ Microbiol 63: 3548-3552

Soanes D M, Kershaw M J, Cooley R N, Talbot N J (2002) Regulation of the *MPG1* hydrophobin gene in the rice blast fungus *Magnaporthe grisea*. Mol Plant-Microbe Interact 15: 1253-1267

Soto T, Beltrán F F, Paredes V, Madrid M, Millar J B A, Vicente-Soler J, Cansado J, Gacto M (2002) Cold induces stress-activated protein kinase-mediated response in the fission yeast *Schizosaccharomyces pombe*. Eur J Biochem 269: 5056-5065

Southern E M (1975) Detection of specific sequences among DNA fragments separated by gel electrophoresis. J Mol Biol 98:503-517

Spanu P (1998) Deletion of *HCf-1*, a hydrophobin gene of *Cladosporium fulvum*, does not affect pathogenicity on tomato. Physiol Mol Plant Pathol 52: 323-334

Sposato P, Ahn J H, Walton J D (1995) Characterisation and disruption of a gene in the maize pathogen *Cochliobulus carbonum* encoding a cellulase lacking a cellulose binding domain and hinge region. Mol Plant-Microbe Interact 8: 602-609

Srikantha T, Morrow B, Schröppel K, Soll D R (1995) The frequency of integrative transformation at phase-specific genes of *Candida albicans* correlates with their transcriptional state. Mol Gen Genet 246: 342-352

Stahl D J, Theuerkauf A, Heitefuss R, Schäfer W (1994) Cutinase of *Nectria heamatococca* (*Fusarium solani* f. sp. *pisi*) is not required for fungal virulence or organ specifity on pea. Mol Plant-Microbe Interact 7: 713-725

Stahl D J, Schäfer W (1992) Cutinase is not required for fungal pathogenicity on pea. Plant Cell 4: 621-629

Strange R N, Deramo A, Smith H (1978) Virulence enhancement of *Fusarium graminearum* by choline and betaine and of *Botrytis cinerea* by other constituents of wheat. Trans Br Mycol Soc 70: 201-207

Strange R N, Majer J R, Smith H (1974) The isolation and identification of choline and betaine as the two major components in anthers and wheat germ that stimulate *Fusarium graminearum* in vitro. Physiological Plant Pathology 4: 277-290

Strange R N, Smith H, Majer J R (1972) Choline, one of two fungal growth stimulants in anthers responsible for the susceptibility of wheat to *Fusarium graminearum*. Nature 238: 103-104

Strasburger E, Noll F, Schenk H, Schimper A F W (2002) Lehrbuch der Botanik für Hochschulen. 35. Auflage, Spektrum Akademischer Verlag Heidelberg · Berlin

Sutton J C (1982) Epidemiology of wheat head blight and maize ear rot caused by *Fusarium graminearum*. Trans Br Mycol Soc 70: 187-192

Suzuki K (2002) MAP kinase cascades in elicitor signal transduction. J Plant Res 115: 237-244

Sweeney M J, Dobson A D W (1999) Molecular biology of mycotoxin biosynthesis. FEMS Microbiol Lett 175: 149-163

Sweigard J A, Chumley F G, Valent B (1992) Disrution of a *Magnaporthe grisea* cutinase gene. Mol Gen Genet 232: 183-190

Tag A, Hicks J, Garifullina G, Ake C, Phillips T D, Beremand M, Keller N (2000) G-protein signalling mediates different production of toxic secondary metabolites. Mol Microbiol 38: 658-665

Tahirovic S, Schorr M, Then A, Berger J, Schwarz H, Mayinger P (2003) Role for lipid signaling and the cell integrity MAP kinase cascade in yeast septum biogenesis. Curr Genet 43: 71-78

Takano Y, Kikuchi T, Kubo Y, Hamer J E, Mise K, Furusawa I (2000) The *Colletotrichum lagenarium* MAP kinase gene *CMK1* regulates diverse aspects of fungal pathogenesis. Mol Plant-Microbe Interact 13: 374-383

Talbot N J, Kershaw M J, Wakley G E, de Vries O M H, Wessels J G H, Hamer J E (1996) *MPG1* encodes a fungal hydrophobin involved in surface interactions during infection-related development of *Magnaporthe grisea*. Plant Cell 8: 985-999

Talbot N J, Ebbole D J, Hamer J E (1993) Identification and charaterisation of *MPG1*, a gene involved in pathogenicity from the rice blast fungus *Magnaporthe grisea*. Plant Cell 5: 1575-1590

te Have A, Mulder W, Visser J; van Kan J A L (1998) The endopolygalacturonase gene *Bcpg*1 is required for full virulence of *Botrytis cinerea*. Mol Plant-Microbe Interact 11: 1009-1016

Teich A H, Michelutti R (1992) Promoting infection of the wheat heads field-inoculated with *Fusarium graminearum* by covering them with plastic bags. Third European Fusarium Seminar. IHAR Radzików pp 71-75

Thines E, Weber R W S, Talbot N J (2000) MAP kinase and protein kinase A-dependant mobilization of triacylglycerol and glycogen during appressorium turgor generation by *Magnaporthe grisea*. Plant Cell 12: 1703-1718

Thines E, Eilbert F, Sterner O, Anke H (1997) Signal transduction leading to appressorium formation in germinating conidia of *Magnaporthe grisea*: effects of second messengers diacylglycerol, ceramides and sphingomyelin. FEMS Microbiol Lett 156: 91-94

Thyagarajan B, Johnson B L, Campbell C (1995) The effect of target site transcription on gene targeting in human cells *in vitro*. Nucleic Acid Research 23: 2784-2790

Tonukari N J, Scott-Craig J S, Walton J D (2000) The *Cochliobolus carbonum* SNF1 gene is required for cell wall-degrading enzyme expression and virulence on maize. Plant Cell 12: 237-248

Trail F, Xu H, Loranger R, Gadoury D (2002) Physiological and environmental aspects of ascospore discharge in *Gibberella zeae* (anamorph *Fusarium graminearum*). Mycologia 94: 181-189

Trembley M L, Ringli C, Honegger R (2002) Hydrophobins DGH1, DGH2, and DGH3 in the lichen-forming basidiomycete *Dictyonema glabratum*. Fungal Genet Biol 35: 247-259

Turk M and Plemenitas A (2002) The HOG pathway in halophilic black yeast *Hortaea werneckii*: isolation of the HOG homolog gene and activation of HwHog1p. FEMS Microbiol Lett 216: 193-199

Ueno Y, Sawano M, Ishi K (1975) Production of trichothecene mycotoxins by *Fusarium* species in shake culture. Appl Microbiol 30: 4-9

Urban M, Mott E, Farley T, Hammond-Kosack K (2003) The *Fusarium graminearum MAP1* gene is essential for pathogenicity and development of perithecia. Mol Plant Pathol 4: 347-359

Valette-Collet O, Cimerman A, Reignault P, Levis C, Boccara M (2003) Disruption of *Botrytis cinerea* pectin methylesterase gene *Bcpme1* reduces virulence on several host plants. Mol Plant-Microbe Interact 16: 360-367

van Kan J A, van´t Klooster J W, Wagemakers C A, Dees D C, van der Vlugt-Bergmans C J (1997) Cutinase A of *Botrytis cinerea* is expressed, but not essential, during penetration of gerbera and tomato. Mol Plant-Microbe Interact 10: 30-38

Vestal E F (1964) Barley scab in South Korea in 1963 and 1964. Plant Dis Rep 48: 754-755

Waffenschmidt S, Jaenicke L (1987) Assay of reducing sugars in the nanomole range with 2,2-bicinchoninate. Anal Biochem165: 337-340

Wang Y Z, Miller J D (1988) Effects of *Fusarium graminearum* metabolites on wheat tissue in relation to *Fusarium* head blight resistance. J Phytopathol 122: 118-125

Wang Z-Y, Yong X-N, Xiao Q-P (1982) The improvement of identification techniques of scab resistance of wheat and the development of resistant sources. Sci Agric Sin 5: 67-77

Wanjiru W M, Zhensheng K, Buchenauer H (2002) Importance of cell wall degrading enzymes produced by *Fusarium graminearum* during infection of wheat heads. European Journal of Plant Pathology 108: 803-810

Wessels J G H (1996) Fungal hydrophobins: proteins that function at an interface. Trends Plant Sci 1: 9-15

Wessels J G H, de Vries O M H, Asgeirdottir S A, Springer J (1991) Hydrophobin genes involved in formation of aerial hyphae and fruiting bodies in *Schizophyllum*. Plant Cell 3: 793-799

Widmann C, Gibson S, Jarpe M B, Johnson G L (1999) Mitogen–activated protein kinase: conservation of a three-kinase module from yeast to human. Physiol Rev 79: 143-180

Windels C E, Kommedahl T (1984) Late-season colonization and survival of *Fusarium graminearum* group II in cornstalks in Minnesota. Plant Dis 68: 791-793

Wojda I, Alonso-Monge R, Bebelman J-P, Mager W H, Siderius M (2003) Response to high osmotic conditions and elevated temperature in *Saccharomyces cerevisiae* is controlled by intracellular glycerol and involves coordinate activity of MAP kinase pathways. Microbiology 149: 1193-1204

Wolf J C, Mirocha C J (1973) Regulation of sexual reproduction in *Gibberella zeae* (*Fusarium roseaum* `Graminearum´) by F-2 (Zearalenone). Can J Microbiol 19: 725-734

Wood T.M, Mahalingeshwara Bhat K (1988) Methods for measuring cellulase activity. Methods Enzymol 160, 87-112

Wösten H A B (2001) Hydrophobins: multipurpose proteins. Annu Rev Microbiol 55: 625-646

Xu J-R, Hamer J E (1996) Map kinase and cAMP signaling regulate infection structure formation and pathogenic growth in the rice blast fungus *Magnaporthe grisea*. Genes Dev 10: 2696-2706

Xu J-R, Urban M, Sweigard J A, Hamer J E (1997) The *CPKA* gene of *Magnaporthe grisea* is essential for appressoria penetration. Mol Plant-Microbe Interact 10: 187-194

Xu J-R, Staiger C J, Hamer J E (1998) Inactivation of the mitogen-activated protein kinase Mps1 from the rice blast fungus prevents penetration of host cells but allows activation of plant defense responses. Proc Natl Acad Sci U.S.A. 95 (21): 12713-12718

Xu J-R (2000) MAP kinases in fungal pathogenes. Fungal Genet Biol 31: 137-152

Xue C, Park G, Choi W, Zheng L, Dean R A, Xu J-R (2002) Two novel fungal virulence genes specifically expressed in appressoria of the rice blast fungus. Plant Cell 14: 2107-2119

Zhang Y, Lamm R, Pillonel C, Lam S, Xu J-R (2002) Osmoregulation and fungicide resistance: the *Neurospora crassa os-2* gene encodes a *HOG1* mitogen-activated protein kinase homologue. Appl Environ Microbiol 68: 532-538

Zhang Z, Gurr S J (2001) Expression and sequence analysis of the *Blumeria graminis* mitogen-activated protein kinase genes, mpk1 and mpk2. Gene 266 (1-2): 57-65

Zhang S, Klessig D F (2001) MAPK cascades in plant defence signaling. Trends Plant Sci 6: 520-527

Zheng L, Campbell M, Murphy J, Lam S, Xu J-R (2000). The *BMP1* gene is essential for pathogenicity in the gray mold fungus *Botrytis cinerea*. Mol Plant-Microbe Interact 13: 724-732

Appendix

A. The Gmap1 MAP kinase from *Fusarium graminearum*

5`-GTAGCCATCAAGAAGGTCACCAATGTTTTTAGCAAGAAGATTCTGGCCAAGCGCGCCCT
GCGCGAGATCAAGCTGCTCCAGCACTTCCGCGGCCACCGCAACGTGAGTTTCTGCCTCGGC
GCAACAGACAAGGGACGCGTATGCTGATAGCTTCATCCCATCAGATCACATGTTTGTACGA
CATGGACATTCCTCGACCCGATAACTTCAACGGGACCTATTTGTACGAGGGTCAGTGACGA
TGCCTCCCCGAAAGACGAAAGAGTGAACAATAAGCTGACACGGCACAGAGCTGATGGAGTG
TGATTTGGCTGCCATCATCCGATCTGGCCAGCCTCTTACCGACGCCCACTTCCAATCCTTT
ATCTACCAGATCCTTTGCGGTCTCAAGTACATCCACTCCGCAAACGTTCTGCACCGAGATC
TCAAGCCCGGTAACCTGCTTGTCAACGCCGACTGCGAGCTCAAGATTTGCGATTTCGGTCT
TGCCCGAGGTTTCTCAGTCGACCCCGAAGAGAATGCTGGATACATGACCGAGTACGTCGCT
ACTCGATGG-3`

Fig. 11: Gene fragment found prior to this work by PCR with degenerate primers (Hanks and Quinn 1991). The sequence showed a high homology to fungal MAP kinases. Starting from this MAP kinase gene fragment the flanking regions were cloned with a TAIL-PCR-strategy (Lui and Whittier 1995). Furthermore, this gene fragment was used to clone a transformation vector for the disruption of the *gmap1* gene of *F. graminearum* and for the amplification of a digoxygenin labeled probe for the detection of the *gmap1* gene by southern blot analysis.

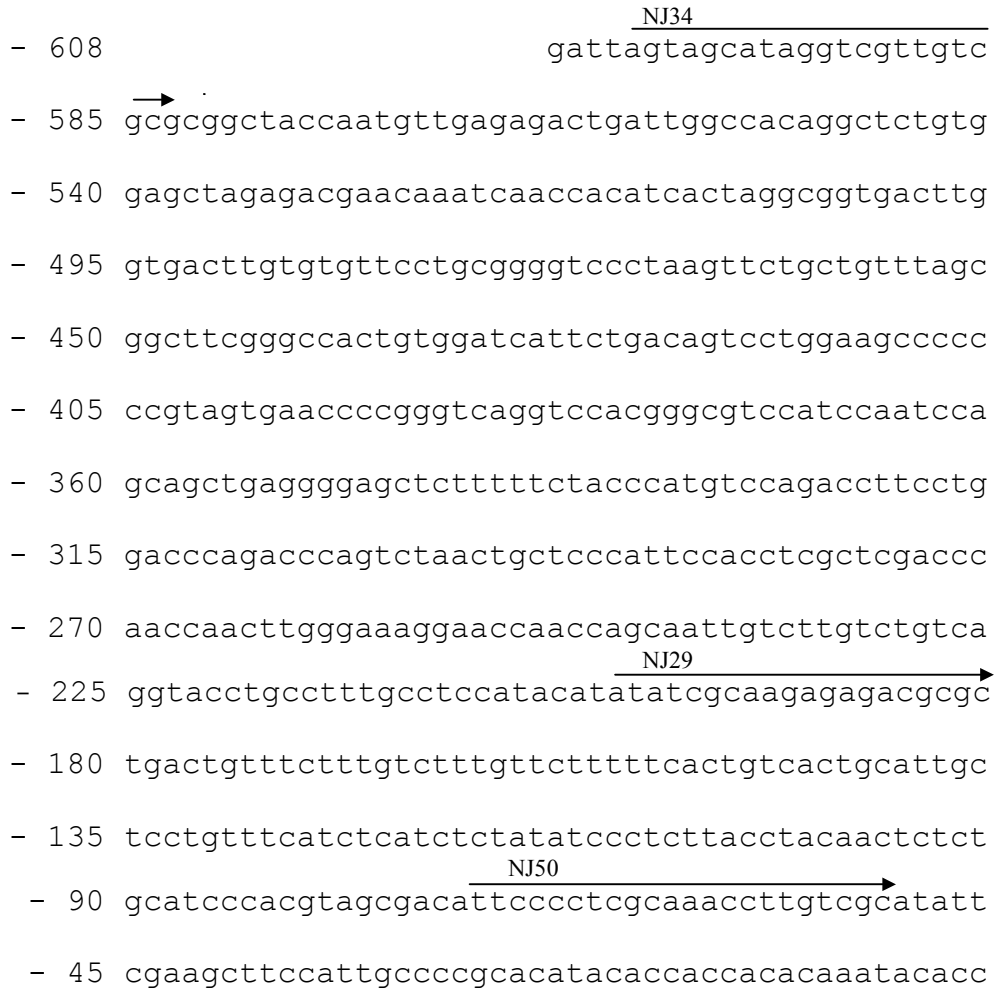

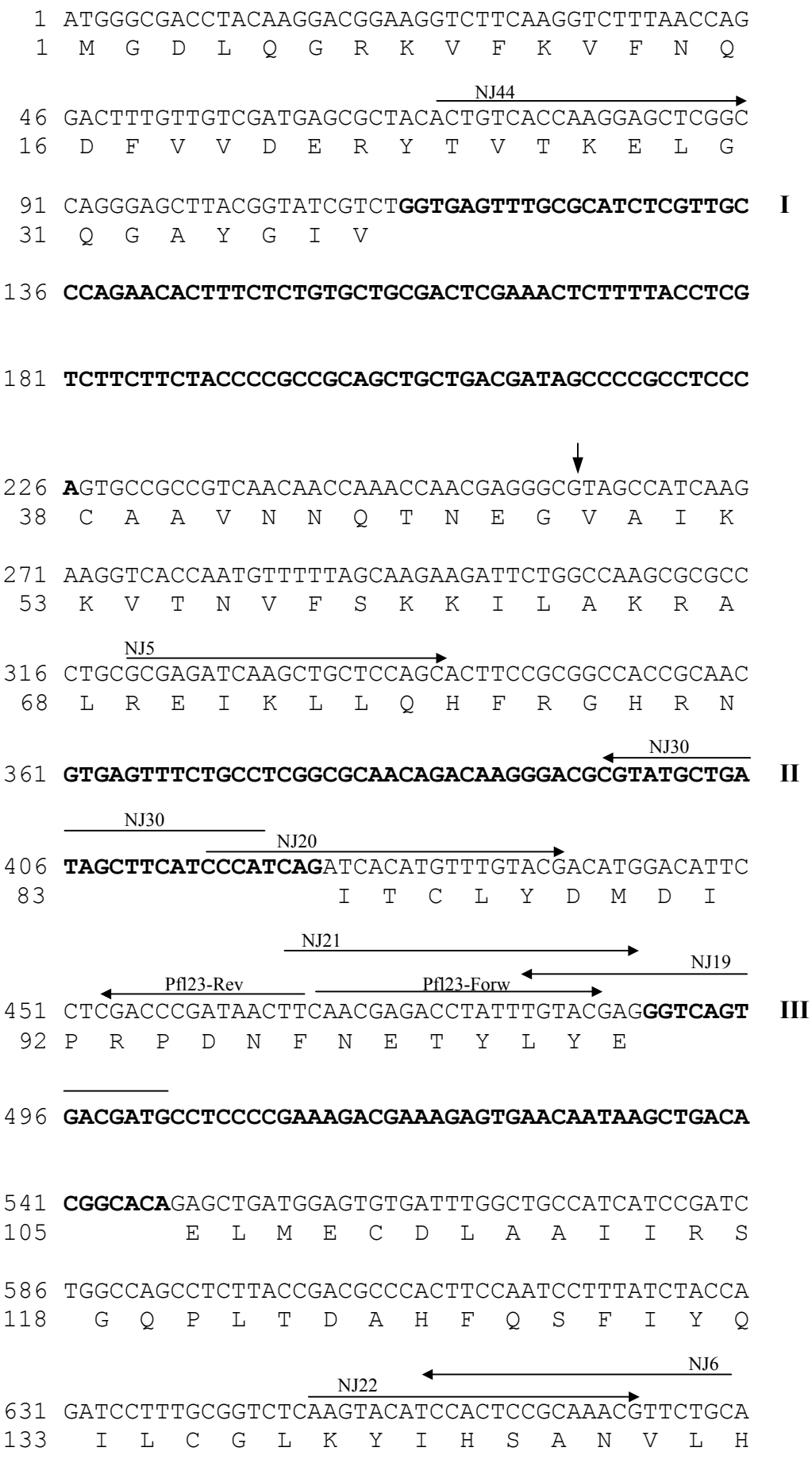
1 ATGGGCGACCTACAAGGACGGAAGGTCTTCAAGGTCTTTAACCAG
1 M G D L Q G R K V F K V F N Q
NJ44
46 GACTTTGTTGTCGATGAGCGCTACACTGTCACCAAGGAGCTCGGC
16 D F V V D E R Y T V T K E L G
91 CAGGGAGCTTACGGTATCGTCTGGTGAGTTTGCGCATCTCGTTGC I
31 Q G A Y G I V
136 CCAGAACACTTTCTCTGTGCTGCGACTCGAAACTCTTTTACCTCG
181 TCTTCTTCTACCCCGCCGCAGCTGCTGACGATAGCCCCGCCTCCC
226 AGTGCCGCCGTCAACAACCAAACCAACGAGGGCGTAGCCATCAAG
38 C A A V N N Q T N E G V A I K
271 AAGGTCACCAATGTTTTTAGCAAGAAGATTCTGGCCAAGCGCGCC
53 K V T N V F S K K I L A K R A
NJ5
316 CTGCGCGAGATCAAGCTGCTCCAGCACTTCCGCGGCCACCGCAAC
68 L R E I K L L Q H F R G H R N
NJ30
361 GTGAGTTTCTGCCTCGGCGCAACAGACAAGGGACGCGTATGCTGA II
NJ30
NJ20
406 TAGCTTCATCCCATCAGATCACATGTTTGTACGACATGGACATTC
83 I T C L Y D M D I
NJ21
NJ19
Pfl23-Rev
Pfl23-Forw
451 CTCGACCCGATAACTTCAACGAGACCTATTTGTACGAGGGTCAGT III
92 P R P D N F N E T Y L Y E
496 GACGATGCCTCCCCGAAAGACGAAAGAGTGAACAATAAGCTGACA
541 CGGCACAGAGCTGATGGAGTGTGATTTGGCTGCCATCATCCGATC
105 E L M E C D L A A I I R S
586 TGGCCAGCCTCTTACCGACGCCCACTTCCAATCCTTTATCTACCA
118 G Q P L T D A H F Q S F I Y Q
NJ6
NJ22
631 GATCCTTTGCGGTCTCAAGTACATCCACTCCGCAAACGTTCTGCA
133 I L C G L K Y I H S A N V L H

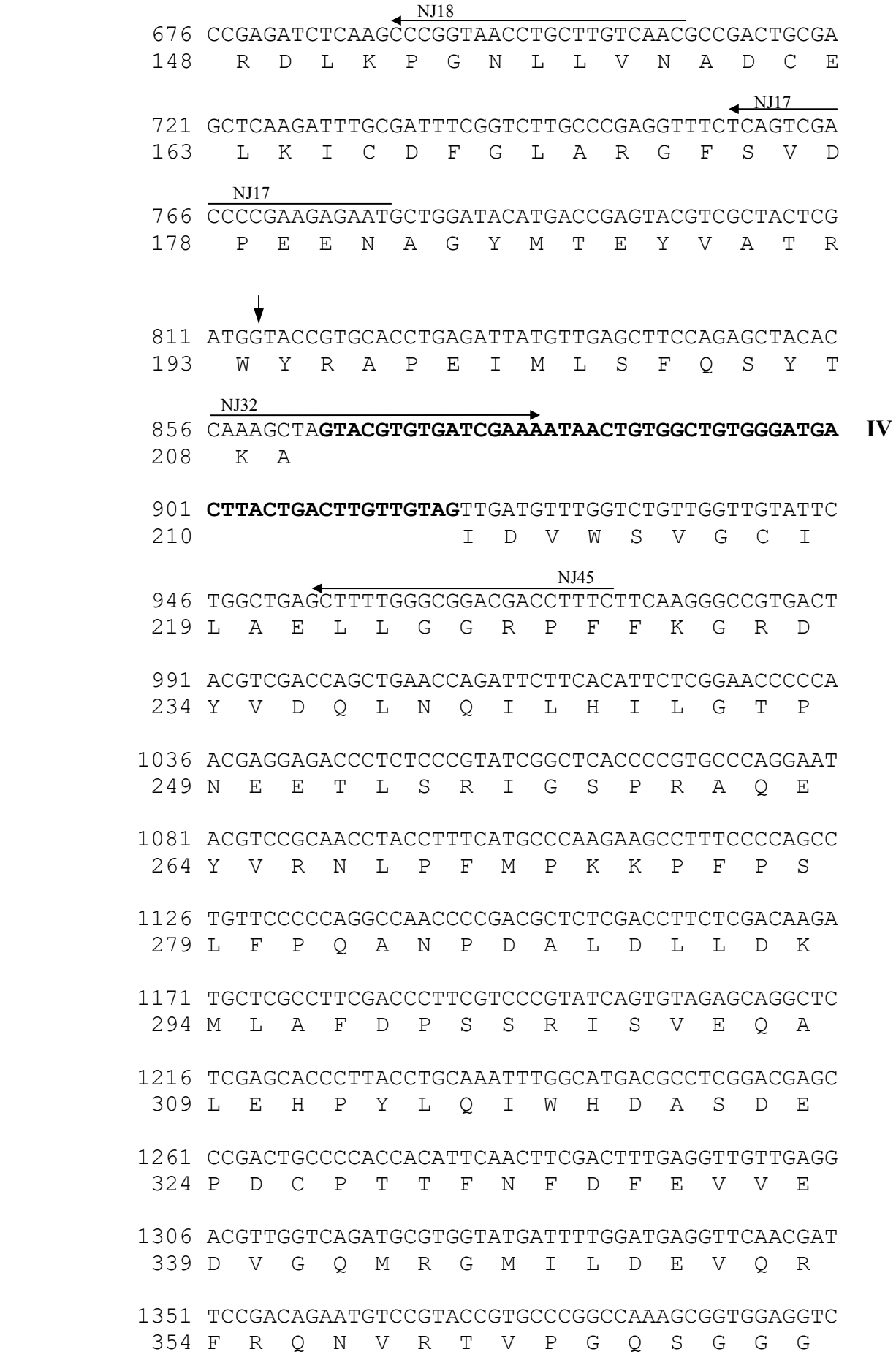
NJ18
676 CCGAGATCTCAAGCCCGGTAACCTGCTTGTCAACGCCGACTGCGA
148 R D L K P G N L L V N A D C E
NJ17
721 GCTCAAGATTTGCGATTTCGGTCTTGCCCGAGGTTTCTCAGTCGA
163 L K I C D F G L A R G F S V D
NJ17
766 CCCCGAAGAGAATGCTGGATACATGACCGAGTACGTCGCTACTCG
178 P E E N A G Y M T E Y V A T R
811 ATGGTACCGTGCACCTGAGATTATGTTGAGCTTCCAGAGCTACAC
193 W Y R A P E I M L S F Q S Y T
NJ32
856 CAAAGCTAGTACGTGTGATCGAAAATAACTGTGGCTGTGGGATGA IV
208 K A
901 CTTACTGACTTGTTGTAGTTGATGTTTGGTCTGTTGGTTGTATTC
210 I D V W S V G C I
NJ45
946 TGGCTGAGCTTTTGGGCGGACGACCTTTCTTCAAGGGCCGTGACT
219 L A E L L G G R P F F K G R D
991 ACGTCGACCAGCTGAACCAGATTCTTCACATTCTCGGAACCCCCA
234 Y V D Q L N Q I L H I L G T P
1036 ACGAGGAGACCCTCTCCCGTATCGGCTCACCCCGTGCCCAGGAAT
249 N E E T L S R I G S P R A Q E
1081 ACGTCCGCAACCTACCTTTCATGCCCAAGAAGCCTTTCCCCAGCC
264 Y V R N L P F M P K K P F P S
1126 TGTTCCCCCAGGCCAACCCCGACGCTCTCGACCTTCTCGACAAGA
279 L F P Q A N P D A L D L L D K
1171 TGCTCGCCTTCGACCCTTCGTCCCGTATCAGTGTAGAGCAGGCTC
294 M L A F D P S S R I S V E Q A
1216 TCGAGCACCCTTACCTGCAAATTTGGCATGACGCCTCGGACGAGC
309 L E H P Y L Q I W H D A S D E
1261 CCGACTGCCCCACCACATTCAACTTCGACTTTGAGGTTGTTGAGG
324 P D C P T T F N F D F E V V E
1306 ACGTTGGTCAGATGCGTGGTATGATTTTGGATGAGGTTCAACGAT
339 D V G Q M R G M I L D E V Q R
1351 TCCGACAGAATGTCCGTACCGTGCCCGGCCAAAGCGGTGGAGGTC
354 F R Q N V R T V P G Q S G G G

```
1396 TTCAGGGCCAGGGTGTCCCCGTTCCTCTGCCTCAGGGCAATGGTC
 369 L  Q  G  Q  G  V  P  V  P  L  P  Q  G  N  G

1441 AATGGACTGCTGAGGACCCTCGACCTCAGGAATATGCTGGTCATG
 384 Q  W  T  A  E  D  P  R  P  Q  E  Y  A  G  H

1486 GTAACACCGGACTTGAGCAGGATCTTCAGGGAGGCCTGGATGCTT
 399 G  N  T  G  L  E  Q  D  L  Q  G  G  L  D  A

                                        <-NJ51
1531 CTCGAAGATAAgagctgctacgcaaagtacaagggttgaaaaagg
 414 S  R  R  *

1576 atatatcctagaggattaagaacggcatgctctctggttcaaaat

1621 gaaagatacacccaaggcactggaaatagggacgatgctaggtgg

1666 gtttcgagtatttaatgcctggaatgagaagagaaggatggaaaa

1711 ataaagcttttggcttcagcaggctgagggggcatgcccttaa

1756 atgggttgagagggcagtgaagcgtttccctcatcttcatttcca

1801 tcatrtgtttttccgaatgagaaacgatatcaatactatatttct

1846 ttatttttatatgatactccgtctttctatcttgttatgattga
                                     <-NJ31
1891 agacgtagaacaacagcgacgatgatgaatatgactatcgtttat

1936 gatgtaccaaggatgacaggtgggaatatgtcatcaatttgaggc

1981 tggtgtcttacaaggaaatcagtactttaatccttgatggagaga

2026 catttcaattcatacgataagacatcatcactggtgcgcagaata

2071 aattataaaggcagtattccatttgatagcaagtagatatggtga

2116 tggttatatgtgccttgacctaaaaatcgccccttaaccttgtgc

2161 cgtttgtagtaagtccttcattagacatcaatatctatccctttc

2206 cttaggggtagccttttgccagactttggggctgttgttgggaat
                                  <-NJ35
2251 ctgttgctagactcctgctggttctccttgttgaaagaattcgtc

2296 ggctttgctccgttgttgataacactgtacaatc
```

Fig. 13: Nucleotide sequence containing the complete *gmap1* gene with flanking regions as well as the putative amino acid sequence. Fat lettered nucleotide sequence areas indicate the location of the four introns (I-IV) found in the *gmap1* gene. Horizontal arrows mark the position of the various primers used. Two vertical arrows indicate the beginning and the end of the initial gene fragment found prior to this work by PCR with degenerate primers.

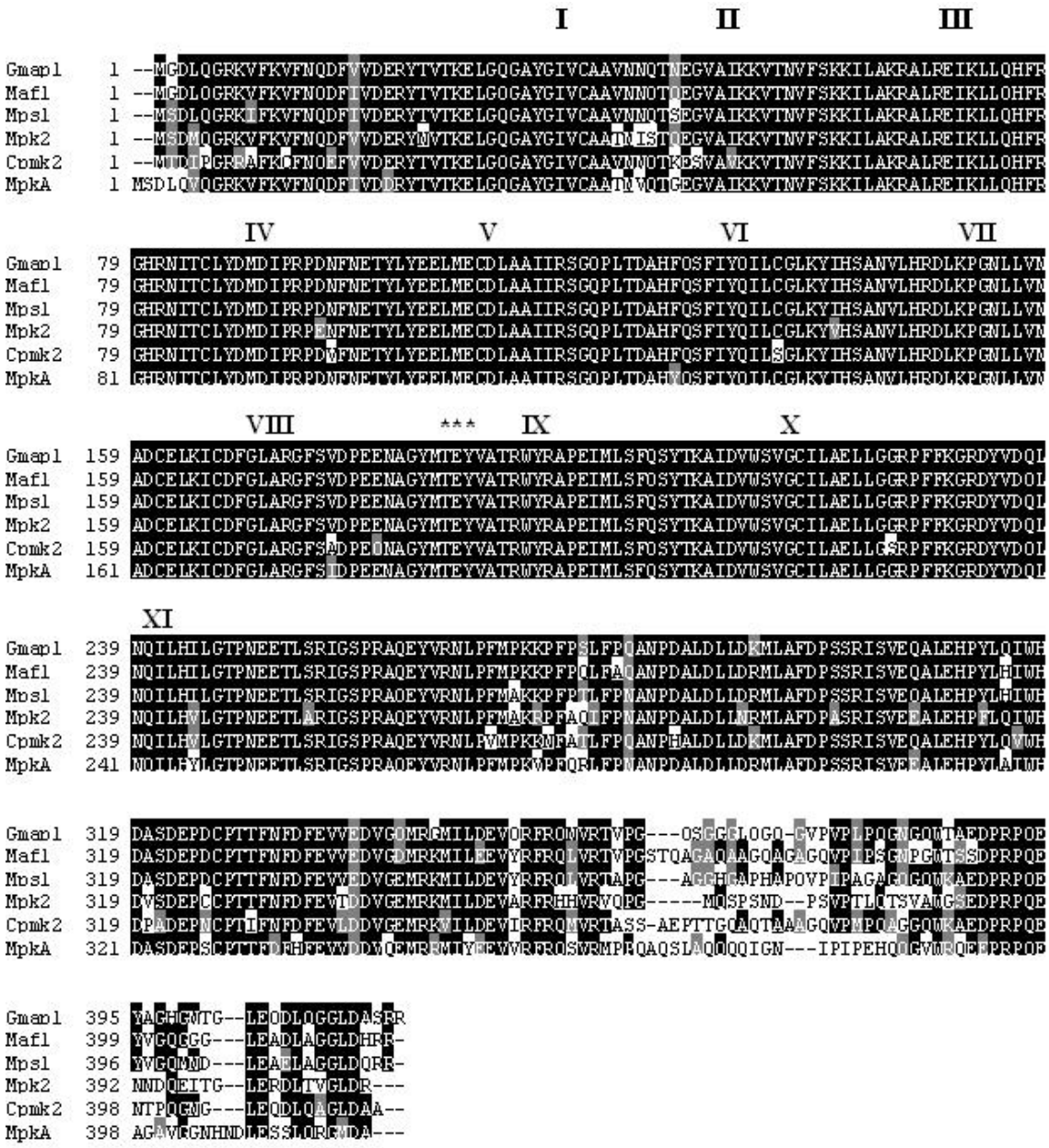

Fig. 14: Alignment of the predicted amino acid sequence encoded by the *gmap1* gene and several fungal MAP kinases. The alignment was performed with the CLUSTAL W 1.8 programme. Identical amino acids are indicated as white letters on a black ground. Similar residues are shown on gray background. Gaps introduced for the alignment are indicated by hyphens. The protein kinase domains of the yeast/fungi extracellular signal regulated kinase subgroup 2 are indicated by Roman numerals (Hanks and Quinn 1991). The TEY sequence required for kinase activation is marked by asterisks (Kültz 1998). The GenBank accession numbers for *C. lagenarium* Maf1, *M. grisea* Mps1, *B. graminis* Mpk2, *C. purpurea* Cpmk2, and *A. nidulans* MpkA are AAL50116, AAC63682, AAG53655, CAC87145 and AAD24428, respectively.

B. The Gpmk1 MAP kinase from *Fusarium graminearum*

5`-GCCAAAAGGTCGCCATCAAGAAGATCACTCCTTTCGATCACTCCATGTTCTGTCTAAGA
ACTCTGCGAGAGATGAAGCTGCTGCGATACTTCAACCACGAGAACATCATTTCTATTCTCG
ACATTCAGAAGCCCCGAAGTTACGAGTCATTTCAGGAAGTCTATCTGATCCAGGTACGAAA
CGCCACTGTTTTGCTGTAGTAAGATCAGCGAGCTAACAAACACTGCAGGAGCTGATGGAGA
CGGATATGCACCGTGTCATCCGCACACAGGATCTTTCCGACGACCACTGCCAGTACTTCAT
CTACCAGACCCTCCGAGCCCTCAAGGCGATGCACTCGGCCAACGTGCTGCACCGAGACTTG
AAGCCCTCCAACCTCCTCCTCAACGCCAACTGTGATCTCAAGGTCTGCGATTTCGGTCTTG
CGCGATCCGCTGCCTCTCAGGAGGATAACTCTGGTTTCATGACCGAATATGTCGCGACTCG
ATGG -3`

Fig. 12: Gene fragment found prior to this work by PCR with degenerate primers (Hanks and Quinn 1991). The sequence showed a high homology to fungal MAP kinases. Starting from this MAP kinase gene fragment the flanking regions were cloned with a TAIL-PCR-strategy (Lui and Whittier 1995). Furthermore, this gene fragment was used to clone a transformation vector for the disruption of the *gpmk1* gene of *F. graminearum* and for the amplification of a digoxygenin labeled probe for the detection of the *gpmk1* gene by southern blot analysis.

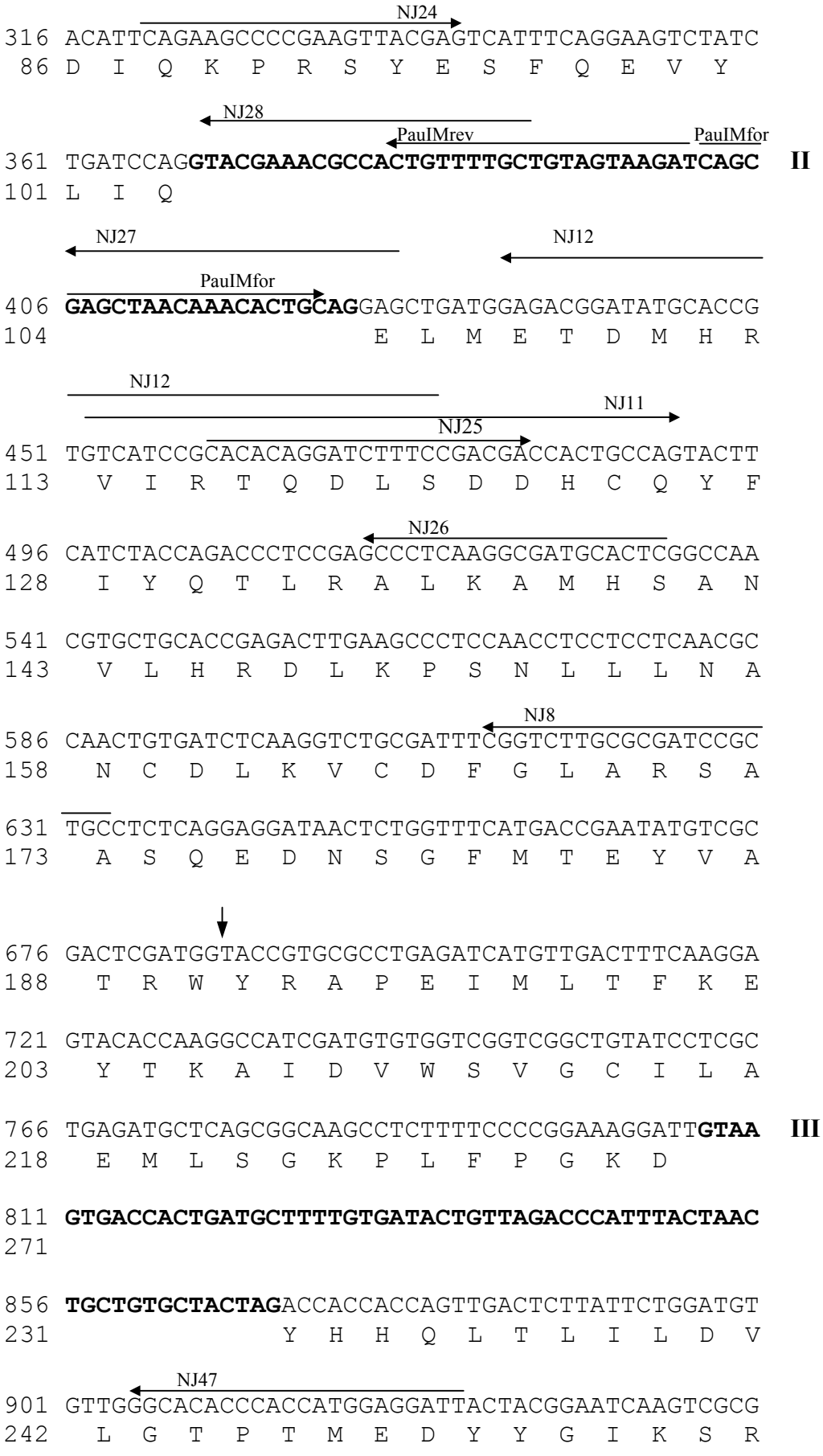
NJ24
316 ACATTCAGAAGCCCCGAAGTTACGAGTCATTTCAGGAAGTCTATC
86 D I Q K P R S Y E S F Q E V Y
NJ28
PauIMrev
PauIMfor
361 TGATCCAGGTACGAAACGCCACTGTTTTGCTGTAGTAAGATCAGC II
101 L I Q
NJ27
NJ12
PauIMfor
406 GAGCTAACAAACACTGCAGGAGCTGATGGAGACGGATATGCACCG
104 E L M E T D M H R
NJ12
NJ11
NJ25
451 TGTCATCCGCACACAGGATCTTTCCGACGACCACTGCCAGTACTT
113 V I R T Q D L S D D H C Q Y F
NJ26
496 CATCTACCAGACCCTCCGAGCCCTCAAGGCGATGCACTCGGCCAA
128 I Y Q T L R A L K A M H S A N
541 CGTGCTGCACCGAGACTTGAAGCCCTCCAACCTCCTCCTCAACGC
143 V L H R D L K P S N L L L N A
NJ8
586 CAACTGTGATCTCAAGGTCTGCGATTTCGGTCTTGCGCGATCCGC
158 N C D L K V C D F G L A R S A
631 TGCCTCTCAGGAGGATAACTCTGGTTTCATGACCGAATATGTCGC
173 A S Q E D N S G F M T E Y V A
676 GACTCGATGGTACCGTGCGCCTGAGATCATGTTGACTTTCAAGGA
188 T R W Y R A P E I M L T F K E
721 GTACACCAAGGCCATCGATGTGTGGTCGGTCGGCTGTATCCTCGC
203 Y T K A I D V W S V G C I L A
766 TGAGATGCTCAGCGGCAAGCCTCTTTTCCCCGGAAAGGATTGTAA III
218 E M L S G K P L F P G K D
811 GTGACCACTGATGCTTTTGTGATACTGTTAGACCCATTTACTAAC
271
856 TGCTGTGCTACTAGACCACCACCAGTTGACTCTTATTCTGGATGT
231 Y H H Q L T L I L D V
NJ47
901 GTTGGGCACACCCACCATGGAGGATTACTACGGAATCAAGTCGCG
242 L G T P T M E D Y Y G I K S R

```
 946 CCGTGCTCGAGAATACATCCGATCGCTCCCCTTCAAGAAGAAGGT
 257   R  A  R  E  Y  I  R  S  L  P  F  K  K  K  V

 991 TCCCTTCCGAACTCTATTCCCCAAGACATCGGATCTGGCCCTCGA
 272   P  F  R  T  L  F  P  K  T  S  D  L  A  L  D

1036 CCTGCTCGAGAAGCTCCTCGCATTCAACCCTGTTAAGCGCATTAC
 287   L  L  E  K  L  L  A  F  N  P  V  K  R  I  T

1081 TGTGGAGGAAGCTCTGAAGCACCCATACCTTGAGCCTTACCACGA
 302   V  E  E  A  L  K  H  P  Y  L  E  P  Y  H  D

1126 CCCCGAGGACGAGCCAACAGCGCCCCCAATCCCCGAGGAGTTCTT
 317   P  E  D  E  P  T  A  P  P  I  P  E  E  F  F

1171 CGACTTTGACAAGCACAAAGACAACCTGAGCAAGGAGCAGCTGAA
 332   D  F  D  K  H  K  D  N  L  S  K  E  Q  L  K

                                                NJ53
1216 GCAGTTGATCTACCAGGAGATCATGAGGTAAacgtggagcctctg
 347   Q  L  I  Y  Q  E  I  M  R  *

1261 taaaaagacgacctgcgaatttggggatatcagatagaccacaac

1306 acaaacctatggacacgcaagcgagcaagcgcatacagaatcacc

1351 agtcgagtttattctgcatatcatgtatctggcatgagtcttttg

1396 ggtcaatcttgctgatcgaggtggttgaatgtaaggaaacaggat

1441 cgagatatgaaatggcgagaaactgagatccagacgggtgataaa

1486 gatgattttatgaattgcacatcgcaaccatttcttattagttgt

1531 tatatcccaaaagaaatattcataatacgtgcttgtttgtatacc

1576 ggttgctttttgtgaatgatggggtacaagtcatgttgagataca

1621 tgtcagtcggagatgatagttggttgatagtgcggcaaacaccgc

1666 atatctcctgatgttgccataaattcgcttggctcattcctttac

1711 ttgccaccattggccattcatgttcgcaacgtgacagtcaaaatc
                                      NJ38
1756 tttcagtgctaaccacggatcaaaggtctagacctaaccaaggcc

1801 cctatgca
```

Fig. 19: Nucleotide sequence containing the complete *gpmk1* gene with flanking regions as well as the putative amino acid sequence. Fat lettered nucleotide sequence areas indicate the location of the three introns (I-III) found in the *gpmk1* gene. Horizontal arrows mark the position of the various primers used. Two vertical arrows indicate the beginning and the end of the initial gene fragment found prior to this work by PCR with degenerate primers.

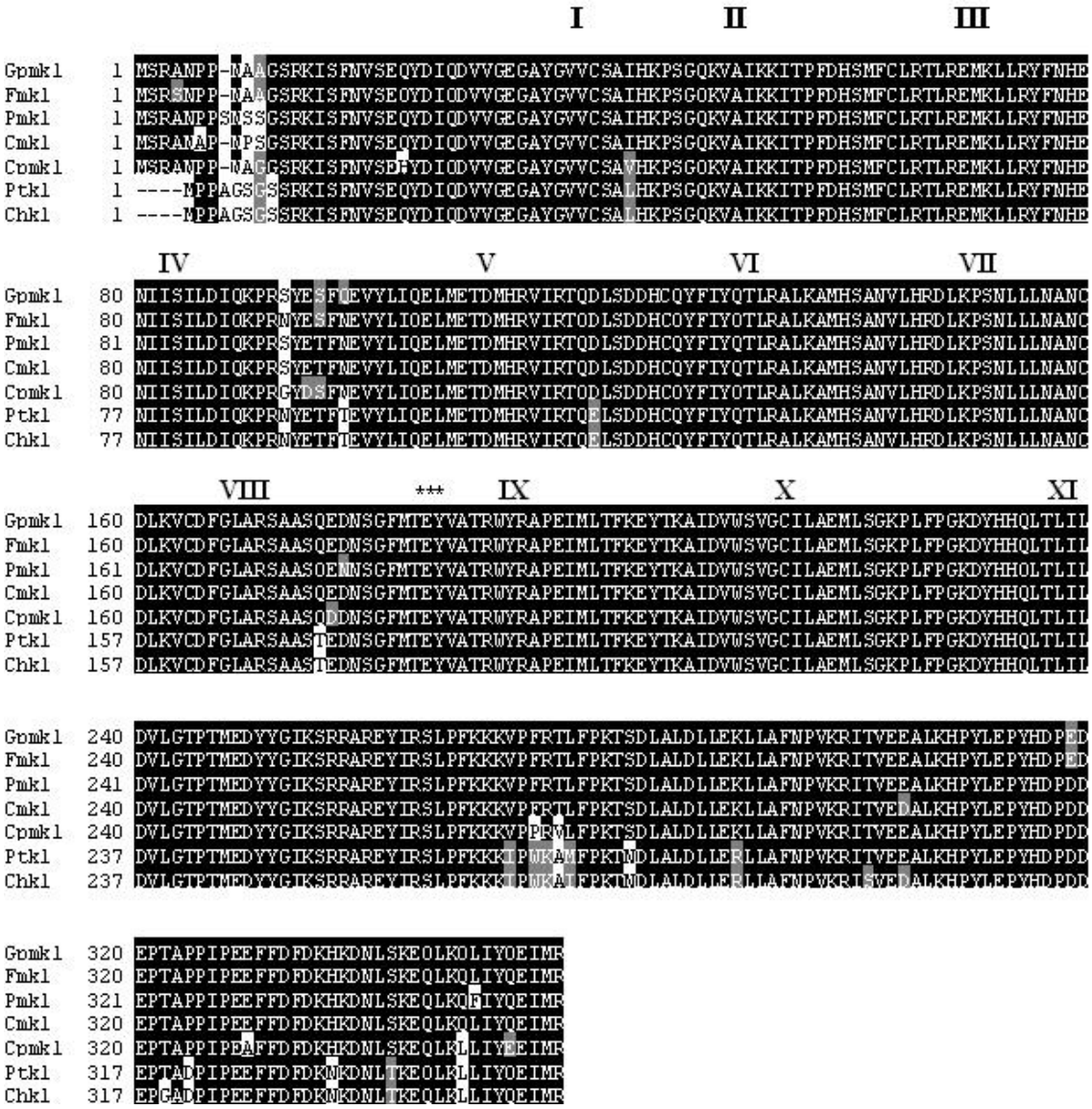

Fig. 20: Alignment of the predicted amino acid sequence encoded by the *gpmk1* gene and several fungal MAP kinases. The alignment was performed with the CLUSTAL W 1.8 programme. Identical amino acids are indicated as white letters on black background. Similar residues are shown on gray background. Gaps introduced for the alignment are indicated by hyphens. The protein kinase domains of the yeast/fungi extracellular signal regulated kinase subgroup 1 are indicated by Roman numerals (Hanks and Quinn 1991). The TEY-sequence required for kinase activation is marked by asterisks (Kültz 1998). Genbank accession numbers for *F. oxysporum* Fmk1, *M. grisea* Pmk1, *C. langenarium* Cmk1, *C. purpurea* Cpmk1, *P. teres* Ptk1, and *C. heterostrophus* Chk1 are AF286533, U70134, AJ318517, AF174649, AF272831, AF178977, respectively.

C. The osmolarity MAP kinase from *Fusarium graminearum*

```
 676 CAGTTCATTCAGTATTTCCTCTACCAGATCATG**GTATGCTCTCAC**  V
 116  Q  F  I  Q  Y  F  L  Y  Q  I  M

 721 **CACGCCTAATTAAGCGGACCTGTTGATCGATGGCCATATTTGCTA**


 766 **ACGTTTGGTTCGTCTACAG**CGTGGACTCAAGTACGTGCATTCGGC
 127                      R  G  L  K  Y  V  H  S  A

 811 CGGTGTTGTCCACCGTGACCTCAAGCCTAGCAACATTCTCGTCAA
 136   G  V  V  H  R  D  L  K  P  S  N  I  L  V  N

 856 CGAAAACTGCGATTTGAAGATCTGCGACTTTGGTCTTGCCCGAAT
 151   E  N  C  D  L  K  I  C  D  F  G  L  A  R  I

              NJ70 ──────────►
 901 CCAGGACCCCCAGATGACTGGCTATGTTTCTACACGATACTACCG
 166   Q  D  P  Q  M  T  G  Y  V  S  T  R  Y  Y  R

 946 AGCTCCCGAGATTATGCTCACCTGGCAAAAATACGACGTTGAAGT
 181   A  P  E  I  M  L  T  W  Q  K  Y  D  V  E  V

 991 TGATATCTGGAGTGCTGGCTGCATTTTCGCTGAGATGCTTGAGGG
 196   D  I  W  S  A  G  C  I  F  A  E  M  L  E  G

1036 CAAGCCTCTTTTCCCTGGAAAGGATCACGTCAACCAATTCTCCAT
 211   K  P  L  F  P  G  K  D  H  V  N  Q  F  S  I

1081 CATCACCGAGCTCCTCGGCACCCCCCCTGATGATGTTATCAACAC
 226   I  T  E  L  L  G  T  P  P  D  D  V  I  N  T

1126 CATCGCCAGTGAGAAC**GTTAGTTATACGATGCCCACGAGTCTTTA**  VI
 241   I  A  S  E  N

1171 **CCCAGGTCTCCAACTAACCATCGATAG**ACTCTTCGGTTTGTCAAG
 246                              T  L  R  F  V  K

1216 TCGCTACCCAAGCGCGAGAGACAGCCCCTCCGTAACAAGTTCAAG
 252  S  L  P  K  R  E  R  Q  P  L  R  N  K  F  K

1261 AACGCAGACGACTCAG**GTACGATTGCAGTCATTGAGATGAACCCG**  VII
 267  N  A  D  D  S

1306 **GACACAACGAGCTGACAACAGTATTAG**CCATTGACCTTCTCGAAC
 272                               A  I  D  L  L  E

1351 GCATGCTTGTCTTTGACCCCAAGAAGCGAATAACTGCCACTGAGG
 278 R  M  L  V  F  D  P  K  K  R  I  T  A  T  E

1396 CTCTCGCTCACGACTACCTTTCTCCCTACCATGACCCTACAGACG
 293 A  L  A  H  D  Y  L  S  P  Y  H  D  P  T  D
```

Fig.49: Nucleotide sequence containing the complete gene for the putative osmolarity MAP kinase from *F. graminearum* with short flanking regions as well as the deduced amino acid sequence. Fat lettered nucleotide sequence areas indicate the location of the eight introns (I-VIII) found in the gene. Horizontal arrows mark the position of the four primers used to analyse the sequence.

Fig. 50: Alignment of the predicted amino acid sequence of the putative osmolarity MAP kinase from *F. graminearum* and several fungal MAP kinases. The alignment was performed with the CLUSTAL W programme. Identical amino acids are indicated as white letters on black background. Gaps introduced for the alignment are indicated by hyphens. The protein kinase domains of the yeast/fungi stress-activated protein kinase subgroup are indicated by Roman numerals (Hanks and Quinn 1991). The TGY-sequence required for kinase activation is marked by asterisks (Kültz 1998). Genbank accession numbers for *N. crassa* osmotic sensitive-2 MAP kinase, *M. grisea* Osm1, *H. werneckii* Hog1p-like protein, and *S. cerevisiae* Hog1 are AAK83124, AF184980, AAM64214 and AAA34680, respectively.

D. Fungal mitogen-acivated protein kinases

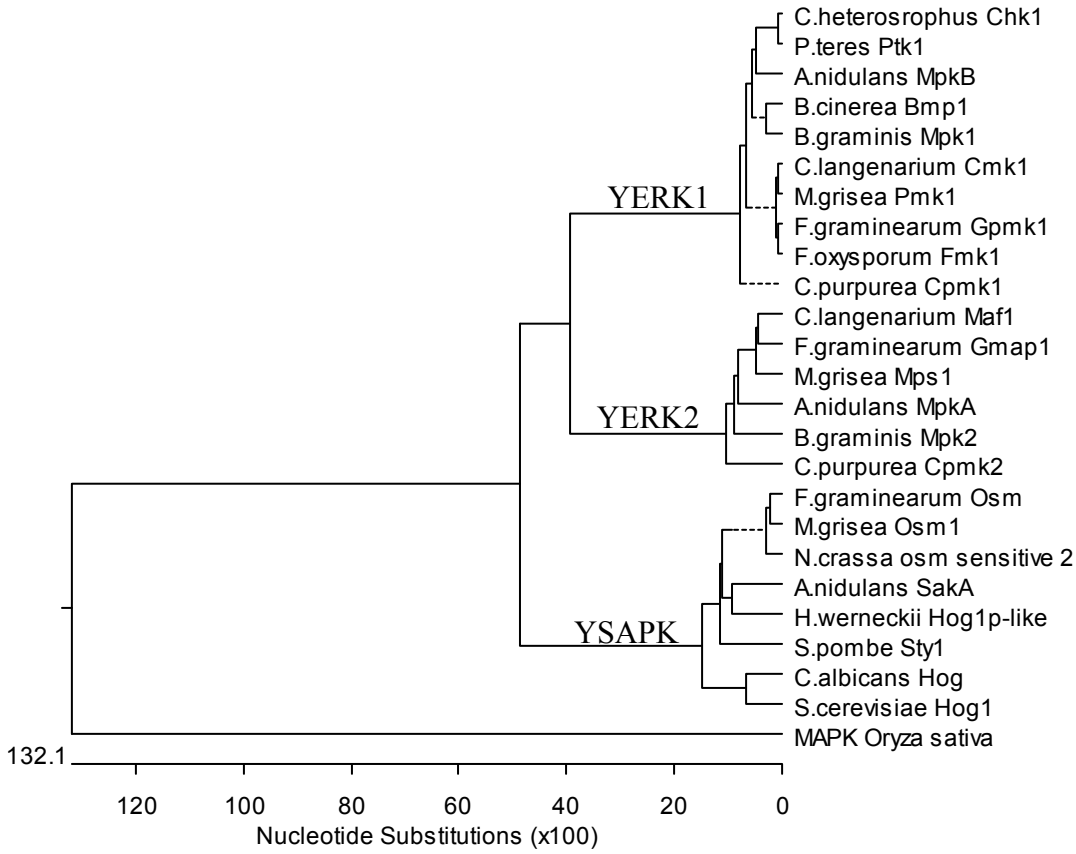

Fig. 15: Phylogenetic tree of various MAP kinases including the three MAP kinases of *F. graminearum*, Gmap1, Gpmk1 and the putative osmolarity MAP kinase, which were isolated in the cause of this work. All amino acid sequences were aligned with the CLUSTAL W programme. The fungal MAP kinases group to the three main classes of fungal MAP kinases, the yeast/fungi extracellular signal regulated kinase subgroup 1 (YERK1) and subgroup 2 (YERK2) and the yeast/fungi stress-activated protein kinases (YSAPK). A plant MAP kinase from *Oryza sativa* (accession number AAO37965) was used as reference. The accession numbers for the fungal MAP kinases are as follows: *C. heterostrophus* Chk1, AAF05913; *P. teres* Ptk1, AAK52840; *A. nidulans*. MPKB, AAF12815; *B. cinerea* Bmp1, AAG23132; *B. graminis* Mpk1, AAG53654; *C. langenarium* Cmk1, AAD50496; *M. grisea* Pmk1, AAC49521; *F. oxysporum* Fmk1, AAG01162; *C. purpurea* Cpmk1, CAC47939; *C. langenarium* Maf1, AAL50116; *M. grisea* Mps1, AAC63682; *A. nidulans* MPKA, AAD24428; *B. graminis* Mpk2, AAG53655; *C. purpurea* Cpmk2, CAC87145; *M. grisea* Osm1, AF184980; *N. crassa* osm sensitive 2, AAK83124; *A. nidulans* SakA, AAF97243; *H. werneckii* Hog1p-like, AAM64214; *S. pombe* Sty1, Q09892; *C. albicans* Hog, Q92207; *S. cerevisiae* Hog1, P32485.

E. Putative hydrophobin from *Fusarium graminearum*

```
- 372                                                agcctcactgaa
                                  NJ94B
- 360 ttccctcctggttgaagaagaacgcgcgccaatgctaaattttgg

- 315 aataaccagcaatcaatcaattaatacaggtaaacattttgaaag

- 270 ggatgtttctgcgattagttataattagattgacttcttggccaa

- 225 aaagagcatagtaccagacatgtaatctcgcttcaataacgatgt

- 180 tgggctagtctttacagactattggaaagctagtggcattagctt

- 135 gctatctcggccttcagcttttattttgttatttgctcgatgtga

 - 90 acaaatgcacttcctccttttttgtttcacttgttctcaacccaa

 -  45 tagttacttctctagcaactgttgaaagccacctgatccaccaag
                                  NJ59
   1 ATGCGATTCACTGCCTTTCTGTTGCCCATCGTTCTCGGTGCTGTA
   1  M  R  F  T  A  F  L  L  P  I  V  L  G  A  V

  46 TCGGCCGGACCCTGTCGACCCTCTAGCGCCGAGAGCAGCGCCGAA
  16  S  A  G  P  C  R  P  S  S  A  E  S  S  A  E
            ↑

  91 ACCACGGAGCTTGGCAGTGTGACCACAACCGATCTGTTCCAAACT
  31  T  T  E  L  G  S  V  T  T  T  D  L  F  Q  T

 136 ATCACCGCGACTCTGTCAACCGACGATACAACCACTGCTGTACCT
  46  I  T  A  T  L  S  T  D  D  T  T  T  A  V  P

 181 ACAACTGAGATCGAATCGGCATCAGCGACGACACAGATGATCGAG
  61  T  T  E  I  E  S  A  S  A  T  T  Q  M  I  E

 226 TCTACGATAGAATCAGCCGCCGCTACTTCTTCCACGACTGCTGCT
  76  S  T  I  E  S  A  A  A  T  S  S  T  T  A  A

 271 TCTCGCCAATGTATTGCACCAGCCGCCTTGCAATGCTGCCTGAGT
  91  S  R  Q  C  I  A  P  A  A  L  Q  C  C  L  S

 316 GTTGGAAAAGCGAACGATGGCCCGGTTGGCCTGATCCTTGGGCTG
 106  V  G  K  A  N  D  G  P  V  G  L  I  L  G  L

 361 CTGGGTATTGTTATTAAGGACCTGAGCATTCCAATTGGACTGACA
 121  L  G  I  V  I  K  D  L  S  I  P  I  G  L  T
```

```
406 TGTGAGTTTCCCACACATCATGCTGTTTATCAATCTAACAATCTC    I

                                  NJ62
451 GTTCCAGGCTCATCTGTTCCTAACGCTGAAGCTTGTGGTGCCAGC
136       C  S  S  V  P  N  A  E  A  C  G  A  S

496 CGCACACCAGTTTGCTGCAGTGGCAACAGCCATGTTAGTATTTTG    II
149  R  T  P  V  C  C  S  G  N  S  H

541 TCTCCTGCAACTATTTACTAAATGTTATTGACTTATATGTTCATA


589 GGGCGGCCTTGTTGCTATTGGCTGTACTTCAGTCTAGtgattaat
160   G  G  L  V  A  I  G  C  T  S  V  *

631 tatttttttaattagaagactaattaatagtaatagataaagcca
          NJ95
676 ctactgaactggttggctgcatggtgaagagaagtcatataataa

721 tagtttcccac
```

Fig. 52: Nucleotide sequence containing the complete gene for the putative hydrophobin from *F. graminearum* with short flanking regions as well as the deduced amino acid sequence. Fat lettered nucleotide sequence areas indicate the location of the two introns (I and II) found in the gene. Horizontal arrows mark the position of the four primers used to analyse the sequence. Fat lettered amino acids indicate the position of the conserved cysteine residues. The vertical arrow shows the signal peptid cleavage site.

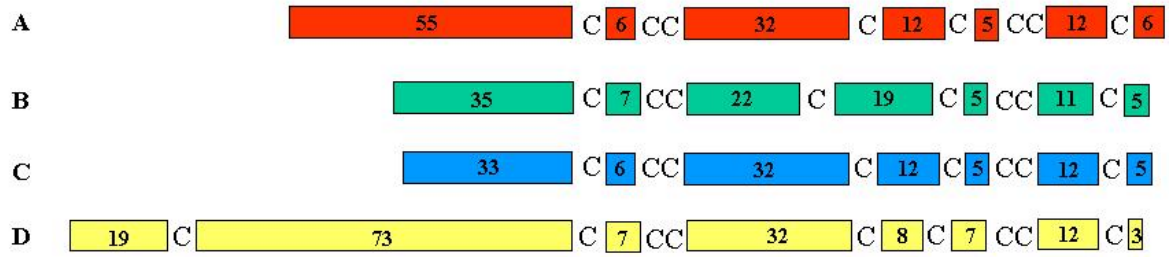

Fig. 53: Spacing of the conserved cysteine residues in various hydrophobins. A) SC3 from *S. commune* (AAA96324); B) Mpg1 from *M. grisea* (AAA20128); C) Fvh1 from *F. velutipes* (BAB17622); D) putative hydrophobin from *F. graminearum*. The cysteine residues are shown with a capital C. The coloured bars indicate the other amino acids of the proteins. The number of amino acids found in each domain between the cysteine residues is specified in the coloured bars.

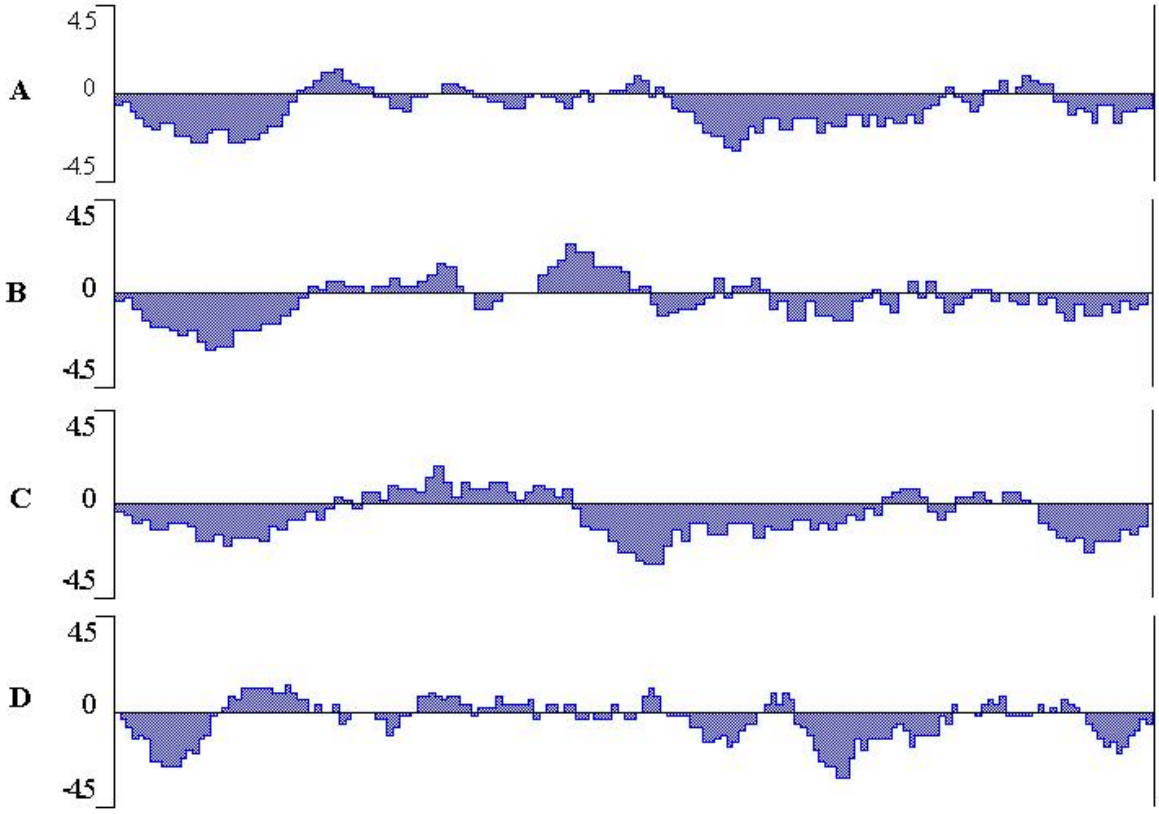

Fig. 54: Hydropathy-Plots (Kyte-Doolittle) of various hydrophobins. A) SC3 from *S. commune* (AAA96324); B) Mpg1 from *M. grisea* (AAA20128); C) Fvh1 from *F. velutipes* (BAB17622); D) putative hydrophobin from *F. graminearum*.

„Special Thank´s to....“

Prof. Dr. Wilhelm Schäfer möchte ich für die Überlassung des Themas, die vielen Diskussionen, die Korrektur der Arbeit und seine stete Hilfsbereitschaft danken.

Für die Übernahme des Zweitgutachtens der Dissertation gilt mein besonderer Dank Prof. Dr. Horst Lörz.

Für die finanzielle Unterstützung, die Bereitstellung der *Fusarium graminearum* cDNA-Bank und für die Durchführung einiger Sequenzierungen geht mein Dank an die BASF AG, Ludwigshafen, und im Speziellen an Dr. Thierry Lacour für sein Verständis und Entgegenkommen.

Dr. Marc Lemmens möchte ich für die Messung der Toxine und für seine wertvollen Tips zur Durchführung der Induktionen und der Interpretation der Ergebnisse danken.

Mein ganz spezieller Dank geht an die Mitglieder der TaRes Gruppe. Es war eine unglaubliche Freude, in einer so gut funktionierenden Gruppe zu arbeiten. Hilfsbereitschaft, Freundschaft, Motivation, Spaß an der Arbeit und natürlich so manche Alberei dominierten das Geschehen. Schon um Euretwillen hat die Arbeit Freude bereitet.
Dr. Anke P. Lösch war mit wertvoller Hilfe, sowohl was Fachfragen als auch Persönliches an ging, immer zur Stelle. Auch wenn ich das erst zu schätzen lernte, als ich wußte, wie man die langen Monologe unterbrechen konnte! Anke, ich schätze Deine Verläßlichkeit und Offenheit sehr! Abschließend, möchte ich mich bei Dir auch noch für die Korrektur der Arbeit bedanken.
Dr. Sascha Malz war, glaube ich, unser aller Sonnenschein! Immer konnten wir mit, als auch über ihn lachen. Fast nie ist ein Tag vergangen, an dem wir uns nicht mit vor Lachen schmerzendem Bauch, gekugelt haben. Sascha, in Deiner Schreibphase haben wir Dich sehr vermißt. Auf einmal wußten wir nicht mehr, wenn wir ärgern sollten. Dir möchte ich für Deine Hilfe bei der Korrektur der Arbeit danken und natürlich für Deine unermüdliche Reparaturarbeit an meinem komischen Computer sowie allen anderen Probleme, die ich mit der Bemerkung „Sascha, ich hab mal ne Frage...“ oder „Sag mal Sascha,...“ eingeleitet habe.
Katrin Quester möchte ich zunächst für Ihre hervorragende Arbeit am Hydrophobin und am Osmo-MAP-Kinase Projekt danken. Ich hoffe, daß Dir die Zusammenarbeit mit mir Spaß gemacht hat. Und wenn nicht, so hatten wir auf jeden Fall sehr viele, lustige Stunden beim Cocktailtrinken im Bolero, auf dem DOM, beim Abrocken oder beim Billard-, Bohnanza oder Carromspielen.
Meike Andermann war für mich immer ein ruhiger Pol, wenn es mal stürmisch war. Unsere Gespräche haben immer geholfen, die Gemüter zu kühlen oder waren einfach interessant, wenn es mal wieder um Urlaubserinnerungen oder andere Themen ging.
Dr. Frank J. Maier hat mir geholfen, mein anfängliches Heimweh an den Bodensee zu lindern. Immer wenn, Du schwäbisch gschwätzt hascht, kam ich mir gar nicht mehr so weit weg vor! Außerdem möchte ich mich bei Dir für die Übergabe der MAP-Kinase-Ursprungsplasmide und für Deine generelle Hilfsbereitschaft danken.
Auch wenn wir TaRes-Leute nun teilweise wohl in alle Winde verstreut werden, so hoffe ich, daß der Kontakt bleibt! Ich wünsche Euch allen das Allerbeste für die Zukunft.

Ein weiterer Dank gilt einer kleinen, aber feinen Damenrunde, mit der ich jeden Mittag das Vergnügen hatte zu essen. Liebe Cathrin, Birgit, Brigitte und Katrin, schön dass Ihr mich aufgenommen habt. Auch wenn Ihr Euch immer nur über die Größe meiner Portionen

lustig gemacht habt! Ich hab´s mit Fassung getragen!! Brigitte möchte ich an dieser Stelle auch ganz herzlich für die sprachliche Korrektur meiner Arbeit danken.

Dr. Attila Gácser danke ich für seine geduldigen Bemühungen uns fußkranken Grazien ein bißchen Gefühl für`s Tanzen beizubringen. Es hat viel Spaß gemacht!

Dr. Angelika Felk möchte ich danken, daß sie mir immer Mut gemacht hat.

Einen besonderen Dank an Dr. Frank Stehr für die nette Zeit zusammen und natürlich für seine Hilfe bei der musikalischen Untermalung der Arbeit.

Dr. Siegfried Salomon und Christian Haase möchte ich für Ihre Diskussionsbereitschaft zum Thema Lipasen und auch für alle weiteren experimentellen Tips danken.

Ich danke natürlich auch noch den vielen anderen AMPIII Mitarbeitern, die da kamen und gingen und die ich hier nicht namentlich genannt habe, für das gute Arbeitsklima.

Den Gärtnerinnen Marion Hagemann und Bärbel Klötzl möchte ich für Ihre großartige Unterstützung bei der Aufzucht und Pflege der Pflanzen danken.

Janbo Nörskau möchte ich für seinen nicht unwesendlichen Einsatz bei meinen unendlichen Computer-Problemen danken.

Einen speziellen Dank auch an Claudia Motz und Julia Steinbrener, die mir beide immer wieder aufs Neue zeigten, wie unerläßlich es ist, wirklich gute Freunde zu haben, auch wenn sie nicht gerade um die Ecke wohnen.

Meinen Eltern gilt ein Dank, da sie mir mein Biologiestudium ermöglicht haben. Ansonsten noch einen allgemeinen Dank für alles Gute, was Sie mir haben angedeihen lassen sowie für die sprachliche Korrektur meiner Arbeit.

Volker, Dir möchte ich dafür danken, dass Du einfach immer da bist, wenn ich Dich brauche! Vielen Dank auch für den moralischen Aufbau, in Zeiten, in denen ich nicht mehr an mich geglaubt habe. Tausend Dank für die Tips zum Etablieren der Enzymtests, die andauernde Bereitschaft, mit mir über mein Thema zu diskutieren und zu debatieren sowie für die letzten drei schönen Jahre im Spritzenweg. Ohne Dich wäre ich einfach nicht so weit gekommen. Danke!